UNCLASSIFIED

AD NUMBER
AD387671
CLASSIFICATION CHANGES
TO: **unclassified**
FROM: **confidential**
LIMITATION CHANGES
TO: **Approved for public release, distribution unlimited**
FROM: **Distribution authorized to U.S. Gov't. agencies and their contractors; Administrative/Operational Use; AUG 1966. Other requests shall be referred to Air Force Rocket Propulsion Laboratory, Edwards AFB, CA.**
AUTHORITY
31 Aug 1978, Group-4, per document marking, DoDD 5200.10; AFRPL ltr, 10 Dec 1985

THIS PAGE IS UNCLASSIFIED

AFRPL-TR-66-135

WAD: R-424-FR VOL I

AD387671

AD No.
DDC FILE COPY

(TITLE UNCLASSIFIED)

FINAL REPORT FOR THE FEASIBILITY DEMONSTRATION OF A LARGE IMPULSE SOLID ROCKET ATTITUDE CONTROL MOTOR

N.J. Rolleri
Wright Aeronautical Division
Curtiss-Wright Corporation

TECHNICAL REPORT AFRPL-TR-66-135, VOLUME I

August 1966

DDC
MAR 11 1968
A

GROUP 4

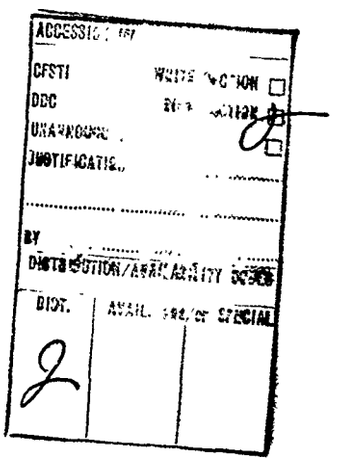
DOWNGRADED AT 3 YEAR INTERVALS;
DECLASSIFIED AFTER 12 YEARS.

In addition to security requirements which must be met, this document is subject to special export controls and each transmittal to foreign governments or foreign nationals may be made only with prior approval of AFRPL (RPPR-STINFO), Edwards, California 93523.

This document contains information affecting the national defense of the United States within the meaning of the Espionage Laws, Title 18, U.S.C. Sects. 793 and 794, the transmission or revelation of which in any manner to an unauthorized person is prohibited by law.

Air Force Rocket Propulsion Laboratory
Solid Rocket Division
Edwards Air Force Base, California 93523

When U. S. Government drawings, specifications, or other data are used for any purpose other than a definitely related Government procurement operation, the Government thereby incurs no responsibility nor any obligation whatsoever, and the fact that the Government may have formulated, furnished, or in any way supplied the said drawings, specifications, or other data, is not to be regarded by implication or otherwise, or in any manner licensing the holder or any other person or corporation, or conveying any rights or permission to manufacture, use, or sell any patented invention that may in any way be related thereto.



COPY 1 OF 260

(TITLE UNCLASSIFIED)

(9) FINAL REPORT, Jan 65 – Jul 66,

(6) FEASIBILITY DEMONSTRATION OF A LARGE IMPULSE SOLID ROCKET ATTITUDE CONTROL MOTOR, Volume I (U). (8)

(10) Norman J. Rolleri

(11) Aug 66

(12) 265p.

(14) WAD-R-424-FR-Vol-1

(15) AF 04(611)-10531

GROUP 4

DOWNGRADED AT 3 YEAR INTERVALS; DECLASSIFIED AFTER 12 YEARS.

(16) AF-3059

(18) AFRPL

(19) TR-66-135

In addition to security requirements which must be met, this document is subject to special export controls and each transmittal to foreign governments or foreign nationals may be made only with prior approval of AFRPL (RPPR-STINFO), Edwards, California 93523.

This document contains information affecting the national defense of the United States within the meaning of the Espionage Laws, Title 18, U.S.C. Secs. 793 and 794, the transmission or revelation of which in any manner to an unauthorized person is prohibited by law.

(381700)

1423

FOREWORD

(U) The Curtiss-Wright Corporation, Wright Aeronautical Division contracted with the Air Force Rocket Propulsion Laboratory, Edwards, California for the feasibility demonstration of a large impulse solid rocket attitude control motor under contract AF04(611)-10531.

(U) The objective of this program was to provide the technology required to design, fabricate, test and demonstrate a solid propellant propulsion system, employing the expandable ("E") dome design concept, that is capable of rapid, precise, command stop-start re-start functions and to demonstrate the requirements specified in Exhibit A of the above contract.

(U) The program effort included the following areas of work:

a. Analyses, design and reliability of the system.

b. Selection and evaluation of the rocket motor materials.

c. Igniter and propellant tailoring to meet the requirements of the system.

d. Pulser and stepping servo development.

e. Static tests at sea level and vacuum conditions.

f. Repetitive firing tests to demonstrate the overall operation of the system.

(U) This final report documents the work accomplished under the above contract from January 1965 through July 1966, and is submitted in complete fulfillment of contract AF04(611)-10531.

(U) The Air Force project engineer was M. Konieczny, Captain, USAF/RPMMA, of the Solid Rocket Division, Air Force Rocket Propulsion Laboratory, Edwards, California, 93523.

(This page is unclassified)

(U) The principal contributors on the project are:

O. Ziegler, B. Scott, A. Bohr, J. Geberth, A. Giordano, S. Flanzenbaum, H. Katz, W. Fioretti, R. Tommasini and P. Schaeffer.

(U) This report has been published in two volumes. Volume I, Confidential, Group IV, describes the design and development of the Solid Rocket System and was distributed in accordance with the CPIA basic list incorporated in Volume I. Volume II Secret Noforn Group III contains system analyses and is available to qualified requestors through the DDC.

(U) This technical report has been reviewed and is approved:

Charles R. Cooke
Chief, Solid Rocket Division
Air Force Rocket Propulsion Laboratory

PRECEDING PAGE BLANK-NOT FILMED

CONFIDENTIAL ABSTRACT

Design, Analyses, and Reliability

(U) Rocket motor optimization studies show that a rectangular motor configuration with an L/D ratio of 2:1 using a simple flat end-burning grain was optimum to provide minimum weight, volume, and sprocket wheel inertia. The design of the rocket motor was based on a quartz-phenolic base, a pre-molded rubber grain inhibitor, a silicone expandable (E) dome, CMP-13 propellant, and a pyrofuze wire pyrotechnic overspray ignition system. The weight of the WSR-101 rocket motor is .0246 pounds.

(U) The final version of the pulser housing assembly was made of stainless steel. The titanium sprocket wheel included provisions to withstand rocket motor failures. The weight of the pulser housing assembly is 5.64 pounds.

(U) The inlet-exit chute assembly design incorporates a cleated belt to feed the rocket motors into the pulser and extract fired rocket motors from the sprocket wheel. The weight of this unit is 1.01 pounds.

(U) A static firing fixture was designed to house the rocket motors during sea level and vacuum firing tests and simulate the firing conditions in the pulser housing assembly.

(U) Heat transfer analyses showed that no problems would exist with the E dome, nozzle throat, sprocket wheel, or pulser housing. A problem would be encountered, however, with the exit cone for extended periods of firing. This did not present a problem for this program. For system applications which would require long periods of firing, suitable materials could be incorporated in the exhaust nozzle extension cone to meet the duty cycle.

(C) System analyses, using the requirements of a post boost propulsion system were conducted for the encapsulated solid propellant pulse rocket system. (Volume II)

(C) Specific impulse computations were performed which showed that 8% aluminum was optimum for the WSR-101 motor. Motor tests produced an Isp of 255 seconds at sea level conditions and an expansion ratio of 14:1, and an Isp efficiency of 96%.

(C) Vacuum stability tests on the CWP series propellants showed excellent storability characteristics at 10^{-6} Torrs and 150°F.

Pulser Development

(U) The pulser system consists of those components which combined together produce the sprocket wheel stepping action to move capsules into firing position.

(U) A prototype solid state, high response relay type, feedback servo combined with a printed electrical motor was developed which met the program requirements for torque and step time.

Fabrication

(U) Standard transfer and compression molds were used to fabricate the rocket motor components. The assembly of the rocket motor components and tape assemblies was accomplished by manual methods using fixtures as required for curing and positioning.

Test

(U) Rocket motor development tests were conducted to establish the configuration of the motor.

(C) Performance repeatability tests on 100 motors showed the reproducibility of total impulse and specific impulse to be 2.47% and 2.3% respectively.

(C) Thermal vacuum firing tests of the rocket motors showed the components to be compatible in space and operable over a temperature range of -30 to +150°F. Ignition delays obtained in vacuum were two to three times longer than those experienced at sea level depending upon the exposure temperature.

(C) A failure mode analysis was made for each component of the WSR-101 system. The observed reliability for the repetitive firings is .926.

(C) A preliminary study of the maintainability requirements for an encapsulated solid propellant pulse rocket motor system shows that only routine checks need be performed to assure operational readiness. The system also has unique characteristics which permit effective checkout and maintenance procedures.

Materials Evaluation

(U) The selection and evaluation criteria for rocket motor materials were based on design requirements and consideration of methods of component fabrication. The materials selected for each rocket motor component are as follows:

Nozzle Base - Fiberite MX 1344-50
E - Dome - Silicone Rubber S-55 and Gen Gard V-57
Inhibitor - Gen Gard V-57
Nozzle Plug - Urethane Foam
Tape - Teflon - Fiberglass TB-5E
Adhesives - Aerospace Sealant 92-018 with Silicone Primer 4094

Igniter Development

(U) Several experimental igniter compositions were prepared and tested in the WSR-101 rocket motor. The aluminum based igniters performed well in the motors but require further improvement. Magnesium based igniters produced rapid rates of pressure rise which ruptured the elastic motor dome.

(U) A spray pyrotechnic igniter was selected as being the most feasible and reliable for the final motor configuration. The ignition system incorporates a Hi-R .004 inch diameter, Pyrofuze initiator and a pyrotechnic booster.

Propellant Development

(C) By means of processing changes, which can be precisely controlled, a reproducible burn rate of 1.9 inches per second was achieved.

(U) Repetitive firing tests were made which combined the operation of all components (rocket motor tape assembly, pulser housing assembly, stepping servo and motor system) of the system.

(U) Two problems were encountered during these tests, namely missed ignition of the rocket motor and E dome extrusion which jammed the pulser assembly. These problems were resolved by modification to the tooling to insure better positioning and spacing of the rocket motors on the tape and the use of higher durometer material for the dome.

(This page is unclassified)

TABLE OF CONTENTS

SECTION	TITLE	PAGE NO.
I.	INTRODUCTION	1
II.	DESIGN, ANALYSIS AND RELIABILITY	3
	A. Design	
	B. Analysis	
	C. Reliability Analysis	
III.	MATERIALS EVALUATION	107
IV.	IGNITER DEVELOPMENT	131
	A. Experimental Igniter	
	B. Spray Igniters	
V.	PROPELLANT DEVELOPMENT	141
	A. Specific Impulse Computations	
	B. Composition Development	
	C. Processing Development	
	D. Characterization of Ballistic and Physical Properties	
	E. Vacuum Stability	
VI.	PULSER DEVELOPMENT	155
	A. Stepping Servo and Pulser Motor	
	B. Prototype Servo and Motor System	
VII.	FABRICATION	191
VIII.	TEST	195
	A. Rocket Motor Tests	
	B. Repetitive Firing Tests	
IX.	CONCLUSIONS	259

LIST OF ILLUSTRATIONS

Figure	Title	Page
1	Encapsulated Solid Propellant Rocket (U)	4
2	WSR-101 Prototype System (U)	5
3	Single Square Grain (U)	7
4	Single Square Grain (U)	8
5	Star Shaped Grain (U)	9
6	Star Shaped Grain (U)	10
7	Concentric Square Grain (U)	11
8	Concentric Square Grain (U)	12
9	Single Flat Grain (a/b = 1.0) (U)	13
10	Single Flat Grain (a/b = 1.58) (U)	14
11	Single Flat Grain (a/b = 2.92) (U)	15
12	Single Flat Grain (a/b = 1.0) (U)	16
13	Single Flat Grain (a/b = 2.89) (U)	17
14	Single Flat Grain (a/b = 2.0) (U)	18
15	Single Flat Grain (a/b = 1.0) (U)	19
16	Single Flat Grain (a/b = 2.3) (U)	20
17	Nozzle-Base Weight Reduction (U)	21
18	Single Flat Grain, Capsule Mass Ratio Versus Capsule Proportions (U)	24
19	Capsule and Tape Assembly WSR-101 (U)	26
20	WSR-101 Capsule Assembly (U)	27
21	WSR-101 Capsule Component (U)	28
22	Nozzle Base WSR-101 (U)	31
23	Nozzle Base Stress Summary (U)	32
24	Expandable Closure WSR-101 (U)	33
25	WSR-101 Propellant Grain (U)	34
26	Boot Inhibitor (U)	37
27	WSR-101 Nozzle Plug (U)	38
28	Tape WSR-101 (U)	39
29	Igniter Wire (U)	40
30	WSR-101 Sprocket Wheel (U)	45/46

LIST OF ILLUSTRATIONS (Cont)

Figure	Title	Page
31	WSR-101 Sprocket Wheel Freebody (U)	48
32	Sprocket Wheel Stresses (U)	49
33	Pulser Housing (U)	51/52
34	Pulser Housing Clamping Loads (U)	54
35	Housing Deflection Schematic (U)	55
36	Pulser Housing with Nozzle Blocks (U)	56
37	WSR-101 Sprocket Wheel Modification (U)	58
38	Motor Shaft Pin Analysis (U)	61
39	Adjustable Inlet and Exit Chute Assembly (U)	63
40	WSR-101 Prototype Pulser Housing (U)	64
41	WSR-101 Prototype Front Cover (U)	66
42	Prototype Ignition Assembly (U)	68
43	WSR-101 Prototype Chute Housing (U)	70
44	Static Firing Fixture (U)	71
45	Expandable E Dome Capsule Configuration (U)	73
46	Expandable Capsule Temperature Distribution in GenGard V-57 Chamber Dome and Sprocket Wheel (U)	79
47	Expandable Capsule Temperature Distribution in Fibrite Nozzle Throat (U)	80
48	Nozzle Exit Cone Temperatures (U)	82-83
49	Failure Mode Analysis (U)	86-94
50	Ground Check-Out System Schematic (U)	104/105
51	Effect of Vacuum Storage and Temperature on V-57 Rubber (U)	109
52	Instron Tensile Testing Machine with Low Temperature Unit in Place for Dome Material Tests (U)	111
53	Jaw Detail of Instron Machine with Dome Material in Place and Cold Jacket Removed (U)	112
54	Test Samples of Dome Materials after Oxy-Acetylene Torch Test (U)	113
55	Test Samples of Nozzle Base Materials after Oxy-Acetylene Torch Test (U)	116
56	Nozzle Closure Test Fixture (U)	122

LIST OF ILLUSTRATIONS (Cont)

Figure	Title	Page
57	Capsule Transport Tape TB-5E Tape .004-.005 Thick (U)	123
58	Boot Inhibitor and Mold (U)	129
59	Theoretical Propellant Performance CWP Solid Propellant Optimization Study (U)	144
60	Burning Characteristics of CWP-9 Propellant (U)	151
61	Burn Rate of CWP-13 Propellant (U)	152
62	Motor Weight Vs. Load Inertia and Stepping Time (U)	157
63	Stepping Servo Block Diagram and Relay Action (U)	158
64	Pulser Stepping Servo Wiring Diagram (U)	159
65	Positioning Accuracy (U)	160
66	Isometric of Mechanical Servo Loop (U)	163
67	Stepping Servo Error Tolerance Diagram Under Static Condition (U)	164
68	Stepping Servo Components Tolerance Limits - WSR-101 (U)	165
69	U9C Printed Motor (U)	167
70	Motor Inertial Load Disc with Position Indicating Slots (U)	168
71	Test Setup (U)	169
72	Variable Frequency and Duty Cycle Pulser Generator (U)	170
73	Power Amplifier (U)	171
74	Power Amplifier (U)	172
75	Experimental Data U9C Printed Motor (SN 153) (U)	173
76	Experimental Data U9C Printed Motor (SN 153) (U)	174
77	Experimental Data U9C Printed Motor (SN 153) (U)	175
78	Experimental Data U9C Printed Motor (SN 153) (U)	176
79	Experimental Data U9C Printed Motor (SN 153) (U)	177
80	U9C Motor - SN 153 - After Test (U)	179
81	U9C Armature Assembly U9C Motor SN 153 After Test (U)	180
82	WSR-101 Breadboard Servo Response (U)	181
83	WSR-101 Breadboard Servo Response (U)	182
84	Stepping Servo and Pulser Motor Breadboard (U)	183
85	WSR-101 Prototype Servo and Motor System (U)	185

LIST OF ILLUSTRATIONS (Cont)

Figure	Title	Page
86	WSR-101 Prototype Servo and Motor System (U)	186
87	WSR-101 Prototype Servo and Motor System (U)	187
88	Prototype Power Requirements (U)	188
89	WSR-101 Prototype Pulser (Acceptance Test Data) (U)	189
90	Two Cavity "E" Dome Mold (U)	192
91	Single Cavity Nozzle Base Mold (U)	193
92	WSR-101 Static Firing Fixture (U)	196
93	Static Firing Fixture on Thrust Cell (U)	197
94	Schematic of Static Test Set-Up (U)	198
95	Hydrostatic Test of Nozzle Base (U)	201
96	Thrust Time Traces, WSR-101, CWP-9 (U)	202-203
97	Thrust Time Traces, WSR-101, CWP-9 (U)	204-205
98	Nozzle Base and Gold Lead Configuration (U)	209
99	WSR-101 Thrust Time Traces Qualification Motors (U)	211
100	Thrust Time Traces, WSR-101, CWP-13 (U)	216-217
101	WSR-101 Pulser Deflection Test (U)	232
102	WSR-101 Pulser Deflection Tests (Deflection Simulating Side Port Firing) (U)	233
103	WSR-101 Pulser Deflection Test (U)	234
104	WSR-101 Sprocket Wheel Shaft Modifications (U)	236
105	WSR-101 Pulser Deflection Tests (Revised Pulser Housing Shaft Supported at Both Ends) (U)	237
106	WSR-101 Pulser Housing Assembly Development (U)	238-242
107	WSR-101 Repetitive Firing Control Panel (U)	245/246
108	WSR-101 Repetitive Check-Out Trace (U)	248
109	WSR-101 Repetitive Firing Trace (U)	259-260

LIST OF TABLES

Table	Title	Page
I	Summary of Basic Rocket Motor Configurations (U)	22
II	Capsule Component Weight Summary (U)	30
III	WSR-101 Initial Pulser Component Weight Summary (U)	42
IV	WSR-101 Prototype Pulser Component Weight Summary (U)	43
V	WSR-101 Capsule Development Tests Single Firings in Firing Fixture-Sea Level (U)	95
VI	Failure Modes of WSR-101 System - Repetitive Firings (U)	98
VII	Expandable Dome Material Testing (U)	110
VIII	Nozzle Closure Plug Tests (U)	118-121
IX	Lap Shear Adhesive Tests as Applied to Tape (U)	125
X	Dome-to-Nozzle Base Adhesive Tests (U)	128
XI	Stoichiometric Mixtures of Metals and Oxidizers (U)	132
XII	Experimental Pyrotechnic Mixtures, Weight Percent (U)	134
XIII	Experimental Igniter Formulations (U)	135
XIV	Motor Tested Experimental Igniter Formulations (U)	137
XV	Effect of Aluminum Concentration on Theoretical Specific Impulse (U)	143
XVI	Effect of Binder Concentration on Specific Impulse (U)	145
XVII	Burn Rate of Aluminum Containing Propellants (U)	147
XVIII	Mechanical Properties of CWP-13 Propellant (U)	153
XIX	Nozzle Base Hydrotest (U)	200
XX	WSR-101 Sea Level Static Firings (U)	207
XXI	Ablation of Dome and Exhaust Nozzle Throat Erosion (U)	208
XXII	WSR-101 Rocket Motor Static Firing Tests (U)	212-215
XXIII	WSR-101 Rocket Motor Static Sea Level Firing Tests (U)	218
XXIV	WSR-101 Performance of Aluminized Propellant CWP-17A8 (U)	220
XXV	WSR-101 Vacuum Ignition Firing Test Summary (U)	222
XXVI	WSR-101 Rocket Motor Thermal Vacuum Tests (U)	223-224
XXVII	WSR-101 Rocket Motor Thermal Vacuum Tests (U)	225-226

LIST OF TABLES (Contd.)

Table	Title	Page
XXVIII	WSR-101 Rocket Motor Vacuum Firing Tests (U)	227
XXIX	WSR-101 Rocket Motor Vacuum Firing Tests (U)	228
XXX	WSR-101 Rocket Motor Vacuum Firing Tests (U)	229
XXXI	WSR-101 Repetitive Firing Summary (Tape No. 1A) (U)	249
XXXII	WSR-101 Repetitive Firing Summary (Tape No. 1) (U)	249
XXXIII	WSR-101 Repetitive Firing Summary (Tape No. 2) (U)	250
XXXIV	WSR-101 Repetitive Firing Summary (Tape No. 3) (U)	250
XXXV	WSR-101 Repetitive Firing Summary (Tape No. 4) (U)	251
XXXVI	WSR-101 Repetitive Firing Summary (Tape No. 5) (U)	251
XXXVII	WSR-101 Repetitive Firing Summary (Tape No. 6) (U)	252
XXXVIII	WSR-101 Repetitive Firing Summary (Tape No. 7) (U)	252
XXXIX	WSR-101 Repetitive Firing Summary (Tape No. 8) (U)	253
XL	WSR-101 Repetitive Firing Summary (Tape No. 9) (U)	253
XLI	WSR-101 Repetitive Firing Summary (Tape No. 10) (U)	254
XLII	WSR-101 Repetitive Firing Summary (Tape No. 11) (U)	254
XLIII	WSR-101 Repetitive Firing Summary (Tape No. 12) (U)	255
XLIV	WSR-101 Repetitive Firing Summary (Tape No. 13) (U)	256

SECTION I

INTRODUCTION

(C) A rocket propulsion system for attitude control of advanced military space vehicles and weapon systems applications must provide single pulses as well as multiple rapid pulse operation. The rocket motors of such a propulsion system must not only deliver high performance but precise and repeatable total impulse per pulse. In addition, it is necessary that the propulsion system be lightweight and withstand long term storability in a space or earth environment.

(U) To meet these requirements, a solid propellant attitude control propulsion system has been developed which has distinct advantages over liquid or gaseous propulsion systems.

(U) The solid propulsion system which was developed to meet the requirements consists of individual solid propellant rocket motors mounted on a transport tape. These motors are fed from a storage container into a firing position by means of a sprocket wheel which is driven by a stepping servo and electric motor.

(U) The configuration of the rocket motor is unique in that a lightweight flexible covering over the propellant-igniter combination expands when the motor is fired within the confines of the sprocket wheel, which serves as the motor case. This feature provides a substantial reduction in motor case weight and system volume.

(U) This final report presents the details of the development program conducted from January 1965 through July 1966. During this program the feasibility of a large solid propellant attitude control propulsion system, which met the above requirements, was demonstrated.

PRECEDING PAGE BLANK-NOT FILMED

SECTION II

DESIGN, ANALYSIS AND RELIABILITY

A. DESIGN

(U) To meet the requirements of the program, a solid propellant propulsion system was designed consisting of individual tape-mounted solid propellant rocket motors, which are fed from a storage container into firing position by means of a stepping motor-driven sprocketwheel. The rocket motors are fired, on command, at any of three positions by a signal from an external electrical source. The operation of a typical system in an attitude control application, is shown schematically in Figure 1.

(U) The individual rocket motors (capsules) consist of an expandable case which is sealed to a rigid, erosion-resistant nozzle and contains the propellant grain and igniter. The sockets of the sprocketwheel and the wheel housing provide a rigid structure within which the capsule expands during operation. Electrical ignition is accomplished via two leads through the rigid part of the capsule. A length of pyrofuze wire is attached to these leads, inside the capsule, and is ignited by the electric current. This ignites a pyrotechnic igniter material which, in turn, initiates burning of the propellant grain. As chamber pressure increases, the flexible case (E-dome) expands within the sprocketwheel to provide the additional volume for combustion. The expandable case also insulates and seals the combustion gases from the structure. The gases exhaust through the capsule nozzle and a nozzle extension which is part of the pulser housing. After firing, the case returns to its original shape and the capsule is ejected through an exit chute.

(U) The prototype assembly which is designated WSR-101 is shown in Figure 2. It consists of a pulser (electric motor, stepping servo, sprocketwheel and housing assembly), adjustable chute and tape containing 100 live capsules plus dummy leader caps. The leader tape section, with its dummy capsules, is threaded through the entrance side of the chute, around the sprocketwheel, and out the exit side. Within the chute, a free wheeling cleated belt engages the entering capsules and is driven by them as they are pulled into position by

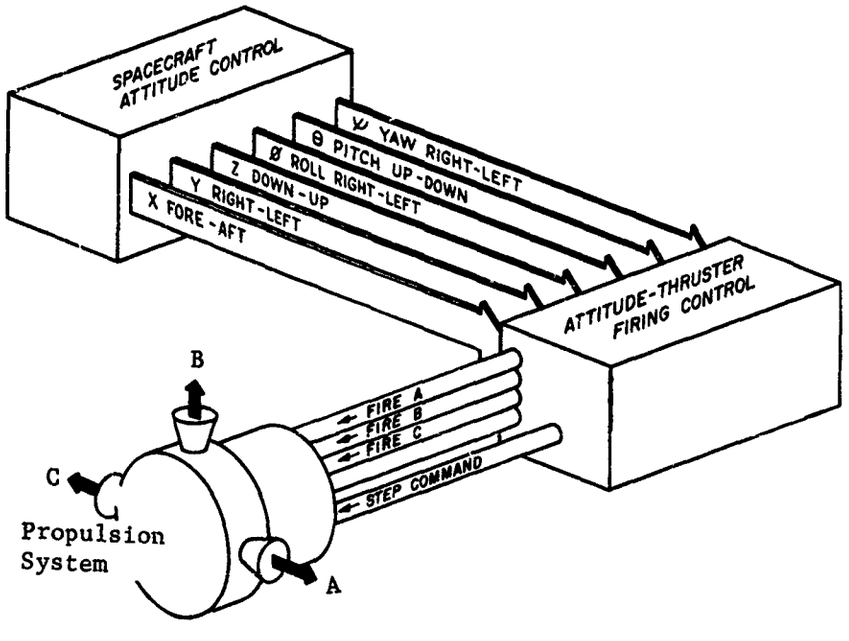


Figure 1. Encapsulated solid propellant rocket.

Figure 1. Encapsulated solid propellant rocket. (U)

66-1182

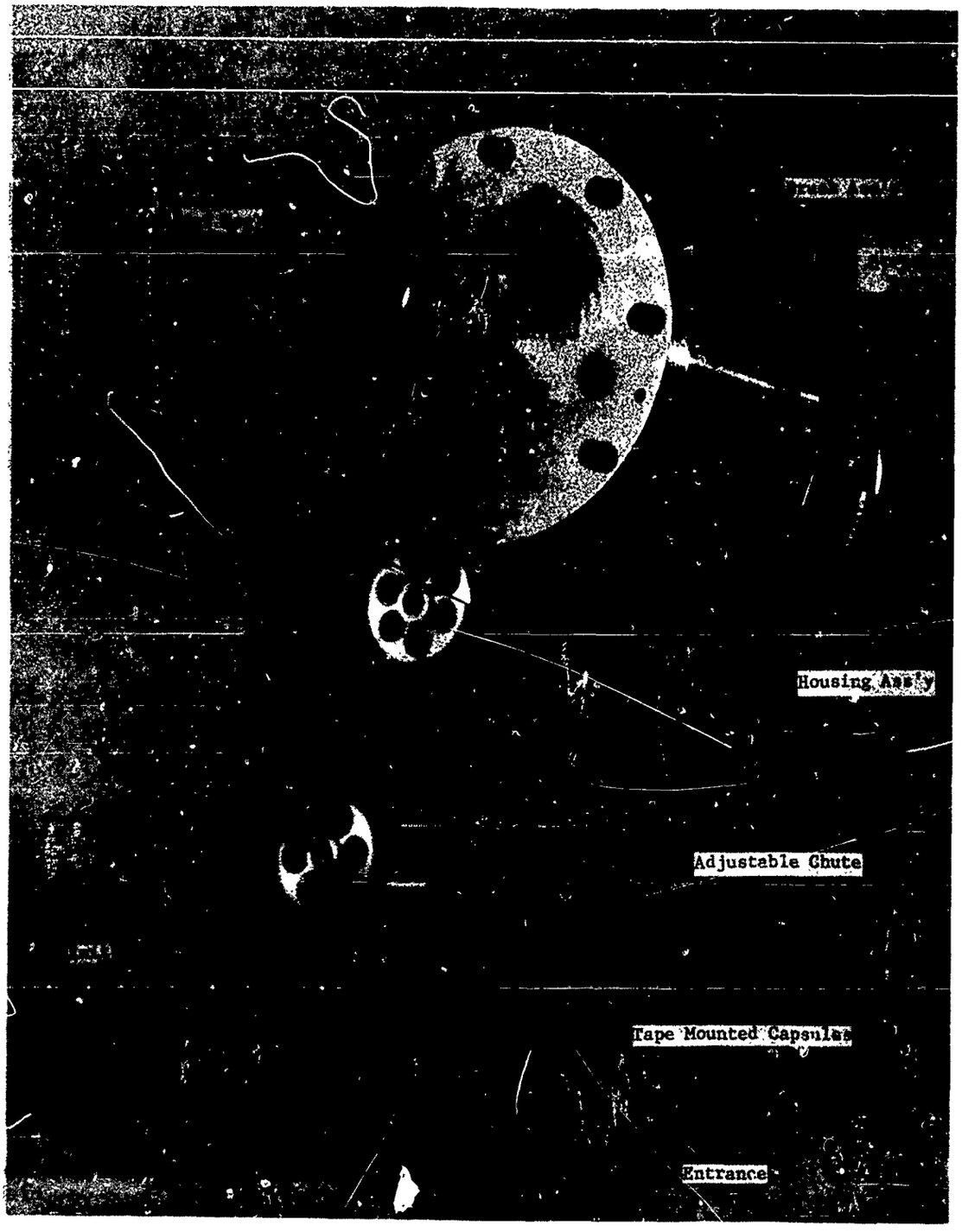


Figure 2. WSR-101 Prototype system. (U)

20-887

(This page is unclassified)

(U) the stepping motor-driven sprocketwheel. On the exit side, the belt engages the spent capsules pulling them out of the sprocketwheel to provide positive ejection.

1. Rocket Motor Optimization

(C) Optimization studies were conducted to establish a rocket motor configuration to best meet the following requirements:

- Mass Ratio 0.50
- Average Thrust 50 lb
- Action Time 50-60 m sec
- Vacuum Specific Impulse (E=20:1) 245 sec
- Reproducible Impulse Bit
- High Reliability
- Simplicity of Design and Assembly

(U) Four basic grain configurations were investigated. These configurations and design data such as total impulse, thrust, chamber pressure, burn time, sprocket wheel diameter, inertia of the sprocket wheel with capsules, nozzle expansion ratio, capsule mass ratio, capsule weight, and packaging volume of the capsules is shown on the following illustrations.

- Single Square Grain (Figures 3 and 4)
- Star Shaped Grain (Figures 5 and 6)
- Concentric Square Grain (Figures 7 and 8)
- Single Flat Grain (Figures 9 through 16)

(C) A ribbed or waffle type nozzle base configuration (similar to Figure 17) was used to assure lightweight with adequate structural strength. The capsule configurations were compared on the basis of a 2000 psia combustion pressure and a propellant burn rate of 2.12 in/sec.

(U) Table I summarizes the design data for these various configuration and high lights the primary design advantages or disadvantages.

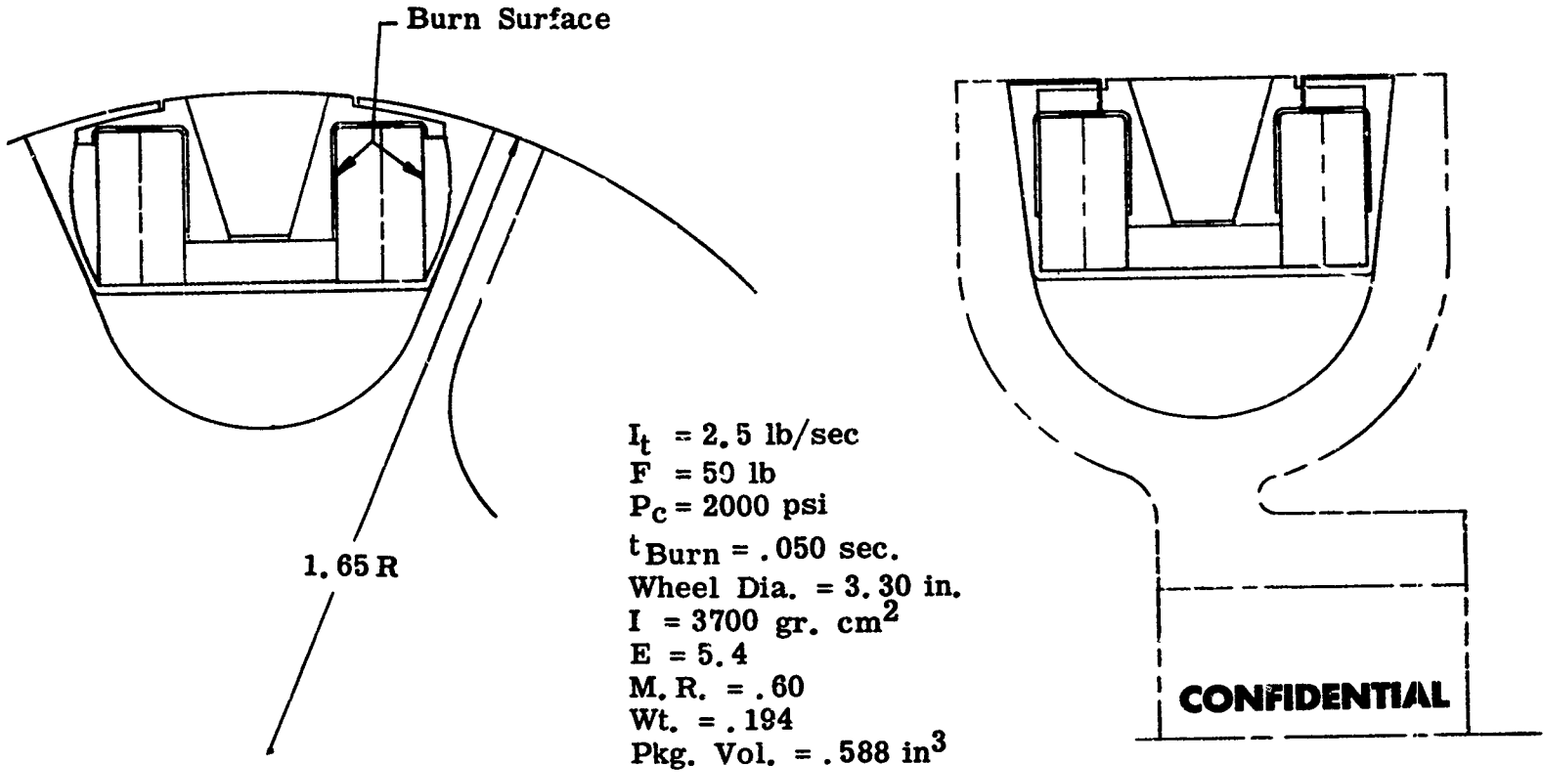


Figure 3. Single square grain. (U)

I_T = 2.5 lb/sec
F = 50 lb
P_c = 2000 psi

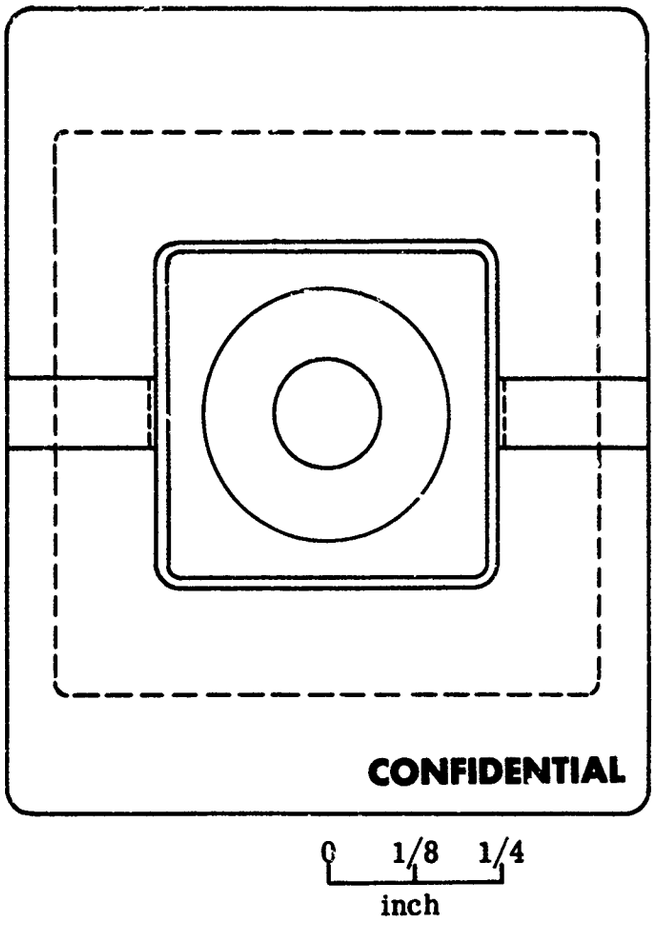


Figure 4. Single square grain. (U)

67-1853

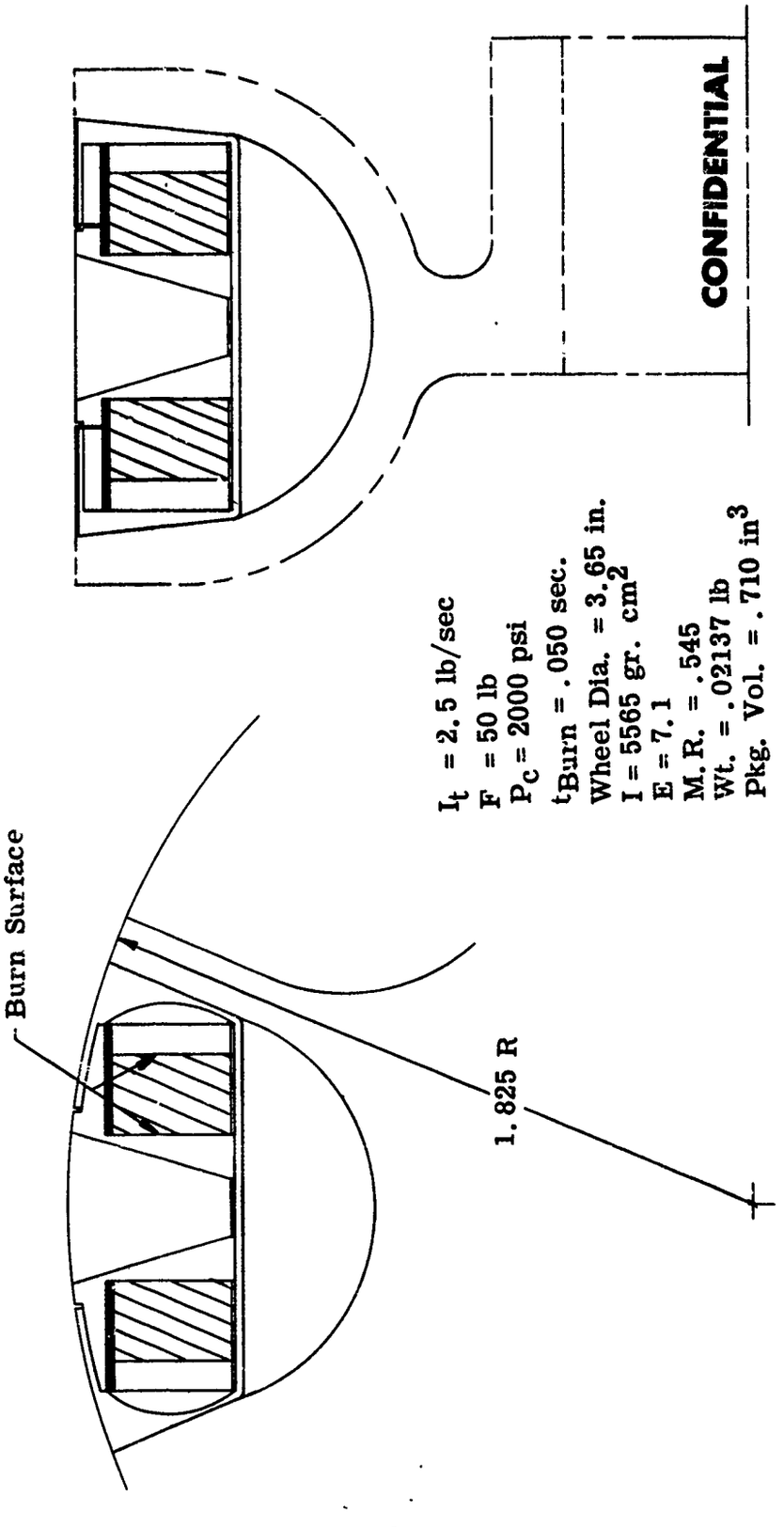


Figure 5. Star shaped grain. (U)

67-1854

I_t = 2.5 lb/sec

F = 50 lb

P_c = 2000 psi

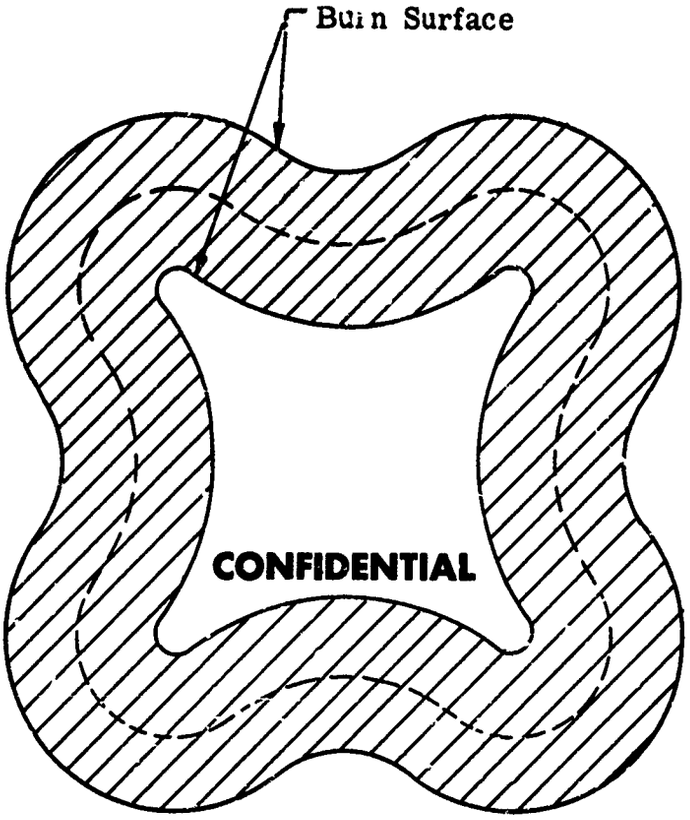
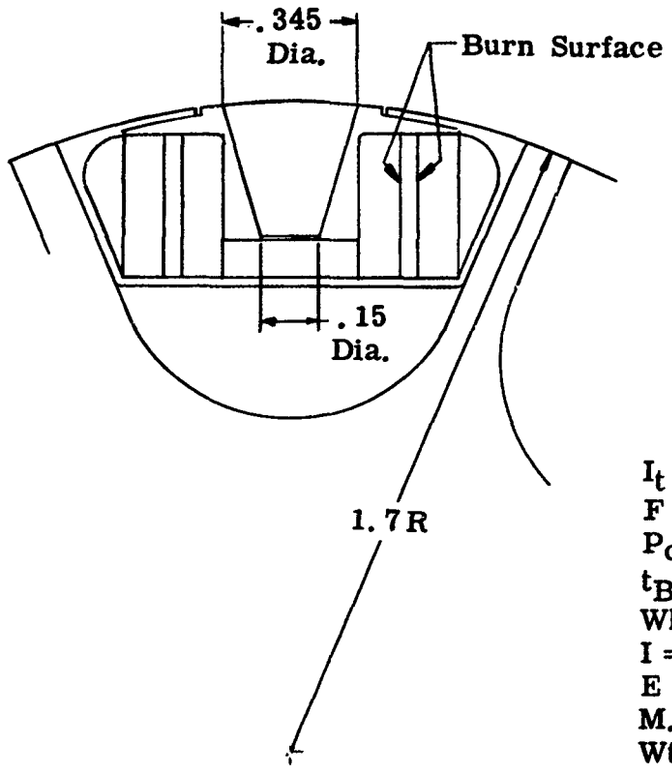


Figure 6. Star shaped grain. (U)



I_t = 2.5 lb/sec
F = 50 lb
P_c = 2000 psi
t_{Burn} = .050 sec.
Wheel Dia. = 3.40 in.
I = 4350 gr. cm^2
E = 5.3
M.R. = .598
Wt. = .01975 lb
Pkg. Vol. = .646 in^3

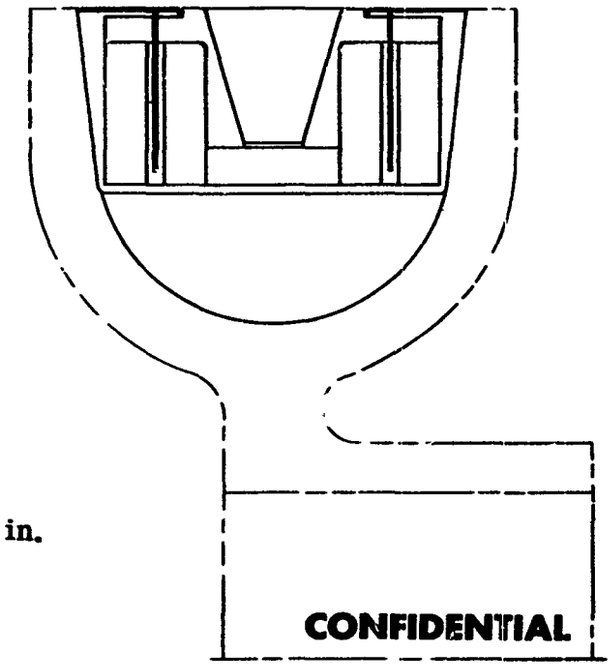


Figure 7. Concentric square grain. (U)

I_T = 2.5 lb/sec
F = 50
P_c = 2000 psi

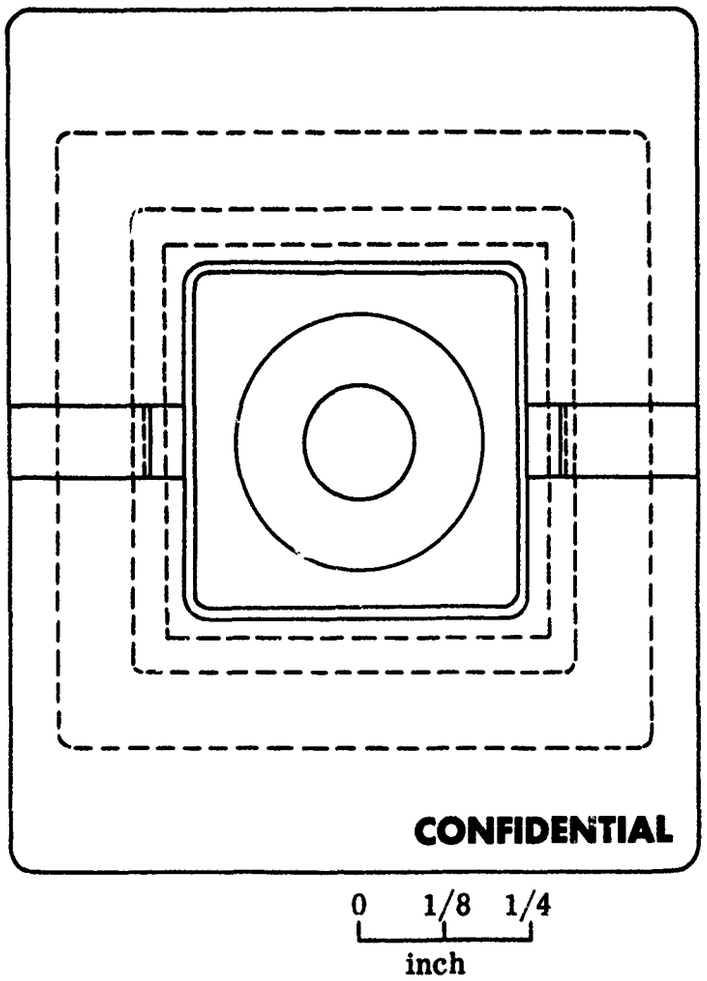


Figure 8. Concentric square grain. (U)

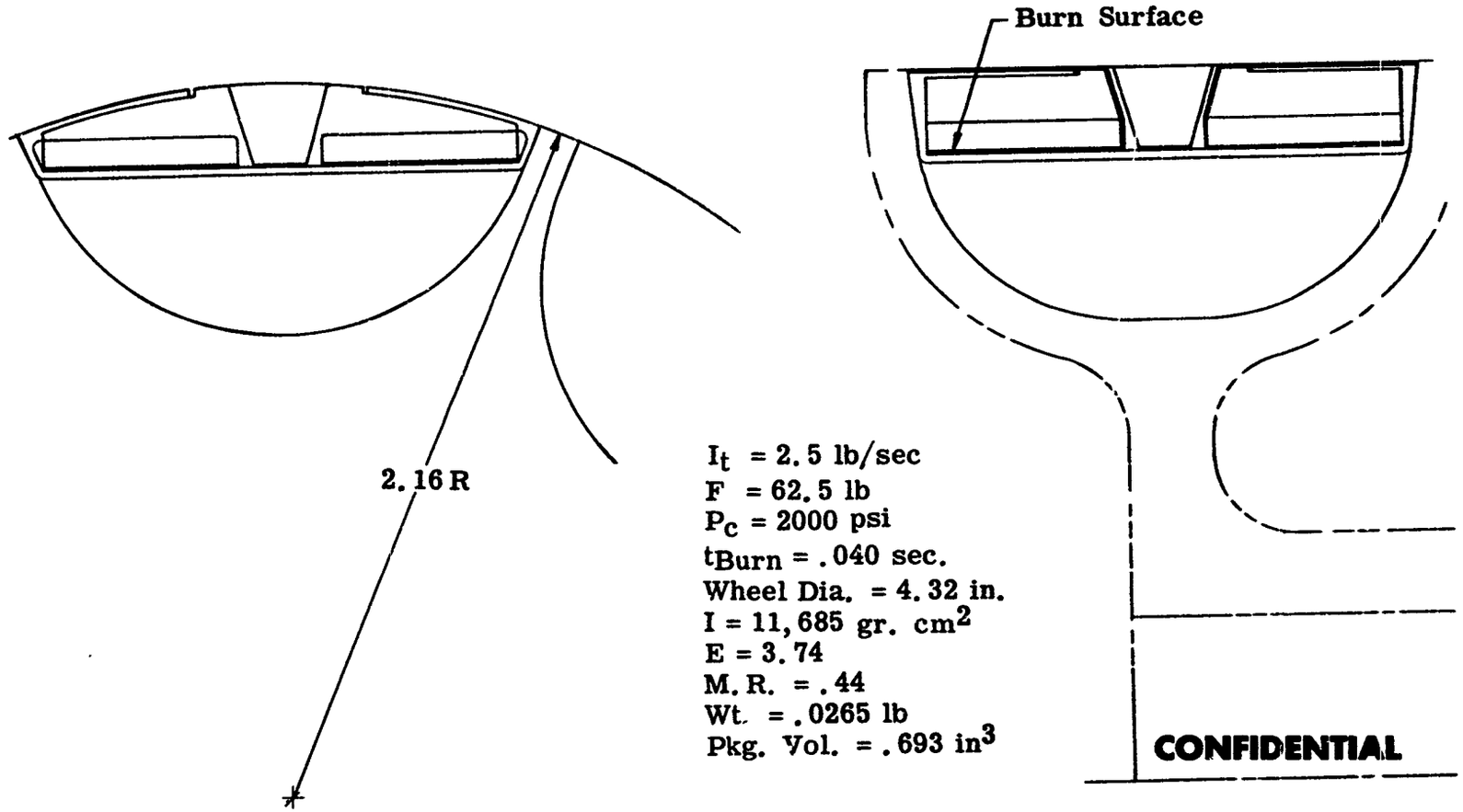


Figure 9. Single flat grain (a/b = 1.0). (U)

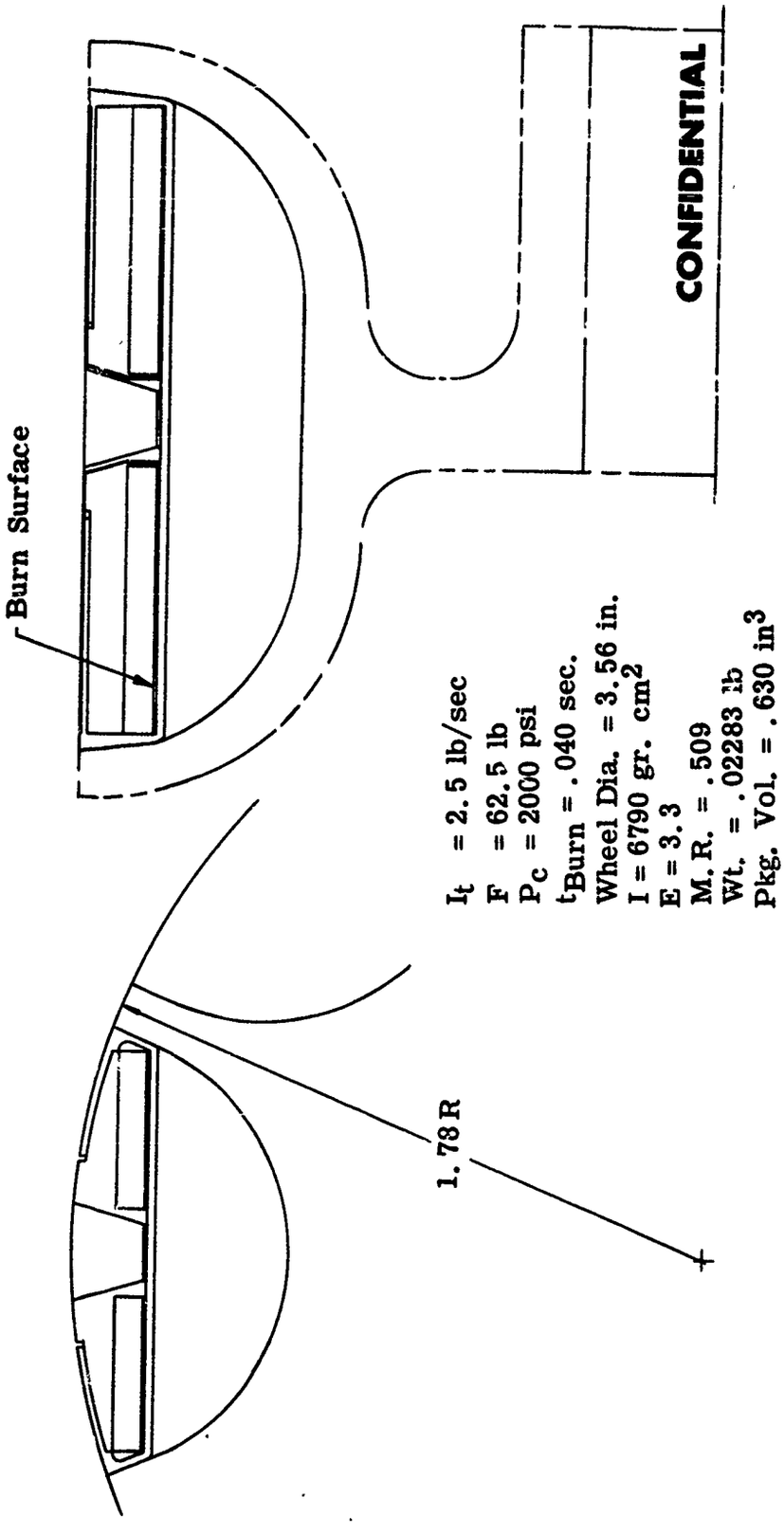
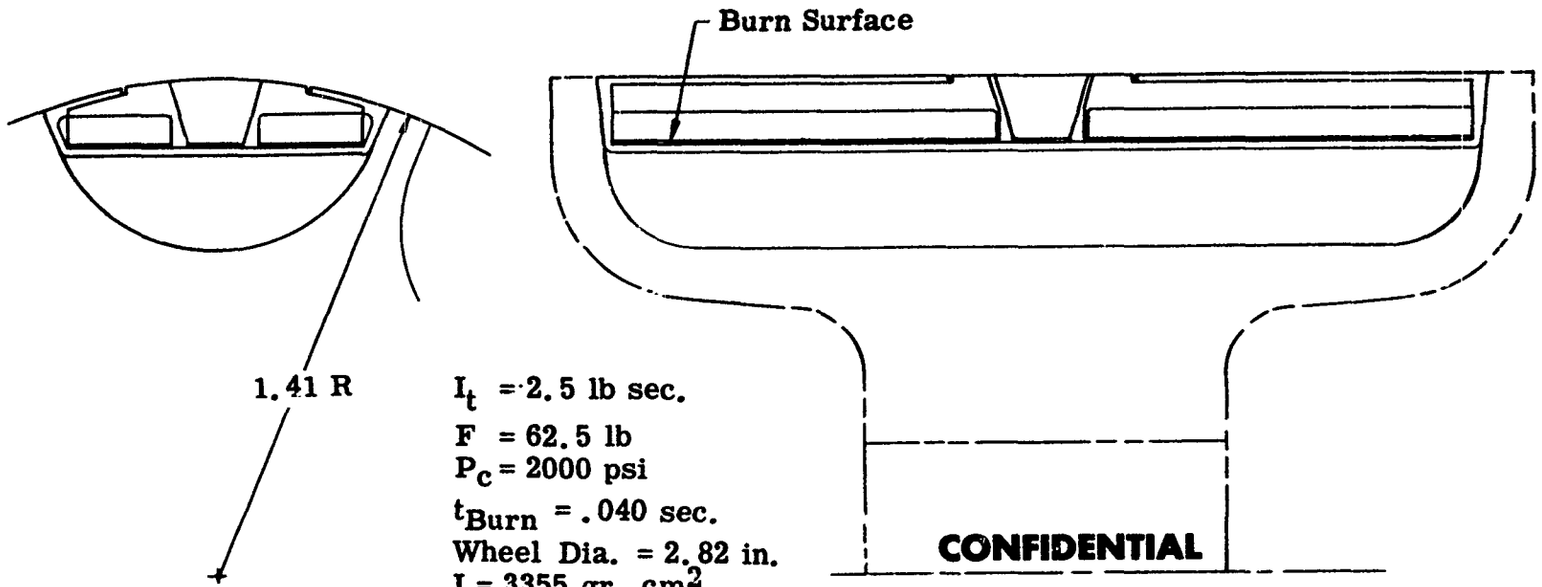


Figure 10. Single flat grain (a/b = 1.58). (U)



I_t = 2.5 lb sec.
F = 62.5 lb
P_c = 2000 psi
t_{Burn} = .040 sec.
Wheel Dia. = 2.82 in.
I = 3355 gr. cm^2
E = 3.0
M.R. = .531
Wt. = .02193 lb
Pkg. Vol. = .536 in^3

Figure 11. Single flat grain (a/b = 2.92). (U)

CONFIDENTIAL

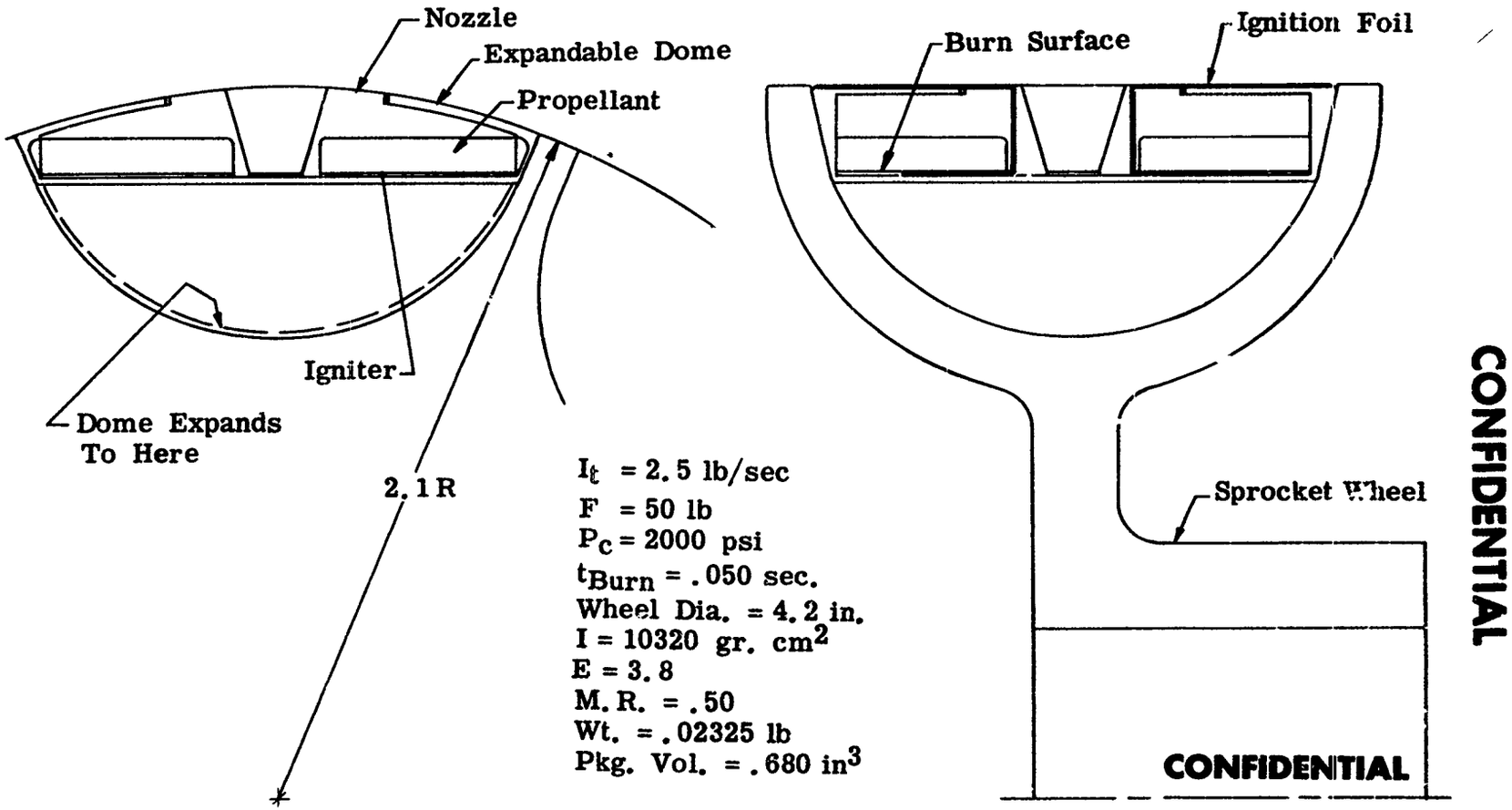


Figure 12. Single flat grain (a/b = 1.0). (U)

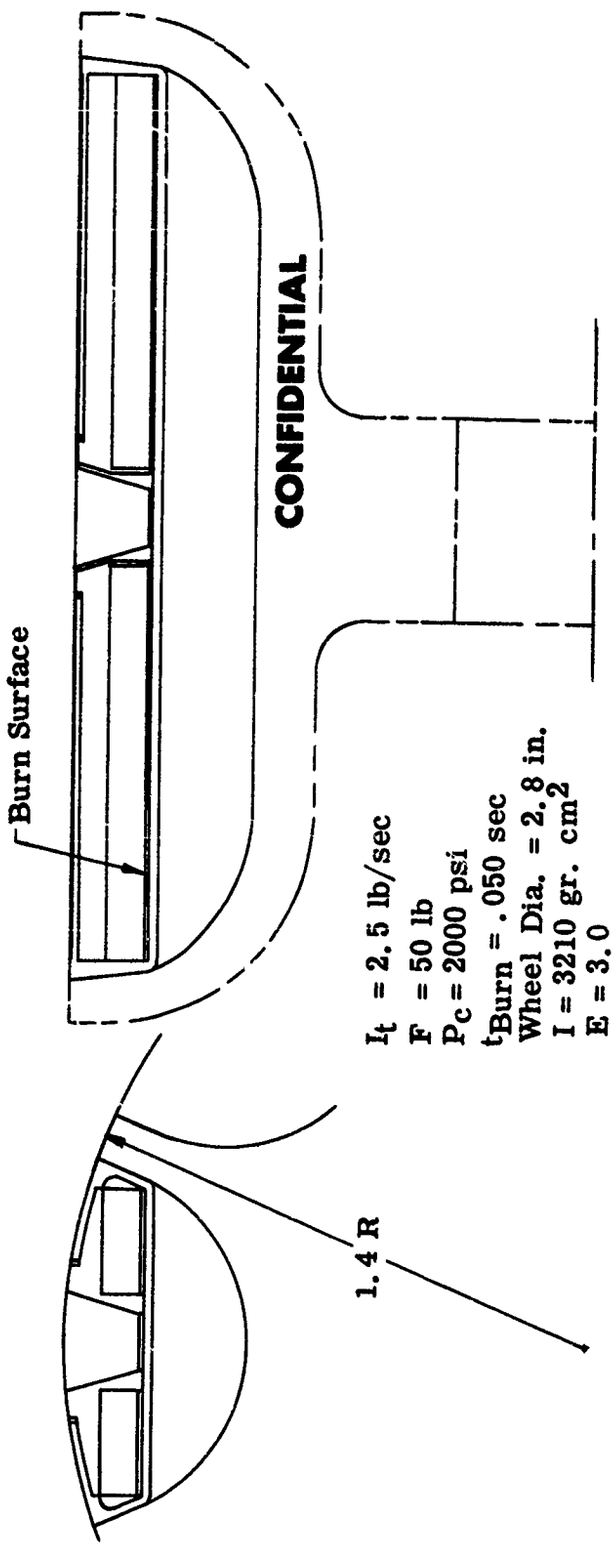


Figure 13. Single flat grain (a/b = 2.89). (U)

Figure 14. Single flat grain (a/b = 2.0). (U)

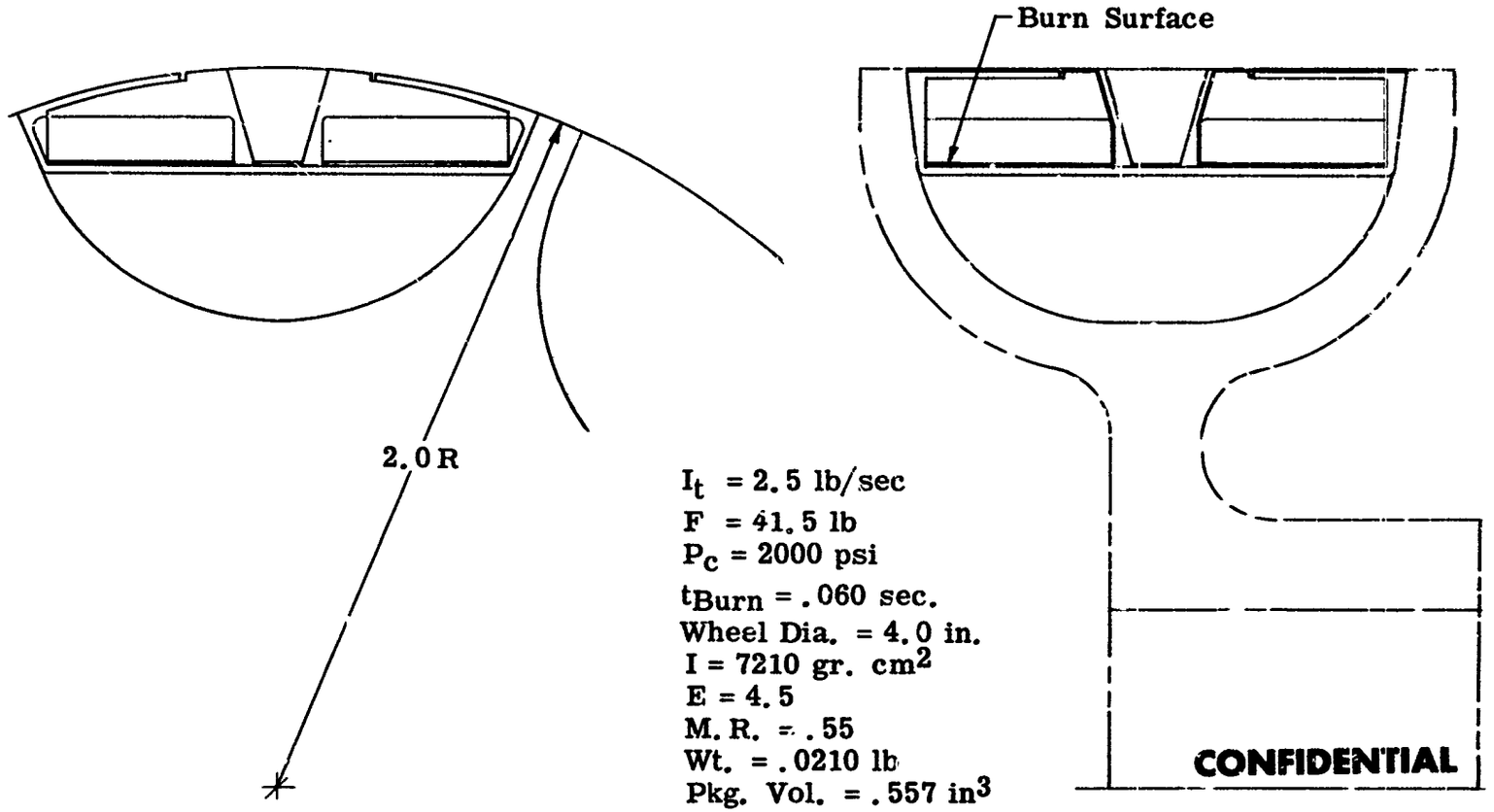
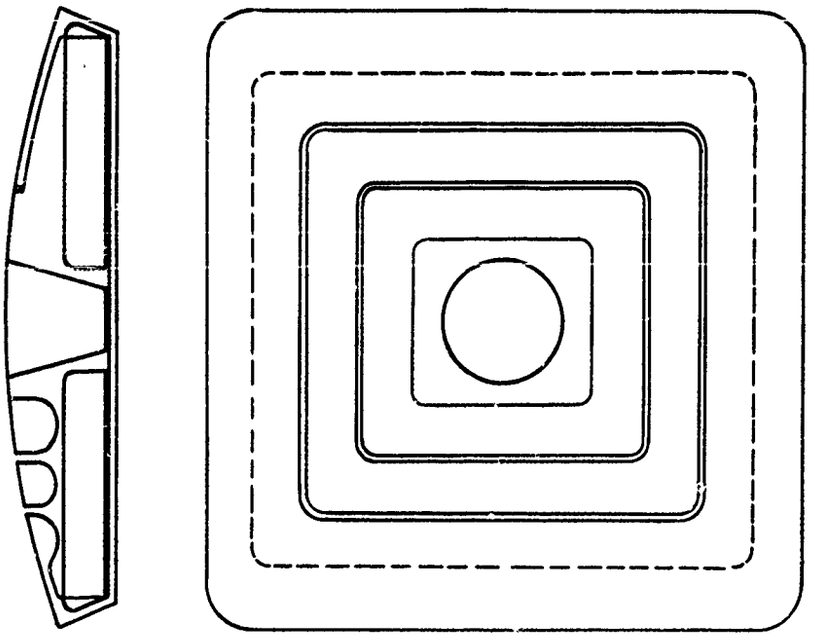
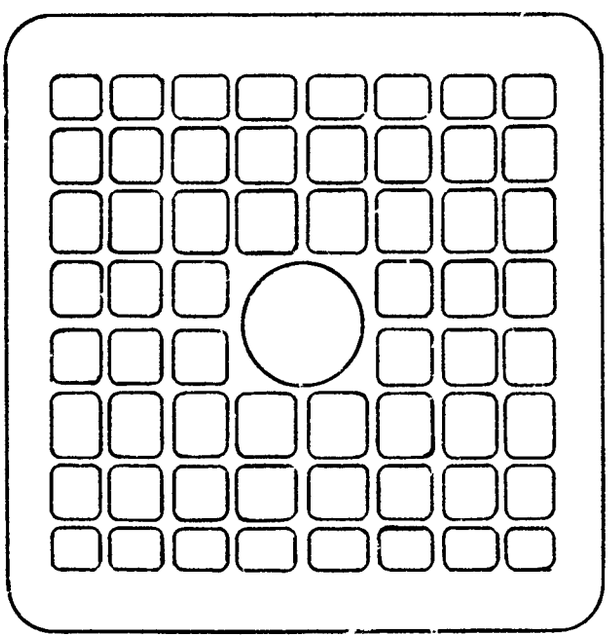


Figure 15. Single flat grain (a/b = 1.0). (U)

Figure 16. Single flat grain (a/b = 2.3). (U)



Ribbed Base



Waffle Base

Figure 17. Nozzle-base weight reduction. (U)

(This page is unclassified)

Table 1. Summary of basic rocket motor configurations. (U)

Design	Burn Time (sec.)	Fig. No.	Grain Shape	E Exh. Nos. Exp. Ratio	Capsule M.R. (Maximum)	I (18 Capsules Included) (GR. CM.^{2})	Motor Weight (For Max. CPS) (Lbs.)	Motor Weight (For 10 CPS) (Lbs.)	M.R. (Without Containers) Max. CPS	M.R. (Without Containers) 10 CPS	Capsule Weight (Lbs.)	Capsule Package Volume (In.^{3})	Remarks	
Single Square Grain	0.05	3-4	sq.	5.4	0.60	3700	6.5 11 CPS	1.06	.447	.567	0.0194	0.588	Igniter might cause Dislocation of Grain During Faulty Ignition	
Star Shaped Grain	0.05	5-6	sq.	7.1	0.545	5565	13 11 CPS	3	.338	.476	0.02137	0.710	Same as No. 1 But less Severe	
Concentric Square Grain	0.05	7-8	sq.	5.3	0.589	4350	6.5 11 CPS	3	.460	.510	0.01975	0.646	Disadvantage of Having a Double Grain Assembly	
Single Grain	0.04 F = 62.5 lbs.	9	sq.	3.74	0.440	11685		3		.395	0.0265	0.693		Best Assembly No Dislocation of Grain During Ignition
		10	Rectang. ($\frac{a}{b}$ = 1.58)	3.3	0.509	6790	13 13 CPS	3	.324	.450	0.02283	0.630		
		11	Rectang. ($\frac{a}{b}$ = 2.92)	3.0	0.531	3355	3 12.5 CPS	1.06	.464	.505	0.02193	0.536	$\frac{a}{b}$ too high Poor Config.	
	0.05 F = 50 lbs.	12	sq.	3.8	0.50	10320		3		.442	0.02325	0.680		
		13	Rectang. ($\frac{a}{b}$ = 2.89)	3.0	0.556	3210	3 11 CPS	1.06	.484	.527	0.02094	0 548	$\frac{a}{b}$ too high Poor Config.	
		14	Rectang. ($\frac{a}{b}$ = 2.0)	3.45	0.545	4450	6.5 11 CPS	3	.417	.480	0.0213	0.620		
	0.06 F = 41.5 lbs.	15	sq.	4.5	0.550	7210		13		.350	0.0210	0.557		
		16	Rectang. ($\frac{a}{b}$ = 2.03)	4.2	0.580	3845		6.5		.436	0.0201	0.542		
							No Value Means 10 CPS 15 Max. CPS		1 Pulser 1000 Capsules			Package Vol. Includes Empty Space Between Capsules		

CONFIDENTIAL

(U) Because of its simple configuration a more detailed analysis was made of the single flat grain. Figure 18 shows the variation in capsule mass ratio as grain proportions and burn times are changed. The capsule mass ratio calculations (propellant weight/total capsule weight) included all the components of the capsule (nozzle base, E dome, igniter wire and spray, gold ignition leads, propellant and inhibitor).

(C) The following assumptions, conditions and ground rules were used for the optimization study.

- The sprocket wheel diameter is proportional to the pitch length of the capsule. Increasing this dimension on the capsule, of course, results in a larger wheel diameter and greater wheel inertia.

- An eight position sprocket wheel was used to allow for multi-directional firing. The weight of the stepping motor depends on the available stepping time and the inertia of the sprocket wheel.

- The available stepping time was determined using the following equation:
  Available Stepping Time = $\frac{1}{\text{cps}}$ - Burntime - .015 sec for Ignition and Tail Off.
  For example, with a .05 sec burn time and a 10 cps cyclic rate the available stepping time is .035 seconds.
  For these conditions and an inertia of 10,320 gm-cm^2, an electric motor weighing 3.0 lb is suitable. With this configuration 10 cps is the maximum rate since no motors are available with reasonable weights which could step in less than .035 seconds.

- Mass ratio, expansion ratio, burn time and grain configuration are all interrelated. For example, with the single flat grain shown in Figure 12 a thin flat configuration

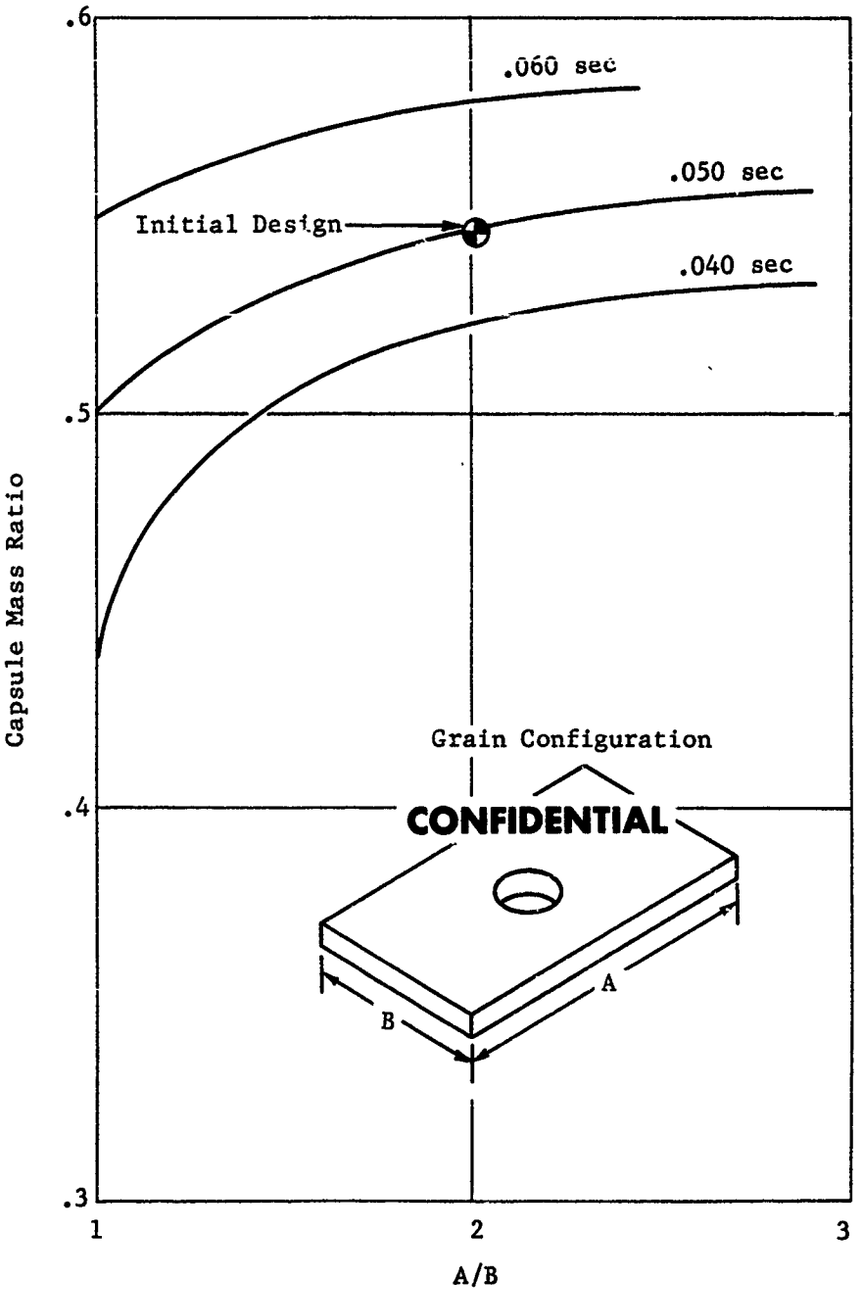


Figure 18. Single flat grain, capsule mass ratio versus capsule proportions. (U)

(C) with a large burn area is needed to meet a .05 second burn time and results in a small expansion ratio and low mass ratio. Past studies have shown the cubic configuration to be most efficient from a packaging standpoint.

- The system mass ratio was calculated using the following equation. No storage container was included since its configuration can vary considerably based on the application.

$$\text{System MR} = \frac{\text{Weight of 1000 grains}}{\text{Weight of 1000 capsules + 1 pulser}}$$

- Package volume was determined by multiplying the height by the spacing by the width of the capsules.

(U) From the studies performed, it was concluded that it is most desirable to keep the inertia of the sprocket wheel to a minimum and thus make use of a lighter stepping motor. Inertia can be reduced using single flat rectangular grains (Figures 13 and 14) rather than single flat square grains. When the rectangular configuration becomes too long (Figures 11 and 13) other problems arise in supporting a long capsule during firing.

(U) Another alternate would be to consider less reliable configurations such as Figures 3, 5 and 7 where the major problem is the location of the igniter. Faulty igniter operation could crack or dislodge the grain causing erratic burning of the propellant.

(U) After consideration of all these factors the single flat rectangular grain having a length twice its width (Figure 14) was selected as the optimum configuration for the capsule design.

2. Capsule Components

(C) a. Capsule (Rocket Motor)

The capsule-tape assembly is shown in Figures 19 and 20 while the size of the major capsule components is shown in Figure 21. The motor contains 4.8779 grams (.01075 lbs) of CWP-13 solid propellant and delivers a total impulse of 2.68 lb-sec at sea level with an overall

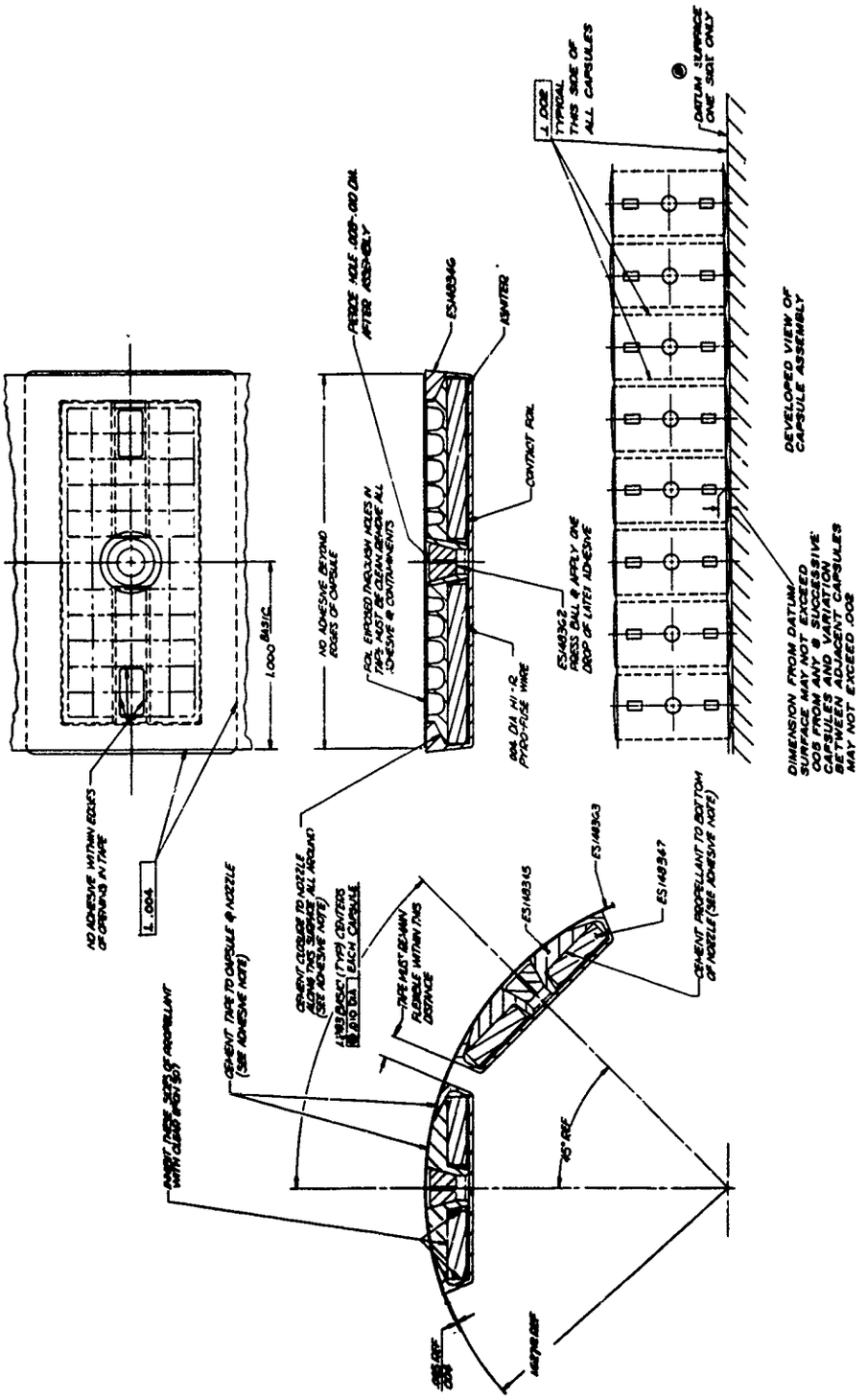


Figure 19. Capsule and tape assembly WSR-101. (U)

66-045

(This page is unclassified)

S - Surface Primed With DC4094 and Apply DC92018 Adhesive
P - Surface Applied With DC280 Press, Sensitive Adhesive
Adhesive - Prime With Dow Corning Silicone Primer 1200 or
Equivalent. Aerospace Sealant 92-018.

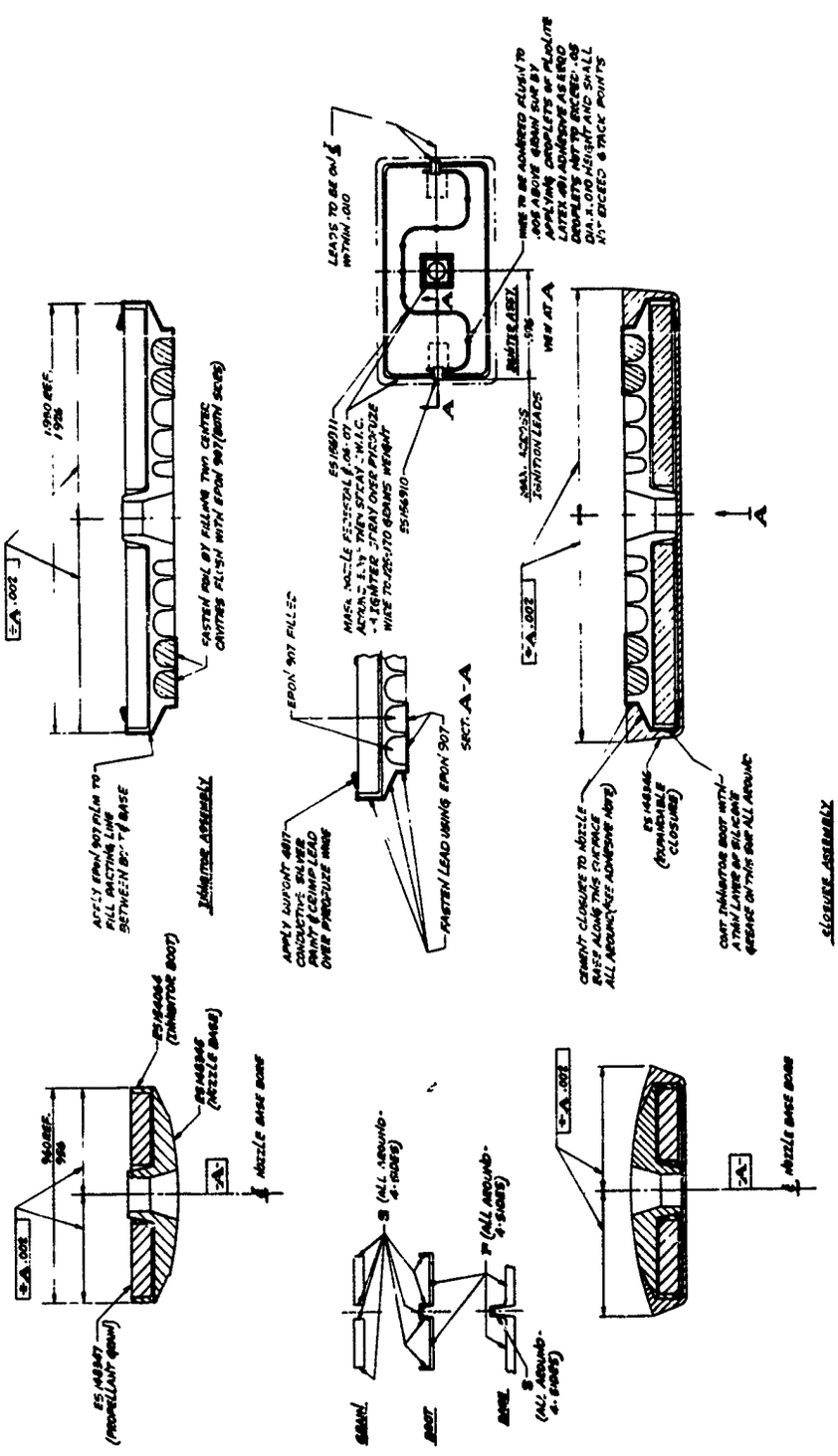


Figure 20. WSR-101 capsule assembly. (U)

20-700

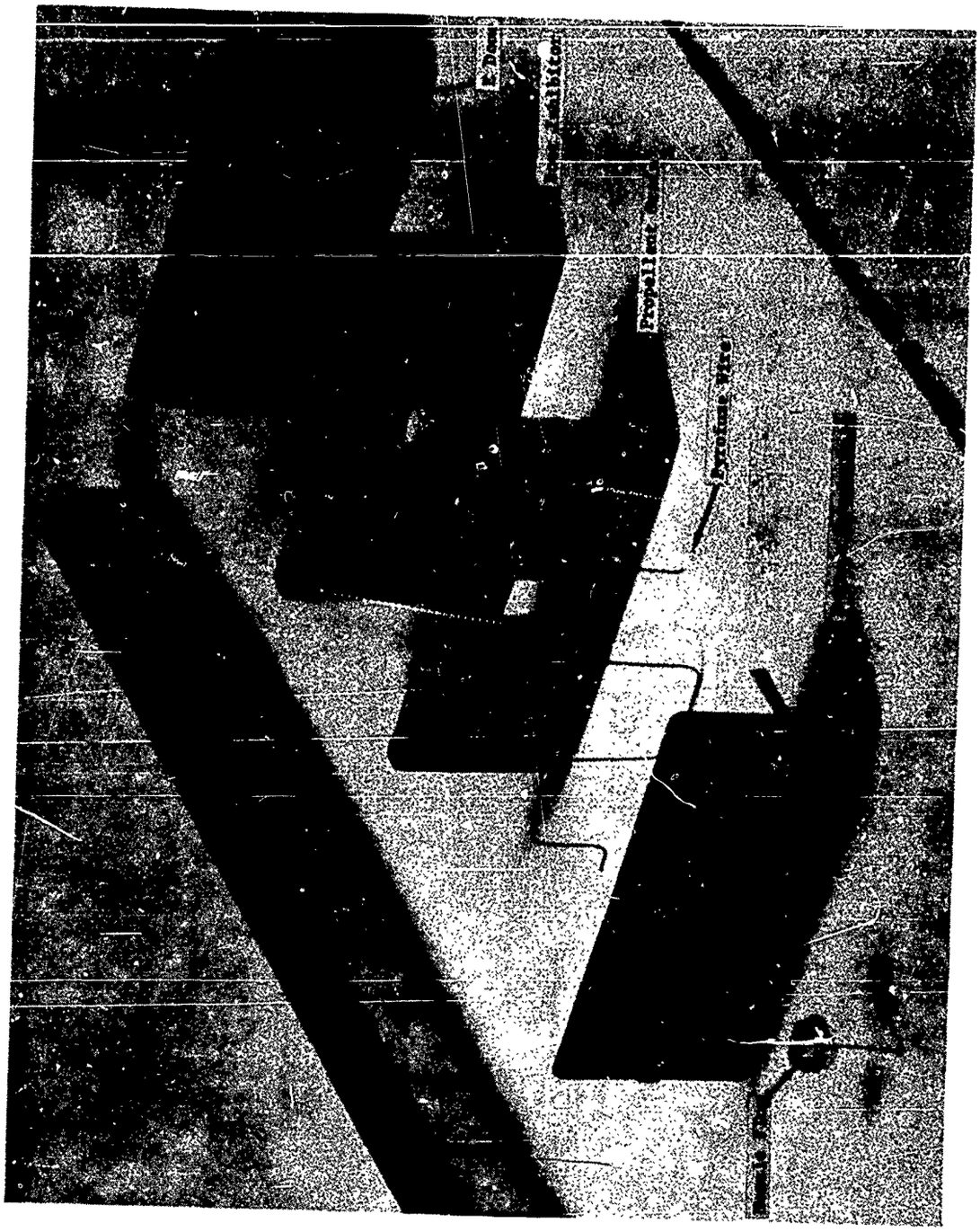


Figure 21. WSR-101 capsule component. (U)

(C) nozzle area ratio of 14:1 (including the nozzle block extension). The nozzle area ratio of the capsule is 2.31:1. Design chamber pressure is 2000 psia and the grain burn time is 46.8 milliseconds. A summary of the weights of the capsule and its components is presented in Table II.

(U) Design details including a stress summary are presented for the capsule components in the following paragraphs.

Nozzle Base

(U) The nozzle base, Figure 22, is a molded, quartz fiber-filled phenolic plastic FIBERITE MX 1344-50M. The high strength nozzle material is highly resistant to erosion. The nozzle base was designed as a waffle type structure to insure light weight while maintaining structural adequacy. Figure 23 shows the points of high stress in the nozzle base along with the stress mode, magnitude of the stress, and the margin of safety.

Expandable Closure

(U) The expandable closure, or E-dome, Figure 24, is used to contain all the rocket motor components within a sealed, minimum volume enclosure during storage and stepping. The closure material must also provide high elongation for a readily expandable case, good insulation properties, minimum char and ablation, and still retain sufficient flexibility to return to its unfired shape. The E-dome is made of Dow Corning Silastic 55 rubber having a minimum tensile strength of 1200 psi.

(U) The maximum shear stress on the adhesive joint between the E-dome and the nozzle base is 92 psi. This is based on a modulus of 400 psi and a maximum strain of 23%. Since the shear strength of the Aerospace 92018 sealant is 200 psi, the bond is considered adequate.

Propellant Grain and Inhibitor

(U) Based on the capsule optimization studies a flat neutral burning grain configuration was chosen. The grain shown in Figure 25 is punched from a slab of

Table II. Capsule component weight summary. (U)

Component	Weight - Grams
Nozzle Base	2.3364
E - Dome	2.0908
Grain	4.8779
Inhibitor	.3908
Nozzle Plug	.0234
Igniter	.1500
Ignition Foil	.0910
Tape	.3000
Misc. (Adhesives Etc.)	.8761
Total	11.1364 Gms.
	0.024556 Lbs.

Mat'l: Reinforced Phenolic Flexural
Strength Requirement: Approx 15,000 psi

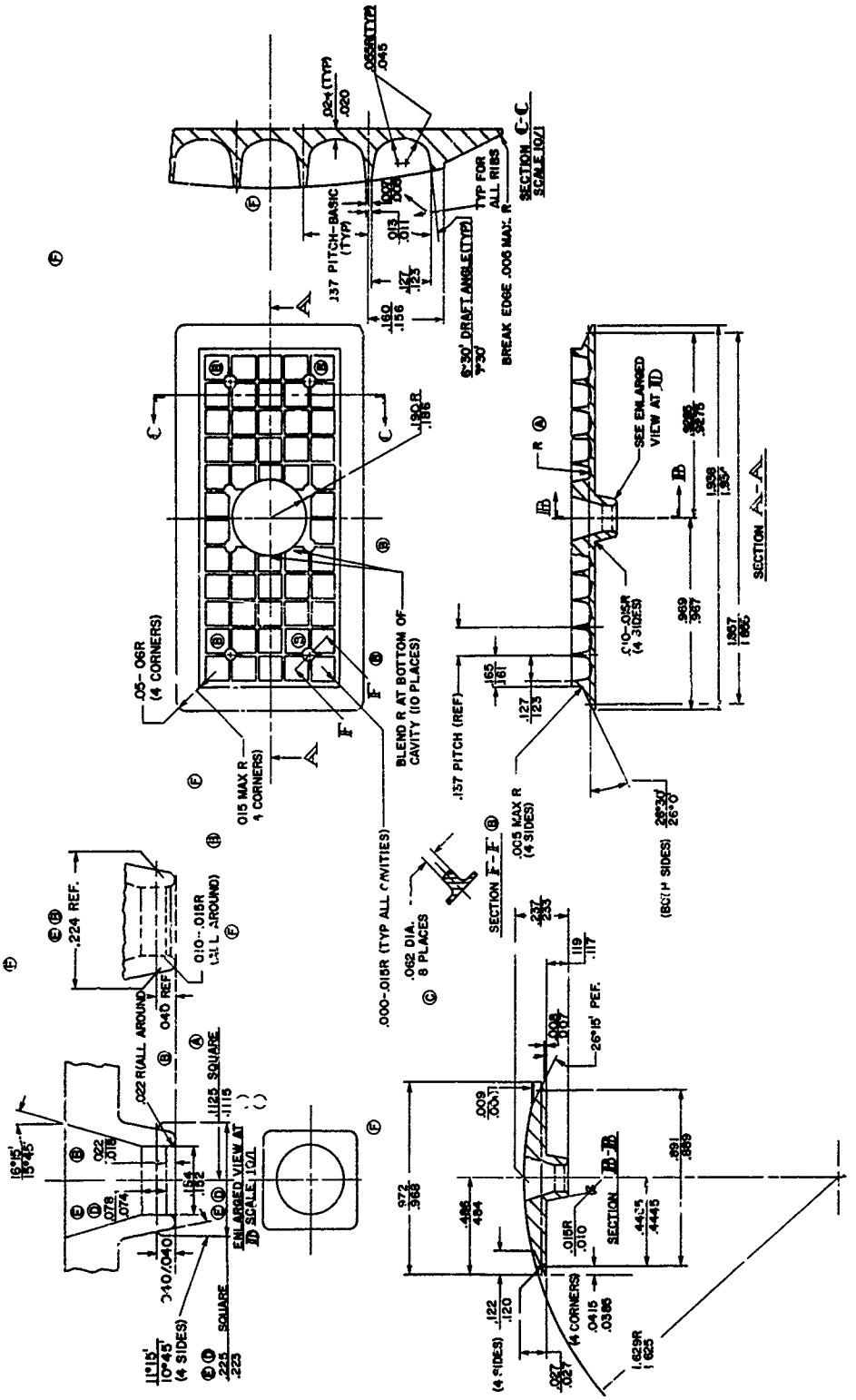
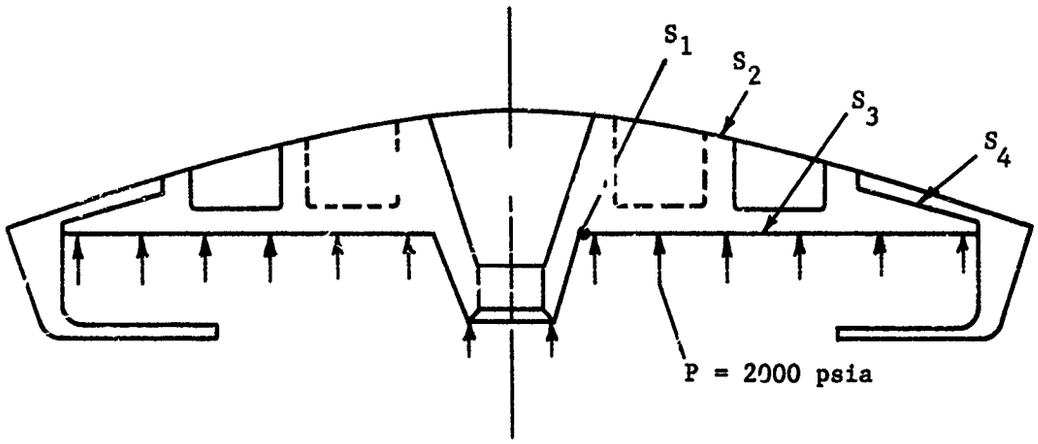


Figure 22. Nozzle base WSR-401, (U)



Point	Stress Mode	Stress Magnitude	Margin of Safety
S_1	Nozzle Shear Out	1180 psi	7.30
S_2	Nozzle Bearing	7300 psi	2.56
	Waffle Panel Bending	2090 psi	3.25
S_3	Adhesive Shear	92 psi	1.17
S_4			

Figure 23. Nozzle base stress summary. (U)

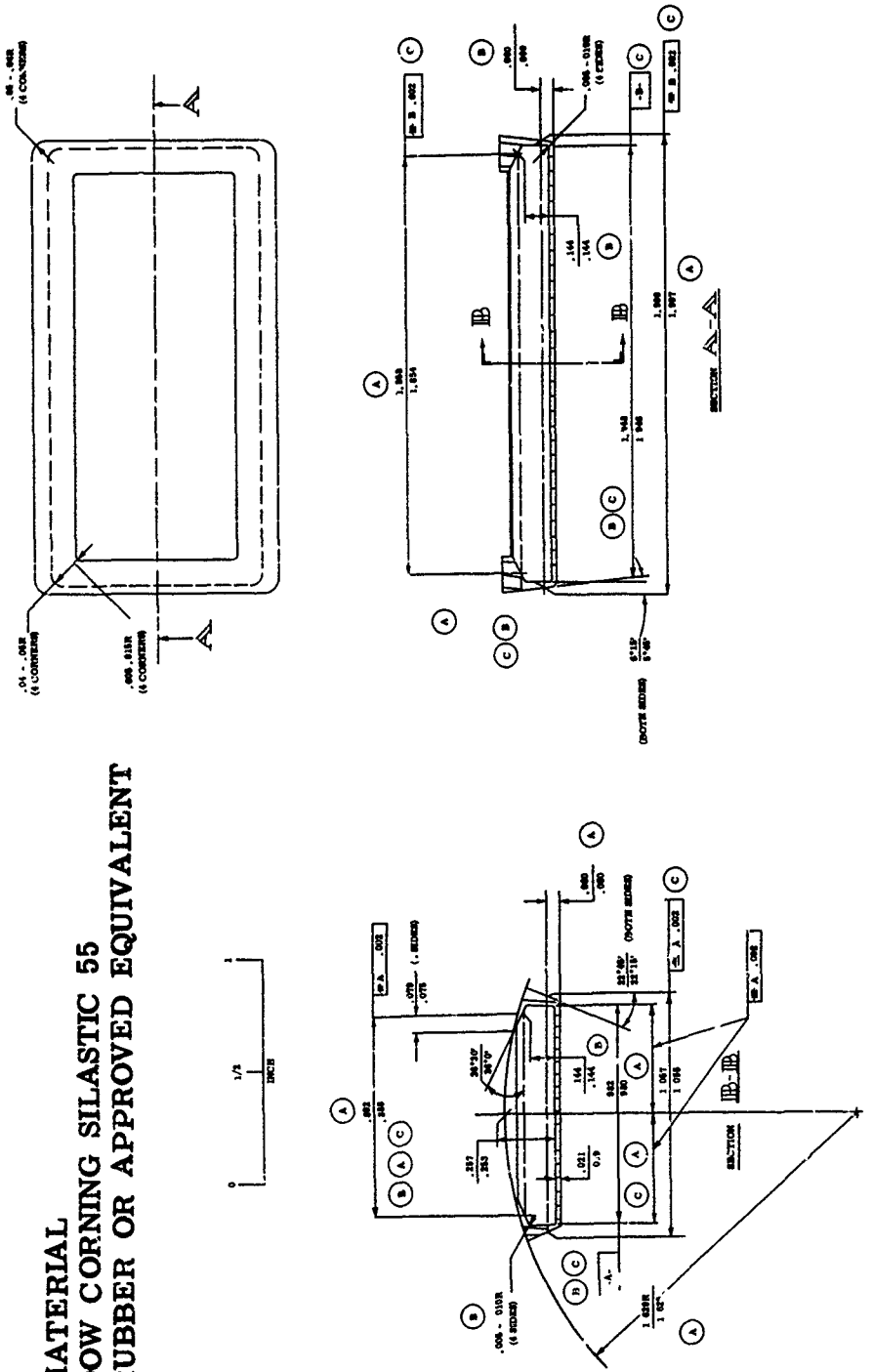


Figure 24. Expandable closure WSR-101. (U)

(This page is unclassified)

Weight = .0115 lbs Min. - .0118 lbs Max.
Material - CWP-13
ES-148347

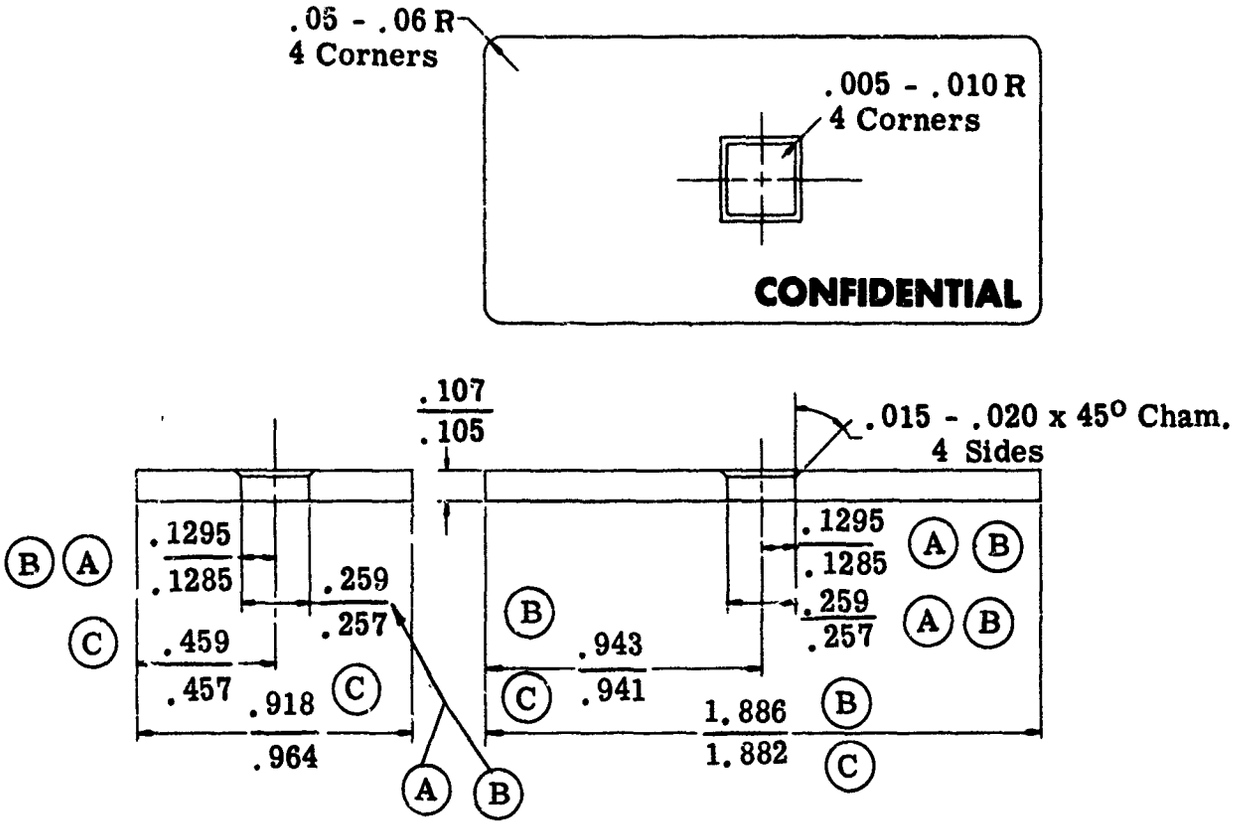


Figure 25. WSR-101 propellant grain. (U)

20-710

(U) CWP-13 propellant. This propellant has been characterized and qualified to be compatible with space environments. It meets the requirements for materials compatibility, impulse, burn rate, physical properties, and sensitivity.

(U) Initially, the inner and outer peripheries of the grain were coated with a 0.20 inch layer of EPON 828 to inhibit burning on these surfaces. The inhibited grain was then adhered to the nozzle base with EPON 828. However, this inhibitor proved to be inadequate during development firing tests. A new inhibitor was designed as shown in Figure 26. This inhibitor is a premolded unit of Gen Gard V-57 material which is adhered to the propellant grain using DC-280 and 92-048 adhesives. The subassembly is then bonded to the nozzle base. The boot inhibitor configuration has proven to be a superior design as shown by the test results and in addition has simplified the assembly procedure.

(U) Nozzle Plug

The nozzle plug, Figure 27, is a small urethane foam ball inserted into the nozzle and bonded in place with Aerospace sealant 92018 adhesive. A 0.010 inch diameter hole is pierced through the closure after it has been bonded in place. The plug enables case pressure to increase quickly in the capsule thus reducing ignition delay. The hole in the plug also permits the internal and external pressure to equalize as external conditions vary, thus preventing premature expansion of the dome during altitude changes (booster rocket operation).

(U) Tape

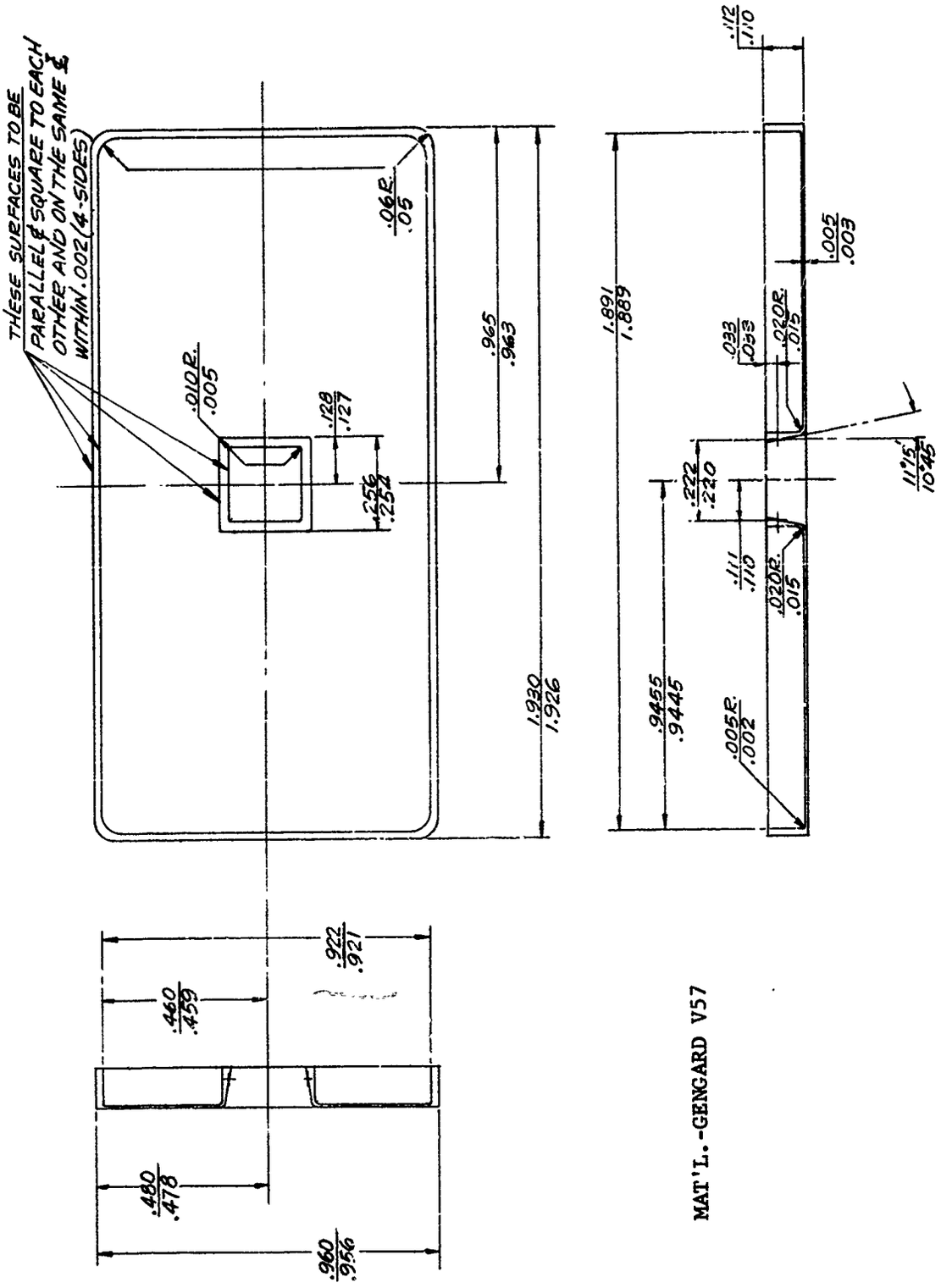
The individual motors are bonded to the teflon coated glass tape, Figure 28, with an Aerospace sealant 92018 adhesive. The tape has high strength and good flexibility. The cutouts in the tape are provided for the nozzle and the two contact foils. Close tolerances on these cutouts were maintained to insure repeatibility from section to section and to maintain pitch accuracy.

(U) Ignition Leads

Two NEYORO G ignition leads were originally molded into the nozzle base. The thin foils extended down the length of the nozzle through the base surface and were bonded to the waffle surface of the base. During static firing tests, a structural problem developed in the area of the exhaust nozzle and the ignition lead. An investigation showed that the gold lead was not being properly positioned by the molding die. This resulted in exposure of the gold lead or the thinning down of the nozzle material. During firing, this section would break out causing a blockage of the nozzle and a resultant failure of the capsule. A revised ignition lead contact configuration was designed which placed the foils at the ends of the capsule (Figure 20) and removed them from the nozzle area completely.

(U) Igniter Assembly

The igniter sub-assembly consists of a preformed length of 0.004 inch diameter Hi-R pyrofuze wire (Figure 29), spot bonded to the propellant grain surface with Pliolite latex 491 adhesive. The wire ends are attached to the ignition leads at the ends of the nozzle base (Figure 20). A pyrotechnic igniter material (CWIC-8) is sprayed onto the propellant grain as shown in Figure 20 and is cured in a vacuum oven to remove any volatile materials.



MAT'L.-GENGARD V57

Figure 26. Boot inhibitor. (U)

Mat'l: Koppers Co. Inc., Pittsburg, Pa. Dylite F40. Expand At 225°F For Approx. 10 Minutes. Screen To Obtain .192 to .198 Beadsize. If Needed, Use Optional Molding Method.

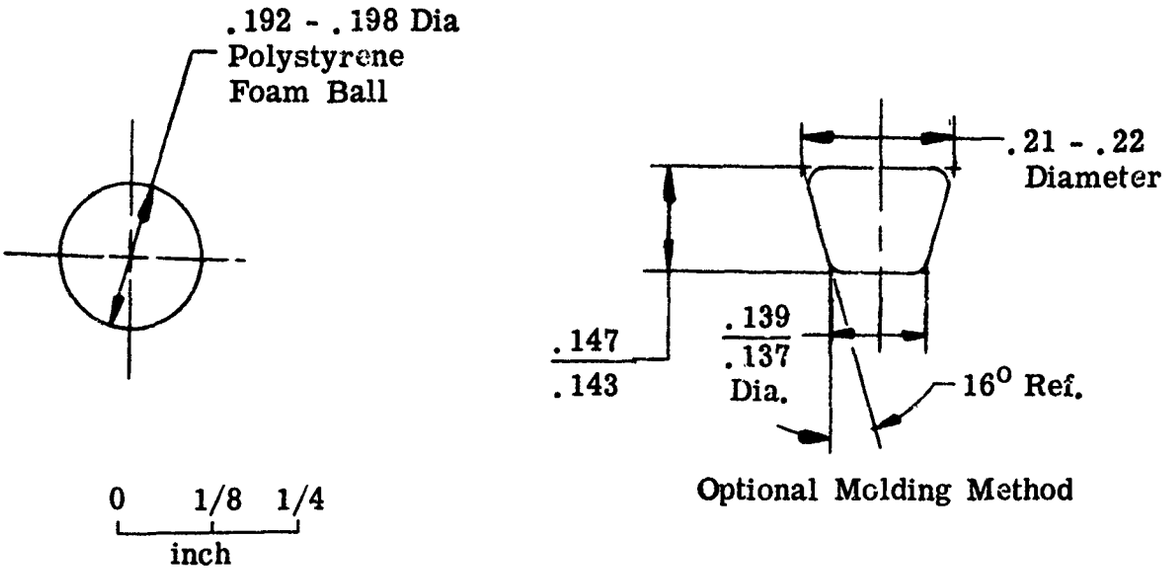


Figure 27. WSR-101 nozzle plug. (U)

Mat'l: Teflon Coated Fiberglass TB-3E
Length of Tape: As Required
No Fraying at Edges or In Holes of Tape
ES148363

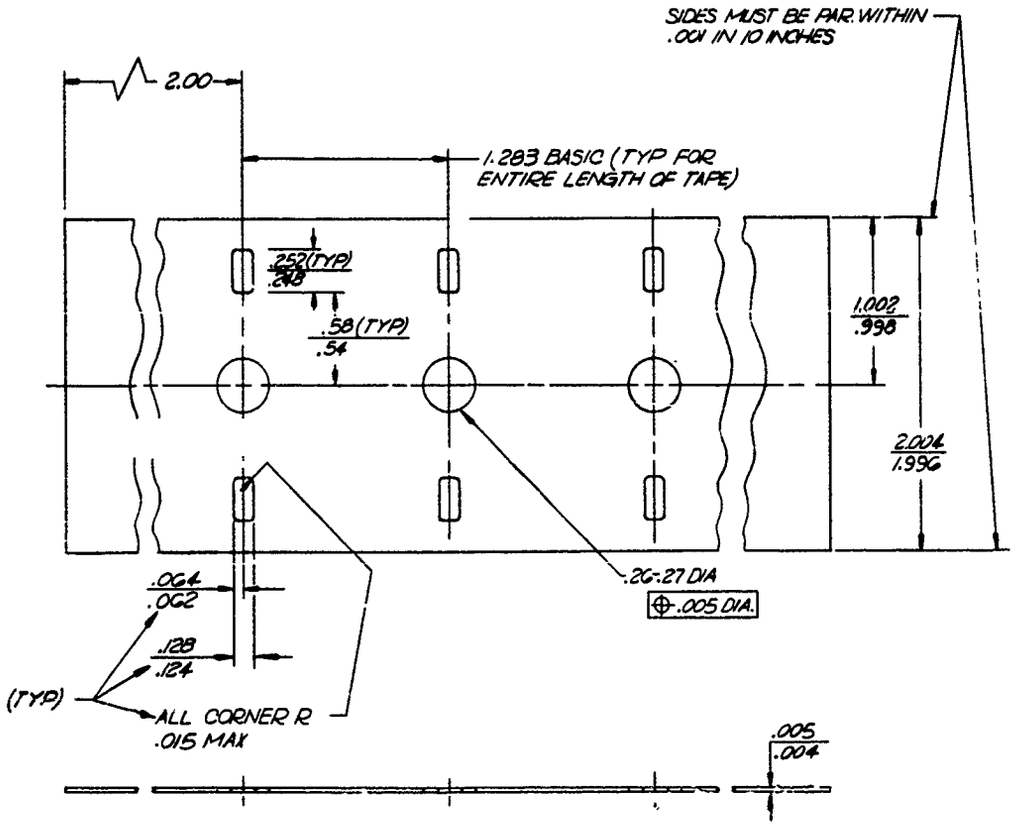


Figure 28. Tape WSR-101. (U)

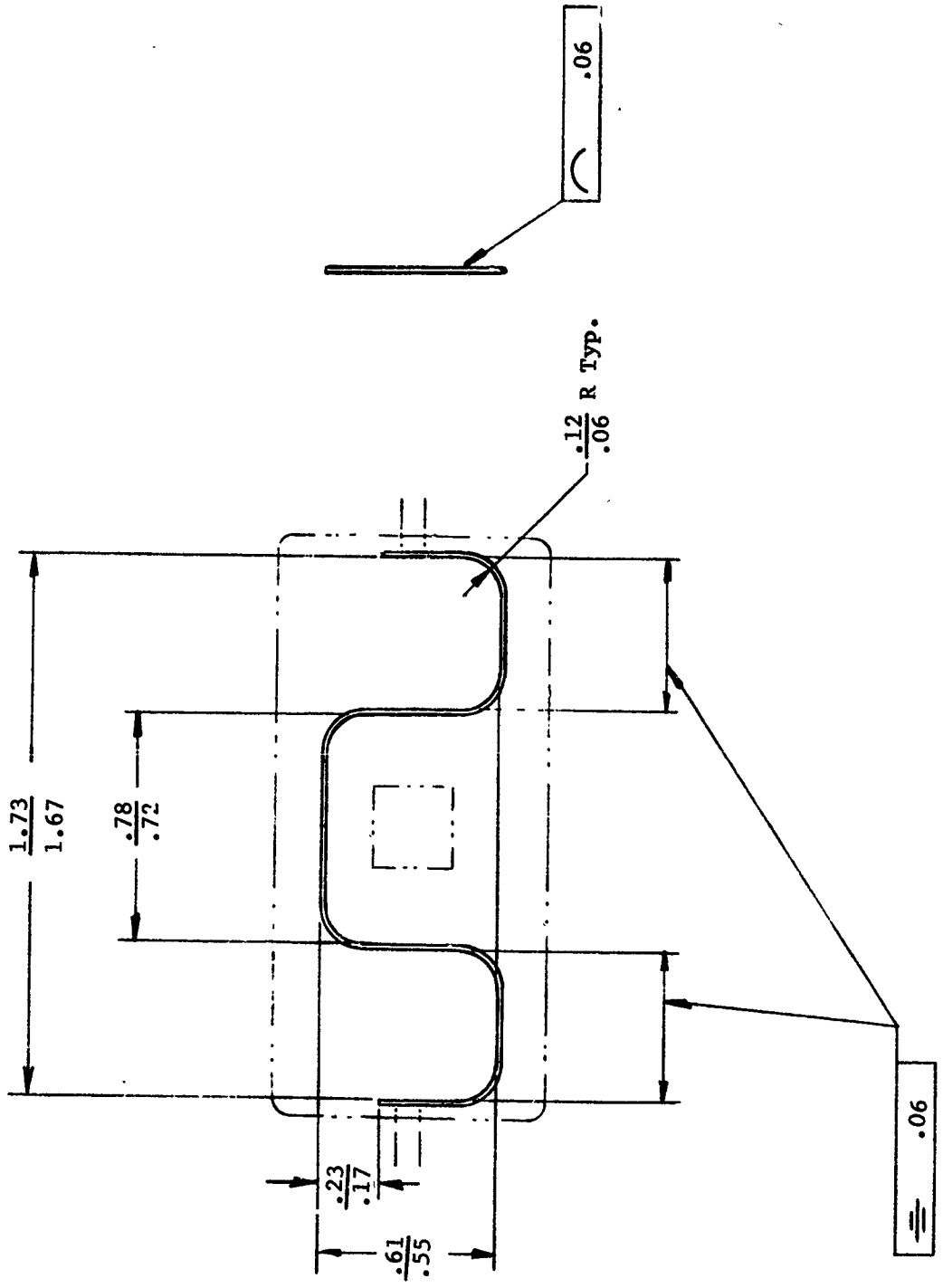


Figure 29. Igniter wire. (U)

66-047

(U) 3. Pulser Housing Assembly

The design of the pulser housing assembly was conducted in two phases. The original design was based on an aluminum housing and a front cover plate made of stainless steel. The front cover provided a cantilevered shaft for the sprocket wheel, however, tests showed that excessive deflections of the shaft were encountered when the sprocket wheel was under load. This caused an additional gap between the wheel and housing and resulted in capsule failures during firing. A design modification eliminated the cantilevered shaft. Additional tests uncovered the fact that the aluminum housing was inadequate for repetitive firings.

(U) A second design phase was initiated and a stainless steel prototype configuration evolved. This configuration, with some minor modifications made during test, met the requirements of the program. Weight summaries for both configurations are presented in Tables III and IV.

a. Initial Pulser Configuration

Sprocket Wheel

(U) The sprocket wheel, Figure 30, is one of the major components of the WSR-101 pulser assembly and considerable effort was expended towards its design. The sprocket wheel is made of Titanium 6AL4V alloy heat treated to 170,000 psi yield strength.

(U) The E-dome capsule requires close support by the sprocket wheel. On the other hand, feeding of the tape without jamming of the capsules under the worst possible tolerance condition requires an allowance for clearance. This necessitated a detailed tolerance study incorporating the manufacturing tolerances encountered in past designs. Cavity dimensions were established to provide the following range of overall clearances between capsule and cavity walls.

Capsule Short Length Clearance	0.014 to 0.020 in
Capsule Long Length Clearance	0.020 to 0.028 in

Table III. WSR-101 initial pulser component weight summary. (U)

Component	Weight
Housing	1.383 lb.
Sprocket Wheel	.900
Nozzle Block (3)	.840
Front Cover	1.090
Adapter Plate	.424
Reduction Gear	.100
Seal	.007
Needle Bearing	.251
Thrust Bearing	.030
Bearing Spacer Ring	.018
Ignition Assembly	.109
Stepping Motor	3.180
Chute Assembly	2.830
Misc. (Screws and Pins)	.047
TOTAL	11.209 lb.

Table IV. WSR-101 prototype pulser component weight summary. (U)

Component	Weight
Housing	2.57 lb.
Sprocket Wheel	.90
Front Cover	1.13
Adapter Plate	.30
Reduction Gear	.10
Taper Bearing (2)	.22
Bearing Spacer	.02
Ignition Assembly	.11
Shaft	.26
Stepping Motor	3.18
Chute Assembly	1.01
Misc. (Screws)	.05
TOTAL	9.83 lb.

(2) Heat treat per AMS 4967, sec 6:1 heat to 1750°F ±25°. Hold for 1-2 hr. quench in agitated water, heat to 1000°F ±15° hold for 4-8 hr. and aircool. Hardness R_C 43 minimum teflon coat .0005-.001 thick all sur marked per AMS 2515.
Dim. locating true pos. holes are basic.
All dimensions apply after coating.
Break sharp edges .01 maximum and blend.

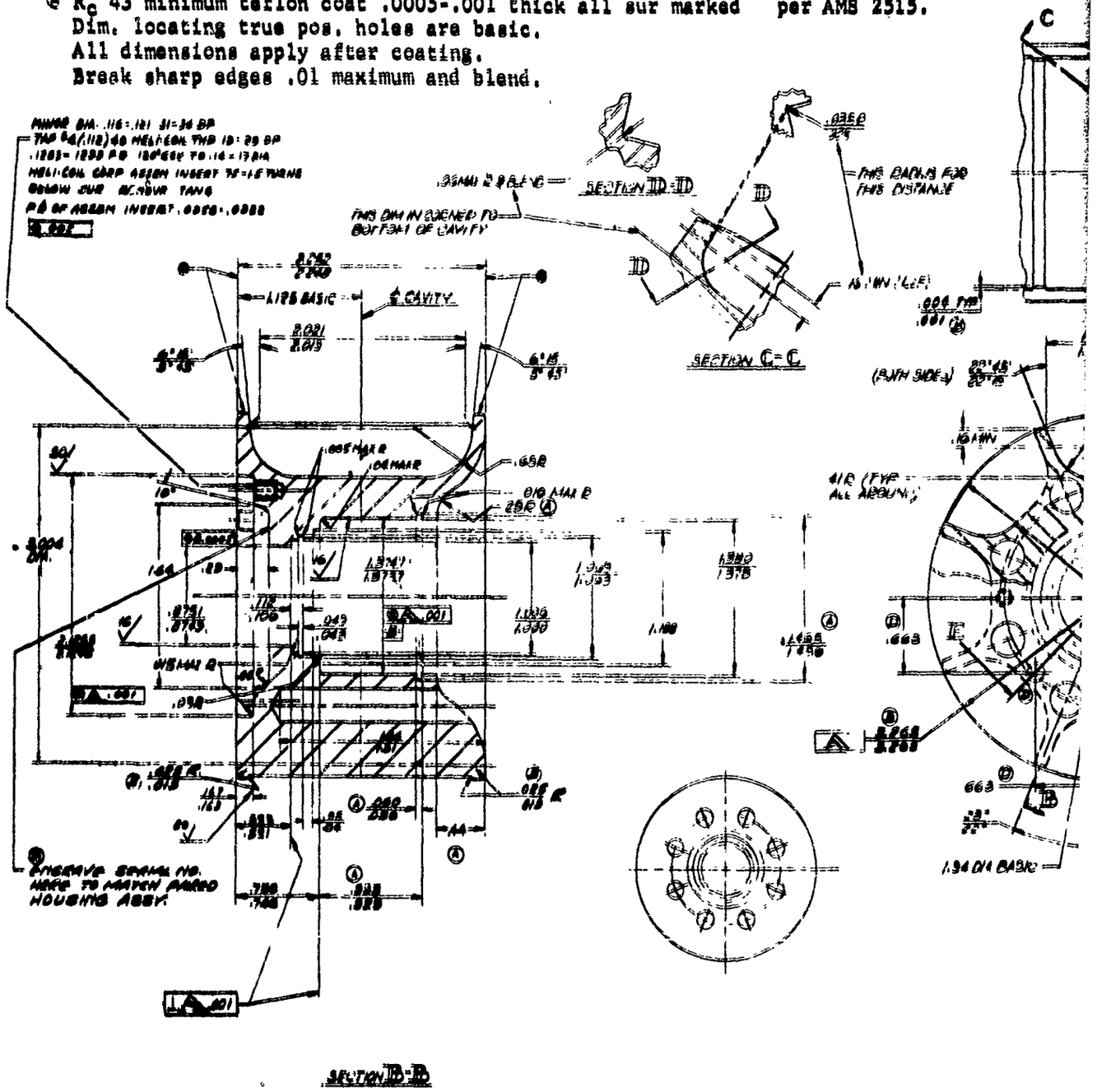


Figure 30. WSR-101 sprocket wheel.

at to 1750°F ±25°. Hold for 1-2 hr. quench
150 hold for 4-8 hr. and aircool. Hardness
l thick all sur marked per AMS 2515.
asic.

lend.

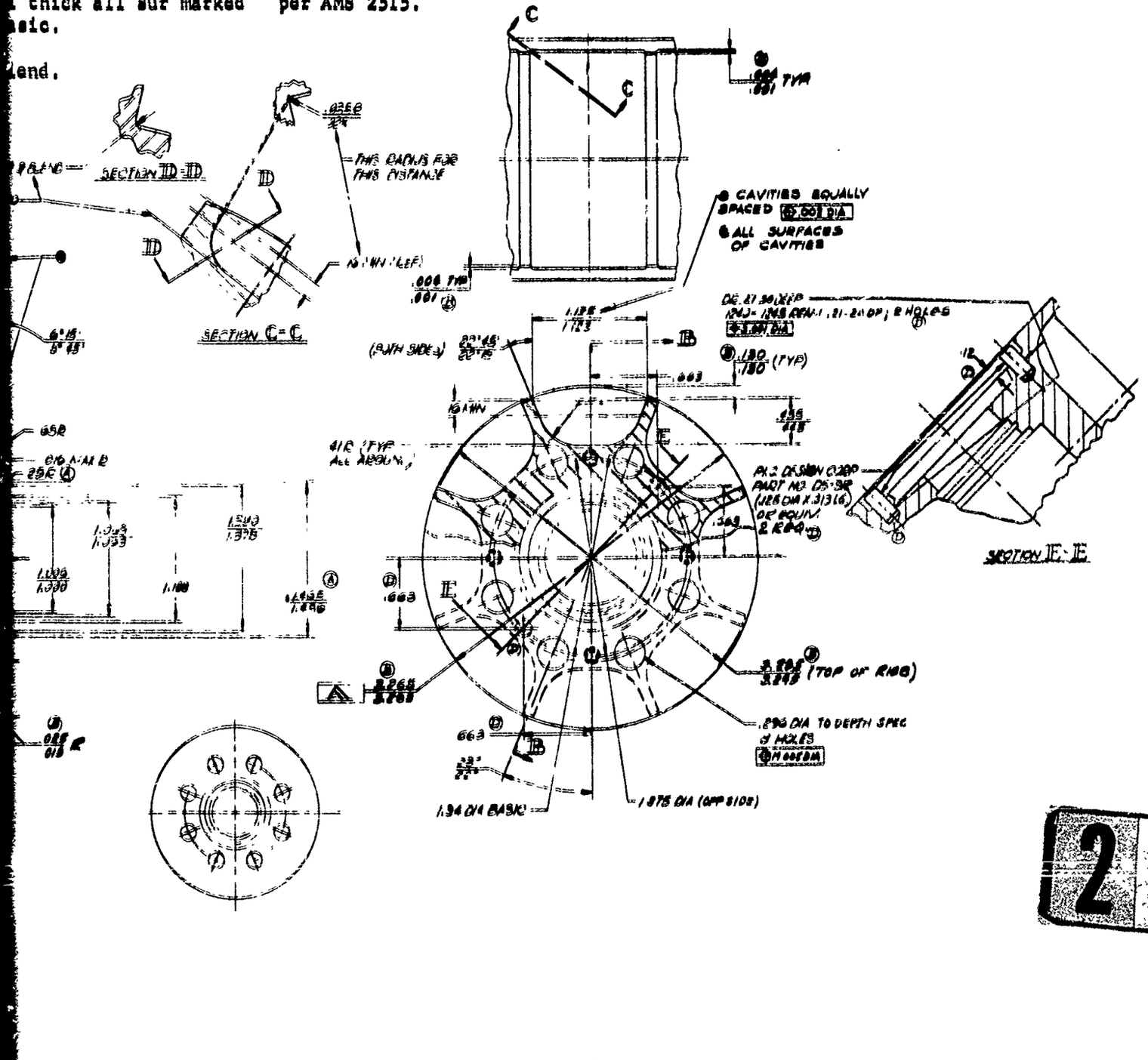


Figure 30. WSR-101 sprocket wheel. (U)

(U) A clearance tolerance was established between the sprocket wheel and the pulser housing. This clearance, based on previous experience, was sufficiently small to prohibit failure of the E-dome yet large enough to provide adequate clearance. The required diametral clearance is 0.0110 to 0.0145 inches.

(U) A structural analysis was conducted on the various load carrying walls of the sprocket wheel. These include the two side walls and the longitudinal wall between the cavities. A freebody diagram of the sprocket wheel is shown in Figure 31. The inter-cavity wall was analyzed for bending as a simple cantilever beam of unit width and variable cross-section under a uniformly distributed load. The results of the analysis are presented in Figure 32.

(U) A similar analysis cannot be conducted for the two side walls since the effect of hoop restraint is not included. Therefore, the side walls were analyzed as flat plates of uniform thickness subject to a uniformly distributed load. The following edge conditions were assumed; one long edge free, one long edge fixed, and two short edges supported. The maximum bending stress of 77,000 psi occurs at the center of the fixed edge. The resulting stress was adjusted for the actual thickness at the fixed edge. The margin of safety, based on a yield strength of 140,000 psi at 150°F, is 0.82.

(U) The weight of the sprocket wheel is 0.900 pounds. The calculated inertia load of the titanium sprocket wheel is .772 gram-cm^2.

Pulser Housing

(U) The pulser housing provides three firing ports at ninety degree intervals. The initial housing, Figure 33, was made of 2024-T6 Aluminum and weighed 1.383 pounds. The base of the housing was attached to the adjustable chute while both ends of the housing were doweled and held securely by screws to the front cover and adapter plate. During firing, the capsule bears against the housing and imparts a load of 4000 pounds. This load is carried in shear by ten dowel pins (five on each side). The shear stress on each pin is 14,500 psi and the margin of safety is 3.10.

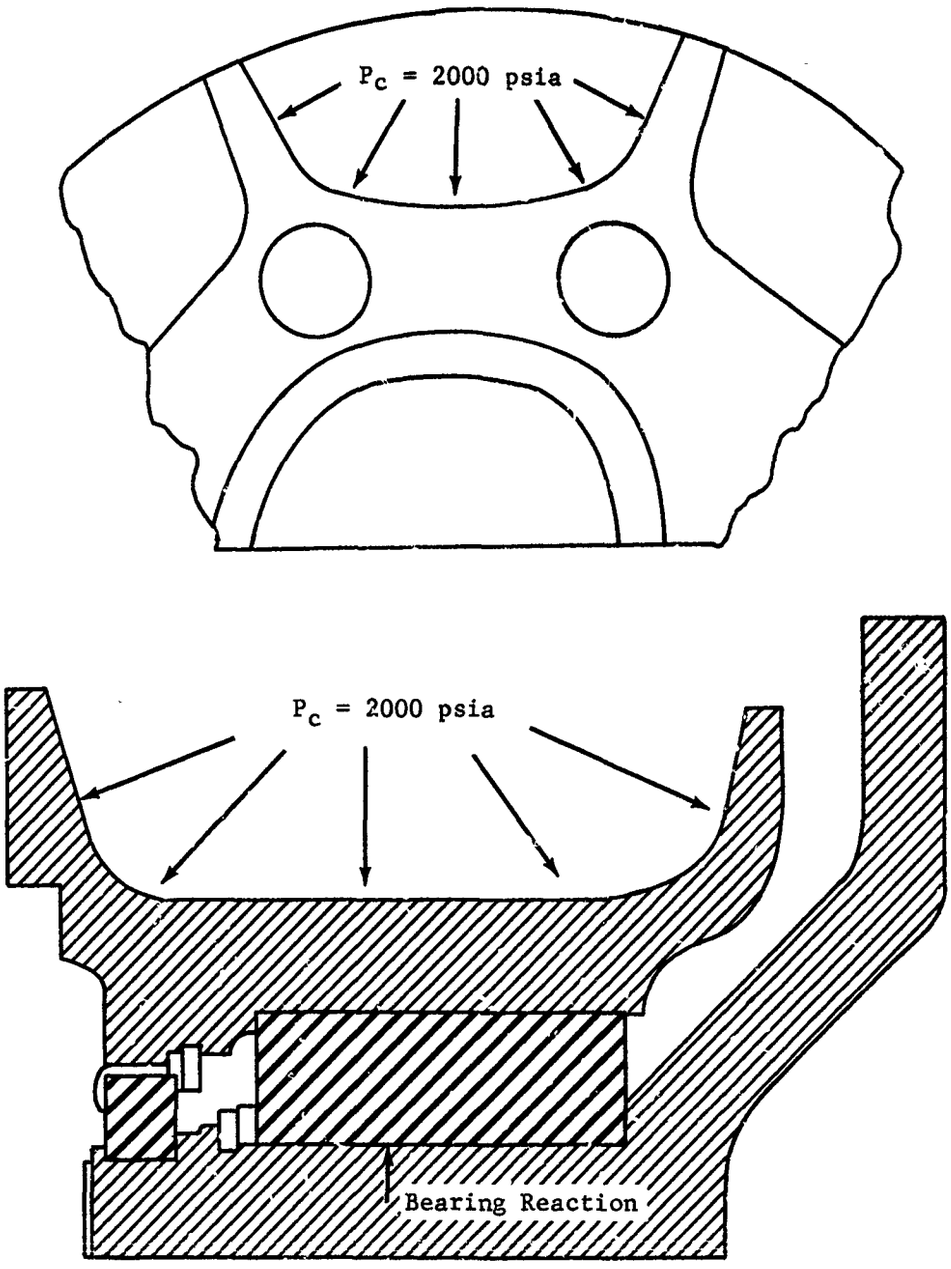
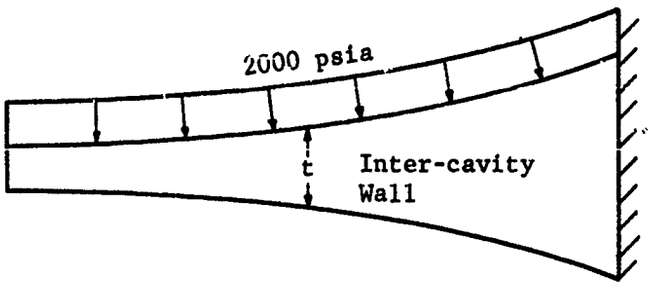


Figure 31. WSR-101 sprocket wheel freebody. (U)



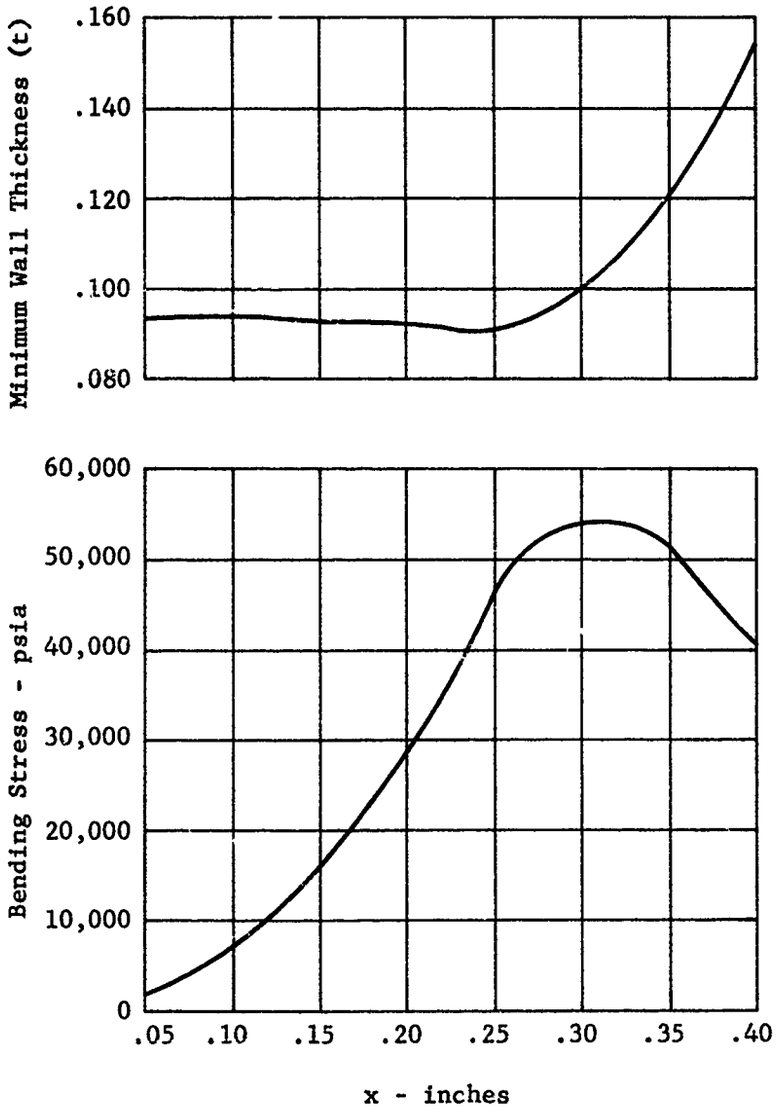


Figure 32. Sprocket wheel stresses. (U)

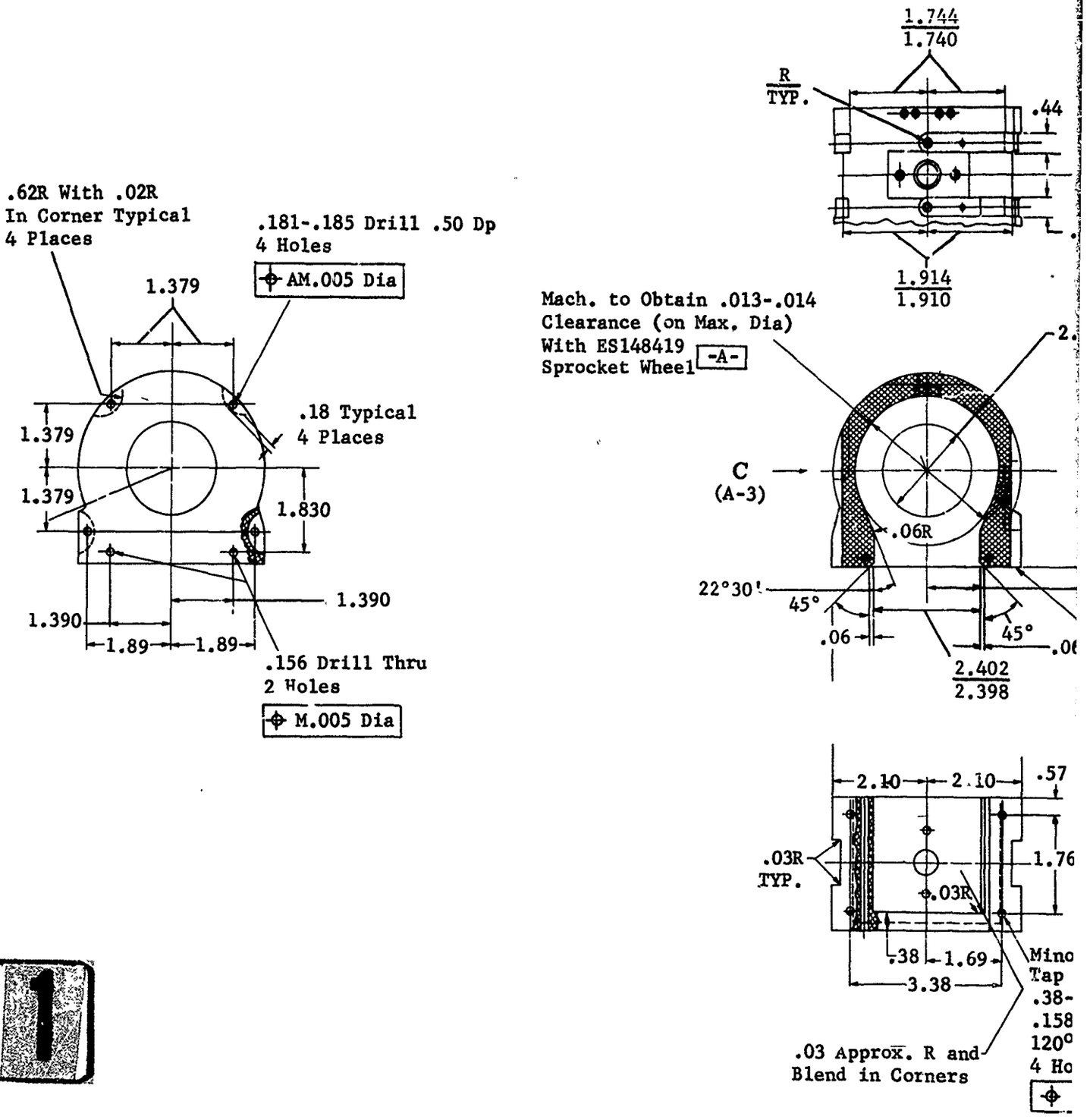
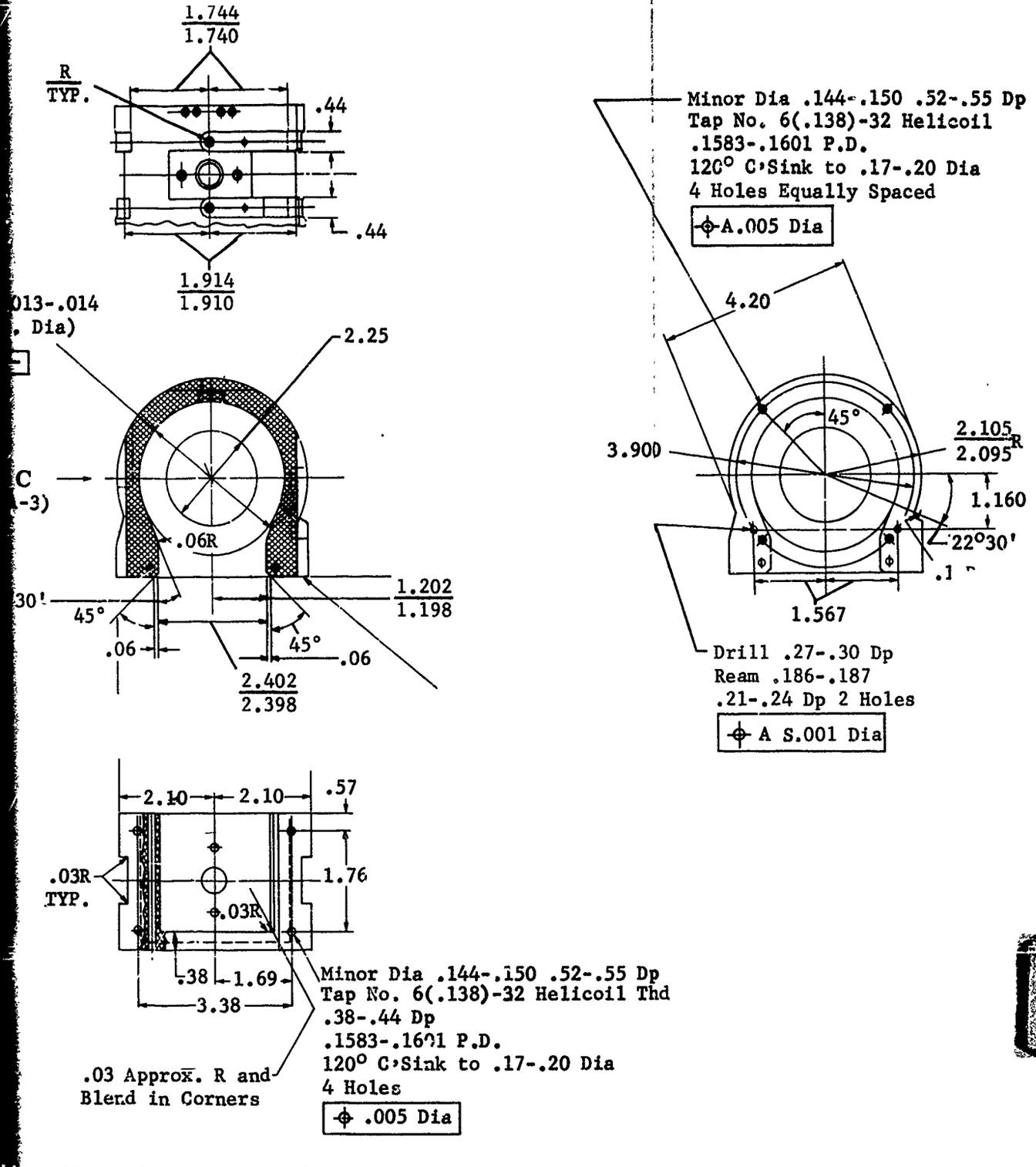


Figure 33. Pulser housing. (U)



ure 33. Pulser housing. (U)

(U) In addition to carrying the bearing load, the dowel pins serve to realign the pulser should it be disassembled, and stiffen and maintain the roundness of the housing during firing.

(U) The cap screws joining the pulser housing to the adjustable chute frame and the cap screws holding the frame to the bench fixture are subject to both tensile and/or shear loads depending on which firing port is used. Figure 34 shows the loading, stresses and margins of safety for the cap screws.

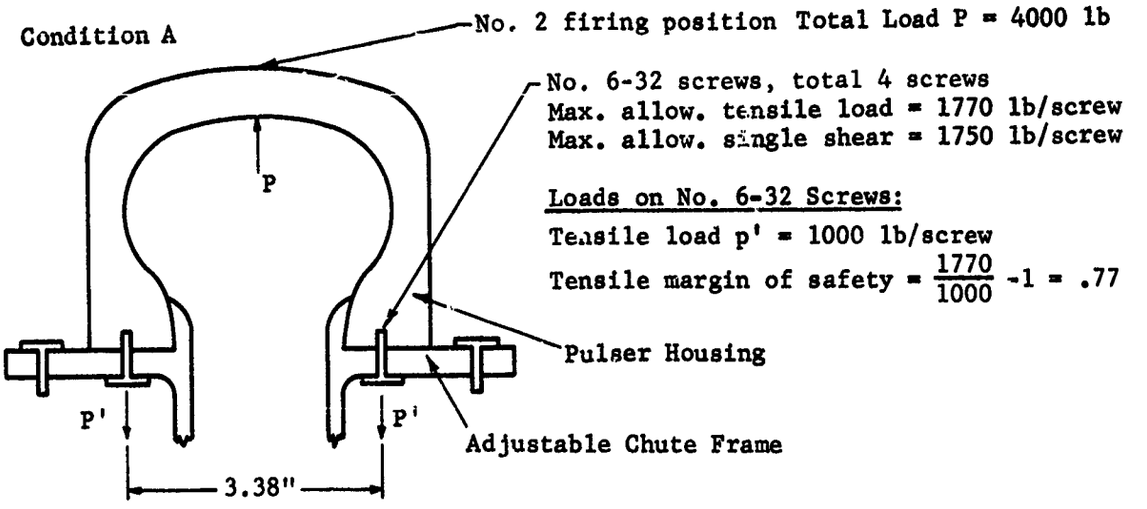
(U) The ID of the pulser housing was bored out to close tolerances to provide an exact clearance (.0110 to .0145 inches on diameter) for the sprocket wheel.

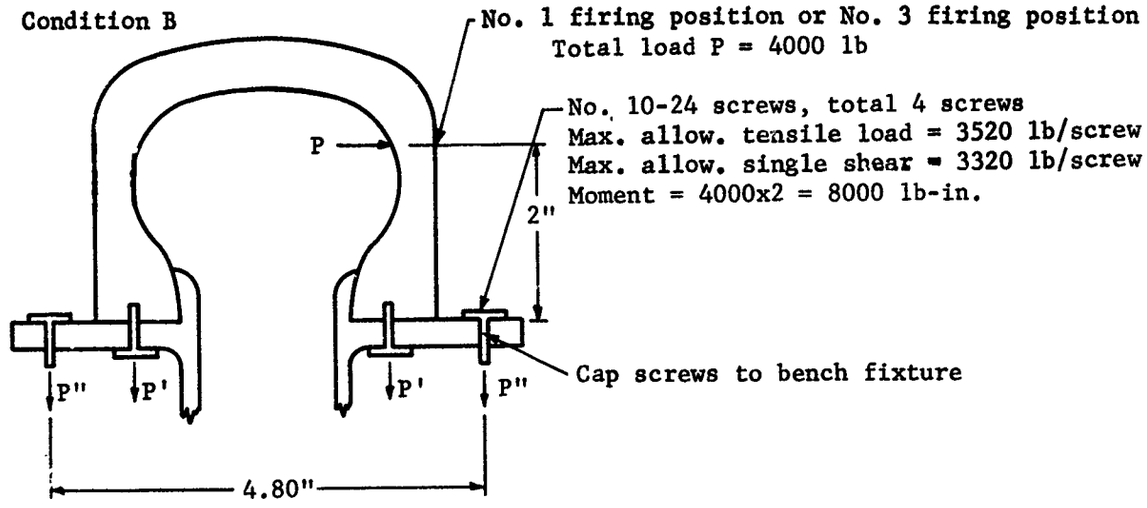
(U) An analysis was conducted on the deflection of the pulser housing in the region of the exhaust nozzle. This analysis, based on the deflection of a uniformly loaded fixed end beam of unit width and constant cross section, indicated a range of mid-point deflections from 0.0036 to 0.0590 inches depending on the assumed thickness of beam. The analysis is conservative since it does not include the effect of hoop restraint which reduces deflections as shown in Figure 35a. Based on the above analysis, exhaust nozzle blocks, Figure 35b, were designed to reduce the maximum mid-point deflection to acceptable limits.

Nozzle Blocks

(U) The nozzle blocks serve two functions. First they provide the nozzle exhaust cone extension and secondly, act as backup supports for the housing at the nozzle opening to minimize housing deflection.

(U) The nozzle blocks shown in Figure 36 are made of 6061-T6 aluminum and are securely tied into the two end rings of the housing. Although, each block was designed to take the full load of 4000 pounds, an interaction analysis between the nozzle block and the housing "beam" indicates that only 2800 pounds will be transmitted to the nozzle block. Therefore, the nozzle block design is conservative and the actual mid-point housing deflection will be only 0.0015 inches. The maximum bending stress in the block is 15,500 psi. Each nozzle block weighs 0.28 pounds.





Loads on No. 10-24 screws:

Tensile load $P'' = \frac{8000}{4(4.80)} = 417$ lb/screw

Tensile margin of safety $= \frac{3520}{417} - 1 = 7.4$

Shear load = 1000 lb/screw

Shear margin of safety $= \frac{3320}{1000} - 1 = 2.32$

Loads on No. 6-32 screws:

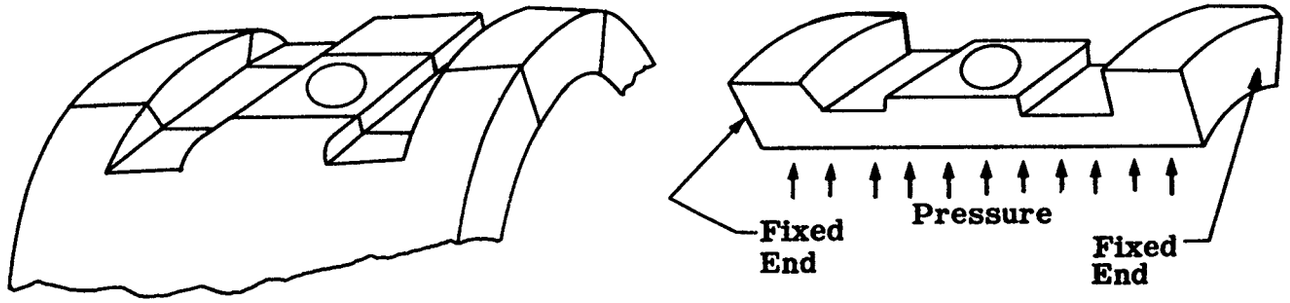
Tensile load $P' = \frac{8000}{4(3.38)} = 593$ lb/screw

Tensile margin of safety $= \frac{1770}{593} - 1 = 2.0$

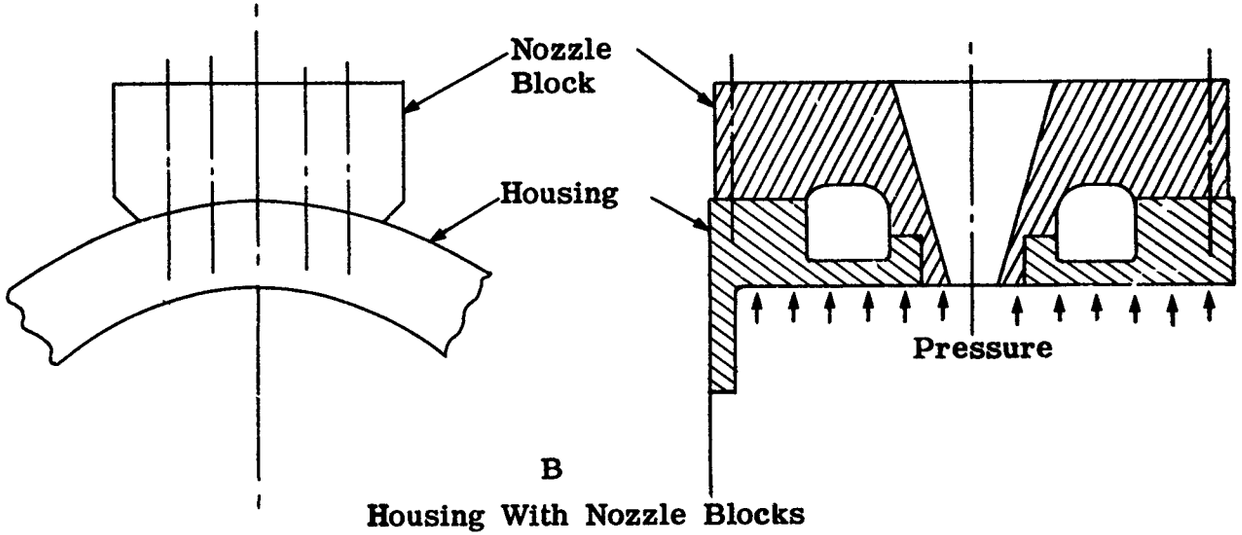
Shear load = 1000 lb/screw

Shear margin of safety $= \frac{1750}{1000} - 1 = .75$

Figure 34. Pulser housing clamping loads. (U)



A
Unsupported Housing



B
Housing With Nozzle Blocks

Figure 35. Housing deflection schematic. (U)

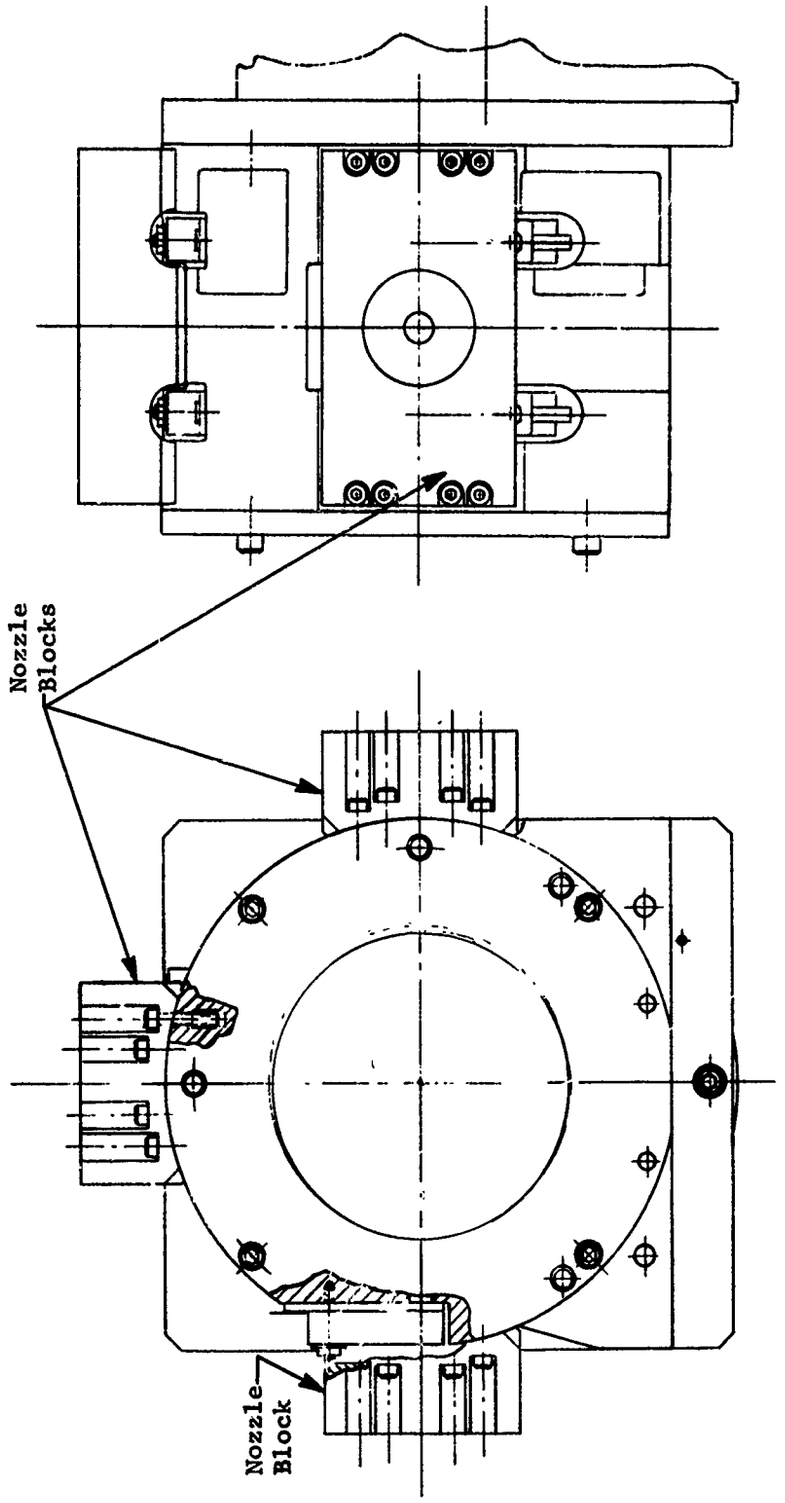


Figure 36. Pulser housing with nozzle blocks. (U)

Front Cover

(U) The front cover weighs 1.09 pounds and is made of 431 stainless steel having a yield strength of 148,000 psi at 500°F. The cover is joined to the side of the pulser housing by five dowel pins and four cap screws.

The primary function of the front cover is to provide a shaft for the support of the sprocket wheel. The firing load of 4000 pounds from the capsule is transmitted through the sprocket wheel and needle bearing to the shaft. The maximum bending stress in the shaft is 86,000 psi resulting in a margin of safety of 0.74. The calculated deflection at the end of the shaft was 0.0045 inches which decreased to 0.00087 inches when the stiffness of the inner race of the needle bearing was included. However, deflection tests of the assembled pulser showed the actual deflection of the shaft to be 0.007 inch at 1000 psi. Therefore, a design modification was made to the front cover to increase its strength and eliminate the cantilevered shaft. This modification is shown in Figure 37.

Bearings

(U) Two bearings were employed in the original WSR-101 pulser housing. One was a heavy duty roller bearing while the other was a low torque ball bearing. A Torrington HJ-142212 bearing and outer race with an IR-101416 inner race served as the roller bearing. The ball bearing was a Borden SFR6FF3 thrust bearing having a flanged deep groove with a double flexeal seal and pressed steel retainers. The roller bearing, which was under the radial firing load of 4000 pounds, had a static capacity of 10,300 pounds resulting in a 1.58 margin of safety. A spacer ring was provided as an extension to the outer race to support the end seal. The ball bearing resisted any side load due to thrust misalignment which would be small and negligible.

The inertia loads were calculated as 165 and 10.6 gram-cm^2 for the roller bearing and the ball bearing respectively. The combined weight of the bearings, spacer ring and seal is 0.299 pounds.

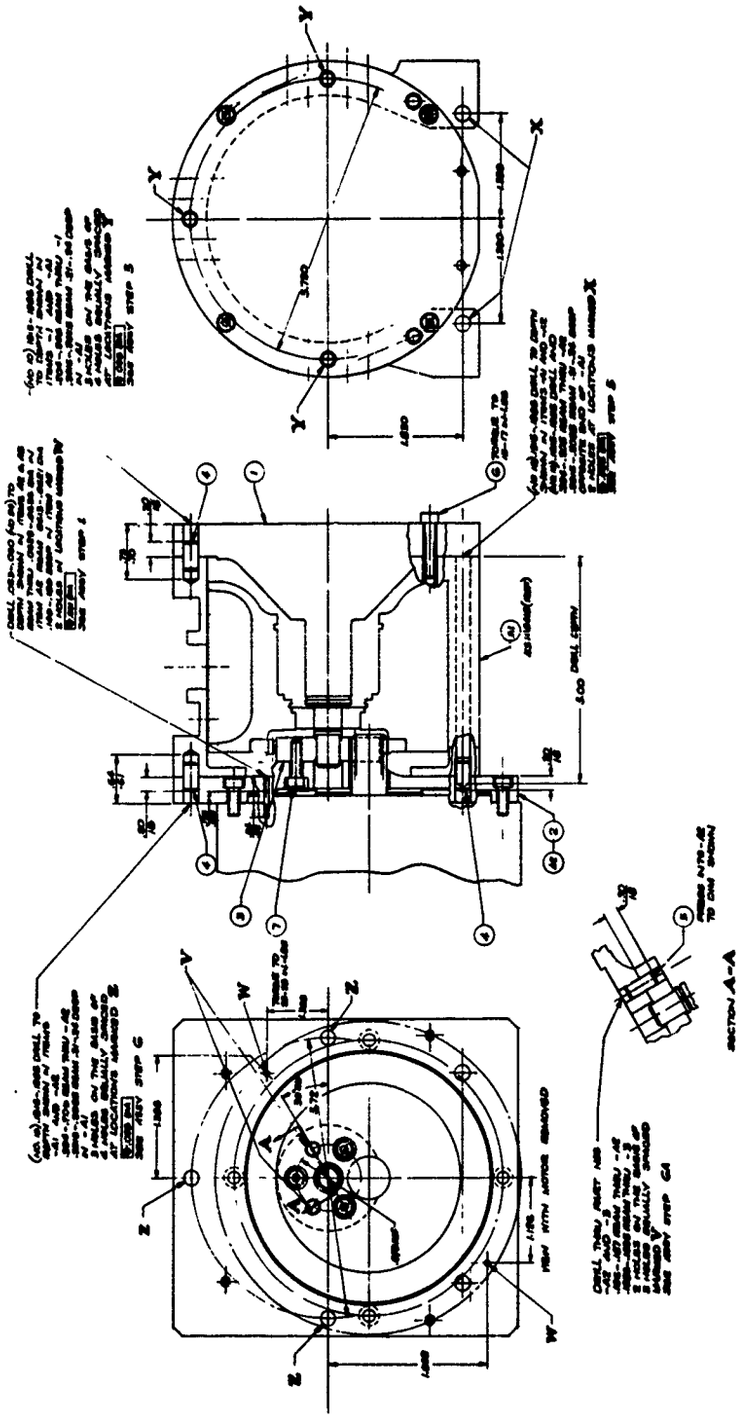


Figure 37. WSR-101 sprocket wheel modification. (U)

Reduction Gear

(U) The reduction gear was designed to permit the sprocket wheel to step at 45 degree intervals while the U9C motor steps at 180 degree intervals. The gear is made of AMS 6475 material, having a Rockwell core hardness of C38-43 and a nitrided surface. The gear is doweled to the sprocket wheel and held in place with four 4-40 socket head cap screws. Based upon a motor stall torque of 150 ounce-inches and a dynamic load factor of 2.0 (because of the suddenly applied loads) a compressive contact stress of 250,000 psi exists on the gear teeth. Control of gear tooth backlash is provided at assembly. The inertia load of the reduction gear is 216 gram-cm^2 and its weight is 0.100 pounds.

(U) Based on maximum deflection of the bearing shaft, the maximum deflection of the reduction gear is 0.00087 inches. When capsule firing takes place in either the 3 o'clock or 9 o'clock positions, the tendency is for the reduction gears to rotate a distance equal to the maximum deflection of the gear, namely 0.00087 inches of arc or 0.0662 degrees. The stepping motor pinion, which is free to rotate must rotate through this same arc length. This results in a force of one pound transmitted to the pinion to overcome the inertia and frictional torque of the motor. This force is negligible compared with the normal stepping force of 50 pounds. The angular acceleration of the pinion due to the bearing shaft deflection is 44.5 radians/sec^2. This compares with the normal operating (stepping) acceleration of 3490 radians/sec^2 based on a 0.030 second stepping time.

Seal

(U) The lip seal at the side wall of the sprocket wheel is a composite structure composed of a silicone rubber ring stretched over and bonded to an aluminum disc. The aluminum disc is slotted to permit bending of tabs to form a conical surface for the rubber seal. The seal sits over the reduction gear and is fastened to the sprocket wheel with the same four screws that secure the reduction gear. The rubber lip of the seal is pinched against the housing thereby sealing off the capsule from the bearings. If a capsule should blow, then the seal would prevent any particles from entering and possibly damaging the bearings.

Adapter Plate

(U) The adapter plate which joins the U9C stepping motor to the pulser housing is made of 6061-T6 aluminum and weighs 0.424 pounds. The motor is doweled in two places to the adapter plate and held in place with four 6-32 socket head cap screws. The plate is in turn doweled to the housing with five pins and held in place with four 6-32 socket head cap screws. The doweling insures that the motor pinion gear and reduction gear always mate in an identical manner regardless of the number of disassemblies. Because of shaft deflections encountered during tests, the rear adapter plate was modified to support the end of the shaft thus eliminating the cantilever shaft configuration. This modification is shown in Figure 37.

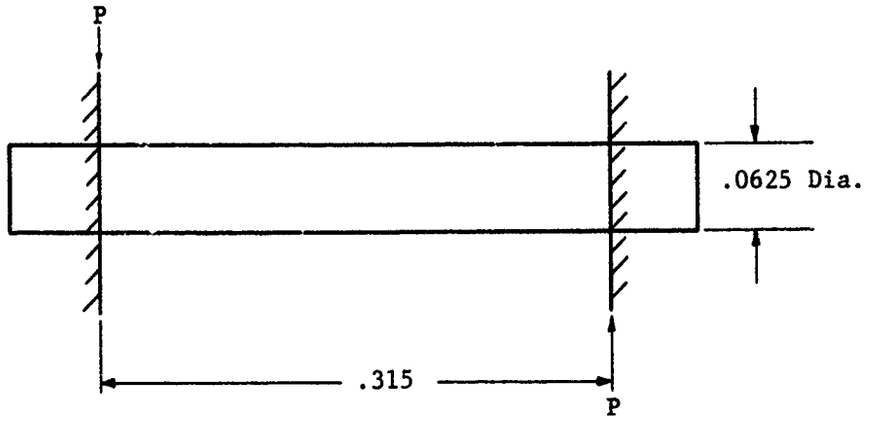
Motor Gear Assembly

(U) Stepping motor torque is transmitted to the reduction gear by the pin connected coupling shown in Figure 38. Testing has shown that the actual torque load can be from 2 to 6 times the maximum motor static torque of 150 inch-ounces.

(U) The motor gear is machined on the end of a short, partially hollow shaft and pinned to the motor shaft. The pinion gear is made of the same material used for the reduction gear AMS 6475. Two pins (.0625 inch diameter) set at 90 degrees to each other, are used to attach the gear to the shaft. The AMS 5688 pins are press fitted into both the gear and the shaft, therefore only a shear failure mode was considered for these pins. The maximum shear stress is 28,200 psi at each shear surface resulting in a margin of safety of 3.96.

Ignition Assembly

(U) The ignition system is composed of two separate ignition assemblies at each firing port. Each assembly consists of a contact brush, insulator, cover, washer and stud. The contact brush is made of a beryllium copper material having a minimum yield strength of 160,000 psi. The contact pin at the end of the brush is made of Paliney 7 material and is riveted to the brush.



Actual torque = 150 in. oz.

Maximum torque = 2x6 x 150 = 1800 in. oz.

Material: AMS 5688

Shear strength = 140,000 psi

Endurance limit, 10^8 cycles = 100,000 psi

$$P = \frac{1800}{(2).315} = 2860 \text{ ounces} = 179 \text{ lb}$$

$$\sigma_{max} = \frac{179}{(2)\ \pi(.0625)^2} = 28{,}200 \text{ psi}$$

Margin of safety = 3.96

Figure 38. Motor shaft pin analysis. (U)

(U) The brush was analyzed as a curved cantilever beam subject to a concentrated load at the end. Limitations for the design of the brush were the 0.19 inch maximum deflection and an end load in the order of a few ounces. The result of the analysis indicated a brush thickness of .0050 to .0055 inches and a maximum bending stress of 57,300 psi. The margin of safety is 1.80.

(U) A urethane rubber cover enclosing the ignition assembly provides a surface which acts as an upper deflection stop for the brush. The refrasil phenolic insulator, which provides an opening sufficiently large for the contact pin only, acts as a lower deflection stop for the contact brush. The deflection gap is .080 to .095 inches (.100 to .105 inches less than the thickness of the brush and the height of the rivet head). The deflection gap is included in the maximum design deflection of .190 inches.

Adjustable Inlet and Exit Chute Assembly

(U) The adjustable chute shown in Figure 39 incorporates a cleated belt to pull the fired capsules from the sprocket wheel. The belt is cast polyurethane and has a pinch of 1.75%. The chute housing, guide wheels, and side guide blocks are aluminum. Teflon guide blocks support and locate the belt and also guide the tape and capsules at the chute inlet and exit. Friction is minimized by use of teflon coatings on the side guides for the tape. This chute configuration was chosen because it expedites loading and is preferred where a relatively large number of load-unload cycles take place.

b. Prototype Pulser Configuration

Sprocket Wheel

(U) The sprocket wheel configuration was not changed for the prototype configuration.

Pulser Housing

(U) The revised pulser housing design was based on use of 440 stainless steel. This housing, shown in Figure 40, also provides for three firing ports at 90 degree intervals. Three basic considerations are incorporated in the

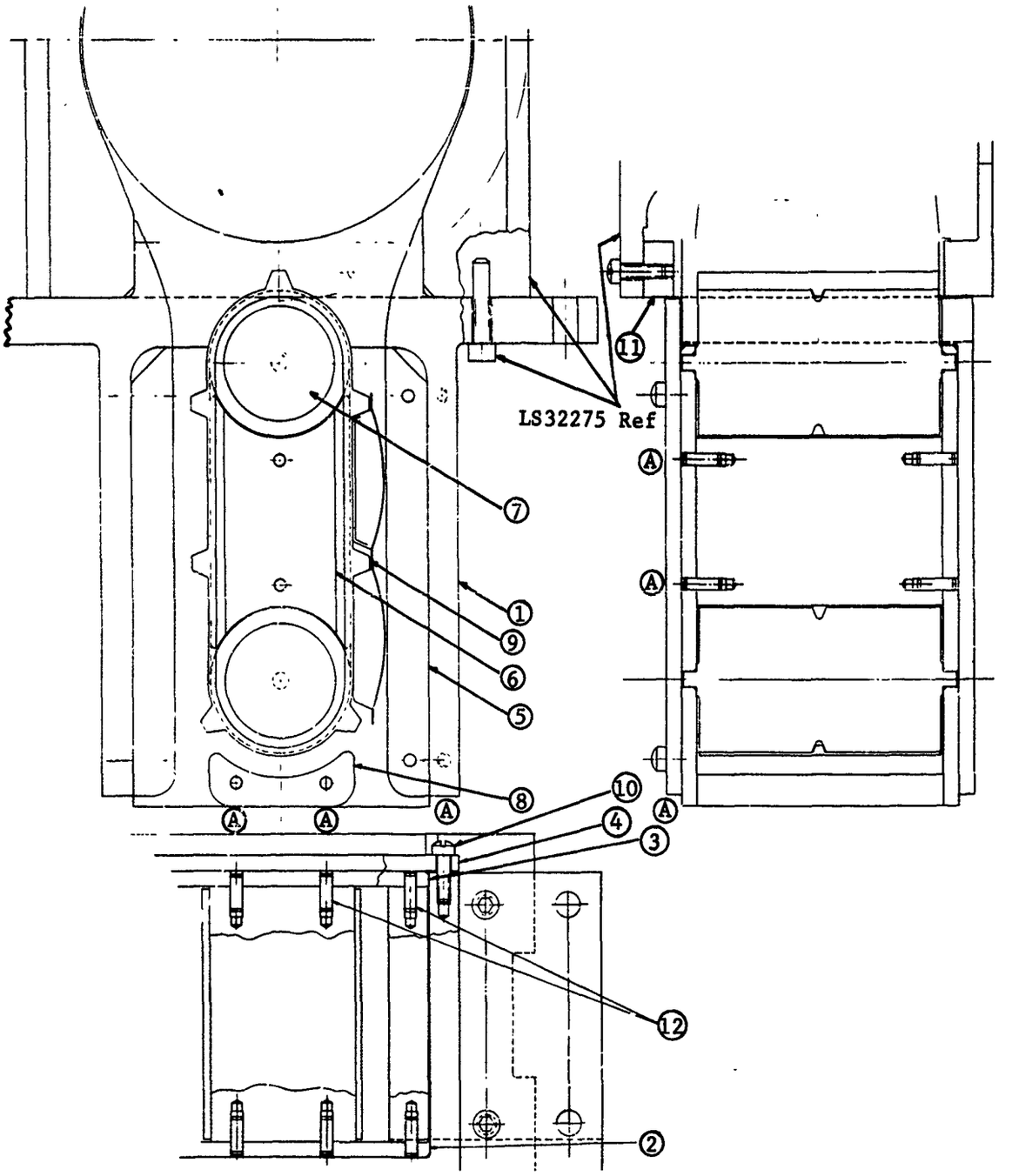


Figure 39. Adjustable inlet and exit chute assembly. (U)

66-046

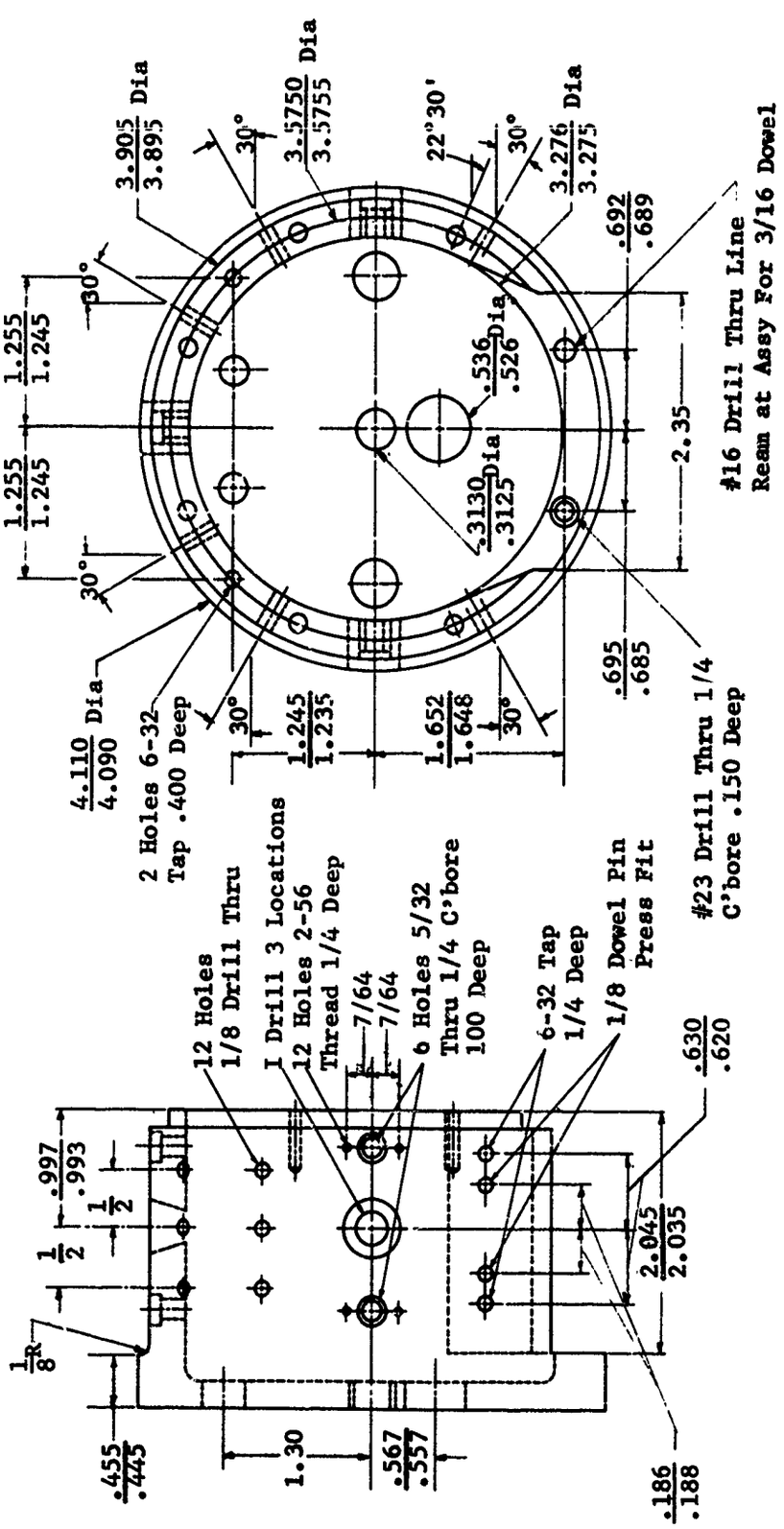


Figure 40. WSR-101 prototype pulser housing. (U)

20-691

(U) design. The first is a close fitting pilot (line on line) with the front cover to reduce deflections during firing. The second is there are no undercuts for the contact brush assembly at the firing ports. This in conjunction with the material change reduces the deflection at the firing port from a nominal .005 inch for the initial design to .001 inches. The deflection is considered negligible in that the analysis does not include the hoop restraint which would further reduce deflection. Therefore the nozzle blocks which provided backup support in the initial configuration have been eliminated from the design. The third consideration, which resulted from testing, is the addition of holes located strategically around and in back of the housing to provide venting in case of capsule failure and overpressurization. The weight of the prototype housing is 2.57 pounds.

Front Cover

(U) The front cover, Figure 41, is made of 440 stainless steel and weighs 1.13 pounds. As mentioned, the front cover is piloted on the pulser housing and is joined to the housing by six high strength cap screws. In the initial configuration, the sprocket wheel shaft was machined as an integral part of the cover. In the prototype design, the shaft is a separate element. The front cover has vent holes, similar to the housing, to provide for capsule failures and overpressurization during repetitive firings.

Sprocket Wheel Shaft

(U) The prototype design has an independent shaft configuration. The shaft is press fitted in the pulser assembly in holes in the front cover and rear section of the pulser housing. The configuration allows the sprocket wheel and bearings to be assembled to the shaft prior to installation in the housing to provide closer control of clearances in the tapered bearing. The shaft material is 440 stainless steel and weighs 0.26 pounds.

Bearings

(U) The roller and thrust bearings used in the original design were replaced with two tapered roller bearings. The tapered bearings provide

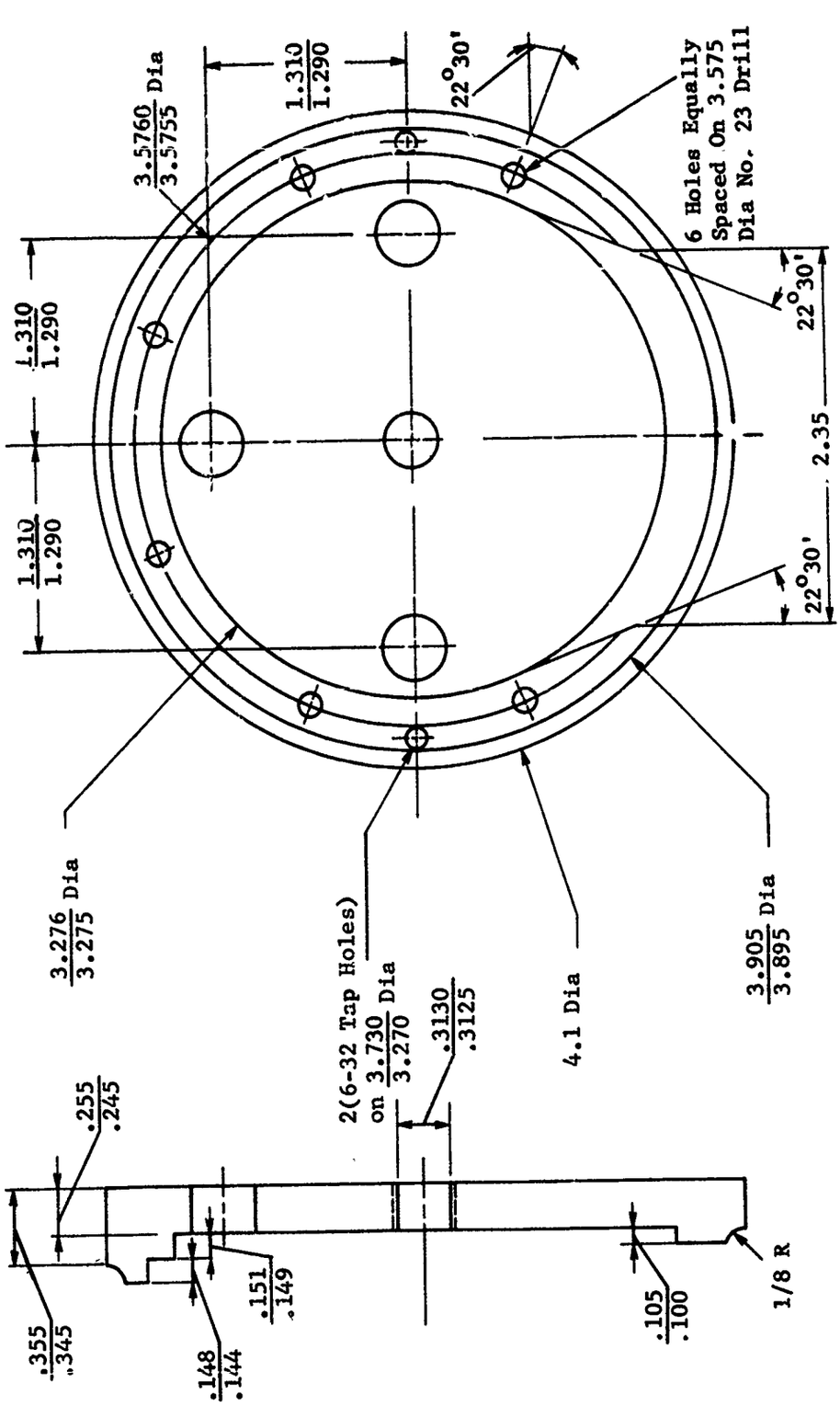


Figure 41. WSR-101 prototype front cover. (U)

66-039

(U) smaller clearances and better firing load distribution. The combined weight of the two bearings and spacers is 0.24 pounds.

Adapter Plate

(U) The adapter plate design was modified to mate with the U9C motor and the revised pulser housing. The plate is made of 6061-T6 aluminum and weighs 0.30 pounds. The motor is attached to the plate with four 6-32 socket head cap screws. The plate is in turn attached to the housing rear section with four 6-32 cap screws. The adapter plate is relieved in the area where the vent holes are located in the rear section of the pulser housing to permit gas to escape in the case of a capsule failure.

Ignition Assembly

(U) The ignition system was redesigned to provide for more contact force between the pin and capsule and to withstand a capsule failure in the pulser. The configuration, shown in Figure 42, is composed of a tungsten contact pin fitted into a phenolic block. Tungsten is used because of its resistance to damage by arcing. The contact pin unit is assembled by means of springs at each end to a steel block which is fastened to the pulser housing. The attaching springs provide a contact force of 4 ounces. The springs also allow the brush assembly to ride smoothly over irregularities on the tape without jamming. Two cap screws are placed through slots in the phenolic block and are screwed into the steel block to limit the travel of the pin assembly in case of a capsule failure. Teflon inserts are provided in the steel block and the pulser housing to prevent short circuits. Two ignition assemblies are located at each firing port.

Reduction and Motor Gear Assembly

(U) No design changes from the original configuration were made to the reduction gear or motor gear assembly. The lip seal was removed from the assembly.

Adjustable Inlet and Exit Chute Assembly

(U) The design modifications incorporated in the chute assembly reduced

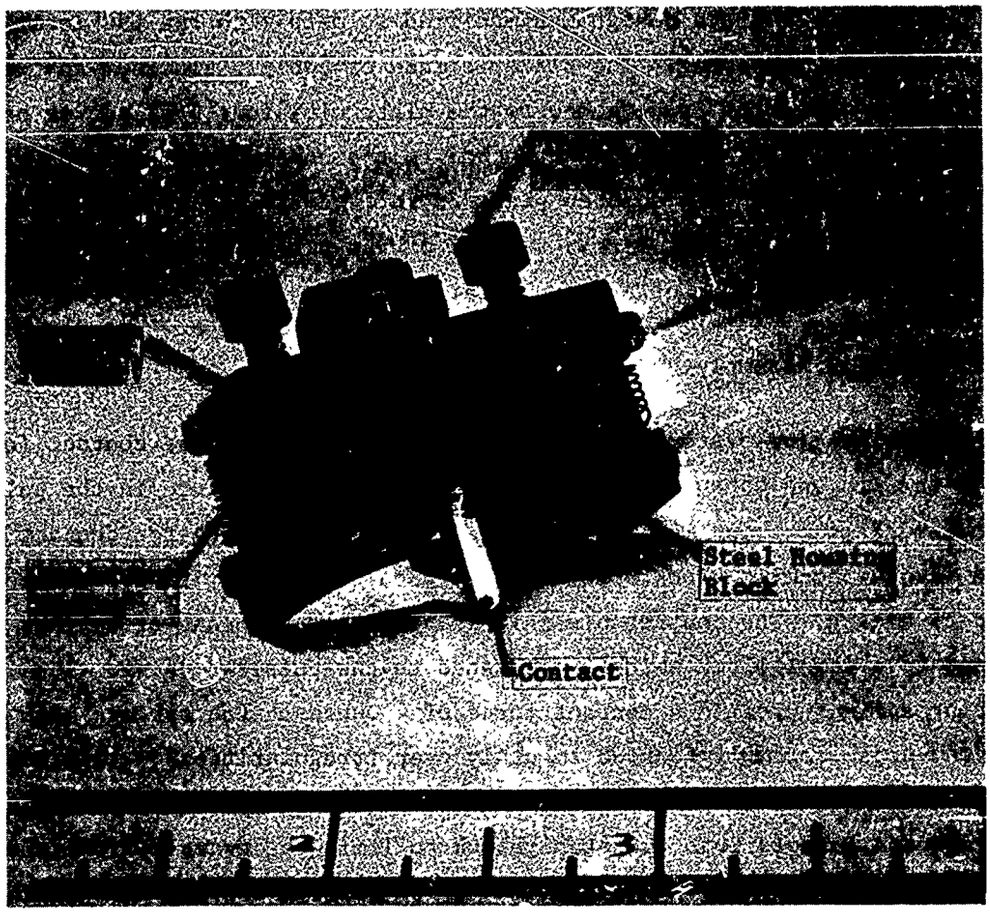


Figure 42. Prototype ignition assembly. (U)

(U) the weight of the assembly and reduced the friction of the belt and guide wheels. The weight of the revised assembly is 1.01 pounds. The weight reduction was achieved by modifying the housing assembly and incorporating the side guide blocks into the housing (Figure 43). Friction was minimized by adding miniature ball bearings to the guide wheels.

4. Static Firing Fixture

(U) The static firing fixture, shown in Figure 44, was designed to house the capsule during sea level and vacuum firing tests. The fixture is composed of four basic components: a high strength phenolic base, a stainless steel body containing an exact duplicate of the sprocket wheel cavity, a refrasil phenolic cover with a 14:1 exit cone extension, and a steel cover plate. The entire fixture is bolted together with eight 10-24 screws. The spacing between the cavity and the refrasil cover can be adjusted by the insertion of shims to simulate various sprocket wheel-to-housing clearances.

(U) During the test program, a modification was incorporated which combined the steel cover plate and phenolic cover into one unit.

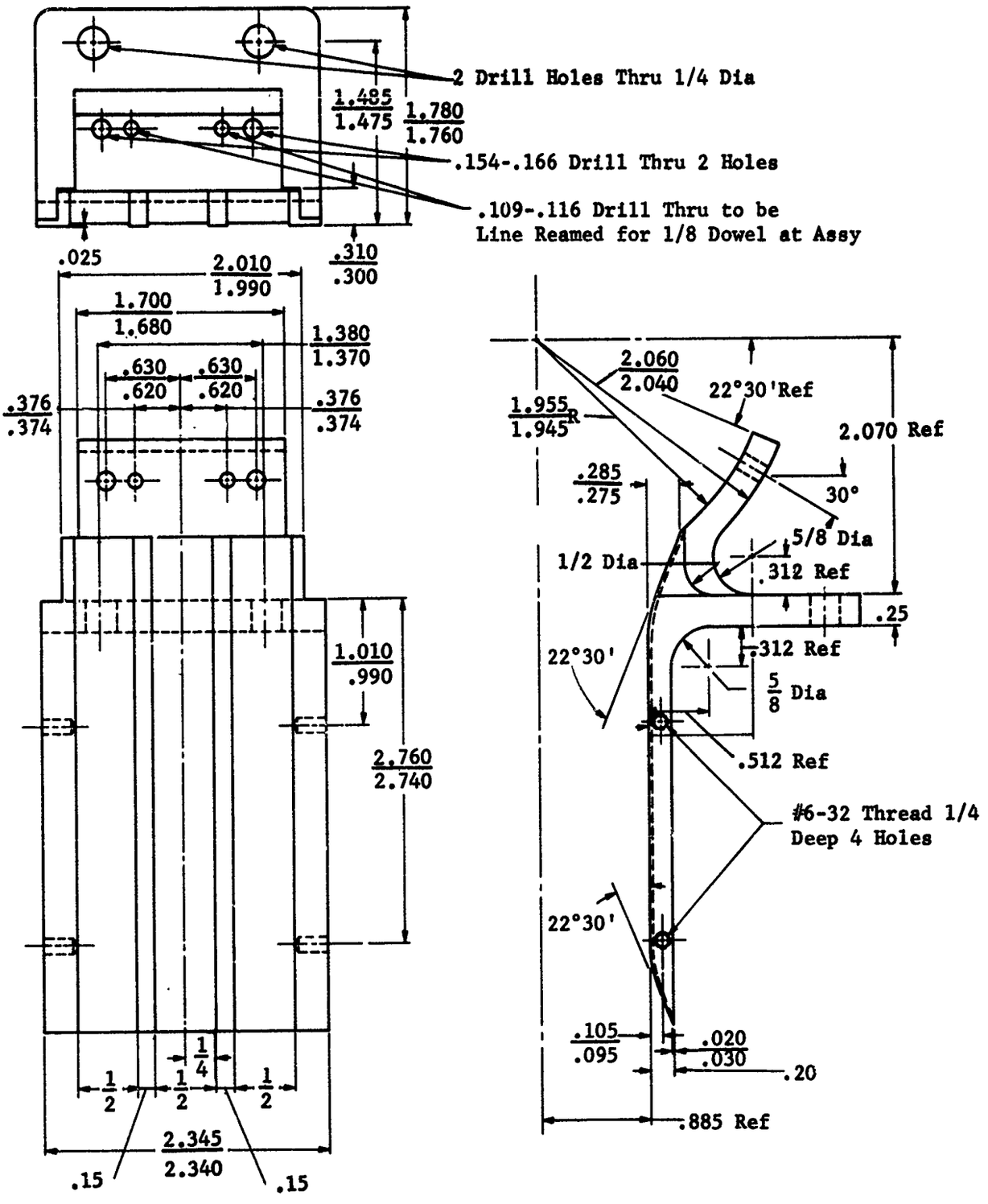
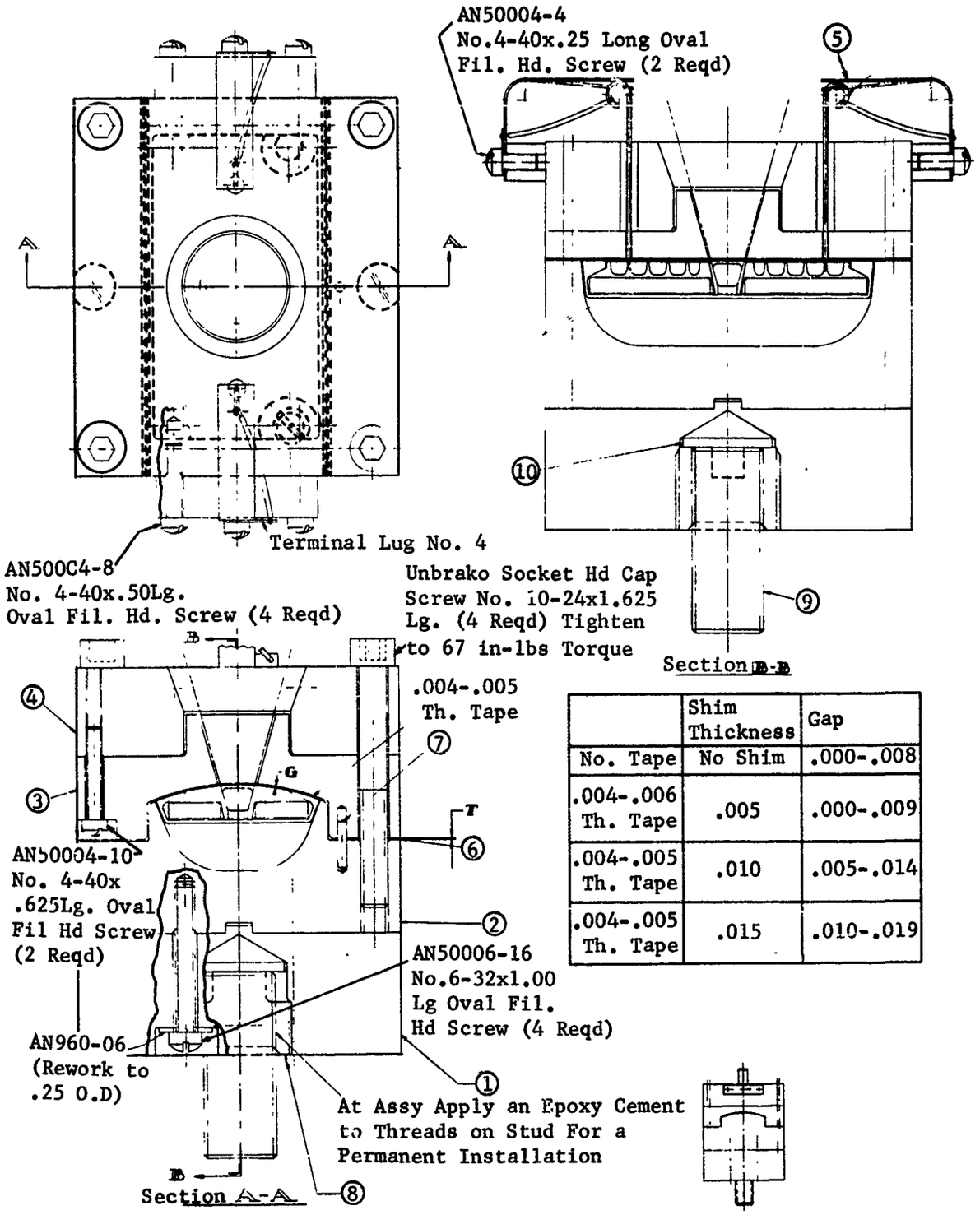


Figure 43. WSR-101 prototype chute housing. (U)

66-095



	Shim Thickness	Gap
No. Tape	No Shim	.000-.008
.004-.006 Th. Tape	.005	.000-.009
.004-.005 Th. Tape	.010	.005-.014
.004-.005 Th. Tape	.015	.010-.019

Figure 44. Static firing fixture. (U)

66-048

(This page is unclassified)

B. ANALYSIS

(C) 1. Heat Transfer

With the establishment of the capsule design, a series of one-dimensional heat transfer analyses were conducted on the capsule E-Dome configuration, sprocket wheel, and nozzle throat for a .05 second firing.

(U) a. Analyses

1) Chamber Dome and Sprocket Wheel -- The capsule configuration prior to and during firing is shown in Figure 45. The section analyzed consisted of a .02 inch thick Gen-Gard V-57 Expandable dome backed by a .0025 inch thick teflon coating and a .125 inch thick section of the aluminum sprocket wheel.

(C) During firing, the Gen-Gard dome is heated by convection and radiation from the 4390°F combustion gases of the burning solid propellant grain and is expanded against the constraining sprocket wall.

(U) The total heat rate to the chamber dome may be expressed as follows:

$$Q_T = Q_C + Q_R = (h_C + h_R)\, A_C\, (T_G - T_S) \qquad (1)$$

Where A_C = Heat transfer surface area-ft^2

h_C = Convective heat transfer coefficient - BTU/hr-ft^2 - °R

h_R = Radiative heat transfer coefficient - BTU/hr-ft^2 - °R

T_G = Combustion gas temperature - 4390°F

T_S = Surface temperature of dome - °F

Q_T = Total heat rate to surface of dome - BTU/hr

Q_C = Heat rate by convection - BTU/hr

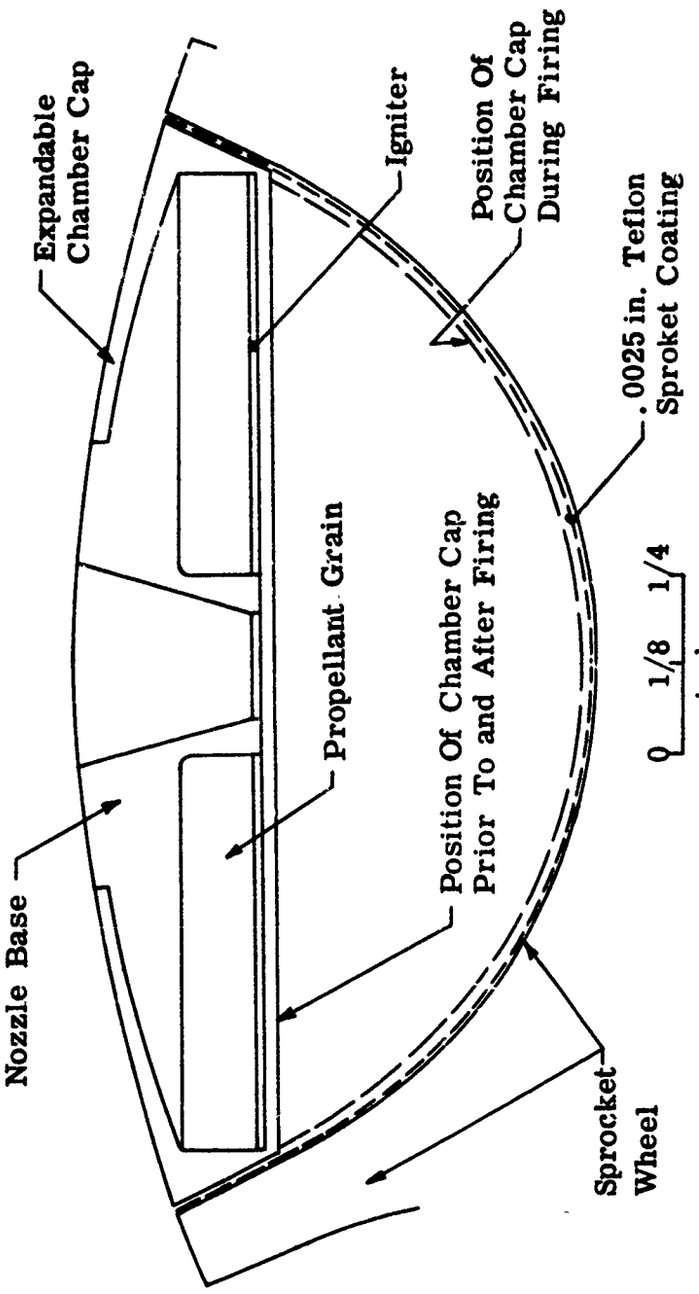


Figure 45. Expandable E dome capsule configuration. (U)

20-726

Q_R = Heat rate by radiation - BTU/hr

(U) A conservative estimate of the heat transfer convective coefficient was obtained by assuming that the combustion gases would flow along the dome wall before exhausting through the nozzle. The following relationship presented in Reference 1 was used to calculate an average convective coefficient for turbulent flow of combustion gases.

$$(Nu)_L = .036 \, (P_R)^{1/3} \, (R_e)_L^{\ .8} \qquad (2)$$

Where

$(Nu)_L$ = Average Nusselt Number of gas = $h_c L/k$

P_R = Prandtl Number of gas = $C_p \mu / k$

$(R_e)_L$ = Reynolds Number of gas flow = $\frac{LG}{\mu}$

L = Effective length along heated dome surface - ft

G = Mass flow rate - lb/sec - ft^2 of gas

μ = Viscosity of combustion gas - $\frac{lb}{ft - sec}$

C_p = Specific heat of combustion gas - BTU/lb - °F

k = Thermal conductivity of combustion gas - $\frac{BTU}{hr\text{-}ft\text{-}°F}$

(U) The estimation of the radiative coefficient, h_r, was based on the following expression of Reference 2:

$$h_R = \frac{Q_R}{A_R \, (T_G - T_S)} = \frac{\sigma A_R \, (\varepsilon_G T_G^4 - \alpha_G T_S^4)}{A_R \, (T_G - T_S)} \qquad (3)$$

$$h_R = \frac{\sigma (\varepsilon_G T_G^4 - \alpha_G T_S^4)}{(T_G - T_S)}$$

(U) Where σ = Boltzmann's Constant - $.173 \times 10^{-8}$ $\frac{BTU}{hr - ft^2 - °R^4}$

A_R = Effective area for radiation - ft^2

Q_R = Radiation heat transfer - BTU/hr

h_R = Coefficient of radiation - BTU/hr-ft^2-°R

T_G = Combustion gas temperature - °R

T_S = Surface temperature of dome - °R

ε_G = Emissivity of combustion gas

α_G = Absorptivity of gas

(U) 2) Nozzle -- The nozzle throat section, subjected to the maximum heat flux within the motor, was analyzed to determine the possibility of overheating and ablation of the Fiberite nozzle construction.

(U) During capsule firing, both the inner and outer nozzle surfaces are exposed to convective and radiative heating by the combustion gases. The total heat rate to the nozzle is given by:

$$Q_T = Q_o + Q_i = (h_{c_c} + h_{R_o}) \; A_o \; (T_G - T_{S_o}) + (h_c + h_R) \; A_i \; (T_G - T_{Si}) \qquad (4)$$

Where

Q_T = Total heat transfer rate to nozzle throat - BTU/hr

Q_o = Heat transfer rate to nozzle outer surface - BTU/hr

Q_i = Heat transfer rate to nozzle inner surface - BTU/hr

A_o = Outer surface area of nozzle - ft^2

A_i = Inner surface area of nozzle - ft^2

(U) h_{c_o} = Convective heat transfer coefficient from gas to nozzle outer surface - $\frac{BTU}{hr\text{-}ft^2\text{-}°F}$

(U) h_{c_i} = Convective heat transfer coefficient from gas to inner surface - $\frac{BTU}{hr\text{-}ft^2\text{-}°F}$

(U) h_{r_o} = Radiation heat transfer coefficient from gas to nozzle outer surface - $\frac{BTU}{hr\text{-}ft^2\text{-}°F}$

(U) T_{s_o} = Outer surface temperature of nozzle - °R

(U) T_{s_i} = Inner surface temperature of nozzle - °R

(U) The values of h_{c_o}, h_{r_o}, and h_{r_i} were calculated from the expressions of equations (2) and (3).

(U) The nozzle inner surface convective coefficient, h_{c_i}, was calculated from the relationship presented in Reference 3.

$$h_{c_i} = \left(\frac{.026}{D_t^{.2}}\right)\left(\frac{\mu^{.2}\, C_p}{P_R^{.6}}\right)\left(\frac{P_c\, g}{C^*}\right)^{.8}\left(\frac{D_t}{R_c}\right)^{.1}(\sigma) \qquad (5)$$

(U) Where D_t = Throat diameter - ft

μ = Viscosity of combustion gases - $\frac{lb}{ft\text{-}hr}$

C_p = Specific heat of combustion gases - BTU/lb - °R

P_R = Prandtl Number of combustion gases

P_C = Chamber pressure - lbs/ft^2

g = Acceleration due to gravity - ft/hr^2

C^* = Characteristic combustion gas velocity - ft/hr

(U) R_c = Radius of curvature of throat - ft

(U) σ = Factor to account for variation of transport properties of gas across boundary layer.

(U) The velocity of ablation at the nozzle throat may be calculated as follows:

$$V_{A_i} = \frac{Q_{A_i}/A_i}{\rho F \left[1 + Cp \frac{(T_a - T_\infty)}{F} \right]} = \frac{(h_{C_i} + h_{R_i})(T_G - T_A)}{\rho F \left[1 + C_p \frac{(T_A - T_\infty)}{F} \right]} \quad (6)$$

(U) Where

Q_{A_i} = Heat transfer rate from combustion gases to nozzle inner surface at ablative temperature - BTU/hr

A_i = Nozzle inner surface area - ft^2

ρ = Density of nozzle material - lb/ft^3

C_p = Specific heat of nozzle material - $\frac{BTU}{lb - °R}$

T_A = Ablation temperature of nozzle material - °R

T_∞ = Initial temperature of nozzle - °R

F = Effective heat of ablation of nozzle material - BTU/lb

V_{A_i} = Ablation or erosion rate of nozzle material at nozzle inner surface - ft/hr

b. Results and Discussion

(This page is unclassified)

(C) 1) Chamber Dome and Sprocket Wheel -- The temperature distribution within the chamber dome and sprocket wheel immediately after the .05 second firing is shown in Figure 46. The hot surface of the Gen-Gard V-57 chamber cap will reach a maximum temperature of 1165°F, which indicates a small quantity of charring of the expandable dome (charring temperature of Gen-Gard V-57 is approximately 1000°F). The sprocket wheel will remain relatively cold (60°F) during capsule firing and will, therefore, not be subjected to overheating during continuous repetitive capsule firings.

(C) 2) Nozzle -- The temperature distribution within the nozzle throat section, immediately after capsule firing, is shown in Figure 47. The results of the nozzle analysis indicate that the nozzle inner surface will ablate approximately .0057 inch which represents 11% of the nozzle wall thickness. The hot inner surface of the nozzle will be at the ablation temperature of Fiberite (2000°F). The outer surface of the nozzle which is exposed to a lower heat flux from the chamber combustion gases, will reach a maximum temperature of 540°F.

(U) The results of the forementioned analyses were obtained by the use of a thermal analyser program and a high speed digital computer.

(U) 3) Pulser Exhaust Nozzle Exit Cone -- A two dimensional analysis was conducted to determine the temperature distribution in the exit cone of the pulser assembly and also for the contact brush assembly for a typical duty cycle. Figure 48 shows that for the two materials considered (aluminum and graphite cloth) the contact brush assembly and the rear portion of the pulser housing are not affected by the high exhaust gas temperatures. However, the inner wall of the exit cone, using either material, will erode after 26 firings from a single port.

(U) For the test program exit cone heating was not a problem. For system application, which require continuous pulsing for long periods of time, suitable materials can be incorporated into the exhaust nozzle extension cone to meet the duty cycle dictated by the system.

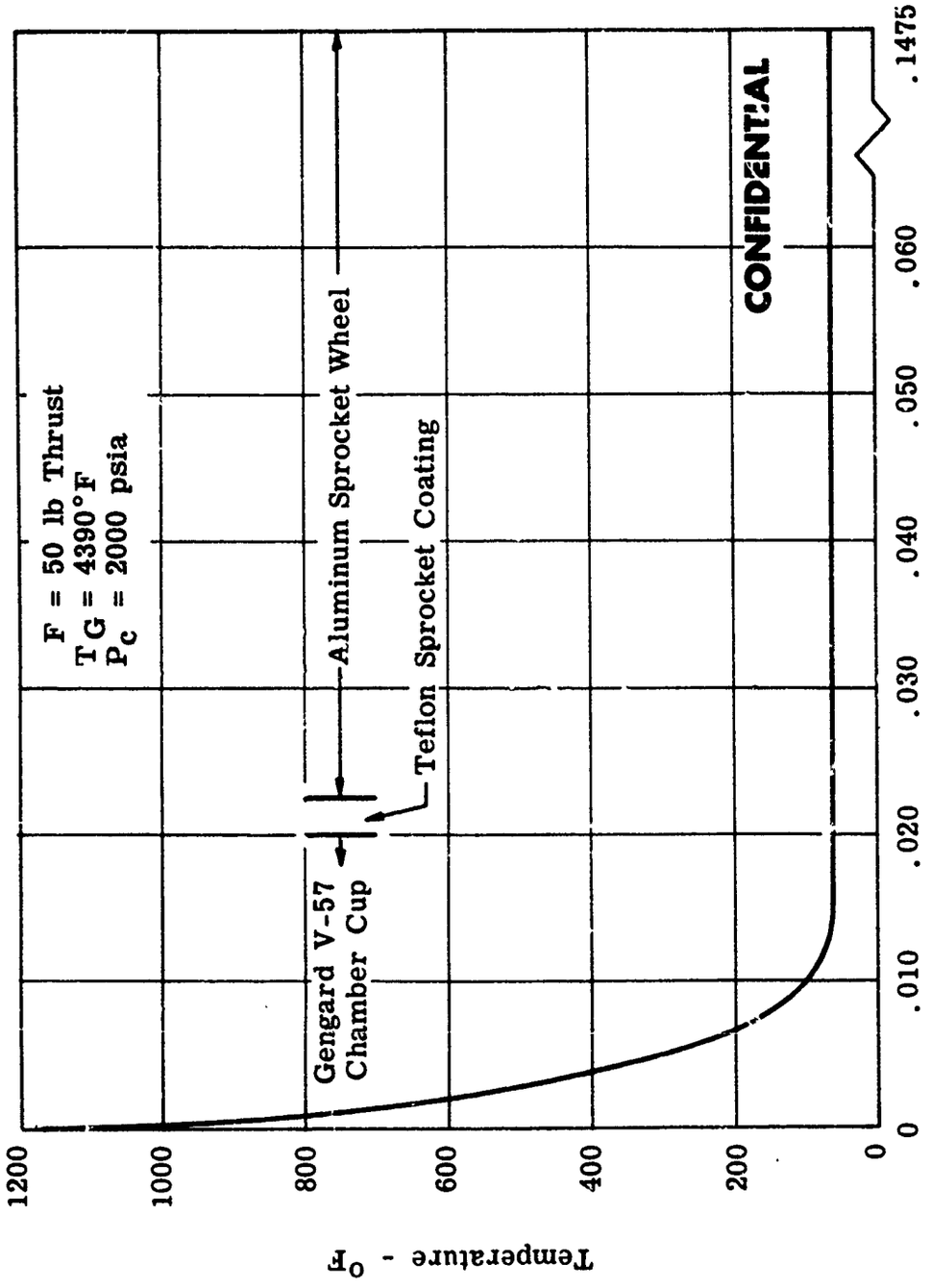


Figure 46. Expandable capsule temperature distribution in GenGard V-57 chamber dome and sprocket wheel. (U)

20-717

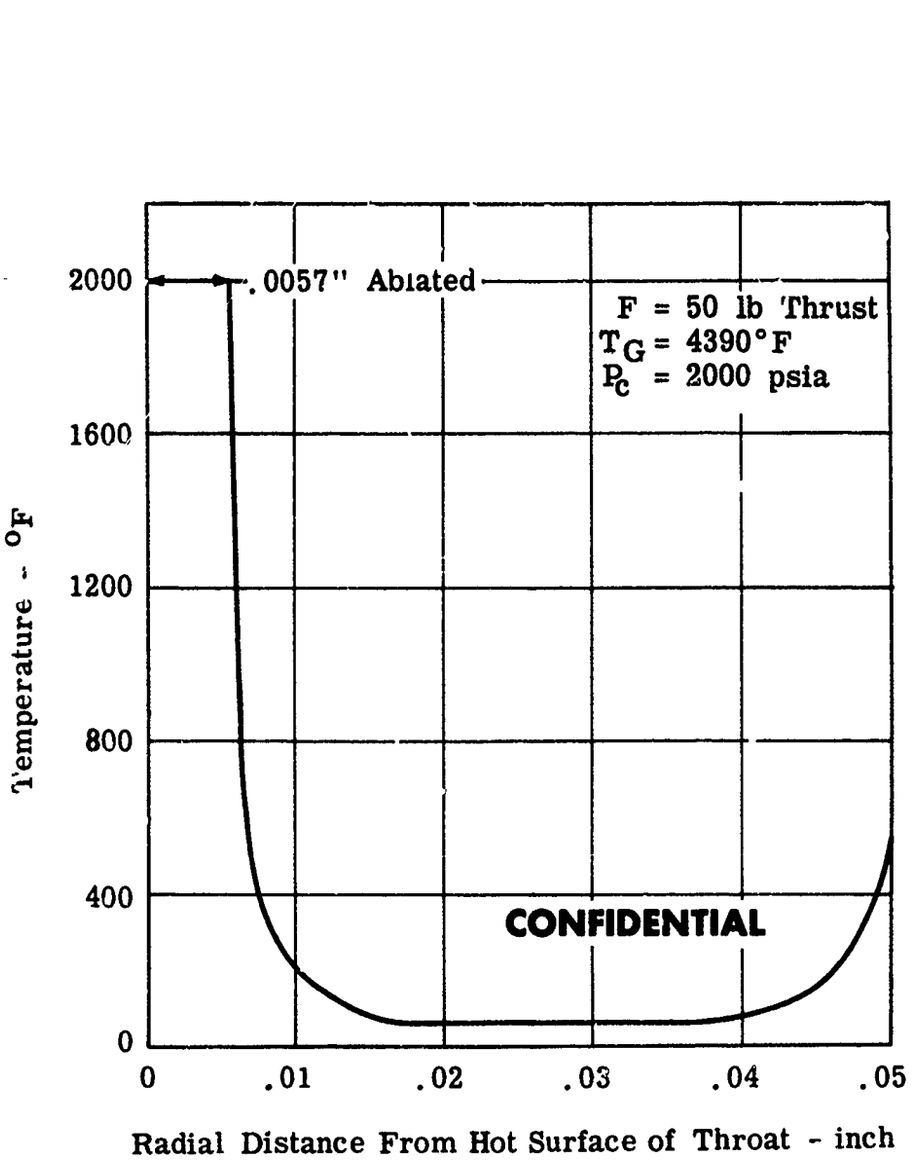
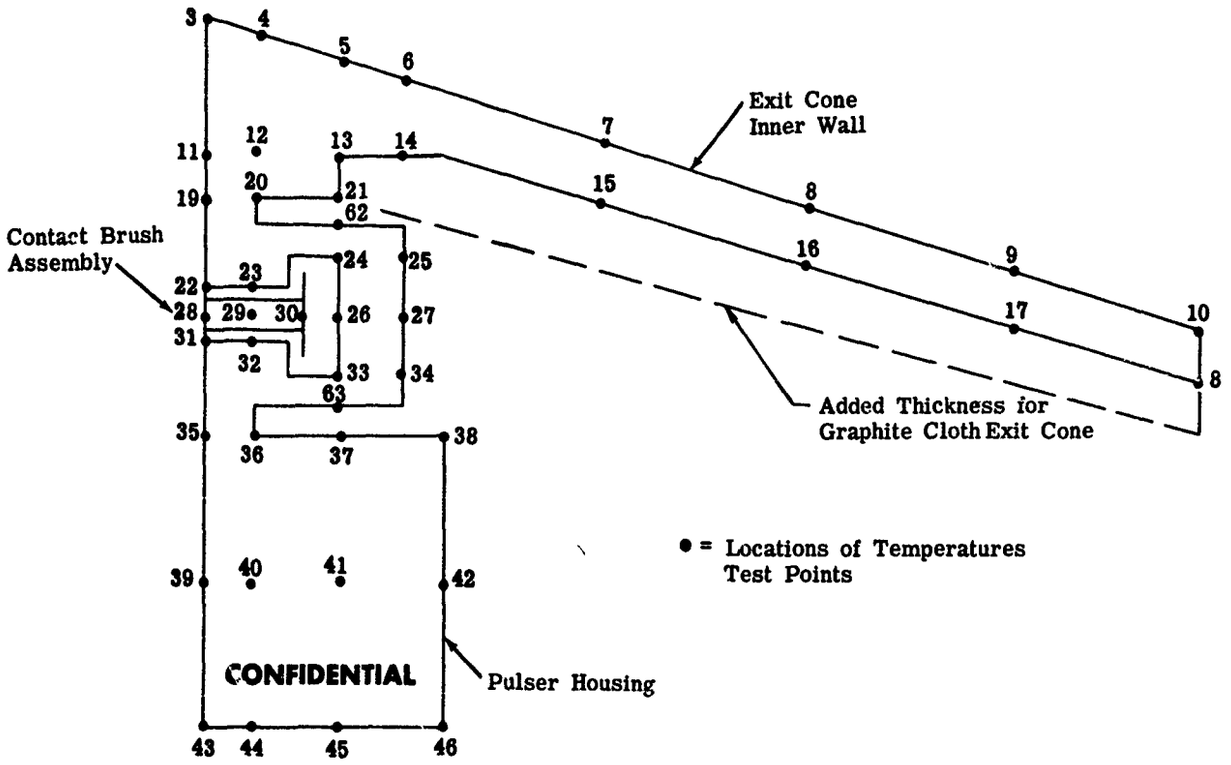


Figure 47. Expandable capsule temperature distribution in fibrite nozzle throat. (U)



Test Point	Temp. °F
3	2441
4	2376
5	2276
6	2219
7	1841
8	1400
9	1100
10	993
11	2022
12	2027
13	2051
14	2079
15	1777
16	1358
17	1068
18	968

Figure 48. Nozzle exit cone te

Temperature Distribution After 26 Firings From Single Port

Aluminum Nozzle Extension

Test Point	Temp. °F	Test Point	Temp. °F	Test Point	Temp. °F
3	2441	19	1978	34	127
4	2376	20	1990	35	125
5	2276	21	2021	36	125
6	2219	22	198	37	125
7	1841	23	193	38	125
8	1400	24	154	39	125
9	1100	25	130	40	125
10	993	26	125	41	125
11	2022	27	137	42	126
12	2027	28	125	43	125
13	2051	29	125	44	125
14	2079	30	125	45	125
15	1777	31	125	46	125
16	1358	32	125	62	1293
17	1068	33	125	63	125
18	968				

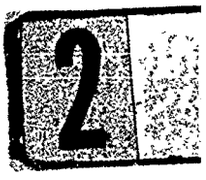
CONFIDENTIAL

Graphite Cloth Nozzle Extension

Test Point	Temp. °F	Test Point	Temp. °F	Test Point	Temp. °F
3	4250	19	214	34	125
4	3940	20	215	35	125
5	3372	21	215	36	125
6	2865	22	128	37	125
7	1353	23	128	38	125
8	1072	24	125	39	125
9	805	25	125	40	125
10	616	26	125	41	125
11	218	27	125	42	125
12	218	28	125	43	125
13	314	29	125	44	125
14	226	30	125	45	125
15	163	31	135	46	125
16	154	32	125	62	129
17	145	33	125	63	125
18	140				

CONFIDENTIAL

Nozzle exit cone temperatures. (U)



List of References

(U) 1. Kreith, Principles of Heat Transfer, p. 286, International Text Book Co., 1963.

2. McAdams, Heat Transmission, p. 89, McGraw-Hill 3rd Edition, 1954.

3. Bartz, D. R., A Simple Evaluation for Rapid Estimation of Rocket Nozzle Convective Heat Transfer Coefficients, pp. 49-51, Jet Propulsion, Jan. 1957.

C. Reliability Analysis

1. Failure Mode Analysis

(C) The results of a component failure mode analysis for a large solid propellant propulsion system employing the expandable "E" dome design concept are shown in Figure 49.

(C) The major failure modes can be grouped according to the effect on overall system reliability as follows:

- A component failure results in immediate system failure.
  P (system failure/single component failure) = 1.

- A component failure will not result in immediate system failure. However, a series of such failures could result in system failure.
  P (system failure/single component failure) $\neq$ 1.

(C) Those failures resulting in immediate system failure are:

- Mechanical failure due to bearing seizure, jamming of tape, tearing of belt in chute, and extrusion of "E" dome material between sprocket wheel and housing.

- Permanent loss of continuity in the fire circuit due to failure of igniter contacts.

- Pulser housing and motor damage resulting from capsule explosion while caps are in non-firing locations.

- Failure of electronic equipment (power supply, pulse generator, logic and fire circuits (these are not included in the failure mode analysis), stepping motor winding and brushes.

(C) Those failures which will not result in immediate system failure are:

- Missed ignition due to failure of pyrofuze wire or igniter overspray (listed as "dud" in the failure summaries).

WSR-101 Motors ("E" Dome Capsules)

Component	Failure Mode	Assumed Cause of Failure	Effect on System	Compensating Design Features
Expandable Dome	"E" dome: burn through.	Excessive local temperatures.	Possible system failure, performance loss.	Propellant is shielded with an inhibitor thus protecting the sides of the dome. Dome has sufficient thickness to withstand the expected ablation.
	"E" dome: seam leak.	Seam separation due to poor adhesion.	Performance loss, possible system failure.	High shear strength adhesives used.
	"E" dome: extrusion.	Excessive local pressures.	Possible system failure.	All edges on "E" dome have extra material. Control on clearance between OD of sprocket wheel and ID of housing.
Nozzle Base Assembly	Base: gas leak or burn through in any part of the nozzle base assembly.	Excessive local temperatures and pressures.	Performance loss, possible system failure.	Material of high ablative temperature is used, also protected by inhibitor. Hydrotest has shown nozzle base rupture pressure safety margin of 3.25.
Urethane Foam Ball	Dome expansion before capsule is in firing position.	Blockage of the vent hole.	System failure.	Quality control monitoring by 100% vacuum testing of capsules.

Figure 49. Failure mode analysis.

WSR-101 Motors ("E" Dome Capsules)

Component	Failure Mode	Assumed Cause of Failure	Effect on System	Compensating Design Features
Propellant	Propellant: physicla break-down, chemical decomposition, loss of energy, loss of ignitabil-ity	Propellant leakage or out-gassing in space environment.	Possible system failure.	Space storable propel-lant demonstrated by vacuum testing.
	Cracked propel-lant grain	Excessive loads during handling	Possible system failure.	Capsules on tape X-rayed
Igniter	Igniter: fails to ignite pro-pellant.	Broken circuit in capsule.	Performance loss.	New capsule immediately advanced to firing position.
	Igniter: delay greater than maximum value specified causing firing out of position.	Improper igniter composition.	Possible system failure.	"E" dome expands almost instantaneously creating friction hence prevent-ing stepping of the motor until pressure is relieved.
	Igniter: rough combustion.	Ignition peak P/t is greater than equilib-rium chamber P/t.	System failure if overpressurization occurs, performance loss.	Capsule designed with sufficient pressure safety margin.
Contacts	Contacts: no ignition contact.	Improper alignment of contacts with brushes.	Performance loss.	New capsule immediately advanced to firing position. Control of capsules onto tape with respect to pitch of

Figure 49 (Continued).

WSR-101 Motors ("E") Dome Capsules)

Component	Failure Mode	Assumed Cause of Failure	Effect on System	Compensating Design Features
Contacts (Cont'd)				capsules, possible off set with each other and perpendicularity in direction of motion.
Contacts	Contact: damage due to arcing.	Capsule not positioned prior to current flow.	Performance loss.	Ignition pulse is synchronized with the movement of the sprocket wheel to ensure capsule positioning prior to current flow.

Figure 49 (Continued).

CONFIDENTIAL

CONFIDENTIAL

Tape and Tape Assembly

Component	Failure Mode	Assumed Cause of Failure	Effect on System	Compensating Design Features
Tape	Tape: jamming.	Twisting and tangling of tape in chute.	System failure.	Chute provides a positive guide during transport.
	Tape: elongation.	Excessive loads.	Probable system failure.	Tape has high resistance to elongation (teflon-fiber glass reinforced).
	Tape: torn or broken.	Excessive loads and bending.	Probable system failure.	Design safety margin of 4.4 based on break strength. Average cycles to failure - 15,000 on the M.I.T. Fold Endurance Tester.
Tape	Tape: burned through.	"E" done corner blow.	Possible system failure.	Sprocket wheel steps out portion of tape that burns through.
	Capsule: sheared off.	Excessive loads.	System failure.	Tape has high lap shear strength.

Figure 49 (Continued).

Pulser System

Component	Failure Mode	Assumed Cause of Failure	Effect on System	Compensating Design Features
Housing	Housing: deflection and/or deformation.	Excessive temperatures and loads.	Possible system failure.	Clearance allowance for sprocket wheel. Design based on deflection criteria in region of nozzle.
	Housing: stress-rupture at firing position.	Excessive loads.	Possible system failure.	"Beefed-up" E-dome minimizes blow-by.
	Screws: stress-rupture.	Excessive vibration and loads.	Possible system failure.	Design safety margin of 0.75 based on shear.
Contact Brush Assembly	Igniter contact spring: fatigue failure.	Excessive vibration and loads.	Possible system failure.	Design safety margin of 1.8 based on 0.2% Yield.
	Igniter contact pin: cold welding.	Excessive contact load and low temperatures.	Possible system failure.	Metals used which resist cold welding. Space qualified material.
	Igniter contact pin: excessive wear.	Excessive loads.	Performance loss.	Contact load is small.
	Igniter contact pin damage due to arcing.	Pin misalignment with "E" dome contacts.	Possible system failure.	Capsule contact foil area provides safety margin.
	Igniter contact pin: jamming.	Contamination.	System failure.	Close clearance between pin and hole in housing.

Figure 49 (Continued).

Component	Failure Mode	Assumed Cause of Failure	Effect on System	Compensating Design Features
	Ignition leads: fail open.	Excessive vibration, temperatures, electrical loads.	System failure.	Leads harnessed and clamped to minimize vibration.
	Ignition leads: short circuit.	Excessive vibration, temperatures, electrical loads.	System failure.	Leads insulated from housing.
Sprocket Wheel Assembly	Sprocket wheel: misalignment, distortion, buckling.	Excessive vibration, loads and temperatures.	Possible system failure.	Clearance allowance to compensate for misalignment. Tapered bearing and locknut prevent axial misalignment.
	Cavities: stress-rupture.	Excessive loads and temperatures.	Probable system failure.	Design safety margins: a. Inter-cavity wall - 1.55 based on 0.2% Yield. b. Side walls - 0.82 based on 0.2% Yield.
	Pinion gear: teeth worn.	Excessive loads and vibration.	Possible system failure.	Surface nitrided resulting in excellent wear properties.
	Pinion or internal gear: teeth broken.	Excessive loads and vibration.	System failure	Pulser testing has shown ability of the gears to withstand overloading conditions.
	Internal gear: teeth worn.	Excessive loads and vibration.	Possible system failure.	Surface nitrided resulting in excellent wear properties.

Figure 49 (Continued).

CONFIDENTIAL

Component	Failure Mode	Assumed Cause of Failure	Effect on System	Compensating Design Features
Sprocket Wheel Assembly	Screws: stress-rupture.	Excessive loads and vibration.	Possible system failure.	Loading on these screws essentially negligible.
	Snap ring: stress-rupture.	Excessive loads and vibration.	Probable system failure.	Axial loads on snap ring negligible.
Bearing	Tapered bearing: seizure.	Excessive loads and improper lubrication.	System failure.	Designed with safety margin based on static capacity.
	Tapered bearing: excessive wear.	Improper lubrication and contamination.	Performance loss, possible system failure.	Controlled bearing contour minimizes wear. Space compatible dry film lubricant is used.
Cover Assembly	Cover: stress-rupture.	Excessive loads and vibration.	Possible system failure.	Design safety margin of 0.74 based on bending stress.

Figure 49 (Continued).

CONFIDENTIAL

Chute

Component	Failure Mode	Assumed Cause of Failure	Effect on System	Compensating Design Features
Belt	Belt: elongation.	Excessive loads.	Possible system	Belt is free wheeling hence essentially no load.
	Belt: tear.	Excessive loads and vibration.	System failure.	Urethane has excellent tear resistance properties.
Inlet and Exit	Guide: misalignment.	Excessive vibration.	Probable system failure.	Guides pinned in designed location.
Bearing	Bearing: seizing.	Contamination.	System failure.	Sealed, self-lubrication space compatible bearings.

Figure 49 (Continued).

CONFIDENTIAL

CONFIDENTIAL

Stepping Motor

Component	Failure Mode	Assumed Cause of Failure	Effect on System	Compensating Design Features
Front & Rear Bearings	Bearing: galling or sticking.	Improper lubrication, excessive loads and vibration.	Probable system failure.	Space compatible dry film lubricant is used.
Brushes	Brushes: excessive wear, fragmentation.	Excessive loads and vibration.	System failure.	Graphite should act as a lubricant at anticipated altitudes.
Brush Return Springs	Springs: permanent set or fatigue failure.	Excessive loads and vibration, overheating.	Probable system failure.	Designed springs with large safety margin.
Armature	Armature: buckling, distortion.	Excessive electrical loads and temperatures.	Probable system failure.	Maintain current within specified limits.
Shaft	Shaft: stress rupture.	Excessive loads and vibration.	System failure.	Stresses introduced by motor onto shaft are essentially negligible.

Figure 49 (Concluded).

(C) . Missed ignition resulting from out-of-synchronization firing.

. Capsule inhibitor failure.

(U) The failure mode analysis lists the existing design features to reduce failure frequency. The following paragraphs discuss the reliability design aspects of the WSR-101 System more fully, including results of design changes incorporated during static and repetitive firing and areas needing further reliability improvement.

(C) The results of the sea level static firings conducted during the development program of the WSR-101 capsule are summarized in Table V. This table presents three major capsule configurations and their effect on capsule performance. The predominant failure modes were "E" dome ruptures because of overpressurization due to inhibitor failure and duds (no ignition) because of a poor joint between the pyrofuze wire and gold lead. The higher failure rate of the vendor assembled capsules was the direct result of going from laboratory assembly techniques to semi-production tooling and assembly methods. The changes to the capsule configuration in conjunction with modified assembly methods resulted in a significant reduction of "E" dome ruptures and a definite improvement in ignition reliability.

(C) Rupture or extrusion of the "E" dome during static firings had a relatively small effect (basically a loss in performance). However when the capsules are fired in the pulser assembly repetitively, this type of failure could result in system failure when the "E" dome material extrudes into the clearance space between the pulser housing and sprocket wheel.

(C) During the initial pulser development firing tests, there were 11 cases of "E" dome failures in the first 29 firings. This was due to excessive clearances between the sprocket wheel and the pulser housing resulting from deflections during firing. This clearance was reduced by incorporating configuration changes to the pulser housing assembly. These modifications increased the reliability in this mode; there was only one failure in the next eleven firings. Although the failure frequency in this mode was further reduced by a modification to the "E" dome, 25 failures in 333 repetitive

Table V. WSR-101 capsule development tests single firings in firing fixture-sea level. (U)

Part No.	Capsule Features Affected By Development	Results of Tests					
		Assembled in WAD Lab.			Semi-Production Assembly (Vendor)		
		Good	Failed	Dud	Good	Failed	Dud
ES148364	a-Contact leads molded into nozzle block b-Pyrofuze wire connection at center c-Inhibitor;consisted of clear Epon 907 plus asbestos powder	114	23	0	34	23	3
ES156912	a-Contact leads attached as loose detail around ends of capsule b-Pyrofuze wire connection at ends of capsule c-Inhibitor; same as ES148364	29	1	0	52	20	5
ES156985	a-Contact leads; same as ES156912 b-Pyrofuze wire connection; same as ES156912 c-Inhibitor; Gengard V57 rubber mold attached to grain with silicone rubber and DC280 contact adhesive.	6	0	0	146	1	0

(C) firings occurred for a 93.5% reliability for this failure mode (Table VI).

(C) Since extrusion of the dome was of particular concern with respect to system reliability, two 25-shot tapes were fabricated using Gen-Gard V-57 material for the E dome instead of Silastic S-55. The Silastic S-55 silicone rubber had been selected because of its excellent elongation properties even at the -30°F temperature. The Gen-Gard V-57 rubber, on the other hand, provides a higher durometer material (durometer of 75 vs. 60 for S-55) and has been used successfully on other programs which did not have such a low temperature operating requirement.

(C) The results of the repetitive firing tests on these two 25-shot tapes proved that the higher durometer material reduced extrusion and increased the reliability of the system. One capsule on each of the tapes produced a high overpressurization. One of these capsules showed no signs of rupture while the other had a minor dome failure. Neither capsule jammed the pulser which would have resulted in a catastrophic failure of the system. A momentary delay from the overpressurization was experienced and was corrected by the servo system.

(U) A minimum clearance must be maintained between the sprocket wheel and pulser housing to provide the maximum area of support for the "E" dome. Therefore, it will be necessary to incorporate a design change to prevent extrusion under any circumstances. One of the changes which could be considered uses a molded high strength material which shrouds the sides of the capsule and would prevent extrusion of the "E" dome material in the event of overpressurization during firing.

(C) A failure to the pulser housing assembly was experienced during the initial repetitive firing tests. The cause of failure was attributed to insufficient venting of the pulser housing assembly. This was resolved by incorporating three 3/8 inch diameter holes in the front and rear face plates and six 1/8 inch and one 1/4 inch diameter holes in the pulser housing between firing ports. Several severe overpressurizations occurred during subsequent repetitive firings, yet the pulser operation was unaffected and no damge was experienced to the pulser assembly.

(C) Brush failure was the other failure mode causing system shutdown during the repetitive firings. However these failures occurred during early testing and addition of vent holes in the brush holder area plus adding a mechanical stop to prevent the brush from popping out of place eliminated these failures during subsequent firings.

(C) The other failure modes (stepping motor, bearings, transport tape) which could result in an immediate system failure, were not encountered during any tests and are not expected to be major failure modes in the final system.

(U) The stepping motor used in this design has been subjected to a variety of MIL specification tests by the vendor, Photo Circuits Corporation. These environmental tests have included temperature, shock, vibration, radio frequency interference, humidity, sand, dust, salt spray, fungus, high voltage, and life tests. As an example of the extensive durability and reliability testing that has been accomplished, one motor has been pulsed continuously at 60 cps for 19,600 hours with only one observed failure.

(U) The pulser bearings were examined at the end of testing and there was no physical evidence of any damage.

(U) During the repetitive firings and continuity checks some of the tapes were passed through the pulser 30 - 40 times. There was never any evidence that the tape caused jamming.

(C) Failure of the belt in the chute appears unlikely. The belt is designed with sufficient safety margin to prevent any tear. Examination of this component at the completion of testing showed no visible damage.

(C) The use of highly reliable components for the electronic subsystems will provide a very high reliability over the relatively short mission times associated with PBPS applications.

(C) From Table VI it is seen that component failures resulting in system failures (jamming and brush failures) totaled 28 (25 + 3) and resulted in an observed reliability for this mode of $R_1 = \frac{333+47-28}{333+47} = .926$.

Table VI. Failure modes of WSR-101 system - repetitive firings. (U)

Failure Mode	Frequency	Effect on System	Remarks
Minor Seam Leaks	42	Small performance loss	These were minor leaks which would still deliver 80%-90% of required thrust.
Overpressurization	14	Performance loss	No significant thrust delivered.
Jamming	25	System failure	All jams caused by capsule failures which allowed the "E" dome material to extrude between sprocket wheel and housing.
Brush failure	3	System failure	Failures occurred during early tests. Design fix incorporated which eliminated this mode of failure.

(C) To determine total system reliability observed during repetitive firing successive performance loss failures, which would cause system failure, must be considered. Overall system reliability is:

$$R_{system} = R_1 \times R_2$$

where

R_1 = probability of catastrophic failure

R_2 = probability of not exceeding allowable consecutive performance loss failures.

(C) It is assumed that at least four consecutive performance loss failure are required for system failure. During the repetitive firings there was no instance of four consecutive performance loss failures. In fact, not even three consecutive failures of this type occurred and there were only a few cases where two in a row were evidenced. Therefore $R_2 = 1$

$$R_{system} = (.926)\ (1) = .926$$

(C) Although in this case $R_2 = 1$, the probability of obtaining consecutive misfires depends upon the inherent ignition reliability and the number of capsules required for a particular mission. The reliability is

$$R_2 = \left[1-(P_f)^{4N}\right]^n$$

P_f = probability of not firing a single capsule

N = number of capsules/pulser

n = number of pulser/system

(C)A high probability of not exceeding the allowable performance loss is obtainable even with a relatively high P_f. For example, if $P_f = .01$, $N = 10{,}000$, $n = 4$, $R_2 = .9996$.

(C) During subsequent development phases design changes will be incorporated to minimize ignition failure. These includes:

. Use of a higher capacity stepping motor to overcome tape drag.

(C) . Determing optimum step time to assure synchronization between the step and fire signals.

(U) The design changes already planned or incorporated, coupled with subsequent comprehensive reliability evaluation and improvement programs, will provide a WSR-101 System which is highly reliable.

2. Maintainability

(C) It is recognized that the Air Force objective for a system is a degree of storability and reliability which precludes any need for check-out and maintenance. The encapsulated solid propellant rocket motor system lends itself to this objective very well. It also has unique characteristics which permit effective check-out and maintenance procedures if required.

(C) The objectives of a Maintainability Program are summarized as follows and are based on a Post Boost Propulsion System.

Maximize

Probability of Mission Success
Probability of Mission Readiness
Ease and Accuracy of Performing Maintenance
Efficiency and Economy of System Development

Minimize

Need for Maintenance
Complexity of Required Maintenance
Maintenance Personnel Requirements
Costs of Maintenance
Time Required for Maintenance

(C) A preliminary review of the maintenance and servicing requirements for a Post Boost Propulsion System shows that only routine checks need be performed to assure operational readiness. The minimal need for maintenance occurs due to the following unique features of the WSR-101 system.

(C) . Modular Concept - The pulser and stepping mechanism can be readily removed and replaced in a system through adequate removable access panels. No special tooling is required and aligning dowels ease replacements.

(C) . Subsystem Isolation - Each axial and ACS subsystem can be isolated and checked out separately.

(C) . Redundant Capsules - Since in the rare event of a misfire there is always a fresh capsule to take its place, no firing tests need be performed to assure readiness.

(C) . Unpressurized Storage - There are none of the problems or unknowns associated with pressurized systems. There is no need for remote pressure instrumentation or leakage monitoring . . . there are no propellant lines or connections to leak or storage tanks to corrode . . . there are no critical components whose readiness cannot be checked such as bladders, propellant valves, burst discs or pressure regulators.

(C) Periodic operational readiness checks of Post Boost Propulsion System can be accomplished using a test console which will provide a functional checkout of the following components.

- ACS and Axial Pulser Actuation
- Axial Nozzle Actuation System
- Ignition Circuit Signal Generation
- Channeling of Step and Ignition Signals through the Malfunction and Priority Circuits
- Pulser System Continuity
- Power Supply Condition

(C) A schematic of the Post Boost Control System and the ground checkout equipment is shown in Figure 69. This schematic shows the major components of the system. The X, Y and Z vehicle computer guidance signals refer to displacement and rotational information while θ, ψ, and ϕ refer to pitch, yaw and roll commands. The self-contained test console with test point connections is shown on the lower left hand side of the schematic.

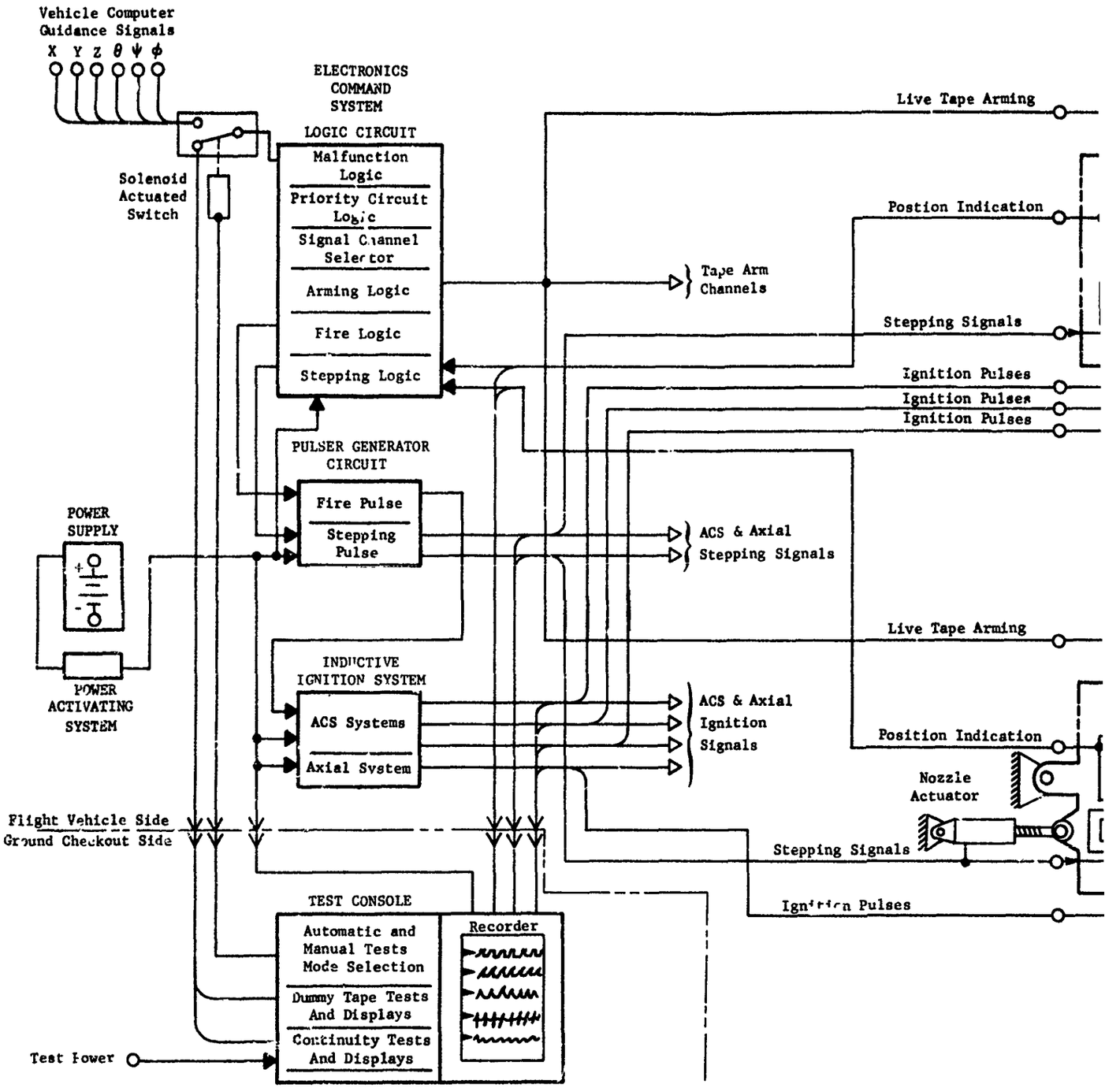


Figure 50. Ground check-out system schematic. (U)

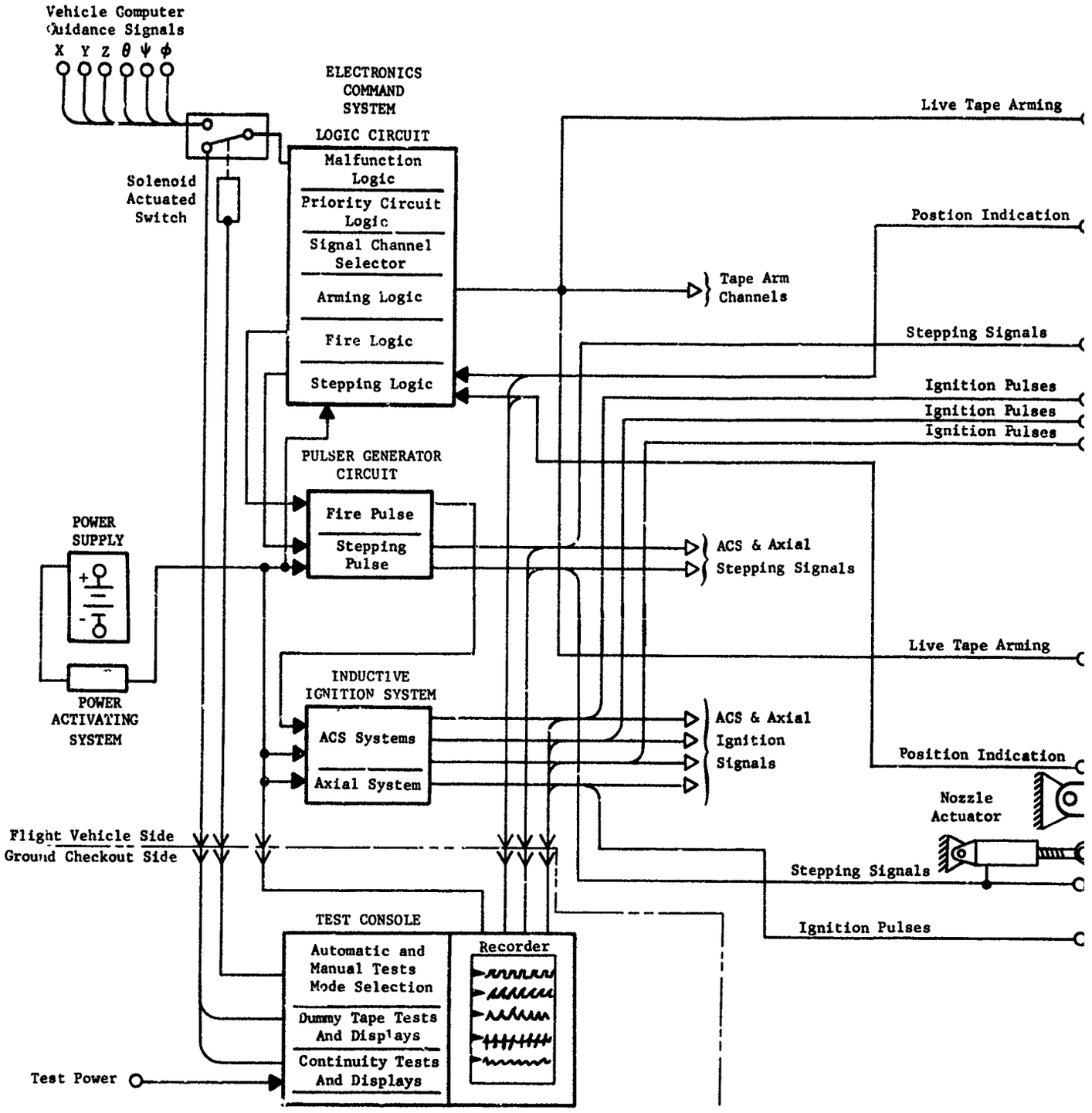
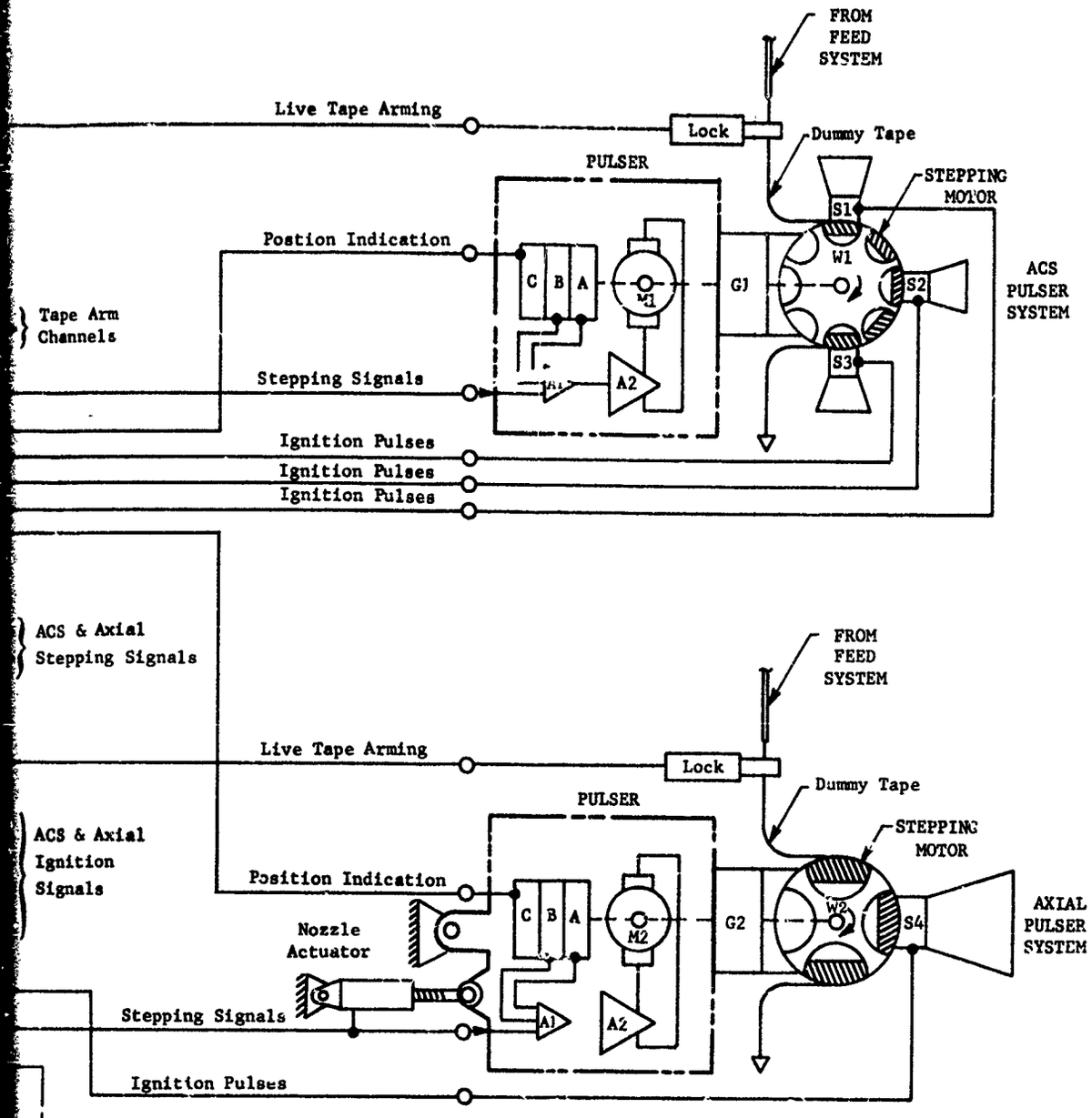


Figure 50. Ground check-out system schematic. (U)



2

system schematic. (U)

(C) The test console and display panel located in the missile control station are connected to the Post Boost Propulsion System guidance input circuit by means of a solenoid actuated switch. Programmed input signals, which simulate operational signals generated by the missile guidance system, are fed to the Post Boost Propulsion System and the feedback controls. Proper functioning of the system components results in specific patterns and readings on the display panel.

(C) To eliminate any introduction of unstable effects, a third potentiometer (C on the schematic) is added to the pulser assemblies to provide an indication of the pulser motor position. The resulting position signal will be displayed on the test console recorder during ground checkout tests. During flight evaluation tests, these signals could serve as a source of telemetered data. The position of the actuator that controls the axial nozzle will be transmitted to the display panel by position indicator limit switches or potentiometers.

(C) The signal generator of the ground test console will feed a series of programmed simulated guidance signals through the Post Boost Propulsion System logic circuits that will step dummy capsules mounted on the initial portions of the tape into firing position. These dummy capsules will have calibrated resistance values, and the receipt of a firing signal at the proper nozzle will result in a correct display on the panel. This checks out the proper functioning of the logic and ignition circuits. Improper signals or malfunctions will result in improper read-outs. A positive mechanical lock precludes the possibility of "live" capsules entering the pulser units. A switching relay will be used to restep the dummy capsules back to their original position.

(U) The state of the battery voltage, servo voltage levels and continuity checks will also be effected from the test console for evaluation.

UNCLASSIFIED

SECTION III

MATERIALS EVALUATION

(U) The selection and evaluation criteria for motor materials were based on design requirements and consideration of methods of component fabrication. Each component of the motor, with the exception of the propellant and the igniter which are reported in Sections IV and V, are detailed separately.

(U) 1. Expandable Dome

At the initiation of the program, the following target values of physical characteristics were established:

Elongation:	Minimum 150%, preferably greater than 300% over the temperature range of + 140°F to -30°F.
Tensile Strength:	Minimum 1500 psi. This was later reduced to 1000 psi based upon design modifications and re-evaluation.
Ablation Resistance:	Low erosion (0.010 inches/second) in the standard ASTM oxy-acetylene torch test.
Space Storable:	No loss of material properties after long term vacuum storage (25 years) and exposure to radiation (2-5 megarads).
Good Snap-back:	Recovery after firing to original volume for high packaging efficiency in the return container.

(U) The expandable dome concept requires a material that will maintain the desired design strength and flexibility through the entire temperature range stated above. Although the General Tire and Rubber Company material (Gen Gard V-57) performed well previously as a dome material in small rocket motors, temperature

UNCLASSIFIED

(U) limitations precluded its use in this program because its elongation is poor at -30°F (Figure 51).

(U) The candidate materials for the dome and their physical properties are listed in Table VII. Values marked with an asterisk (*) were obtained from vendor's data; the remaining data resulted from tests at WAD and oxy-acetylene torch tests at the U.S. Rubber Research Laboratories, Wayne, N.J.

(U) The tensile-elongation samples were prepared by molding the elastomer in a sheet, approximately 6 x 6 x 0.070 inch thick and cutting microtensile samples with a steel rule die. The samples were tested on an Instron Tensile Tester, at a jaw separation speed of two inches per minute.

(U) The Instron Tensile Testing Machine with the cold unit in place for testing at -30°F is shown in Figure 52. The details of the gripping jaws with the insulating flash removed are shown in Figure 53. The oxy-acetylene torch test samples were molded into sheets 4 x 4 x 0.25 inch. The samples were tested by the U.S. Rubber Research Laboratories. The tests were performed by a modification of the standard test described by the tentative method of ASTM Committee D-20, Section III-L. The test results are tabulated in Table VII previously referenced and are shown in Figure 54.

(U) The most promising materials to meet the temperature requirement are the silicones, as they have good low temperature elongation and long term storability. Their major disadvantage is a low tensile strength of less than 1000 psi as compared with ablative rubber compounds at 3000 psi. Silicone ablative compounds have served successfully for the Gemini heat shield but the compounds used for Gemini do not have the strength for a structural membrane as required here. The proven ablation characteristics of the silicones were so attractive that Dow Corning Corporation was contacted for possible new, higher strength compounds. This contact provided information on two new silicone elastometers, Silastic 55 and 955, with tensile strengths exceeding 1000 psi. Their typical properties are:

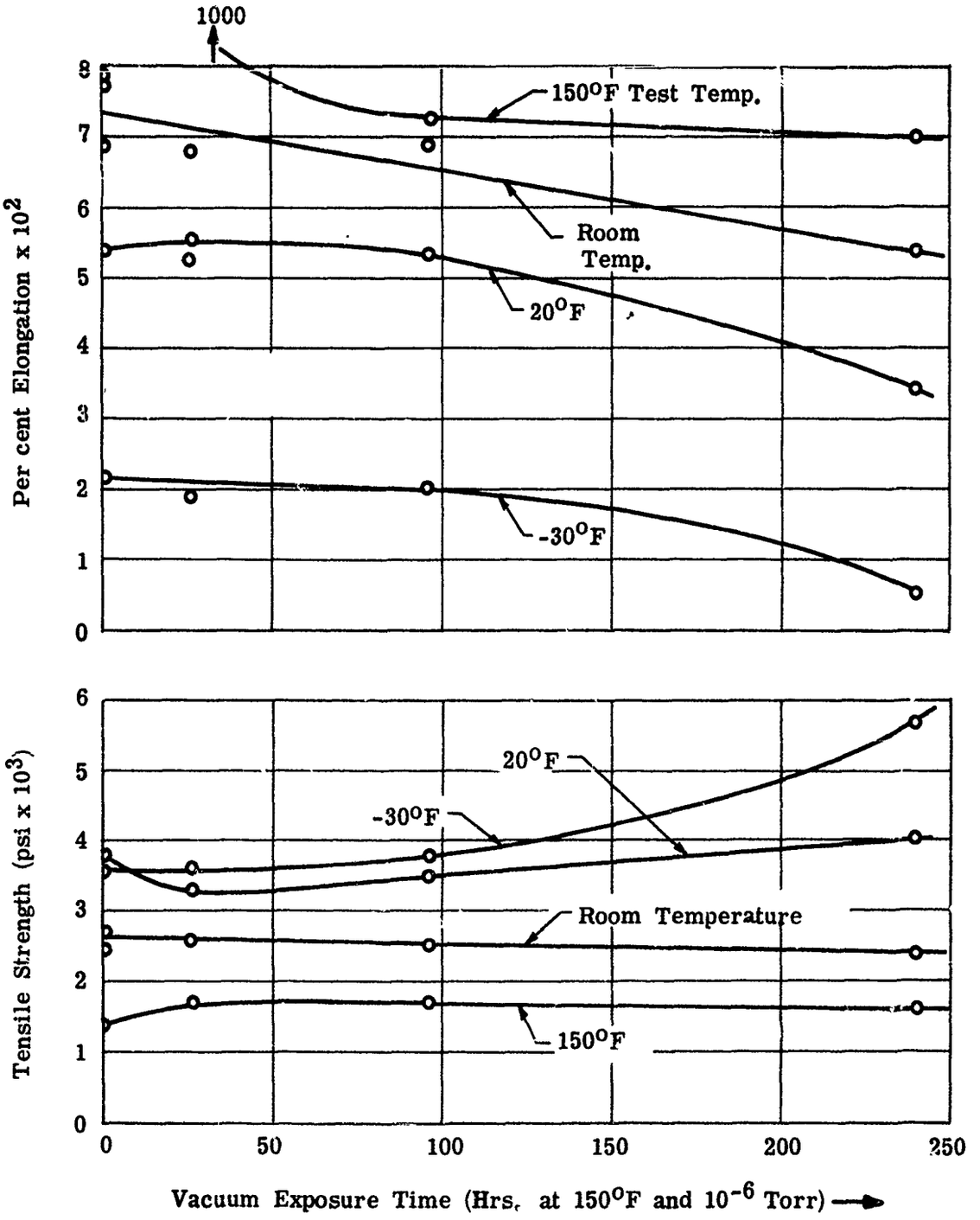


Figure 51. Effect of vacuum storage and temperature on V-57 rubber. (U)

14-650

Table VII. Expandable dome material testing. (U)

Oxy-Acetylene Torch Screening Tests

Application	Material Name	Material Type	Erosion Rate (mils/sec)	Insulation Index (sec/in to 400°F)	Tensile Strength, Psi x 10^3	Elongation % As Molded	Elongation % Aged	Low Temperature Elongation	Material Supplier
E-Dome	Gen-Gard V57, Silica Filled Buna-N		7.9	127.	3.0 ± .5*	700*	375*	Fair	General Tire & Rubber
	Duplicate		7.3	133.	2.6	700			
	Silastic 916, Filled Silicone Rubber		6.1	134.					Dow-Corning Corporation
	Duplicate		6.5	153.	1.0	540	No Change	Excellent	
	Panelyte Grade 5310, Asbestos-Polyisoprene		5.5	154.	1.6*	600*	Lower	Good	Thiokol Panelyte Division
	Duplicate		6.2	135.					
	Gen-Gard V45, Silica Filled Buna-N		6.4	155.	2.0*	450*	200	Fair	General Tire & Rubber
	Duplicate		7.2	128.					
	Gen-Gard V44, Silica Asbestos-Buna N		5.9	153.	.6 to 1.1*	25 to 125*	25*	Poor	General Tire & Rubber
	Duplicate		6.0	155.					
	Garlock 26601, Filled Buna-N		8.6	117.	2.5*	400*	Lower	Fair	Garlock Corporation
	Garlock 47602, Filled Buna-N		12.2	76.	2.5*	400*	Lower	Fair	Garlock Corporation
	Silastic 6557, Silicone Rubber		6.1	148.	1.0*	800*	No Change	Excellent	Dow-Corning Corporation
	Silastic 2048, Silicone Rubber		6.5	152.	.85*	300*	140	Good	Dow-Corning Corporation
	Silastic 1125, Silicone Rubber		9.7	58.	1.1*	450*	No Change	Excellent	Dow-Corning Corporation
	Silastic 2253, Silicone Rubber		22.	45.	1.2*	400*	No Change	Excellent	Dow-Corning Corporation
	Duplicate		23.	44.					
	Asbestos Filled Urethane Rubber		16.7	60.	2.0	420	Lower	Excellent	DuPont
	USR 3009		7.4	122.					U. S. Rubber
	Silastic 55				1.4	500	No Change	Excellent	

Test Conditions:
Oxygen/Acetylene
Vol. Ratio: 1.20
Total Gas Flow
Rate: 225 SCFH
Torch-to-Sample
Distance: 3/4"
Heat Flux:
Approx. 700 BTU/Ft^2/Sec

* Material Supplier's Data

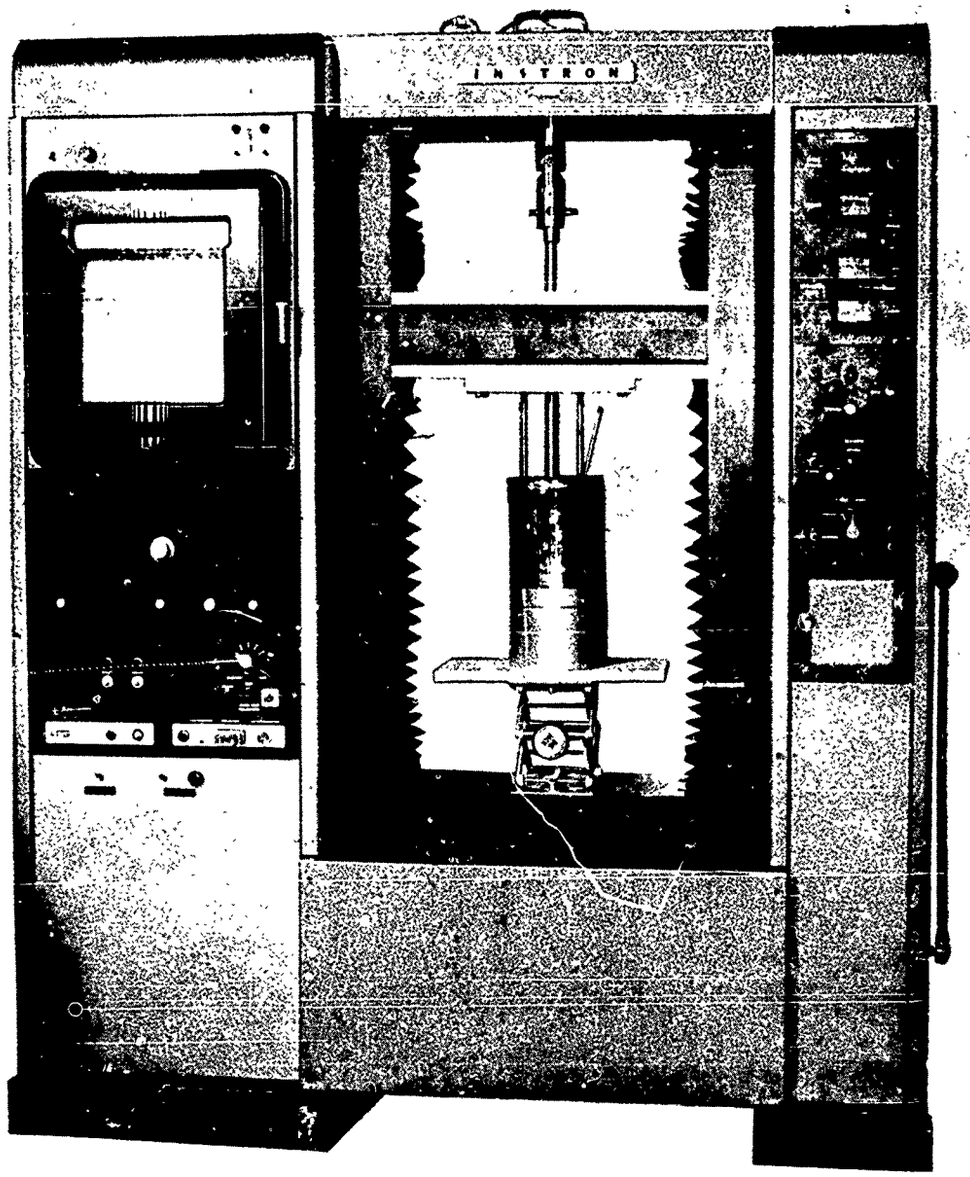


Figure 52. Instron tensile testing machine with low temperature unit in place for dome material tests. (U)

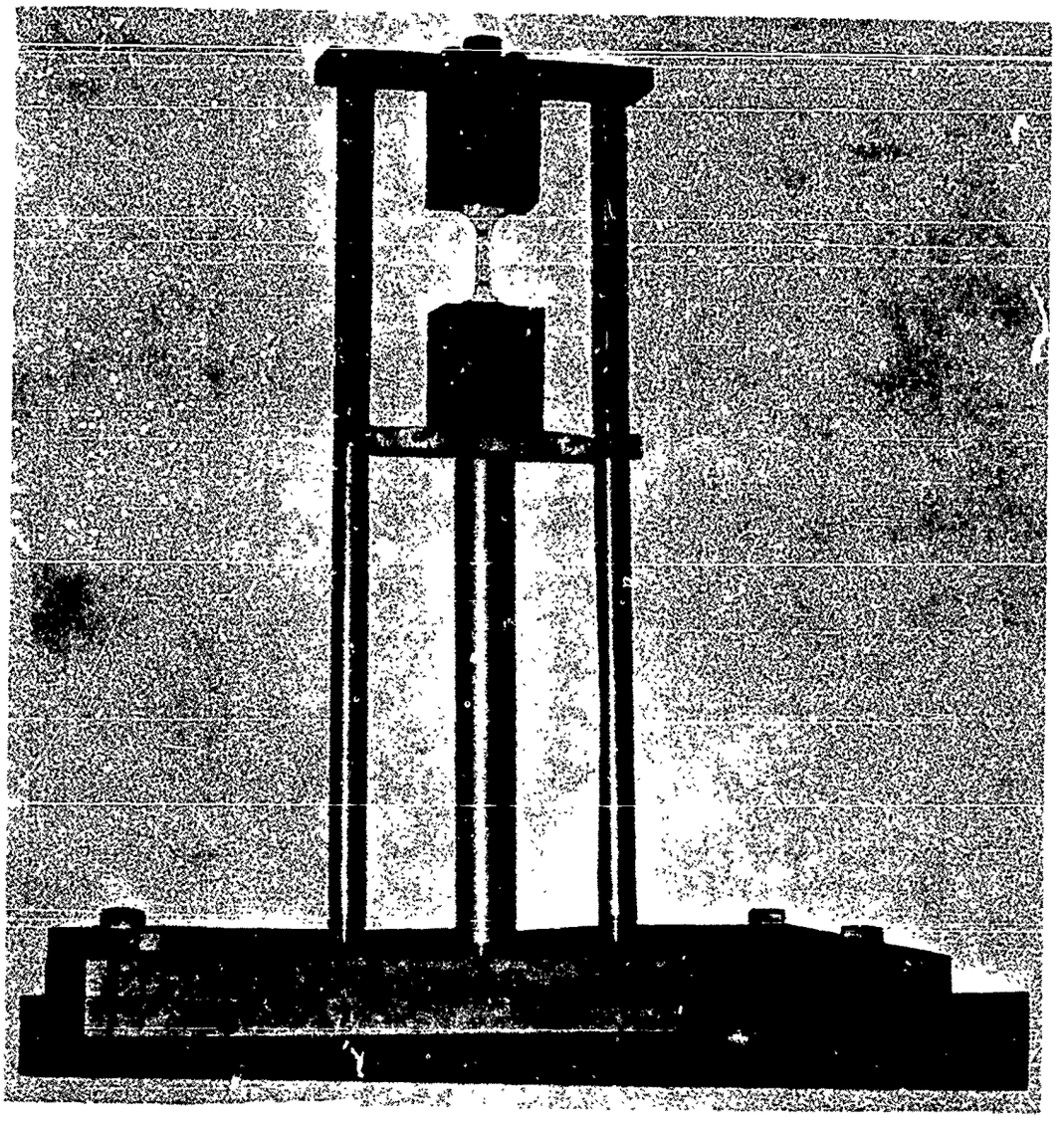


Figure 53. Jaw detail of instron machine with dome material in place and cold jacket removed. (U)

Dow Corning Corporation



Silastic 916
Filled Silicone
Rubber



Silastic 916
Filled Silicone
Rubber



Silastic S-2253
Silicone Rubber



Silastic S-2253
Silicone Rubber



Silastic 2048
Silicone
Rubber

General Tire and Rubber Company



Gen-Gard V57
Silica Filled
Buna-N Rubber



Gen-Gard V44
Silica - Asbestos
Buna-N Rubber



Gen-Gard V44
Silica - Asbestos
Buna-N Rubber



Gen-Gard V45
Silica - Asbestos
Buna-N Rubber

Thiokol Corporation



Panelyte Grade 5310
Asbestos - Polyisoprene
Rubber



Panelyte Grade 5310
Asbestos - Polyisoprene
Rubber

DuPont



Filled Urethane Rubber
DuPont Adiprene L-100
+ Asbestos Fibers

Figure 54. Test samples of dome materials after oxy-acetylene torch test. (U)

(U)

	S-55 + 1.5 parts Cadox TS-50	X-955 + 1.75 parts Cadox TS-50
Tensile Strength, psi	1290	1350
Elongation, percent	550	550
Tear Strength, ppi	170	190
Brittle Point, °F	- 115	- 178

(U) The results of physical tests are listed in Table VII and indicate that the tensile strength is well over 1000 psi. Several domes were molded, assembled on motors, and the motors were fired using the materials noted above. Examination after firing showed an apparent low surface erosion rate and satisfactory performance from a strength viewpoint.

(U) Dow Corning S-55 silicone rubber was finally selected as the dome material. Test firings of motors incorporating this S-55 dome material have been completely successful, indicating that the basic properties of this compound could produce satisfactory performance. Expected erosion rates of less than 0.005 inch/sec have been confirmed. No difficulties attributable to the dome material have been found.

(U) In addition to the test firings made with the S-55 compound, several firings were made with domes of Silastic 955 and Silastic 955 plus 10 phr of quartz powder. These materials also performed satisfactorily and could serve as alternates to the basic choice of Silastic 55.

2. Nozzle Base

(U) In order to select the proper material for the nozzle base the following requirements were established:

Readily molded, primarily by transfer molding.

Erosion resistant, especially at the nozzle throat under firing conditions.

Space storable.

Tensile Strength - 8000 psi minimum.

Flexural Strength - 15,000 psi minimum.

Bondable.

(U) Most of the criteria noted above indicated that a phenolic matrix should be the prime selection for the nozzle base as this material is readily moldable, space storable, bondable, and has good strength properties. Erosion characteristics are imparted by the quartz reinforcement which is superior to second choice glass fibers.

(U) As was done with the dome materials, test specimens were prepared and sent to the U.S. Rubber Research Laboratories, for oxy-acetylene torch tests using the same test method as employed for the dome. These data, along with other physical testing data, are shown in Table VIII and in Figure 55.

(U) Upon receipt of the single cavity transfer mold, moldability tests of the candidate compounds were made. Fiberite FM 4005, a glass fiber filled phenolic, showed excellent molding characteristics as had been found on previous programs. Fiberite FM X1944 and X3106 were too weak and produced pieces that were brittle. A quartz fiber base material, ARP276PHQ, manufactured by American Reinforced Plastics Co., Los Angeles, California was tested and did not mold satisfactorily. Similar results were obtained with Fiberite MX 1344-67, also a quartz filled phenolic. However, the same Fiberite system with a lower fiber content MX 1344-50, had good transfer molding properties. Other compounds that showed good moldability were Fiberite MX 2199A and MX 3264-2, and Allied Chemical Corporation Epial 1907.

(U) A prime concern in this application is erosion at the nozzle throat during firing. Quartz fiber phenolic systems have shown good performance in this regard. As a final selection criterion, motor assemblies were made, fired, and the nozzle bases examined after firing. The Epial 1907 exhibited high throat erosion that was considered excessive for the application. The MX 3264-2 material broke at the nozzle throat during the middle portion of the firing. The thrust-time curves for the MX 2199A and MX 1344-50 indicated adequate performance with respect to throat erosion. Post firing examination of the bases showed that the MX 1344-50 was slightly better than the MX 2199A in erosion characteristics.

(U) Therefore, based on physical tests, molding characteristics, erosion test, and firing of completed motors, Fiberite MX 1344-50, a quartz fiber filled

Figure 55. Test samples of nozzle base materials after oxy-acetylene torch test. (U)

(U) phenolic, was selected as the nozzle base material with the MX 2199A as a back-up.

3. Nozzle Closure Plug and Adhesive

(U) The two prime candidates for the nozzle closure plug were styrene foam and urethane foam. These materials will seal the nozzle, are light in weight, and have good space storability. Table IX details the test results of these materials in conjunction with the adhesive required for their retention.

(U) The tests were performed by sealing the plug into a molded nozzle attached to a threaded fitting as shown in Figure 56. After exposure to the vacuum-temperature conditions noted, the fittings were pressurized to expel the plug and the expulsion pressure was recorded.

(U) Based on the test data, the material selected for the nozzle closure plug was a urethane foam, Nopcofoam A-216, manufactured by Nopco Chemical Company, Newark, N.J. This urethane plug with Dow Corning Aerospace Sealant 92-018 as the adhesive, produced the most consistent and satisfactory results under all test conditions. This combination was chosen as the final configuration for the closure system.

4. Transport Tape

(U) The basic requirements for the tape used to carry the capsules from the storage container through the pulser into discard include space storability, bondability, high break strength and non-stretching. Experience on previous programs had shown that fiberglass reinforced Teflon was suitable with the exception of its marginal ability to bond to the capsules. A stress-strain curve of a Teflon-Fiberglass tape is shown in Figure 57 which indicates adequacy for the application.

(U) An effort was made to obtain a tape with better bonding characteristics than the Teflon tape. Five samples of urethane-fiberglass tape were obtained from Gen-Tape Corporation, Bloomfield, N.J. These samples were tested on an M.I.T. Fold Endurance Tester at a load of 1.5 Kg. and by vacuum exposure.

Table VIII. Nozzle closure plug tests.(U)

Test No.	Plug Material	Adhesive	Vent Hole in.	Test Temp. °F	Vacuum Exposure Conditions	Gas Pressure - psi	
						Leakage	Blow-out
1	Urethane	Pliolite 491	None		Ambient	100	250
2	Foam, 5#/ft.^{3}	Pliolite 491				100	375
3		Pliolite 491				75	600
4		Pliolite 491				50	650
5		Pliolite 170				-	170
6						20	40
7						-	120
8						-	185
9			.006			-	160
10						-	120
11						160	180
12						-	175
13					Vacuum 10^{-6} Torr.	150	160
14					20 Hrs. @ 142°F	160	300
15					25.5 Hrs. @ Ambient	40	320
16						120	290
17						50	280
18						-	280

Table VIII (cont). Nozzle closure plug tests (U)

Test No.	Plug Material	Adhesive	Vent Hole in.	Test Temp. °F	Vacuum Exposure Conditions	Gas Pressure - psi	
						Leakage	Blow-out
19	Molded				Vacuum 10^{-7} Torr.	40	600
20	Styrene				25 Hrs. @ 140°-150°F	600	900
21	Foam				17.5 Hrs. @ Ambient	120	475
22						40	660
23						40	590
24						80	180
25						40	960
26						-	620
27						280	500
28						500	620
29		Pliolite 170	.006		17.5 Hrs. @ Ambient	200	200
30						200	200
31						260	280
32						20	300
33						20	240
34	Molded				Vacuum 10^{-5} Torr.	28	290
35	Urethane				21.3 Hrs. @ 150°F	-	330
36	Foam					-	270
37						-	190
38						-	270
39						200	260
40						110	300
41						-	350

Table VIII (cont). Nozzle closure plug tests (U)

Test No.	Plug Material	Adhesive	Vent Hole in.	Test Temp. °F	Vacuum Exposure Conditions	Gas Pressure - psi	
						Leakage	Blow-out
42	Molded Urethane Foam	Pliolite 170 Top Cover Film Bond (1)	.006	-31	10^{-6} - 10^{-7} Torr @ 140 - 150°F / 19 hrs	35	200
43			.006	-31		400	900
44			.006	-31		380	1000
45	Used Thru Test No. 49	Used Thru Test No. 49	.006	-31	Used Thru Test No. 49	0	40
46			.006	150		0	0
47			.006	145		0	0
48			.006	149		0	0
49			.006	145		0	0
50	Molded Urethane Foam	Dow-Corning Aerospace Sealant 92-018 Side Bonded (2)	.006	150	None	120	280
51			.006	150	None	30	140
52			.006	150	None	100	160
53	Used Thru Test No. 57		.006	150	None	40	240
54		Dow-Corning Aerospace Sealant 92-018 Top Cover Film Bond (1)	.006	150	None	0	0
55			.006	150	None	0	0
56			.006	150	None	10	0
57			.006	150	None	0	0
58	Molded Styrene Form	Dow-Corning Aerospace Sealant 92-018 Side Bonded (2)	.006	150	10^{-7} Torr @ 146° to 153°F / 30 hrs	0	20
59			.006	150		0	30
60			.006	150		0	40
61			.006	Room		0	100
62	Used Thru Test No. 65	Used Thru Test No. 65	.006	Room	Used Thru Test No. 65	0	100
63			.006	-30		0	40
64			.006	-30		5	20
65			.006	-30		0	120

Table VIII (cont), Nozzle closure plug tests (U)

Test No.	Plug Material	Adhesive	Vent Hole in.	Test Temp. °F	Vacuum Exposure Conditions	Gas Pressure - psi	
						Leakage	Blow-out
66	Molded Urethane Form	Dow-Corning Aerospace Sealant 92-018 Side Bonded (2)	.006	150	2×10^{-7} Torr @ 152°F / 20 hrs	0	380
67			.006	150		80	100
68			.006	150		0	120
69			.006	Room		100	120
70	Used Thru Test No. 73	Used Thru Test No. 73	.006	Room	Used Thru Test No. 73	10	180
71			.006	-30		0	260
72			.006	-30		0	265
73			.006	-30		0	300
74	Molded Urethane Form	Dow-Corning Aerospace Sealant 92-018 Side Bonded (2)	.006	150	10^{-7} Torr @ 141° to 170°F / 146 hrs	0	260
75			.006	150		0	180
76			.006	150		0	160
77			.006	Room		0	180
78	Used Thru Test No. 81	Used Thru Test No. 81	.006	Room	Used Thru Test No. 81	100	150
79			.006	-30		0	240
80			.006	-30		0	160
81			.006	-30		0	240
82	Molded Urethane Form	Dow-Corning Aerospace Sealant 92-018 Side Bonded (2)	.006	150	8×10^{-5} - 2×10^{-4} Torr @ 130 - 150°F for 670 hrs	0	380
83			.006	150		0	180
84			.006	150		0	170
85			.006	Room		0	280
86	Used Thru Test No. 89	Used Thru Test No. 89	.006	Room	Used Thru Test No. 89	160	290
87			.006	-30		0	380
88			.006	-30		200	500
89			.006	-30		0	220

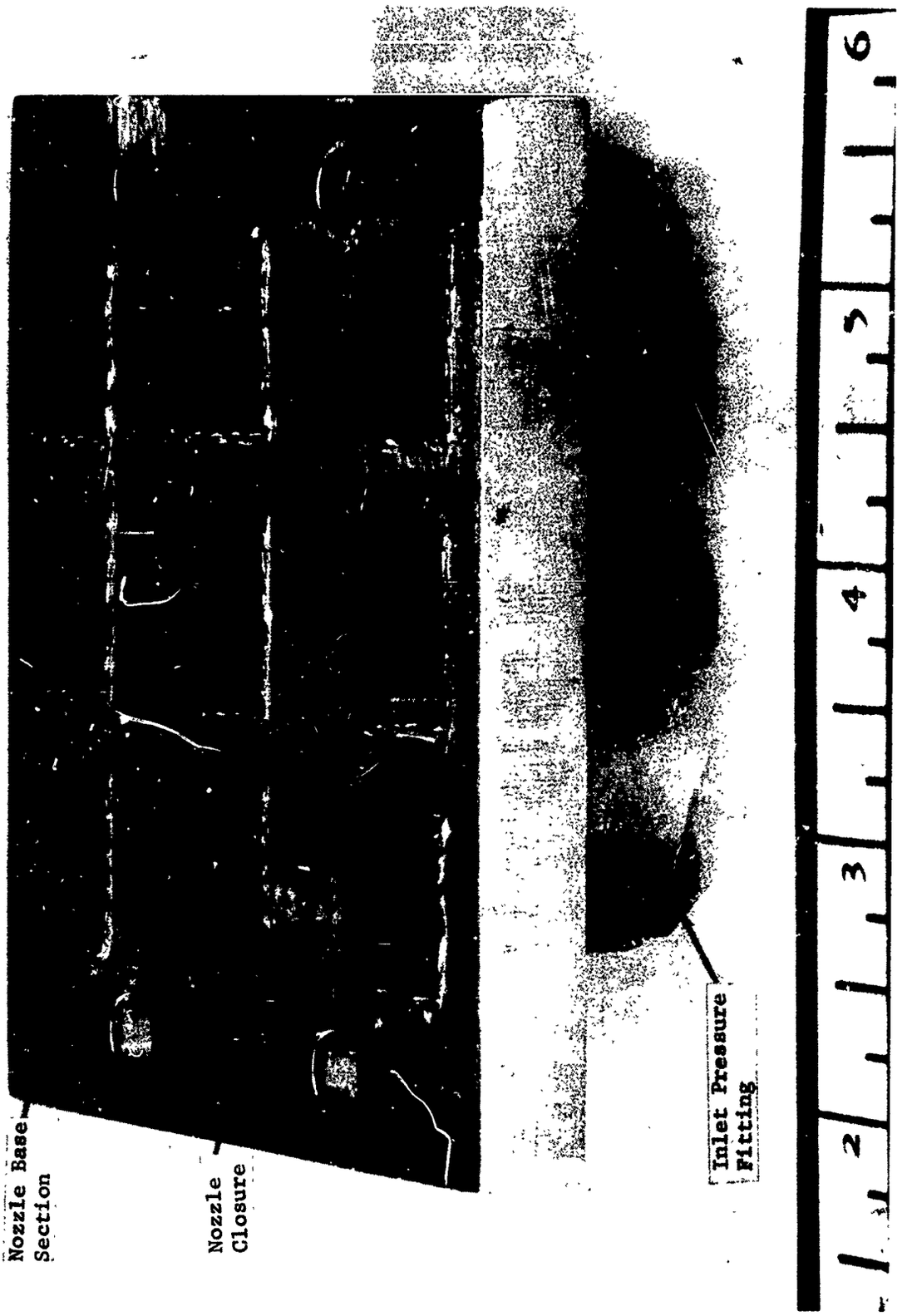


Figure 56. Nozzle closure test fixture. (U)

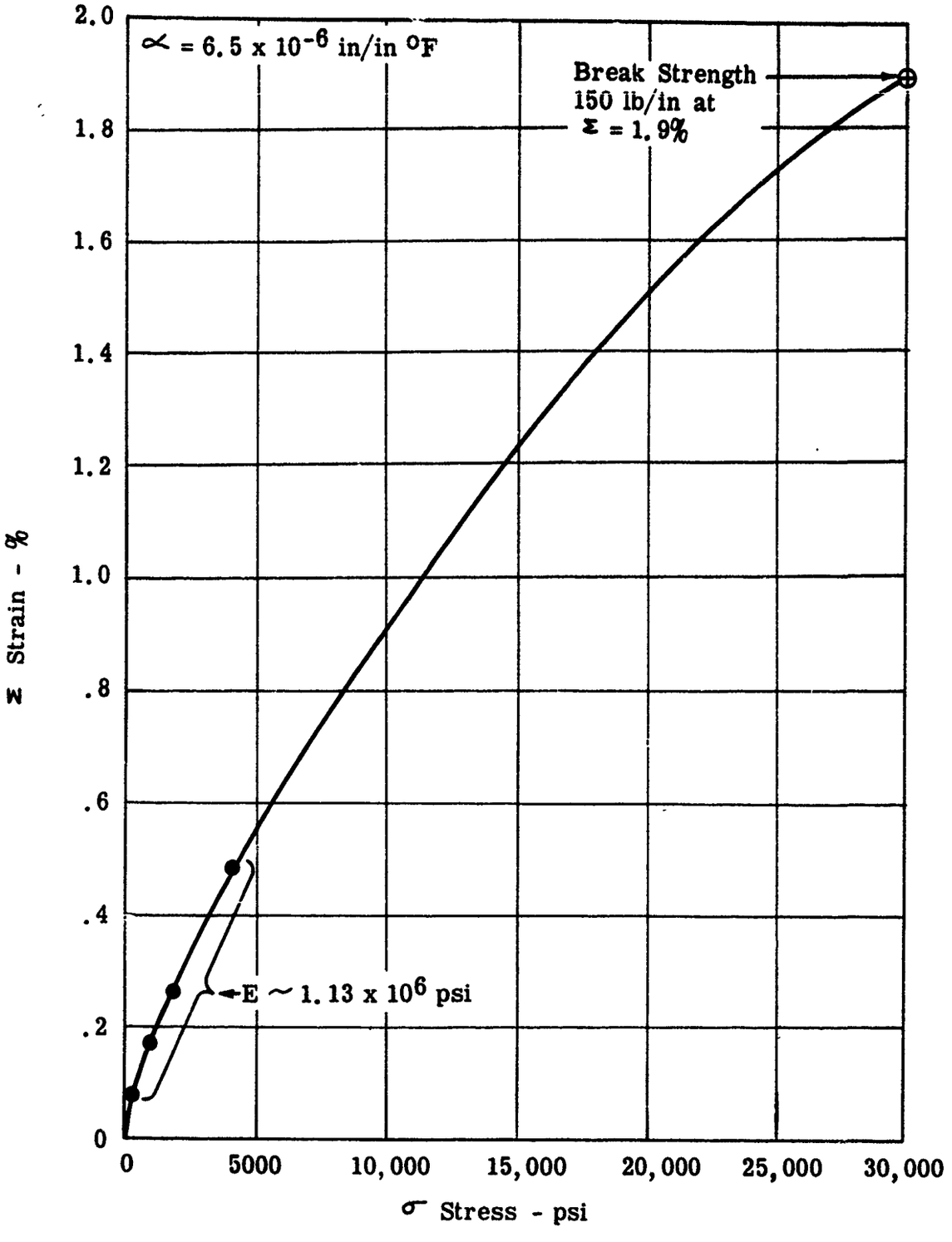


Figure 57. Capsule transport tape TB-5E tape .004-.005 thick. (U)

(U) The data obtained on these materials is listed below:

Material	Fold Endurance, Cycles to Failure	Advantages	Disadvantages
(U) Teflon-Fiberglass TB-5E	15,000	Good vacuum stability. High temperature resistance	Low bond peel strength. Low radiation resistance
Urethane-Fiberglass A	20	- - -	Poor fold endurance
Urethane-Fiberglass B	18	- - -	Poor fold endurance
Urethane-Fiberglass C	50	- - -	Poor fold endurance
Urethane-Fiberglass 4	100,000	Good vacuum stability. Good bond peel strength	Heat seals @ 150°F
Urethane-Fiberglass 5	20,000	Not "heat" sealable. Good bond peel strength	Poor tear resistance

(U) The Teflon-Fiberglass tape met the requirements of the program while the urethane base tapes were unsatisfactory for the reasons noted in the table above.

Dow Corning Aerospace Sealant 92-018 with 4094 primer proved adequate for attachment of the motors to the tape as shown in Table X.

5. Dome to Nozzle Base Adhesive

(U) The choice of a silicone material for the expandable dome created some difficulty in the selection of a suitable adhesive as the silicones are not readily bonded by standard adhesives. The original target specification for this adhesive called for a bond strength of 1000 psi. Later design analysis of the capsule reduced this value to 200 psi which was adopted as the minimum

Table IX. Lap shear adhesive tests as applied to tape. (U)

Tape Material: Teflon-Fiberglass

Adhesive: Dow Corning Aerospace Sealant 92-018

Primer Used	Lap Shear Bond Strength, psi*
None	49.8
1200	158.2
4094	214.0

* Average value of three (3) determinations

Lap shear test: Bonded area - 1/2 x 1/2 inch

Rate of jaw separation - 2.0 inch/min.

(U) bond strength requirement. This lower value eased the problem as silicone compatible adhesives in this strength range were obtained from silicone suppliers.

(U) Lap shear test specimens were prepared using a 1/2 x 1/2 x 0.070 inch square of Silastic 55 filled with 25 parts by weight of Min-U-Sil bonded between two panels of MX 1344-50 1/2 x 1 1/2 x 3/8 inch with the overlap area measuring 1/2 x 1/2 inch. The panels of MX 1344-50 were prepared by blasting with sodium bicarbonate powder and wiping with solvent, Methyl Ethyl Ketone. The Silastic 55 was solvent wiped with Methyl Ethyl Ketone. Adhesive was applied on each panel of MX 1344-50 and the Silastic 55 was placed between them and the assembly was clamped together for cure. The specimens were pulled apart on an Instron Tensile Test machine at a jaw separation speed of two inches per minute. The test data obtained are shown in Table XI.

(U) Dow Corning Aerospace Sealant 92-018 was chosen as the dome to nozzle base adhesive based on the results of the tests described above. The use of a primer was shown to be advantageous as the bond strength was increased by a factor of 4. When applied to the treated surface of the Teflon tape, these primers are also effective in increasing the bond strength of the capsule to the tape. Dow Corning Silicone Primer 4094 was chosen as being the most effective primer.

6. Propellant Inhibitor

(U) In the early phases of the program, propellant inhibition to assure burning from a single surface was accomplished with asbestos filled epoxy resin which was molded around the propellant grain. This inhibition system was found to be laborious and inconsistent in results.

(U) A pre-molded inhibitor was designed and fabricated from General Tire and Rubber Company Gen Gard V-57 as shown in Figure 58. Previously acquired data had shown that Gen Gard V-57 had good ablative properties along with other characteristics typical of an elastomer. When this premolded inhibitor was assembled into motors with suitable adhesives it produced results that were far superior

(U) to those obtained with the epoxy systems. Better control of propellant burning was also obtained as well as a signifficant improvement in consistency. The premolded inhibitor system was used for all motors for the program.

Table X . Dome-to-nozzle base adhesive tests. (U)

Elastomer	Plastic	Adhesive	Primer	Lap Shear Bond Strength (psi)
Dow Corning Silastic 55	Fiber-Filled Phenolic	Dow Corning 92-018	None	90
As Above	As Above	As Above	Dow Corning 1200	440
As Above	As Above	As Above	Dow Corning 4094	370
Dow Corning Silastic 916	As Above	Dow Corning RTV 781	Dow Corning 1200	180

* Specimen: Lap Shear Test. Bonded Area: 1/2 x 1/2 inch

Rate of jaw separation: 2.0 inch/min.

All values are the average of at least three tests.

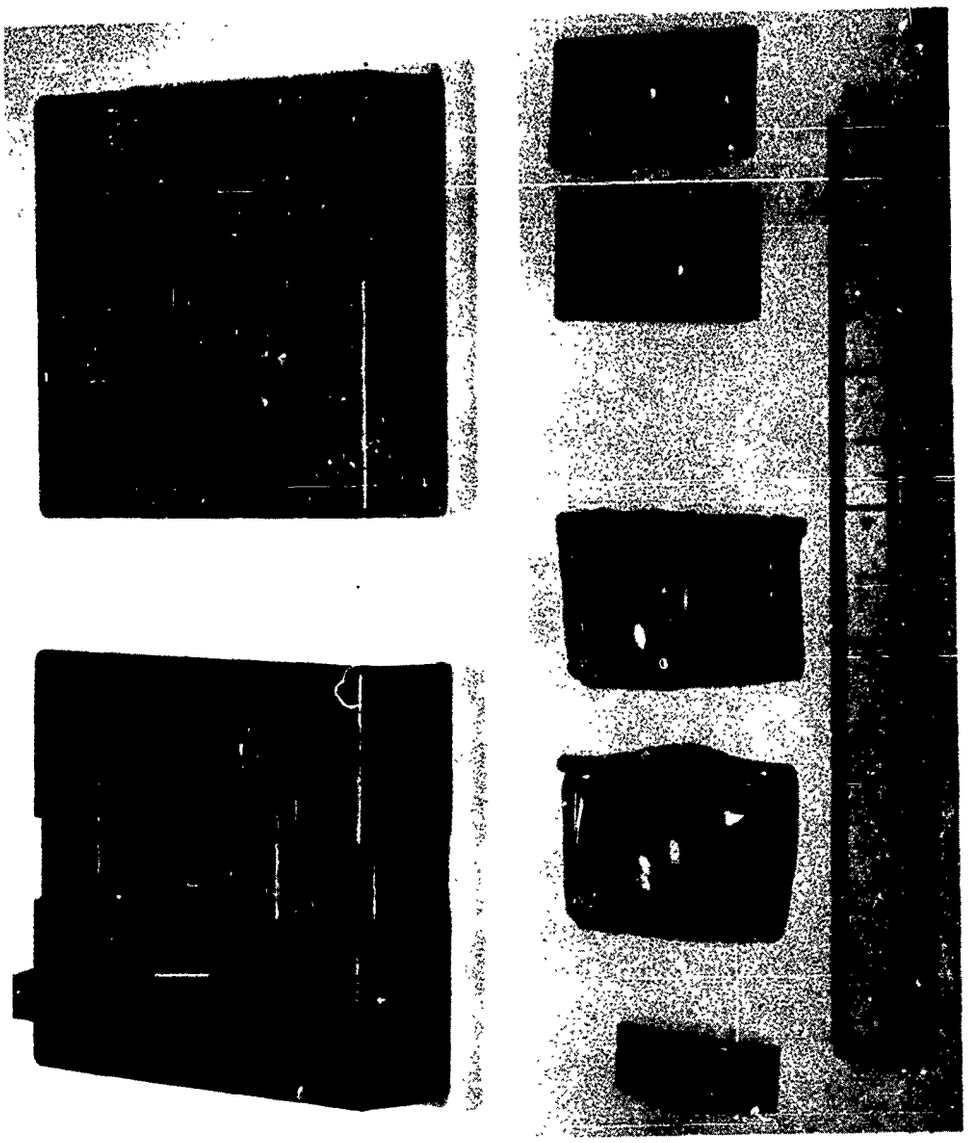


Figure 58. Boot inhibitor and mold. (U)

UNCLASSIFIED

SECTION IV

IGNITER DEVELOPMENT

(U) As an integral part of the program, an igniter study was conducted on a dual approach basis. The objective was the development of a space storable, fast action, reliable igniter that could be fabricated with a minimum of difficulty and, if possible, qualified independently of the other rocket motor components. One facet of this dual approach was a study of various pyrotechnic compositions and fabrication techniques labled Experimental. The other facet continued development of the spray ignitier system devised for previous generation motors aimed at qualification of the system for the WSR-101. This study is labeled Spray Igniters.

1. Experimental Igniters

(U) The experimental igniters studied were primarily of the metallized "high heat content" pyrotechnic type which would produce a minimum of gaseous decomposition products. The development Program Plan included: (1) a screening study based on theoretical heat content, (2) characterization of small size mixes for thermal and shock sensitivity, (3) process development with respect to fabrication, and (4) final characterization through motor firings.

(U) From experience with the previous generation motors it has been found that metallized pyrotechnic compositions achieve fast and efficient ignition of the solid propellant. Therefore, metal additions with various types of oxidizers were considered. The results of the study covering calculated flame temperatures and heats of reaction for five (5) metals in combination with three (3) different inorganic oxidizers is given in Table XII. While the high adiabatic flame temperatures of zirconium and aluminum mixtures made them prime candidates, the high heats of reaction of aluminum, magnesium, and boron were equally attractive.

(U) For preliminary characterization, a group of seventeen (17) pyrotechnic mixtures of metal powder and inorganic oxidizers were prepared in stoichiometric proportions. Deliberate control of particle size was maintained as they exert a major influence on the rate of combustion. Standard autoignition tests,

UNCLASSIFIED

Table XI. Stoichiometric mixtures of metals and oxidizers (U)

Constituents	% Metal	Heat of Reaction Cal/gram	Maximum Adiabatic Flame Temp. °K
Z_R/K Cl O_4	56.8	1584	4600
Z_R/Ba $(NO_3)_2$	46.6	1105	4000
Z_R/KNO_3	53.0	1149	3500
Al/K Cl O_4	34.2	2490	3800
Al/Ba $(NO_3)_2$	25.6	1594	3800
Al/K NO_3	30.8	1761	3800
Mg/K Cl O_4	41.2	2433	3350
Mg/Ba $(NO_3)_2$	31.8	1627	3350
Mg/K NO_3	37.5	1784	3350
Ti/K Cl O_4	48.0	1805	3300
Ti/Ba$(NO_3)_2$	37.9	1204	3300
Ti/KNO_3	44.2	1275	3300
B/K Cl O_4	17.2	2356	3340
B/Ba $(NO_3)_2$	12.1	1341	2520
B/K NO_3	15.2	1495	2520

(U) impact sensitivity, and relative "quickness of burn" tests were conducted on all of the mixtures as shown in Table XIII.

(U) As might be expected from the known nature of zirconium powder, its autoignition temperature was the lowest of all metals used as was its ignitability. While the actual ignition temperatures were not dangerously low, it does indicate a lower safety factor than that encountered with the other metals tested. Impact sensitivity was generally similar for zirconium, aluminum and magnesium while that for boron was appreciably higher.

(U) On a basis of overall comparison, the use of zirconium was terminated as the data did not reveal any significant advantage for its use. The relatively high weights of the metal that were required could affect the overall mass ratio of the system, albeit a small affect; the fairly easy ignition posed a possible safety factor; a very real safety problem in zirconium powder handling during fabrication; and an apparent lack of need for its high adiabatic flame temperature dictated the elimination of zirconium from the program.

(U) The aluminum and magnesium powders in combination with the inorganic oxidizers exhibit a pyrotechnic "sparkler" effect with metal particles showing a long "after burn" relative to the primary combustion. The "sparkler" effect is not considered to be detrimental as it may aid in propogation of ignition over the surface of the propellant grain.

(U) Aquisition of the data described above moved the experimental ignitier work to the next stage, the search for a suitable binder to make the powders useable. Two binders were investigated, nitrocellulose (NC) and polyisobutylene (PIB). The formulations using the NC are shown in Table XIV and were made with single metal powders and single oxidizers in an effort to achieve proper balance between burn rate, ease of processing, and reproducibility. At ambient pressure the magnesium fuel and ammonium perchlorate oxidizer burned rapidly but a fairly high exotherm was observed during mixing operations in which magnesium was used. While the NC has good stoichiometry, fast burning characteristics, stability, and good adhesive properties, the tendency to exotherm when mixing with metallic powders makes its use less than desirable.

Table XII. Experimental pyrotechnic mixtures, weight percent (U)

	1	2	3	4	5	6	7	8	9	10	11	12	13	14	15	16	17
Zirconium	56.8	46.6	53.0	49.2	21.3												
Aluminum						34.2	25.6	30.8	27.7								
Magnesium										41.2	31.8	37.5	34.2				
Boron														17.2	12.1	15.2	13.3
Potassium Perchlorate	43.2					65.8				58.8				82.8			
Barium Nitrate		53.4					74.4				68.2				87.9		
Potassium Nitrate			47.0					69.2				62.5				84.8	
Ammonium Perchlorate				50.8					72.3				65.8				86.7
Barium Chromate					78.7												
Temperature at No Ignition in 3 Minutes (AIT) °C (1)	330	320	330	335	350	>360	>360	>360	>360	>360	>360	>360	>360	>360	>360	>360	>360
Impact Sensitivity, Inches to Impact (2)	3-4	4-5	3-4	3	NI	3-4	2-3	2	3-4	4	1-2	3-4	1/2 tol	5-6	8-9	10-12	5-6
Match Flash Test, Relative Quickness (3)	1	1-2	1-2	2	5	2	2-3	2-3	3	2	3	2	2	4	4	4-5	5

Note: (1) Metal-Oxidizer Prepared In Stoichiometric Proportions
(2) By Impingement With Ball Peen Hammer
(3) Designated By One (1) For Very Fast Burn To Five (5) For Very Slow Burn

Table XIII. Experimental igniter formulations (U)

Batch	1	2	3	4	5	6	7	8	9	10	11	12	13	14	15
AL (5 Micron)	24.93	25.38	26.61	27.71	28.62	29.52	30.77	31.75	32.83						
MG (325 Mesh)										32.97	37.08	30.00	33.74	27.38	30.77
NH_4 CLO_4 (200 Mesh)	65.07	67.22	69.39											52.62	59.23
KNO_3 (200 Mesh)				62.29	64.38	66.48						50.00	56.26		
$KCLO_4$ (200 Mesh)							59.23	61.25	63.17	47.03	52.92				
Nitrocellulose	10.00	7.00	4.00	10.00	7.00	4.00	10.00	7.00	4.00	20.00	10.00	20.00	10.00	20.00	10.00

(U) In an effort to provide improved balance in the overall composition, seven (7) igniter batches were prepared using a combination of metal powders with potassium perchlorate and both NC and PIB as binders. These formulations are described in Table XV. Five (5) rocket motor tests were made with the magnesium base ignitiers and five (5) tests were made with those containing aluminum. These test results were mixed in that ignition delays were not consistent and some motor rupture occurred. The need for more intimate contact between the igniter and propellant was indicated as was modification of the initiation device. While some promise was indicated, it was felt that sufficiently consistent results were not being obtained for adoption into the WSR-101 system.

(U) A prime objective of these igniter experiments was the independent fabrication and qualification of the igniter. To this end, the igniter compositions were applied to various carrier media to which a 0.004 inch Pyrofuge wire had been attached. Various support films were used including Teflon, aluminum, and paper of 1 mil thickness. The igniter mixtures were then applied by buttering and by use of a doctor blade. Sufficient difficulty was encountered in these fabrication techniques with inconsistency, reproducibility, and overall quality to make this system very difficult to handle.

(U) In view of the results of the experiments in igniters where no significant improvement over the basic ignition system used in previous generation motors was obtained, the experimental work was terminated. Efforts were directed to modification and sophistication of the previously used technique as described below.

2. Spray Igniter

(U) A spray type igniter was selected as being the most feasible and reliable for the final motor configuration. This ignition system incorporates a Hi-R, 0.004 inch diameter Pyrofuze initiator and a pyrotechnic booster for ignition of the propellant. The study of the spray igniter was pursued independently of the experimental work with continuous cross exchange of data.

(U) The spray igniter system consists of suspension of the metallic fuel and oxidizer in a volatile solvent in which the binder is dissolved. This mixture is applied with a small spray gun by carefully controlled spraying

Table XIV. Motor tested experimental igniter formulations. (U)

Batch No.	16	17	18	19	20	21	22
Composition							
Magnesium	32.5	34.3	34.3	-	-	-	-
Aluminum	-	-	-	26.2	26.2	20.0	20.0
Boron	4.5	4.7	4.7	4.5	4.5	3.0	4.0
$KClO_4$	53.0	56.0	56.0	59.3	59.3	72.0	72.0
Polyisobutylene	10.0	5.0	-	10.0	-	5.0	4.0
Nitrocellulose	-	-	5.0	-	10.0	-	-
Total Weight %	100.0	100.0	100.0	100.0	100.0	100.0	100.0

(U) conditions covering air pressure, distance, number of passes, and spraying speed. The solvent is evacuated in a vacuum oven so that a weight controlled, reproducible layer of pyrotechnic results.

(U) The previous experience gained with previous generation rockets was utilized to develop a suitable igniter for the WSR-101. The igniter system basically was scaled up from smaller rocket motors (0.1 lb-sec.) with some modifications.

(U) Rather than spraying of the pyrotechnic material onto a fine paper backing or substrate, as was done for the smaller motors, the pyrotechnic was applied directly to the propellant grain after the Pyrofuze wire had been attached. The intimate contact of the pyrotechnic and the propellant grain was a distinct advantage for ignition. The pyrofuze wire was used in a length and shape that placed the wire equidistant from all edges. This configuration allowed equal pyrotechnic ignition over the surface of the grain.

(C) The weight of the pyrotechnic for the WSR-101 was essentially based on the same area to weight ratio as the smaller motors. A value of 145 $\pm$ 25 mg ($\pm$ 20%) was found to be satisfactory for ignition.

(C) It had been noted in previous work that as the size of the motor increased, the ignition delay increased for a given pyrotechnic composition. A particular composition, known as CWIC-4, successfully used for smaller motors, produced an average ignition delay of 60 milliseconds when used in the WSR-101. A new composition, designated CWIC-6, gave ignition delays of about 40 milliseconds in the WSR-101 motor.

(U) Calculation of the total heat content of the CWIC-6 composition showed it to be 4% greater than that of CWIC-4. These data indicated a direction for additional trials in the effort to reduce the ignition delays. Various other compositions were studied and some were tried with varying success.

(C) The final selection of the pyrotechnic composition, designated CWIC-8, was made based on the lowest achievable ignition delay (20 - 25 misec.), total heat content (9% greater than CWIC-4), and the ignitability by Pyrofuze. This formulation did not result directly from the experimental work previously described although some of the information gained in that study was applied.

(C) The pyrotechnic composition (CWIC-8) is a mixture of metallic powders and oxidizer held in form with a resin binder. As previouly described, the mixture is applied by spray with a suitable curing cycle following the application. The composition has an autoignition point of 350°C, well below the temperature generated by the Pyrofuze combustion. Ignition studies at sea level indicated that the burn rate of the pyrotechnic had less influence on ignition delay than the total heat content. Igniters having burn rates at ambient, sea level conditions ranging from 1.0 inch per second to 3.3 inches per second were tested in motors. The burn rate variations were made on the different pyrotechnic compositions of different heat contents, viz., CWIC-4, 6, 8, etc. by varying the application conditions. The final range chosen was 1.5 to 2.0 inches per second.

(C) In the phase of the program concerned with vacuum firing of motors, some difficulty with ignition reliability and excessively long ignition delay was encountered. Further modification of the pyrotechnic was made to assure ignition reliability. A series of tests in vacuum at a simulated altitude of 200,000 feet was performed with the result that a pyrotechnic composition designated CWIC-16 was adopted for use in vacuum firings. This composition was used at a sea level burn rate of 2.0 - 2.5 inches per second. This preliminary work indicated that sea level burn rate can affect the ignitability in vacuum.

(C) While the CWIC-16 composition appears to be in the right direction, ignition delay times in vacuum are somewhat long (50 - 70 msec). A factor that has not been studied is the effect of pressure on the burning characteristics of the pyrotechnic because of time limitation. A prime aim in previous igniter work has been to restrict the composition so that a minimum of gaseous combustion products is obtained. From the limited work done on this program, it appears that in the larger motors, such as the WSR-101, more gaseous combustion products may be desirable to instantly pressurize the capsule and so reduce ignition delay. There are types of oxidizers, fuels, and binders that have characteristics that can produce this instant pressurization. A study in this area of solid propellant ignition appears to be a promising area and should be considered in future efforts.

SECTION V

PROPELLANT DEVELOPMENT

(U) The program for propellant development consisted of five major work areas which follow:

Calculated Specific Impulse

(U) Theoretical computations were made to arrive at an optimum Isp which was to be used as a goal for propellant formulation.

Composition Development

(U) Propellant formulation was made with the idealized theoretical system in mind but tempered with practical ballistic and physical properties requirements. High burn rates and stability in a space environment were major prerequisites in addition to a high delivered specific impulse.

Process Development

(U) This work involved optimum oxidizer blends, uniform fuel and oxidizer dispersion, viscosity, reproducibility and safety.

Characterization of Ballistic and Physical Properties

(U) Testing was conducted on the various propellants to establish burn rates, pressure exponents, density, hardness, sensitivity and mechanical properties.

Vacuum Stability

(C) Stability in vacuum in terms of physical and ballistic constancy was established before, during and after exposure to 10^{-6} Torr at a temperature of 150°F.

A. Calculated Specific Impulse

(C) Theoretical specific impulse computations on the basic CWP-13 composition resulted in a value of 248 lb. sec./lb. at vacuum conditions and an expansion ratio of four as shown in Table XV.

(C) The effects of aluminum powder on the theoretical Isp of the polybutadiene/ammonium perchlorate system are also shown in Table XV with a graphic presertation in Figure 59. The computations were made for 1000 psi chamber pressure and an expansion ratio of four. The optimum aluminum concentration with the CTB binder system is 18% as shown in Figure 59. The 14.7% binder content is standard for the CWP-13 propellant employed in this program. Because of the belief that lower Al contents would minimize nozzle erosion, specific impulse computations were made for a reduction in aluminum content from 18% to 8%. Only a small loss of 5 impulse seconds resulted.

(C) The effect of changing the binder concentration at the expense of the oxidizer relative to Isp values was determined by theoretical computations. Three binder levels (polymer and curative) of 12.7, 14.7 and 16.7% were selected for comparison as shown in Table XVI. A reduction of the binder concentration from 14.7% to 12.7% has a negligible effect on specific impulse while an increase in binder level to 16.7% reduces the specific impulse by only 1.2 seconds. The binder concentration of 14.7% presently employed in the CWP-13 propellant provides maximum impulse and satisfactory processing. This concentration produces a cured propellant which can be machined, shaved and punched to precise dimensions while the physical properties are very satisfactory.

B. Composition Development

(C) During the early phases of the development program, the CWP-9 propellant, which has a burn rate of 1.45 in./sec. at 1000 psi, was used as the propellant to avoid potential delays in hardware test work. Propellant development efforts were initiated and a very reliable, nonmetallized propellant was developed with a burn rate of 1.70 in./sec. at 1000 psi. This propellant designated CWP-13, was then adopted as the standard propellant for the remaining program.

Table XV. Effect of aluminum concentration on theoretical specific impulse (U)

Composition	Weight Percent									
Aluminum	0	2.00	4.00	6.00	9.00	12.00	14.00	16.00	18.00	20.00
NH_4CLO_4	85.30	83.30	81.30	79.30	76.30	73.30	71.30	69.30	67.30	65.30
CTB Polymer	12.92	12.92	12.92	12.92	12.92	12.92	12.92	12.92	12.92	12.92
Epoxy Curative	1.68	1.68	1.68	1.68	1.68	1.68	1.68	1.68	1.68	1.68
Mg O	0.10	0.10	0.10	0.10	0.10	0.10	0.10	0.10	0.10	0.10
Isp (VAC) lb.sec/lb.	247.7	250.6	252.6	254.2	257.7	258.5	260.1	261.2	262.1	261.2
Isp (F.E.) lb.sec/lb	221.9	224.1	225.1	225.8	228.8	227.2	228.1	229.9	231.5	229.8

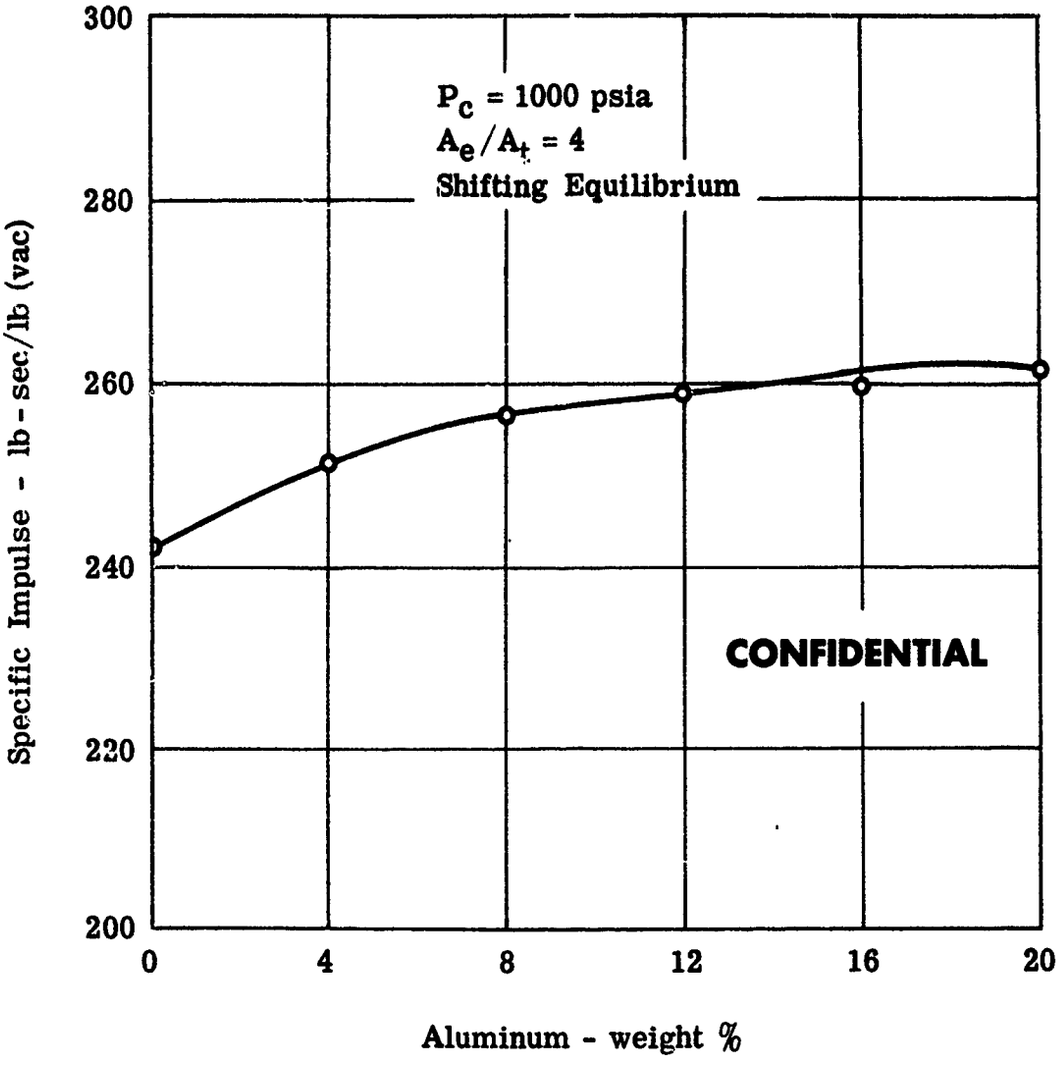


Figure 59. Theoretical propellant performance CWP solid propellant optimization study. (U)

14-649

Table XVI. Effect of binder concentration on specific impulse (U)

Composition	Weight Per cent		
CTB Polymer	11.15	12.92	14.69
Epoxy Curative	1.45	1.68	1.91
Mg O	0.10	0.10	0.10
NH_4CLO_4	68.88	67.30	65.72
Aluminum	18.42	18.00	17.58
Per cent Binder	12.70	14.70	16.70
Isp (VAC) (lb. sec/lb)	262.00	262.10	260.90
Isp (F.E.) (lb. sec/lb)	231.40	231.50	228.40

Note: The oxidizer and aluminum were maintained ar a constant ratio for the three compositions.

(C) The compositions of CWP-9 and CWP-13 are essentially identical; however the high burn rate of the CWP-13 was achieved primarily by reducing the average particle size of the oxidizer and by process improvement. A higher specific impulse was also obtained in CWP-13 as a result of faster induction (decomposition) and reaction time of the more finely divided oxidizer. The high burn rate of this propellant is significant in that a larger web thickness (or shorter burn times) can be employed in rocket motor systems to improve mass ratio.

(C) Initial preparations of CWP-11 (1.25 in./sec.) propellant modified by the addition of 2% by weight of 5 micron diameter aluminum powder yielded slugs which were fissured and porous after cure. As a corrective measure the aluminum powder was then dried under vacuum at 80°C for four hours to remove absorbed volatiles. The propellant prepared after thus treating the aluminum powder was uniform and free of fissures and porosity. The density of two slugs were 1.714 and 1.716 g/cc as compared to 1.690 for the equivalent non-aluminized propellant. The burn rate of the 2% aluminized grain was identical to that of the equivalent non-aluminized propellant.

(C) Specific impulse computations indicated that substituting 8% aluminum in place of ammonium perchlorate in the CWP-13 propellant produced a nine second increase in vacuum specific impulse. When 18% aluminum was substituted another five seconds was added to performance. However, in view of the greater erosive effects of aluminum oxide on the plastic nozzle 8% aluminum was arbitrarily considered the practical limit. Two formulations were prepared with each containing 8% of five micron average diameter aluminum powder as shown in Table XVII. One preparation contained the usual 1.5% Cabosil and the other was prepared without Cabosil. The propellant with the Cabosil exhibited a high burn rate of 1.68 in /sec at 1000 psi and 70°F. The physical properties were also very good compared to those of the more brittle grain which did not contain Cabosil. Thirty grains of each of the two formulations were prepared for experimental motor test firings.

Table XVII. Burn rate of aluminum containg propellants (U)

Composition	Parts to CWP-17A8	Parts to CWP-17A8-1
Ammonium Perchlorate	77.30	77.30
Aluminum	8.00	8.00
Silicon Dioxide (Added)	1.50	---
Magnesium Dioxide	0.10	0.10
Carboxylated Polybutadiene	12.92	12.92
Epoxide Resin	1.68	1.68
Burn Rate in./sec @ 1000 psi	1.68	1.28

C. Process Development

(C) The improvement in burn rate, physical integrity and "punchability" was achieved through a process and particle size change rather than by composition change. A volatile hydrocarbon, namely hexane, is used as a solvent for the polybutadiene binder and the expoxide curative. The binder constituents are completely dispersed throughout the propellant system. The hexane carrier reduces the viscosity of the propellant mix to a semi-fluid consistency by effectively coating the fine ammonium perchlorate with the binder components prior to solvent withdrawal. The hexane carrier is stripped off gradually under a partial vacuum to leave an intimate dispersion of viscous fuel binder on the solid oxidizer.

(C) The uniform distribution of fuel as a thin film on the fine oxidizer particles is responsible for the increase in decomposition rate and combustion rate. Precise controlled measurements were made to ensure removal of all traces of residual hexane from the propellant matrix before the grain shaping and curing operations were performed. Density, hardness and burn rate measurements demonstrated excellent reproducibility.

(U) Continued processing investigation toward the end of the propellant program resulted in a higher burn rate propellant than the CWP-13.

(C) A rate of 1.90 in /sec at 1000 psi and 70°F was measured and confirmed by four repeat propellant batches. The composition of this propellant is the same as CWP-13. The high burn rate was effected without benefit of burn rate catalysts, decomposition catalysts, metal additives and in the complete absence of grain porosity. The 1.90 in /sec carboxy-terminated-polybutadiene composite propellant was designated CWP-19.

D. Characterization of Ballistic and Physical Properties

(U) The experimental and the standard production-run batches of propellant were both prepared and characterized at the Wright Aeronautical Division. The burn rates, pressure exponents and temperature coefficients were determined on a standard Crawford type solid propellant strand burner with a CWP-9 burn

(C) rate plot shown in Figure 60 and CWP-13 burn rate plot shown in Figure 61.

(C) The mechanical properties were determined on an Instron tensile testing machine. Tensile, compression and flexure properties were measured on the Instron using ASTM test procedures. The results obtained are reported in Table XVIII. Properties determined on every production batch included burn rate, density, hardness and uniformity. Tighter-than-conventional burn rate limits of $\pm$ 2% were self imposed to minimize variation in normal rocket motor test work.

E. Vacuum Stability

(C) CWP-9 and CWP-13 propellants were subjected to simulated space vacuum conditions of 10^{-6} Torr pressure and temperatures of 150°F to determine their stability for use in space. The propellants were evaluated for weight change, physical deformation, burn rate and discoloration. The test data given in the following table indicate that the propellants are remarkably stable and the weight loss in vacuum was negligible. The burn rate change was less than the experimental deviation of measurements made with the standard strand burner apparatus.

VACUUM STABILITY OF CURTISS-WRIGHT PROPELLANTS

	CWP-9[1]	CWP-13[2]
Per cent Weight Change After:		
10 Days at 10^{-6} Torr/70°F	0.91%	0.01%
Plus 5 days at 10^{-6} Torr/150°F	1.45%	0.11%
Condition of Propellants after 15 Days at Above Exposure:		
Discoloration	Slight	None
Fissures, Cracks, Etc.	None	None
Deformation	None	None
Burn Rate Change	Very Slight	None
Number of Samples Exposed	8	19

(C) (1) CWP-9 propellant was prepared with random-carboxy-polybutadiene (Goodrich 2000X131). This polymer has been replaced with CTB polymer.

(C) (2) CWP-13 propellant prepared with terminal-carboxy-polybutadiene (Goodrich CTB).

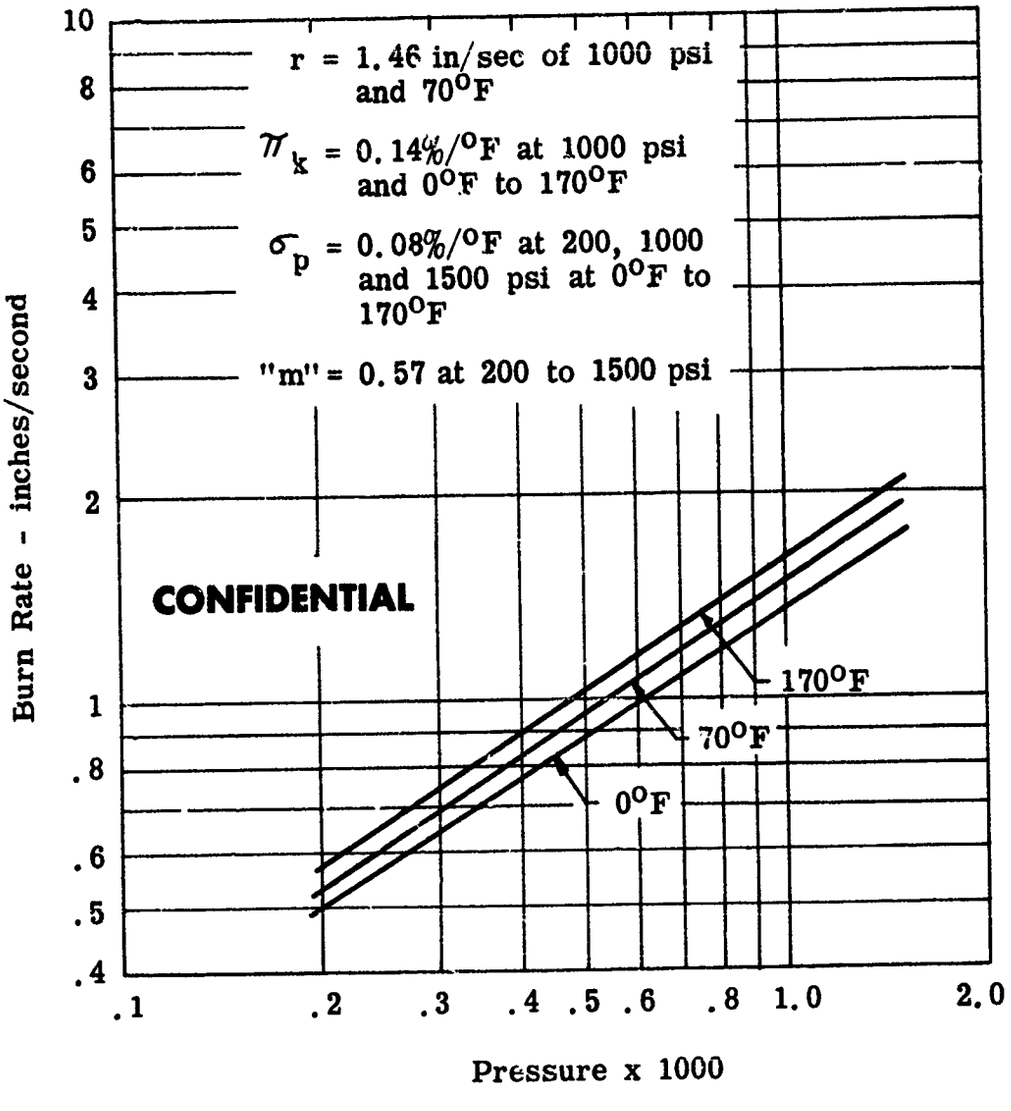


Figure 60. Burning characteristics of CWP-9 propellant. (U)

14-647

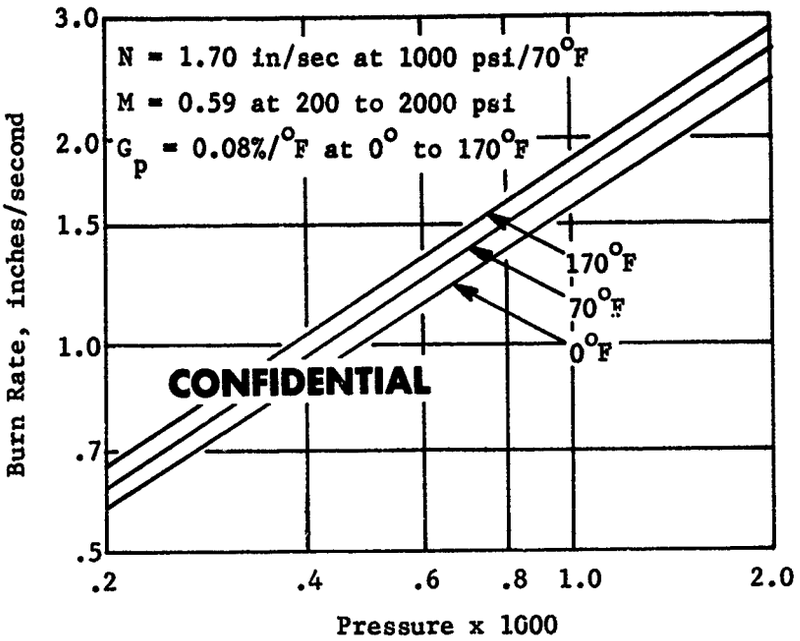


Figure 61. Burn rate of CWP-13 propellant. (U)

Table XVIII. Mechanical properties of CWP-13 propellant.(U)

A. Tensile Properties#

Spec. No.		U.T.S. ksi	Modulus ksi/in.
1-C		1.042	60
2-C		.996	73.45
3-C		1.004	79.4
4-C		1.024	77.3
	Avg:	1.016	72.55
1-L		1.096	83.3
2-L		1.077	100.8
3-L		1.088	100.7
4-L		1.114	88.1
	Avg:	1.094	94.74

B. Compressive Properties##

Spec. No.	C.T.S. ksi	C.Y.S. ksi	Modulus ksi/in.
1	1.9	1.7	58.3
2	1.6	1.2	67.4
3	2.6	1.5	89.9
4	.9	.73	59.4
5	.62	.50	44.7
6	1.1	.79	72.9
7	1.6	1.1	66.9

Note: # Tests conducted on Batch No. 3-2-6B

Tests conducted on Batch No. 3-17-6

SECTION VI
PULSER DEVELOPMENT

(U) The pulser system consists of those components which combine together to produce the stepping action of the sprocket wheel which moves the capsules into the firing position and provides a signal to initiate firing of the capsule.

(C) Since high firing rates are desired and the major portion of the cycle time is required to initiate and complete combustion of the propellant, the time remaining for the stepping action is small.

(C) For example, a stepping time of thirty five milliseconds (.035 sec) is typical for the positioning of a 6600 gm-cm^2 inertial load through an angle of $45^\circ \pm \frac{1^\circ}{4}$ and in the presence of 2 ounce-inches of friction.

(U) This requires a high performance servo system capable of operating in a space environment with a minimum weight and volume. This severely restricted the choice of actuators which could produce the required power levels and power change rates in the alloted times. The selected chosen consisted of a solid state servo driving a printed circuit DC electric motor with the system acting as a relay type servo.

A. Stepping Servo and Pulser Motor

(U) The initial activity in the servo design was to define the load requirement and survey possible actuators which might drive the load.

(U) The initial calculations of the system indicated load characteristics as follows:

Item	Inertia gm-cm^2	lb-in-sec^2
Rotor Wheel	5,290	4.47×10^{-3}
Capsules (15 Live + 5 Fired)	6,210	5.52×10^{-3}
	11,500	9.98×10^{-3}

(U) Improvements incorporated in the capsule design and rotor wheel geometry reduces the total inertia value to 6600 gm-cm^2.

(U) Figure 62 illustrates the effects of inertia and stepping time on motor weight, all motors in this case being a specific type made by "Printed Motors Inc.", Glen Cove, N. Y. Figure 81 also shows the reduction in allowable inertia as stepping time decreases. Typical values are shown below:

Motor	Weight lbs	Inertia For s = .035 sec	Inertia For S = .025 sec
PM #448	6.5	20,600 gm-cm^2	4280 gm-cm^2
PM #368 DS	3.0	14,070 gm-cm^2	3040 gm-cm^2
PM #25805'	1.06	3600 gm-cm^2	704 gm-cm^2

(U) The motor sizing calculation technique automatically accounts for gear ratio reflected inertias and maximum motor and load speed requirements. Only simple servo or torque motor drives were considered. A more complex servo clutch, geneva motion drive was later considered and had certain merits in regard to average power consumption and response. However the simpler printed motor system prevailed and has been the primary type used to accomplish the objectives of the contract.

(U) The basic format of the servo is a relay type closed loop system with position and rate feed as illustrated in Figure 63. A relay servo, in which the power is essentially on all the time but is polarity switched in midstep, is theoretically the fastest responding system available for this application. Figure 64 shows the components and arrangement of the initial breadboard system.

(U) To determine positioning accuracy an analysis was made on the tolerance for the pulser step to aligh the capsule nozzle to the exit cone of the housing and prevent any exit cone misalignment or step in the nozzle contour. These calculations, shown in Figure 65, require positioning of the sprocket wheel within $\pm$ 0.25° of the 45° step.

(This page is unclassified)

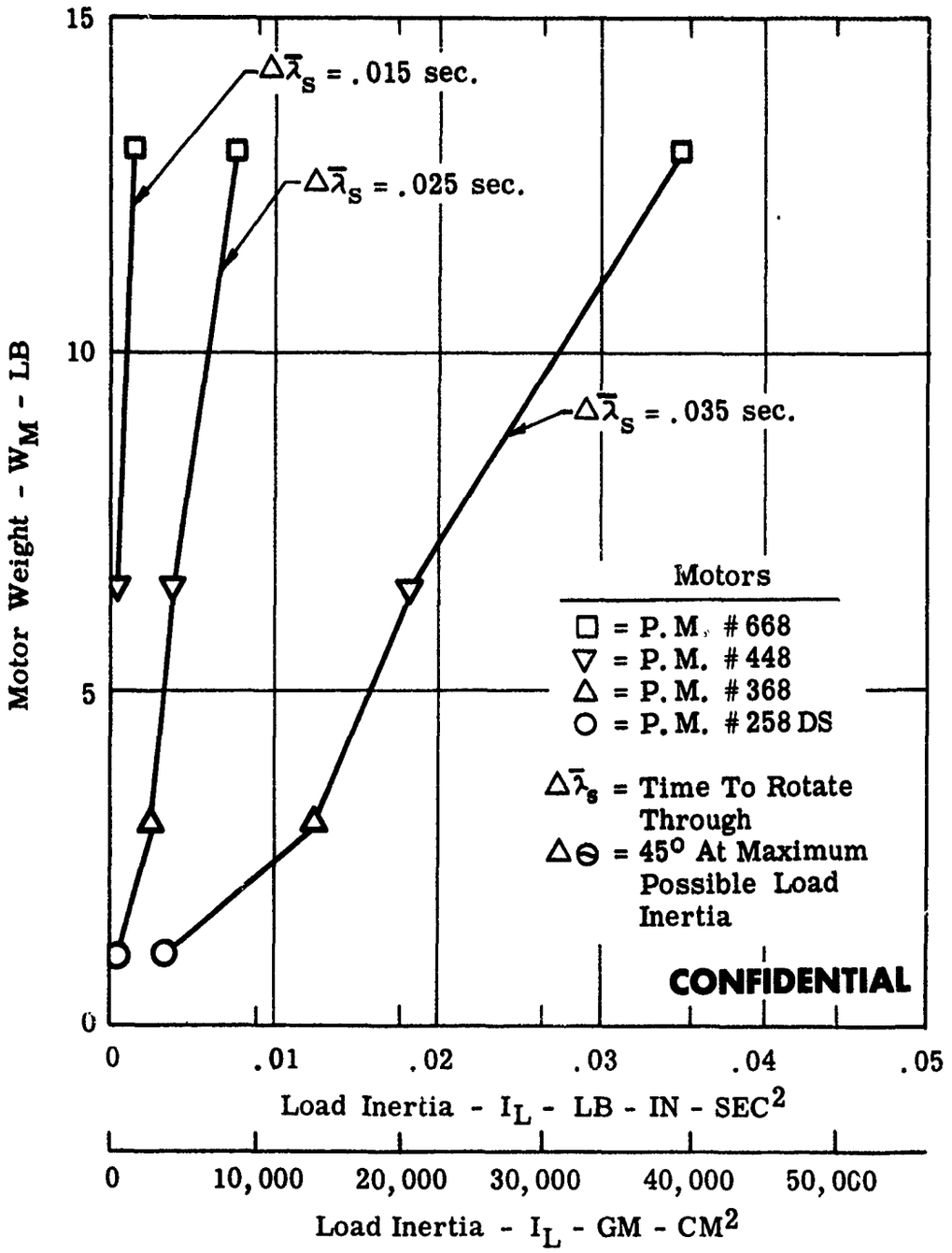


Figure 62. Motor weight vs. load inertia and stepping time. (U)

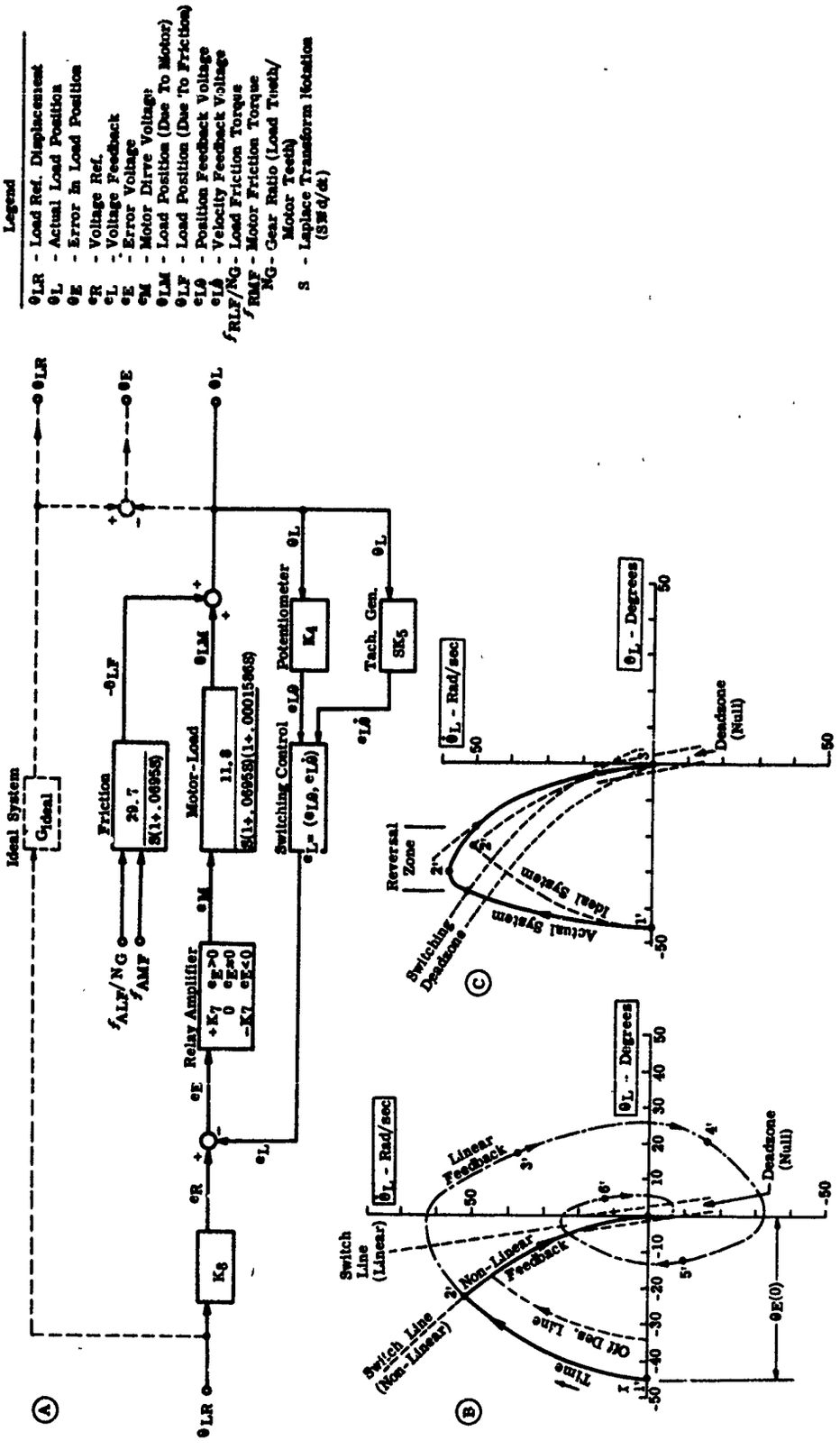


Figure 63. Stepping servo block diagram and relay action. (U)

67-1863

(This page is unclassified)

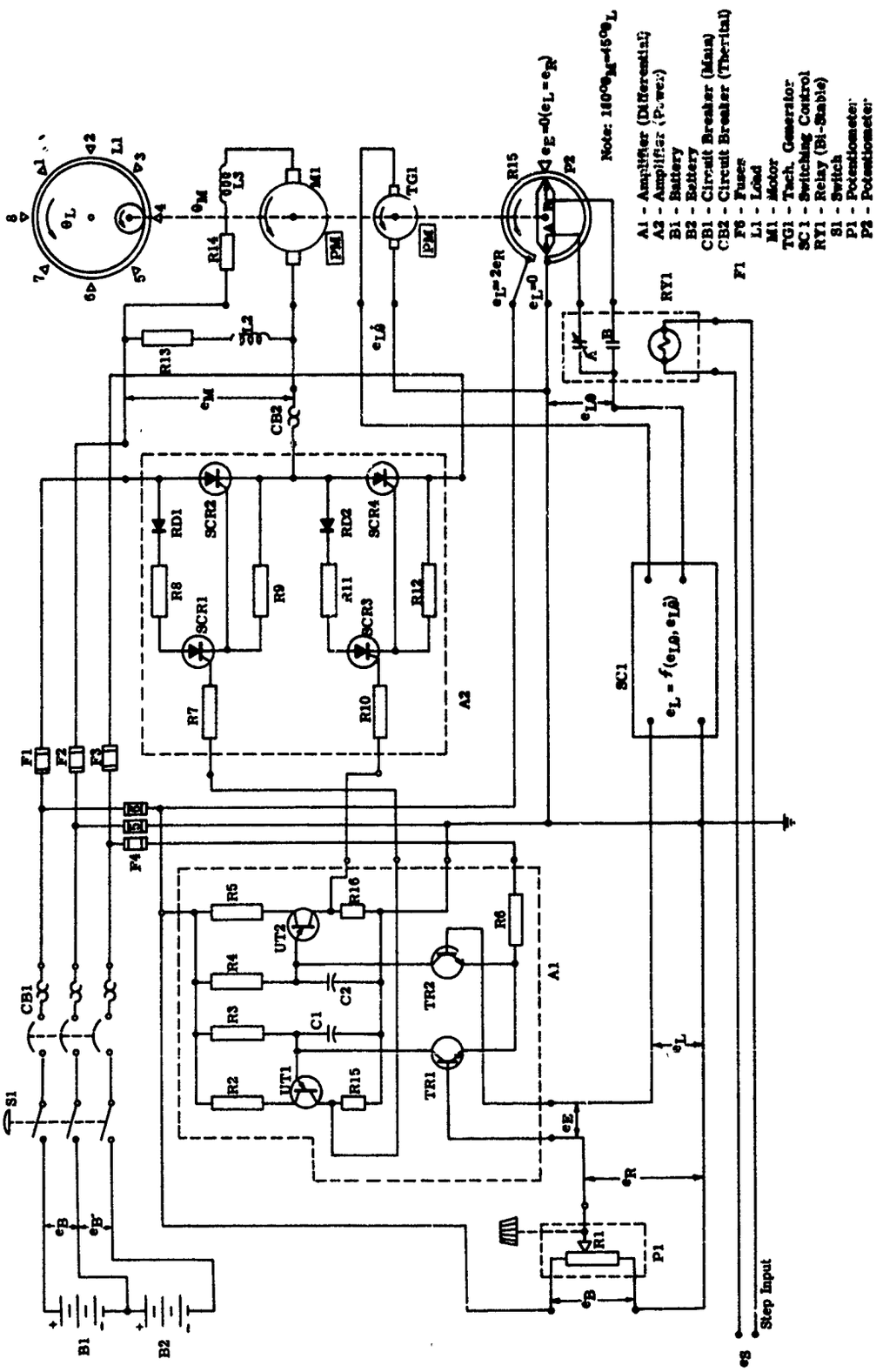
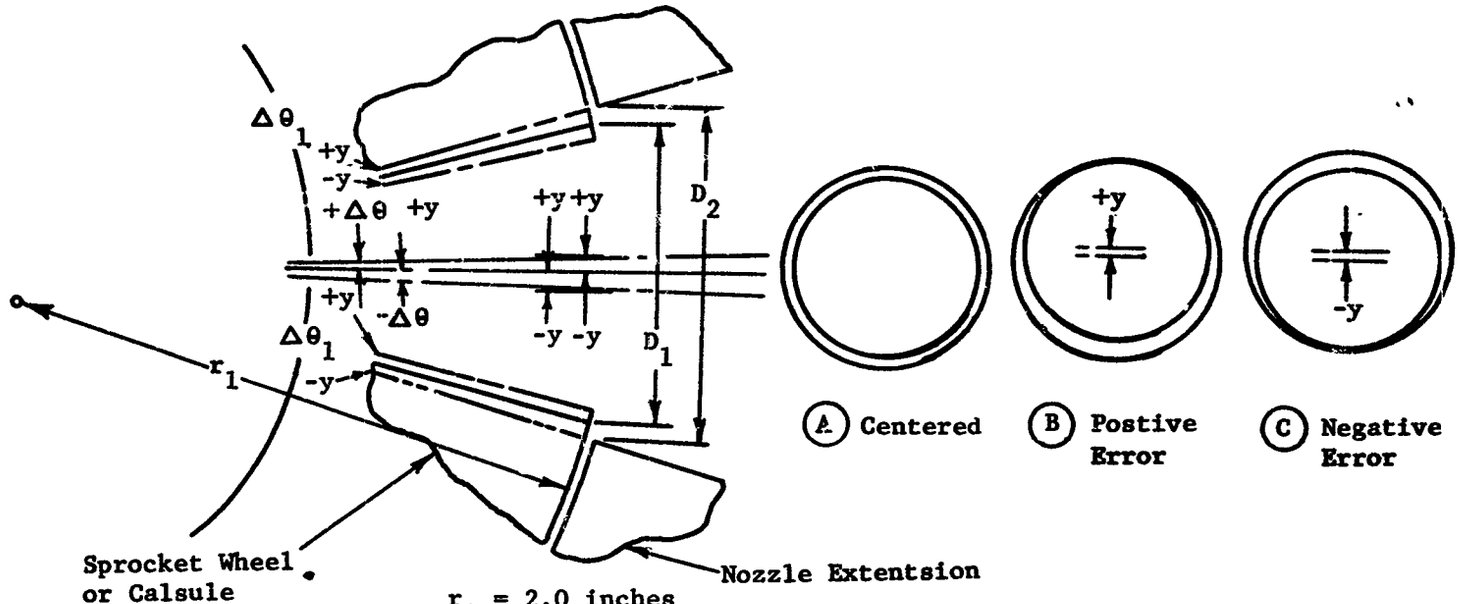


Figure 64. Pulser stepping servo wiring diagram. (U)

14-680



r_1 = 2.0 inches

y = .010 inches

θ_1 = 45° (.7854 Rad.)

$D_1 = D_2 + .020$ inches

$\frac{y}{r_1} = \frac{.010}{2.0} = .005$ radians = 0.2865°

$\theta_{1y} = - \theta_{1y} = 0.2865°$

Use Tolerance of 0.25°

$\theta_1 = 45 \pm 0.25°$

Figure 65. Positioning accuracy. (U)

(U) Following the load positioning analysis, a servo error tolerance analysis was conducted to determine allowable set-up and operating tolerances for all control elements in the system. This included built-in errors (such as alignment of potentiometer dual wiper arms), errors of setting (such as nulling voltages through potentiometer settings) and load disturbance errors (such as frictional forces).

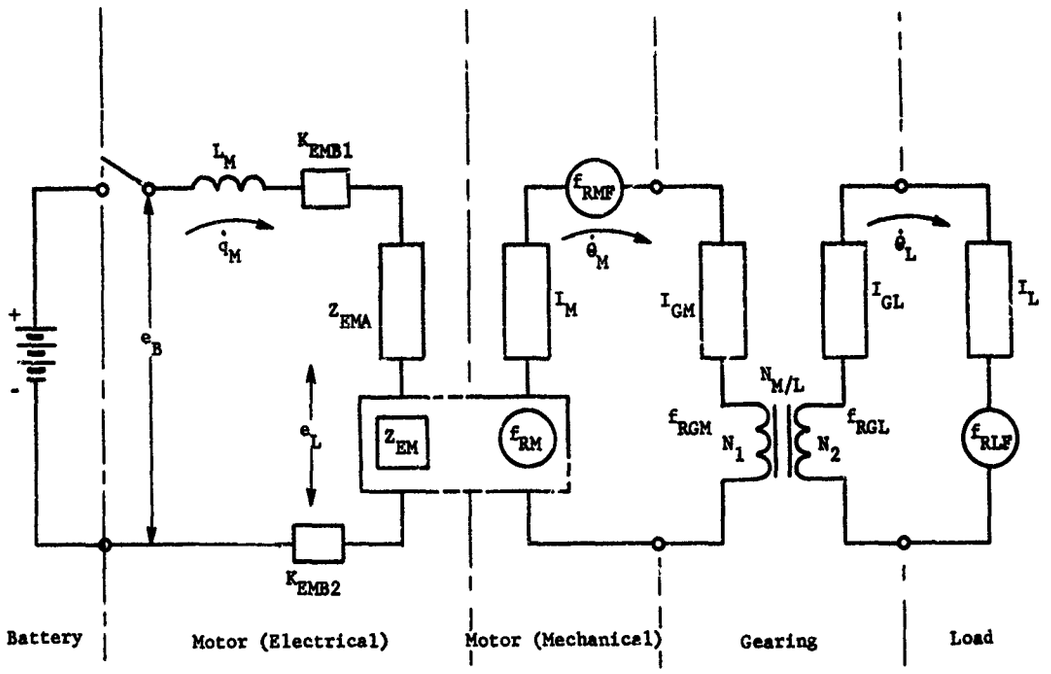
(U) Figure 66 is an isometric view of the mechanical servo loop elements and Figure 67 is a block diagram of the position of error contributors within the control loops.

(U) Figure 68 summarizes the results of the analysis. It is important to note from Figure 68 that the load gear backlash and the load gear-to-nozzle alignment errors are outside of the closed loop servo action envelope and these two errors contribute about 38% of total static error. It is felt this is an acceptable situation because closing the servo loop on the motor side of the gear ratio permits working with angular motions four times larger than load motions and eases resolution problems. Figure 68 indicates that a fairly tight but not impossible tolerance limitation is required in the system components.

(U) Since these errors are not likely to occur simultaneously, at maximum values and in the same direction, a root-mean-square error is computed. The RMS error is listed as 0.0973° out of an allowable 0.25° or approximately 1/3 of the allowable.

(U) A dynamic analysis (shown below) was made relating load position - θ_L to battery voltage - e_B. This analysis includes motor electrical parameters, motor mechanical items (such as inertia and friction), gearing effects, and load characteristics.

(U) These analysis provided an appreciation of the system inter-relationships as well as furnishing design calculations with a basis for both static and dynamic studies.



$$\theta_L(S) = \left[\frac{K_3}{S(K_1 t_{ME} S^2 + K_1 S + K_2)}\right] e_B(S) - \left[\frac{(1 + t_{ME} S)}{S(K_1 t_{ME} S^2 + K_1 S + K_2)}\right] (N_{M/L} f_{RLF} + f_{RMF}) (S)$$

Legend

e_B - Battery Voltage - Volts
L_M - Motor Inductance - Heneries
K_{EMB1} - Motor Brush Resistance - Ohms
K_{EMB2} - Motor Brush Resistance - Ohms
Z_{EMA} - Motor Armature Resistance - Ohms
Z_{EM} - Motor Motional Impedance - Ohms
f_{RM} - Motor Armature Torque - lb-in
I_M - Motor Armature Inertia - lb-in-sec^2
f_{RMF} - Motor Friction Torque - lb-in
I_{GM} - Gear Inertia (Motor Side) - lb-in-sec^2
I_{GL} - Gear Inertia (Load Side) - lb-in-sec^2
f_{RLF} - Load Friction Torque - lb-in
$N_{M/L}$ - Gear Teeth Ratio (Motor/Load = N_1/N_2)
N_1 - Motor Pinion Gear Teeth
N_2 - Load Side Gear Teeth
$\dot{q}_M$ - Motor Current - Amperes
$\dot{\theta}_M$ - Motor Speed - Rad/sec
$\dot{\theta}_L$ - Load Speed - Rad/sec
K_e - Motor Back E.M.F. Constant - Volts/Rad/sec
K_{fr} - Motor Torque Constant - lb-in/Amperes
e_L - Motor Back E.M.F. - Volts (Appears Across Armature)
(S) - Laplace Transform Notation
f_{R2} - Torque at Gear Load Side - lb-in
f_{R1} - Load Torque at Gear Motor Side - lb-in
I_L - Load Inertia - lb-in-sec^2
N_G = Gear Ratio = $1/N_{N/L} = N_2/N_1$

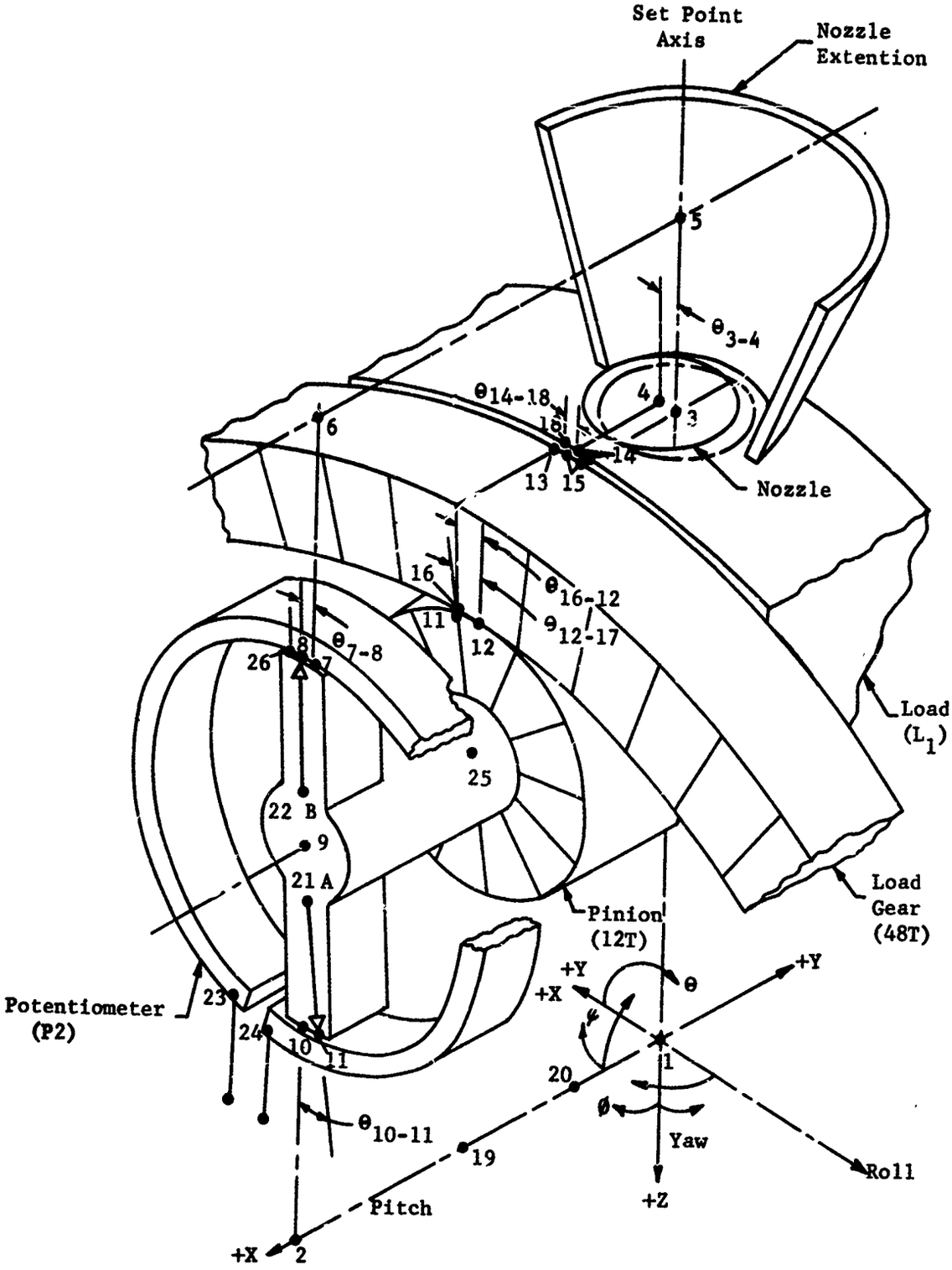


Figure 66. Isometric of mechanical servo loop. (U)

20-718

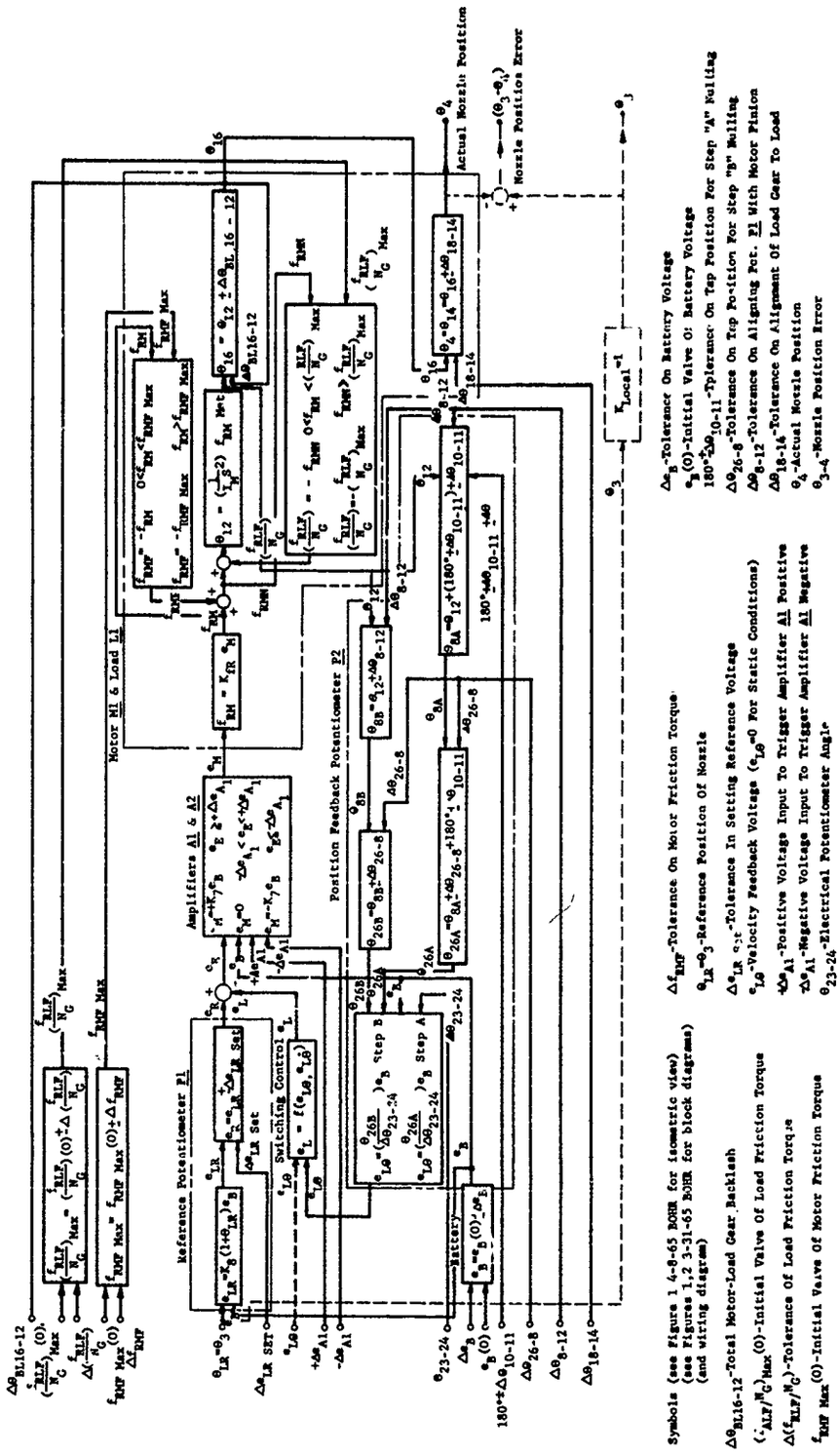


Figure 67. Stepping servo error tolerance diagram under static condition. (U)

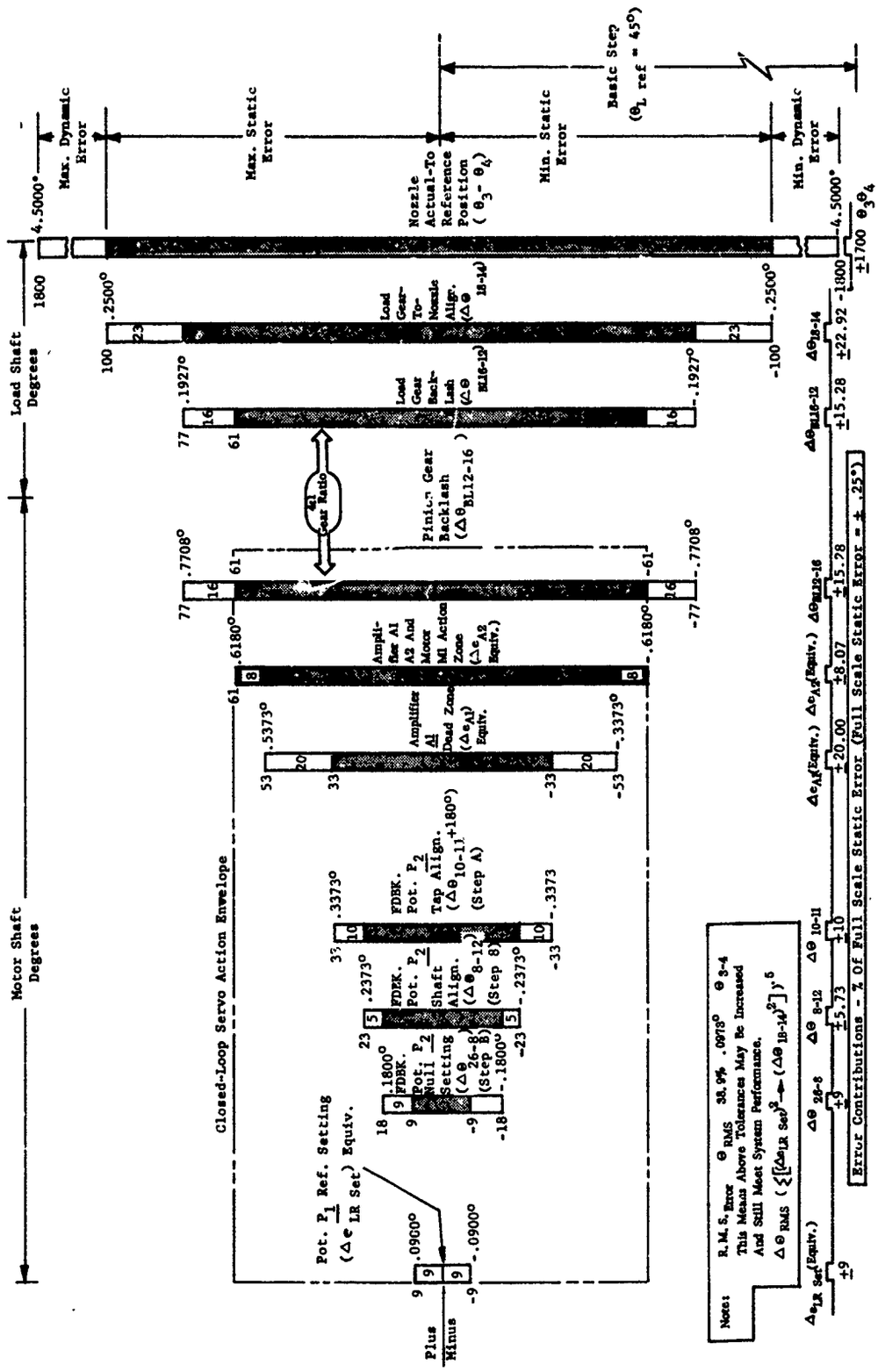


Figure 68. Stepping servo components tolerance limits - WSR-101. (U)

14-678

(This page is unclassified)

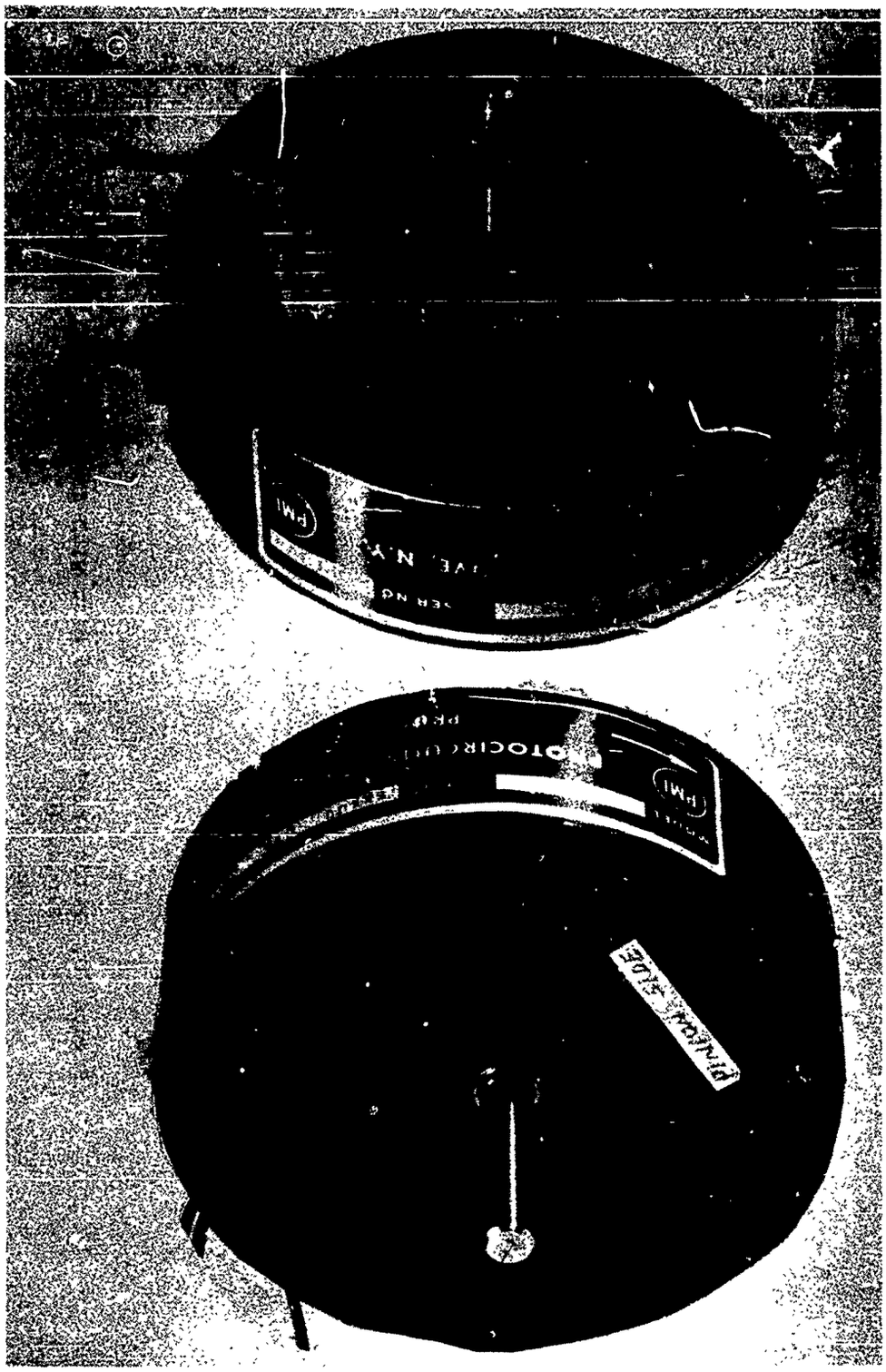
(U) Upon completion of the analyses, a specification was prepared for a drive system capable of meeting the requirements of the program. This specification was issued to several vendors. After surveying the vendor proposals the following drive system was selected. The system consists of a Printed Motor #U9C including a gear reduction of 4:1 to match motor and load inertias and a solid state stepping servo which was subcontracted to M. Ten Bosch Inc. As part of the pulser development phase a program was established to confirm the characteristics of the #U9C motor (Figure 69) under design conditions and to determine absolute limits of operation. The specific objectives of the test program were

- Determine the motor characteristics using an inertial load disc (Figure 70)
- Evaluate the motor characteristics beyond its rated value.
- Determine and evaluate the stepping characteristics of the motor

(C) Figure 71 illustrates schematically the setup used to conduct the tests. A pulse generator was fabricated as shown in Figure 72. This unit is capable of generating 6VDC rectangular waves from 6 to 20 cps both positive and negative. The positive pulses can be modulated from 0 to 100% on-time and the negative pulses can be modulated 0 to 50% on-time. In addition, a special power amplifier was designed and fabricated and is shown in Figures 73 and 74. This amplifier provided the inputs to the motor to simulate various conditions which the motor would experience during operation with the servo system.

(C) The results of these tests are summarized in Figures 75 thru 79. Figure 75B is of particular interest in that it shows that a stepping time of approximately 0.020 seconds might be achieved if a full 28 VDC could be applied to the motor. However, the specification requirement of 0.030 seconds is a more reasonable value in order to minimize motor current and allow for necessary voltage drops in the servo system, while still working from a 22 - 30 VDC source.

(U) The motor used for the tests was Serial Number 153 and was subjected to approximately 10,000 pulses, 8000 of which were within the normal motor rating. The remaining pulses subjected the motor to very high currents (approximately



Brushes and Feedback Elements Side

Pinion Shaft Side

Figure 69. U9C printed motor. (U)

14-671

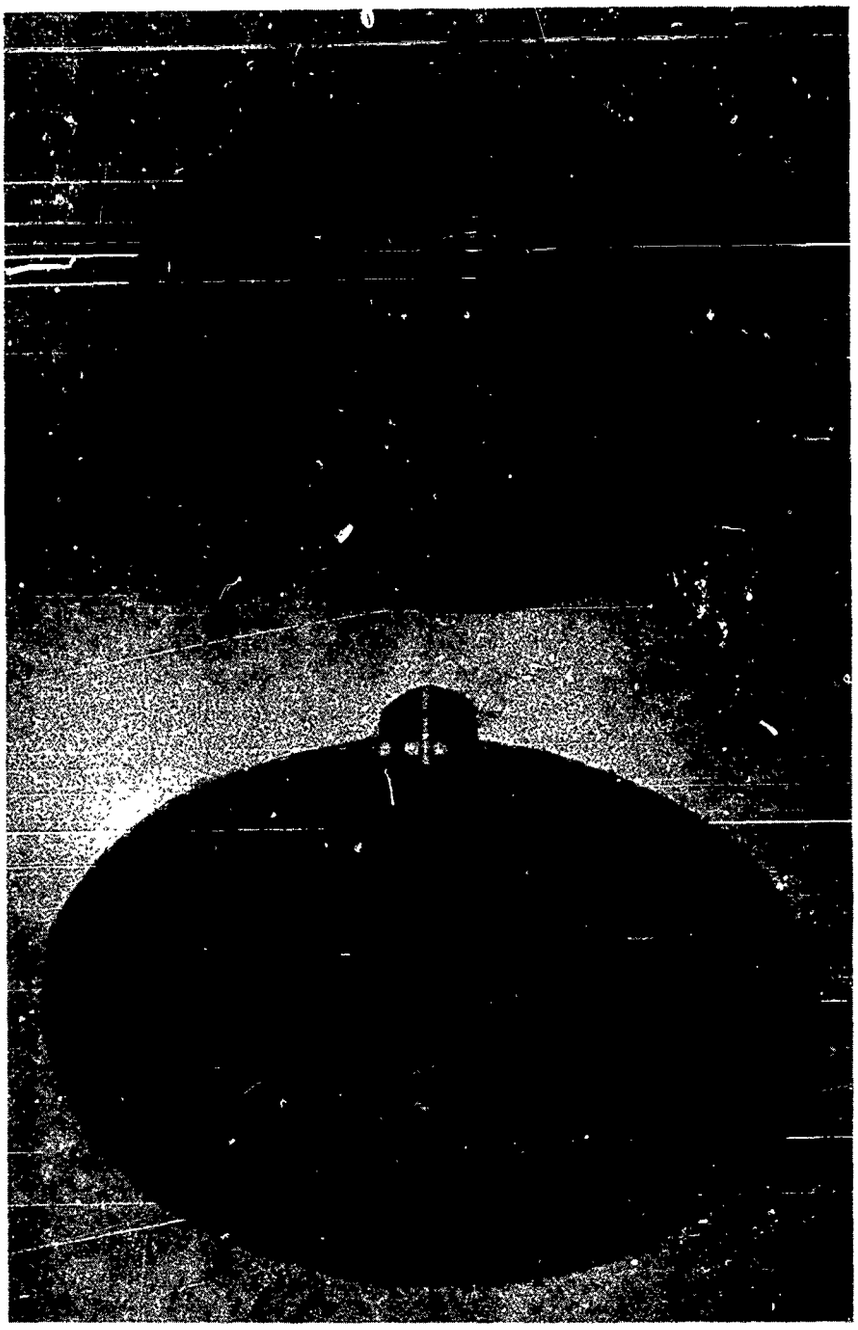


Figure 70. Motor inertial load disc with position indicating slots. (U)

14-677

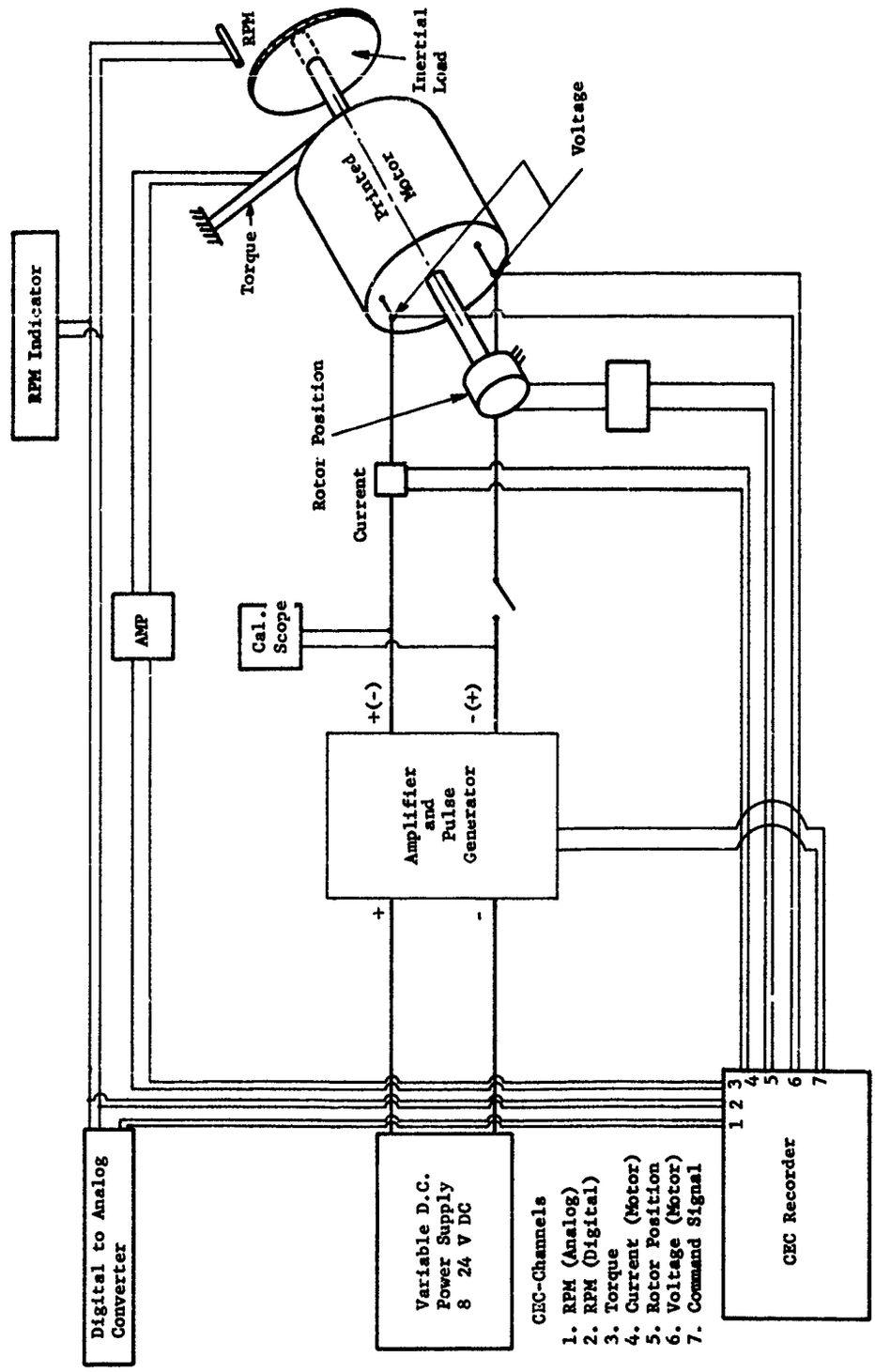


Figure 71. Test setup. (U)

Interior View

Exterior View

Figure 72. Variable frequency and duty cycle pulser generator. (U)

14-665

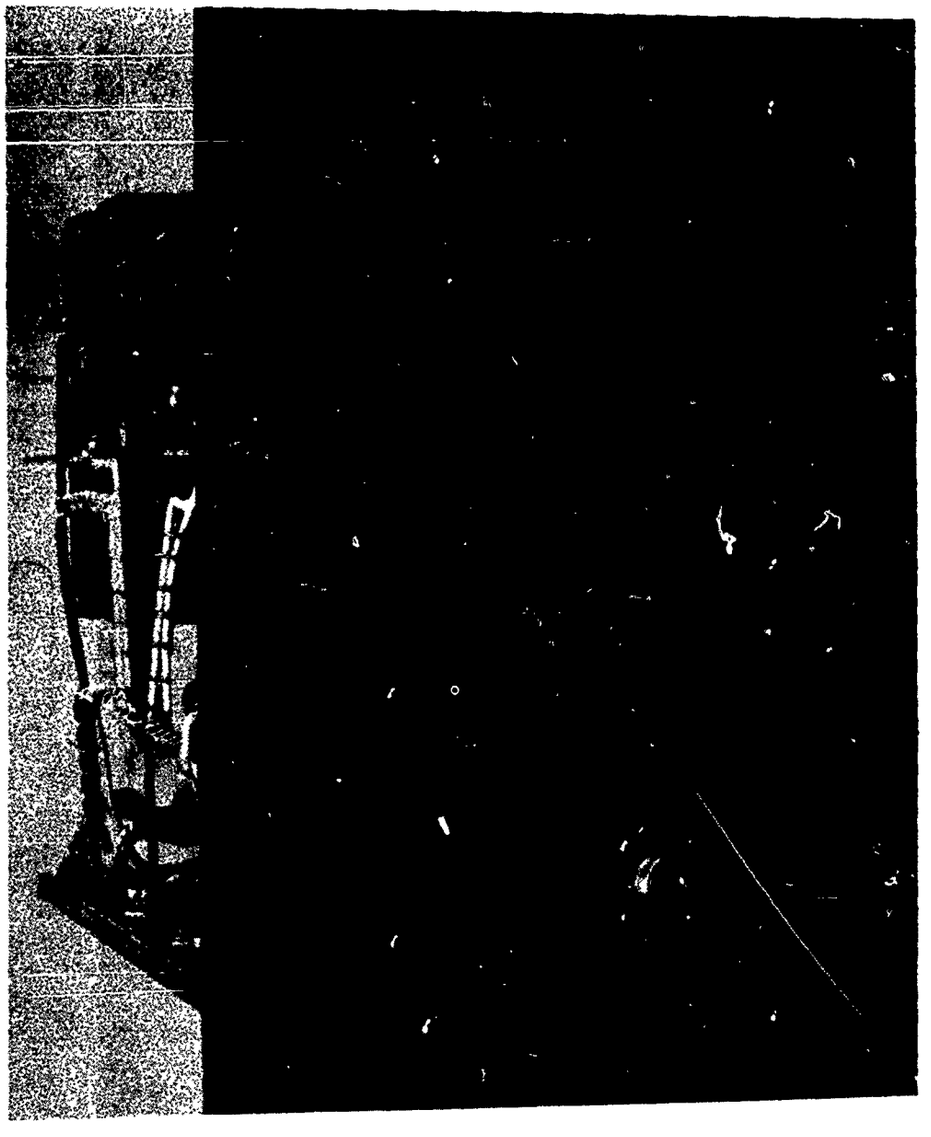
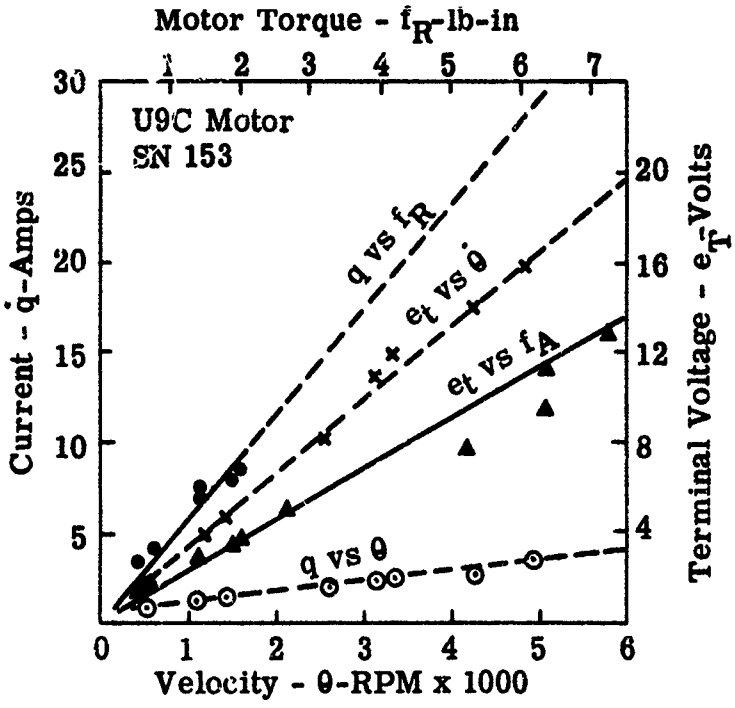


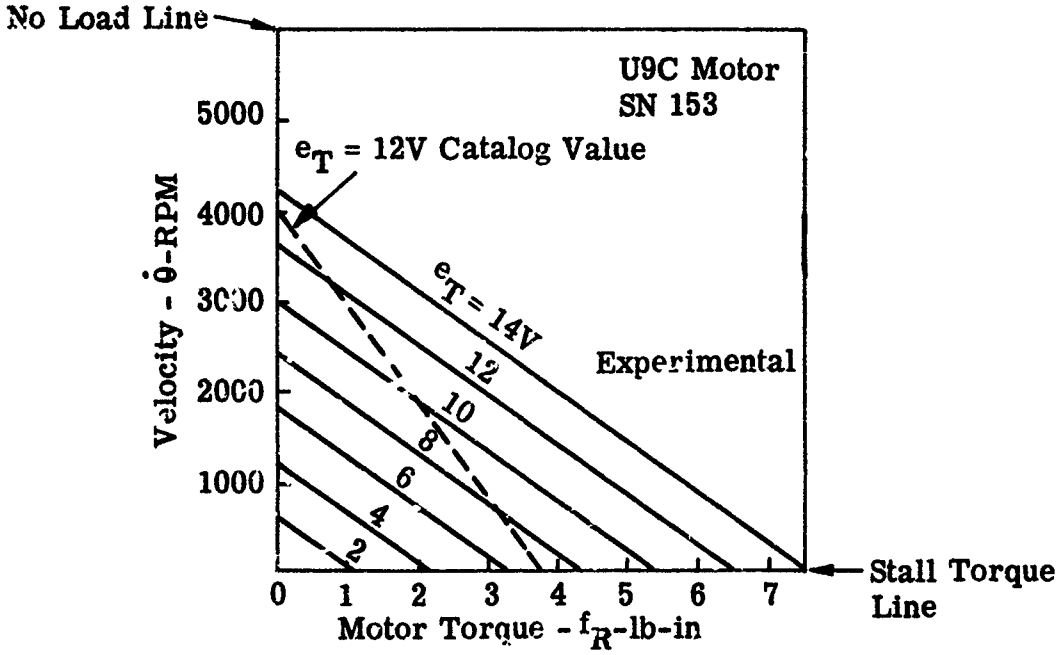
Figure 73. Power amplifier. (U)



Figure 74. Power amplifier. (U)



(a) Steadystate Characteristics

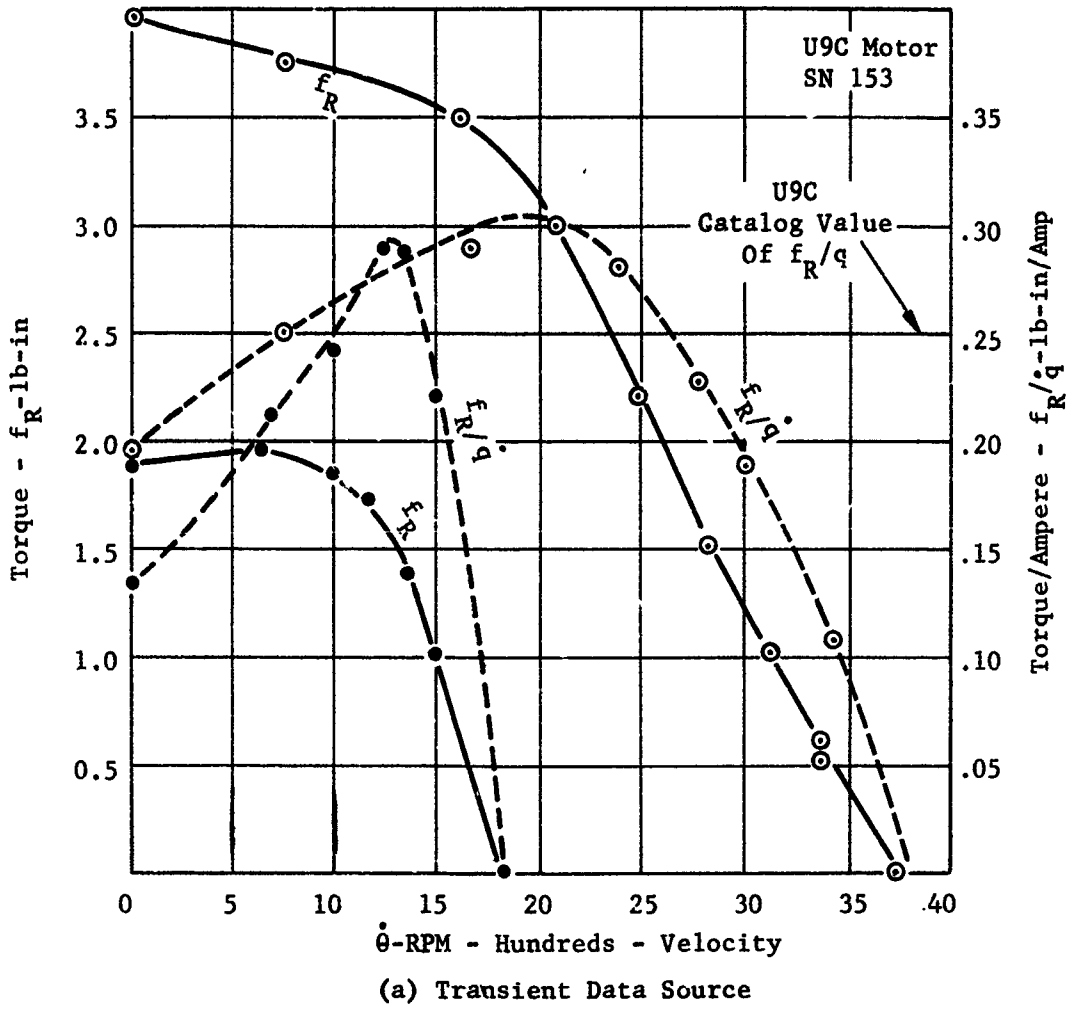


(b) Steadystate Performance

Figure 75. Experimental data U9C printed motor (SN 153). (U)

NOTE: 1. Data For (a) and (b) Obtained by Step Inputs of e_t (Terminal Voltage).

2. e_t Increasses as Speed (θ) Increases Because Back E.M.F. e_B Reduces Motor Current, and Thus Line Voltage Drop From Battery to Motor.



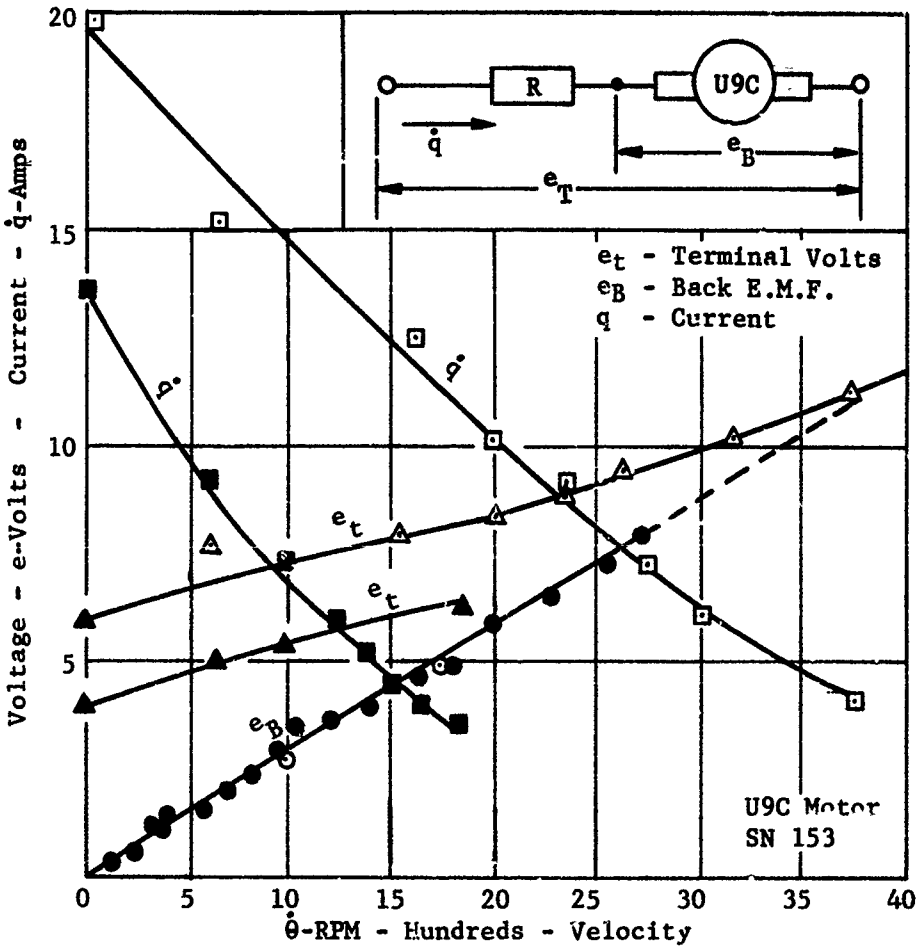
(a) Transient Data Source

Figure 76. Experimental data U9C printed motor (SN 153). (U)

20-862

NOTE: 3. Terminal Voltage Pulse Introduced by First Running Motor in Opposite Direction and Then Switching Terminal Voltage to Oposite Polarity and Level Indicated on Data.

4. All "Hollow" Data Points for $e_t(o)$=6 Volts. All "Solid" Data Points For $e_t(o)$=4 Volts



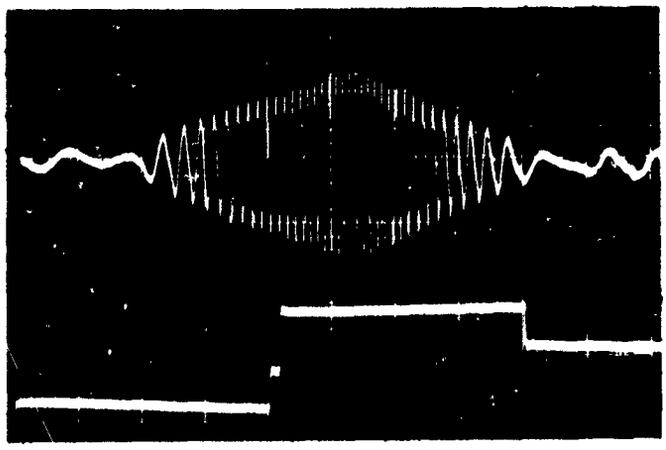
(b) Transient Data Source

NOTE: $(e_B/\dot{\theta})_x$ = 2.91 Volts/1000 RPM Experimental

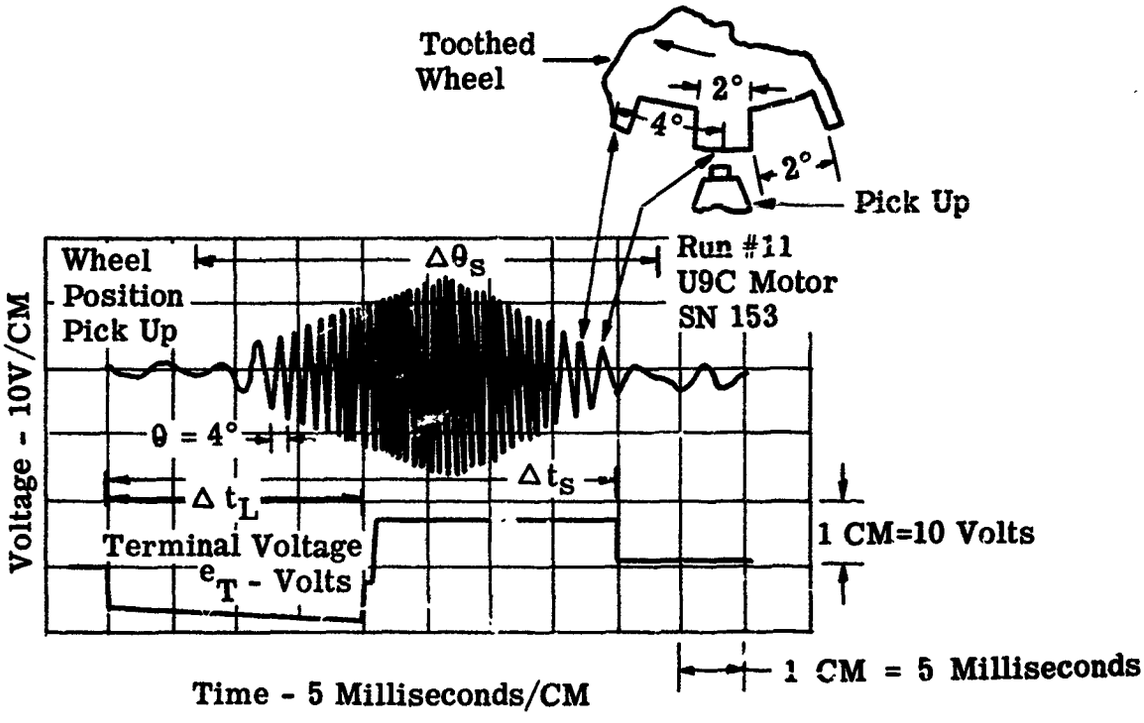
$e_B/\dot{\theta}$ = 2.22 Volts/1000 RPM Catalog Data

Figure 77. Experimental data U9C printed motor (SN 153). (U)

20-900



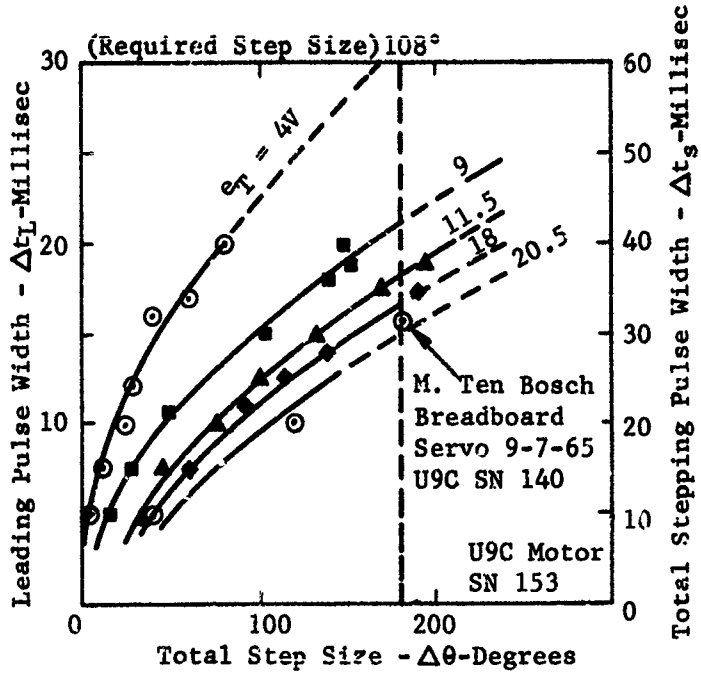
(a) Experimental Data For Shaft Position vs Stepping Pulse



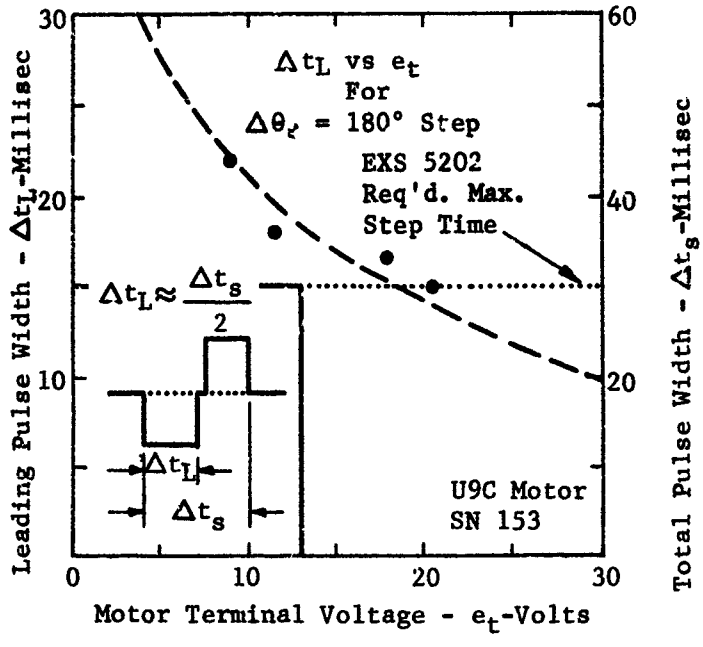
(b) Reduction Of Stepping Data

Figure 78. Experimental data U9C printed motor (SN 153). (U)

20-872



(a) Steadystate Pulse Data



(b) Steady Pulse Data

Figure 79. Experimental data U9C printed motor (SN 153). (U)

20-896

(This page is unclassified)

(U) 40 - 50 amperes) and there was some indication of roughness when hand turning the motor shaft. The motor was disassembled and inspected for damage. The inspection revealed a warped armature due to overheating. This was caused by the excessive current which the motor was subjected to for extended periods. Figures 80 and 81 shows the damage to the armature. The arrows in Figure 80 indicate where the armature was rubbing on the motor housing.

(C) The initial pulser servo breadboard was bench-tested and a step time of 22 milliseconds with an equivalent load of 6000 gm-cm^2 was achieved. However, the breadboard had to be repackaged to a more compact and stable design and required some circuitry changes. These changes resulted in noise pickup and further modifications were required which lowered the system gain and thereby resulted in a lower response. However, the response was within the specification tolerance.

(C) The modified breadboard was bench checked and Figures 82 and 83 present the data of servo motion with an equivalent 6000 gm-cm^2 load. A translation time of approximately .032 seconds with a 1° overshoot with another 4 to 5 milliseconds settling time to the $\pm$ 0.25° requirement was recorded. Figure 102 (b) also presents feedback voltage levels and the effects of adjustment capacitors on response and overshoot. Figure 84 shows the final breadboard configuration of the stepping servo and pulser motor.

B. Prototype Servo & Motor System

(U) The design and fabrication of the prototype servo was based on the knowledge and results obtained from the breadboard and single motor tests. The prototype unit has the following features and improvements:

- Silicon power transistors instead of germanium
- Higher power overload capacity
- Better response
- Packaged as a complete unit including the printed motor

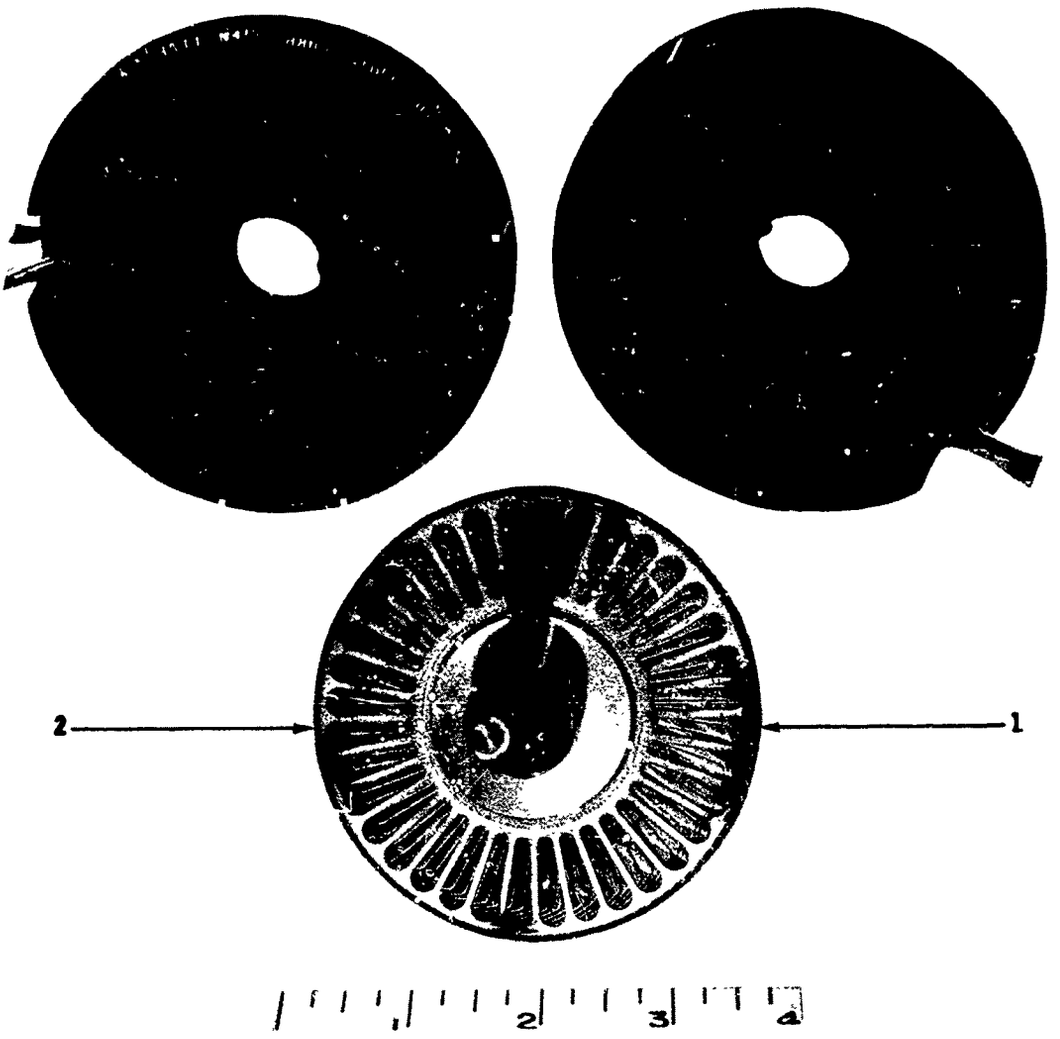


Figure 80. U9C motor - SN 153 - after test. (U)

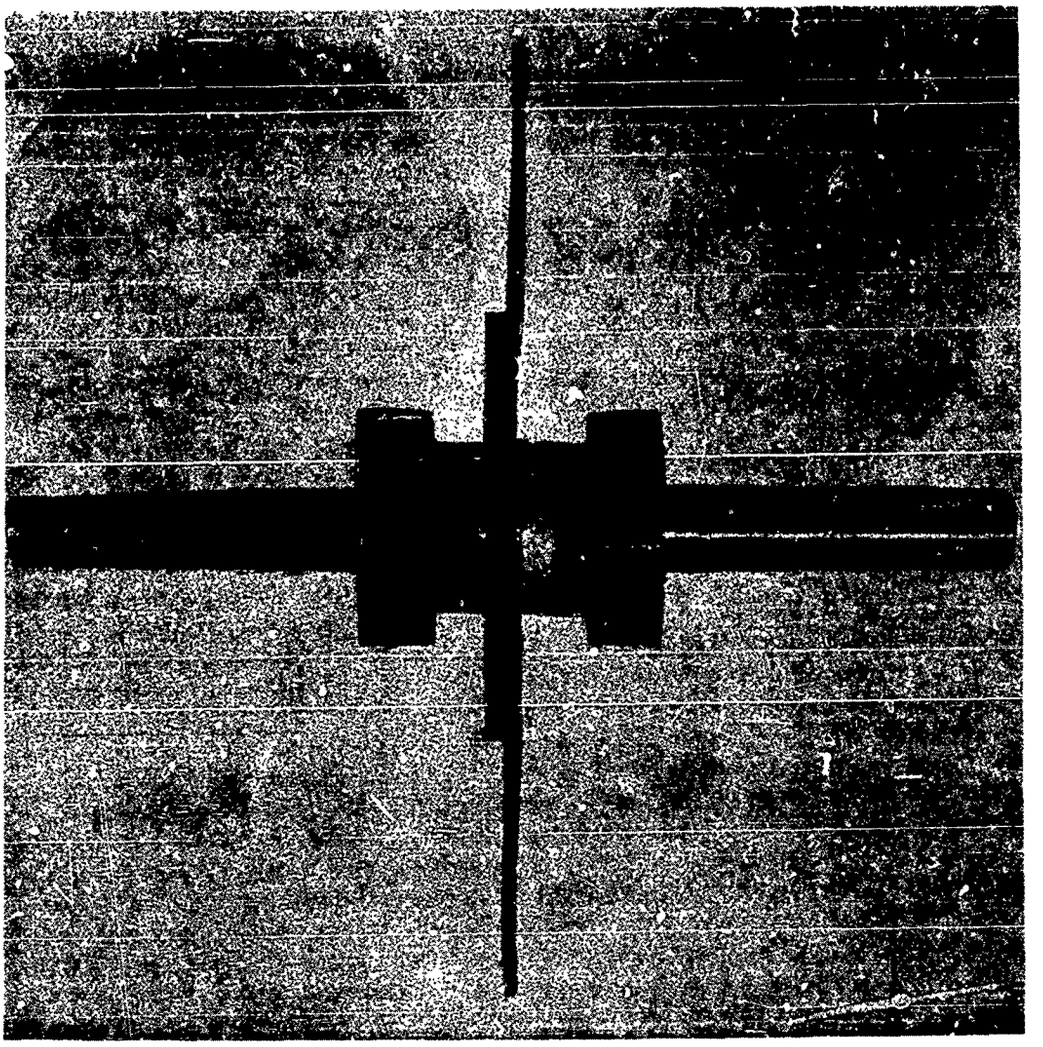


Figure 81. U9C armature assembly U9C motor SN 153 after test. (U)

Test Data - Oscillograph Traces

	Vert. Sens.	Horizontal Sens.	Lead Capacitor
①	1 Volt/cm	10 Millisec./cm	.024 μf
②	1 Volt/cm	10 Millisec./cm	.024 μf
③	1 Volt/cm	10 Millisec./cm	.027 μf

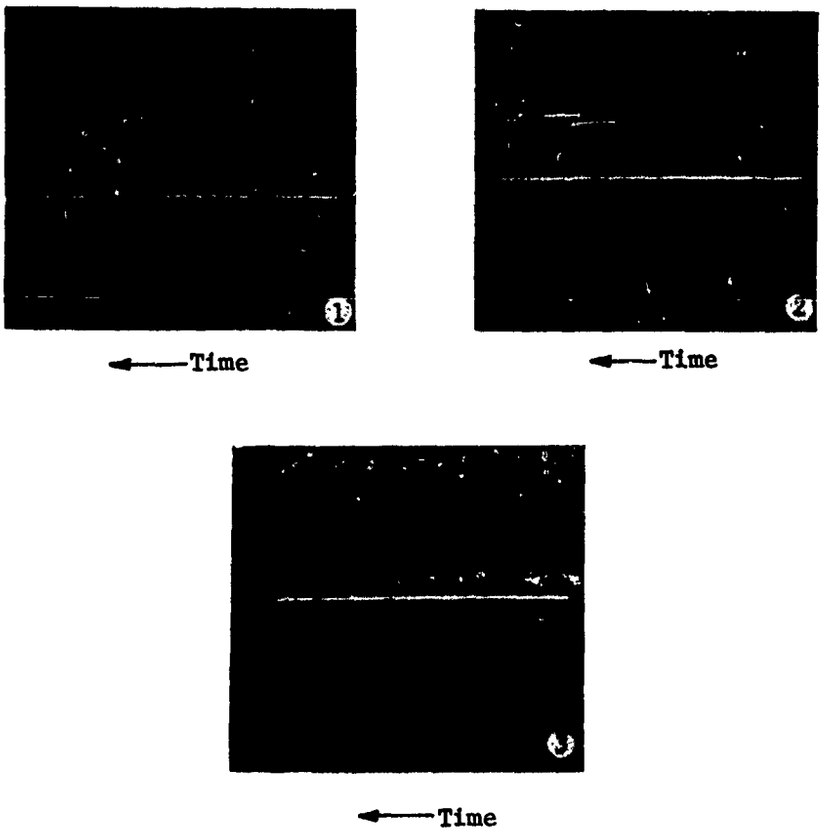


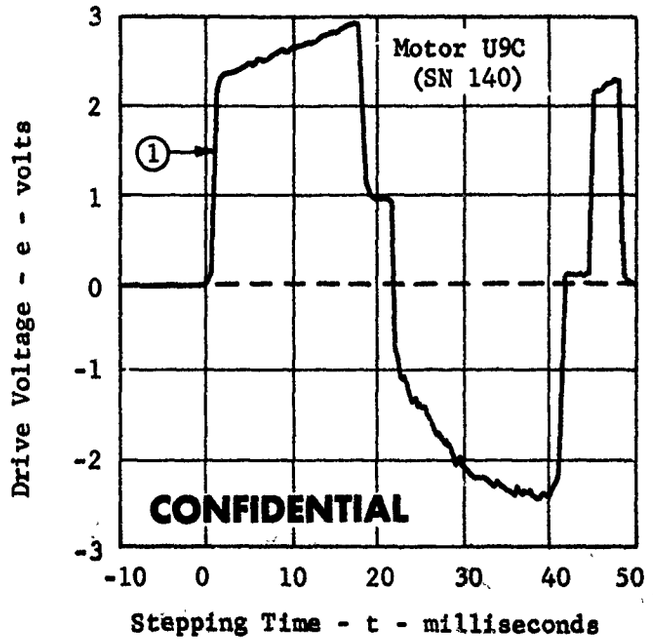
Figure 82. WSR-101 breadboard servo response. (U)

20-877

(This page is unclassified)

INPUT

(a) Potentiometer Feedback Error Voltage vs Time



OUTPUT

(b) Equivalent Shaft Rotation vs Time

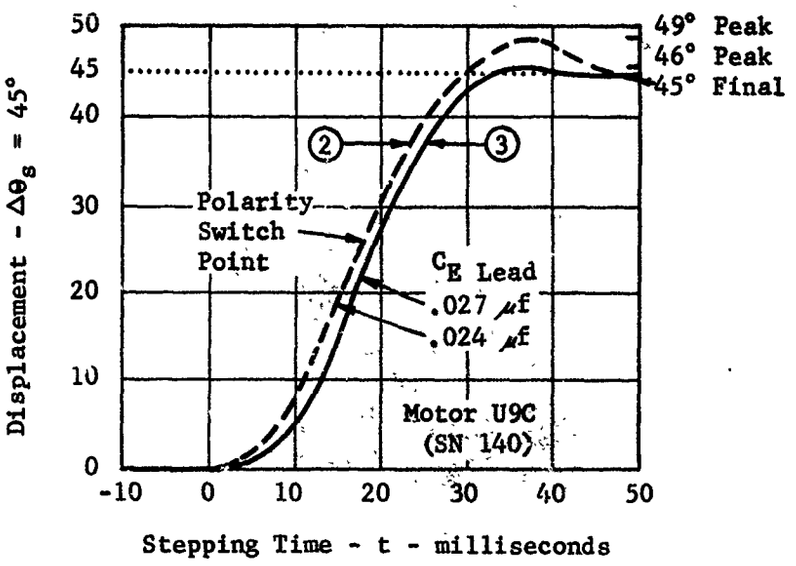


Figure 83. WSR-101 breadboard servo response. (U)

20-909



Figure 84. Stepping servo and pulser motor breadboard. (U)

15-828

(This page is unclassified)

(U) The external and internal arrangement of the prototype servo and motor system is illustrated in Figures 85 through 87.

(U) The prototype design power requirements are presented in Figure 88. During the repetitive firing tests power checks were made which showed the power required to be slightly higher than predicted. This resulted from imperfections in the hand made tapes which added friction to the system. It is estimated that the requirements of Figure 88 can be met with production tapes.

(C) The prototype was acceptance tested before being used for repetitive firings. Figure 90 shows the test data obtained for single pulses and for 10 pulses per second, and indicates that the pulse is completed in 0.030 seconds.

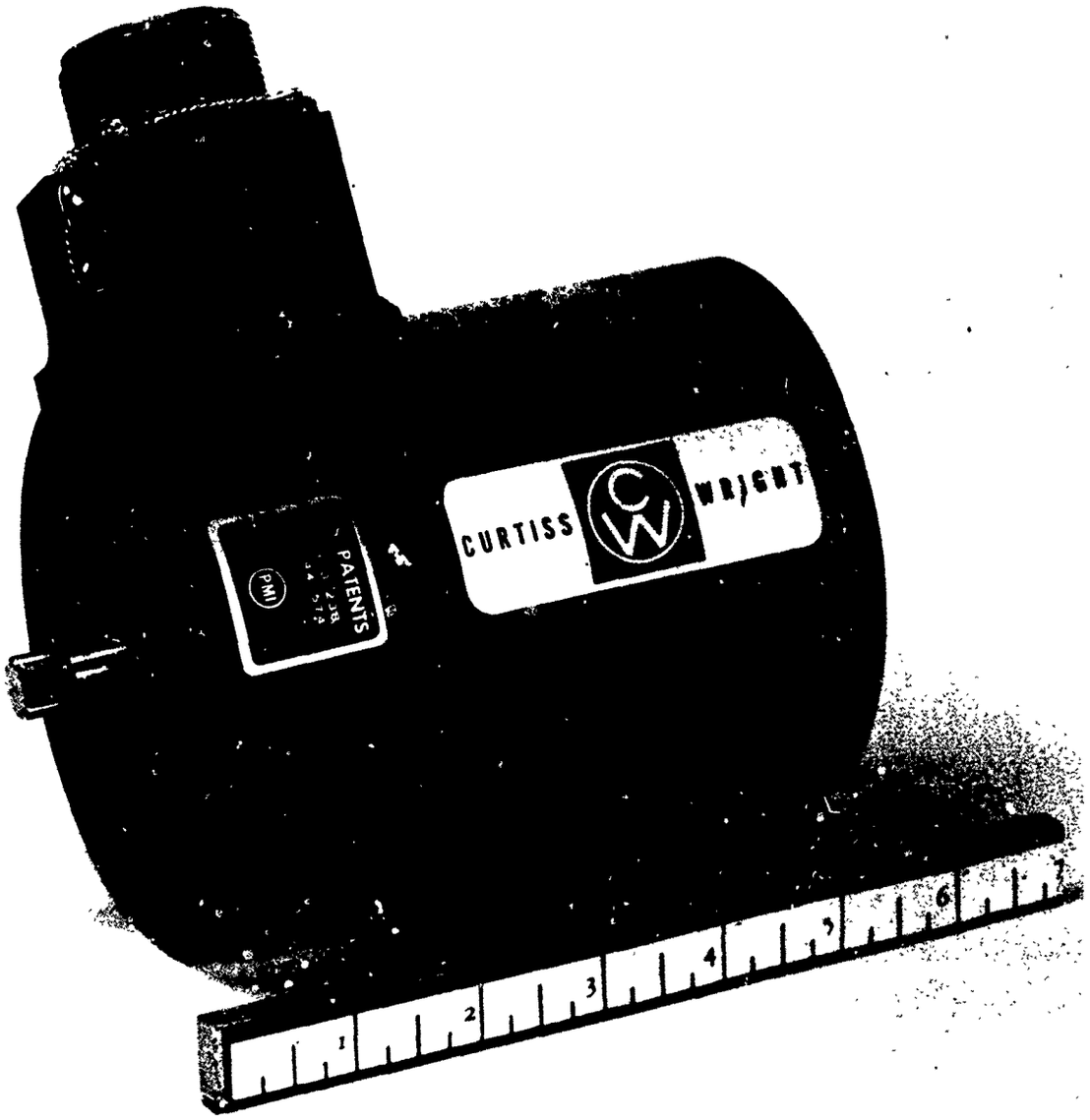


Figure 85. WSR-101 prototype servo and motor system. (U)



Figure 86. WSR-101 prototype servo and motor system. (U)

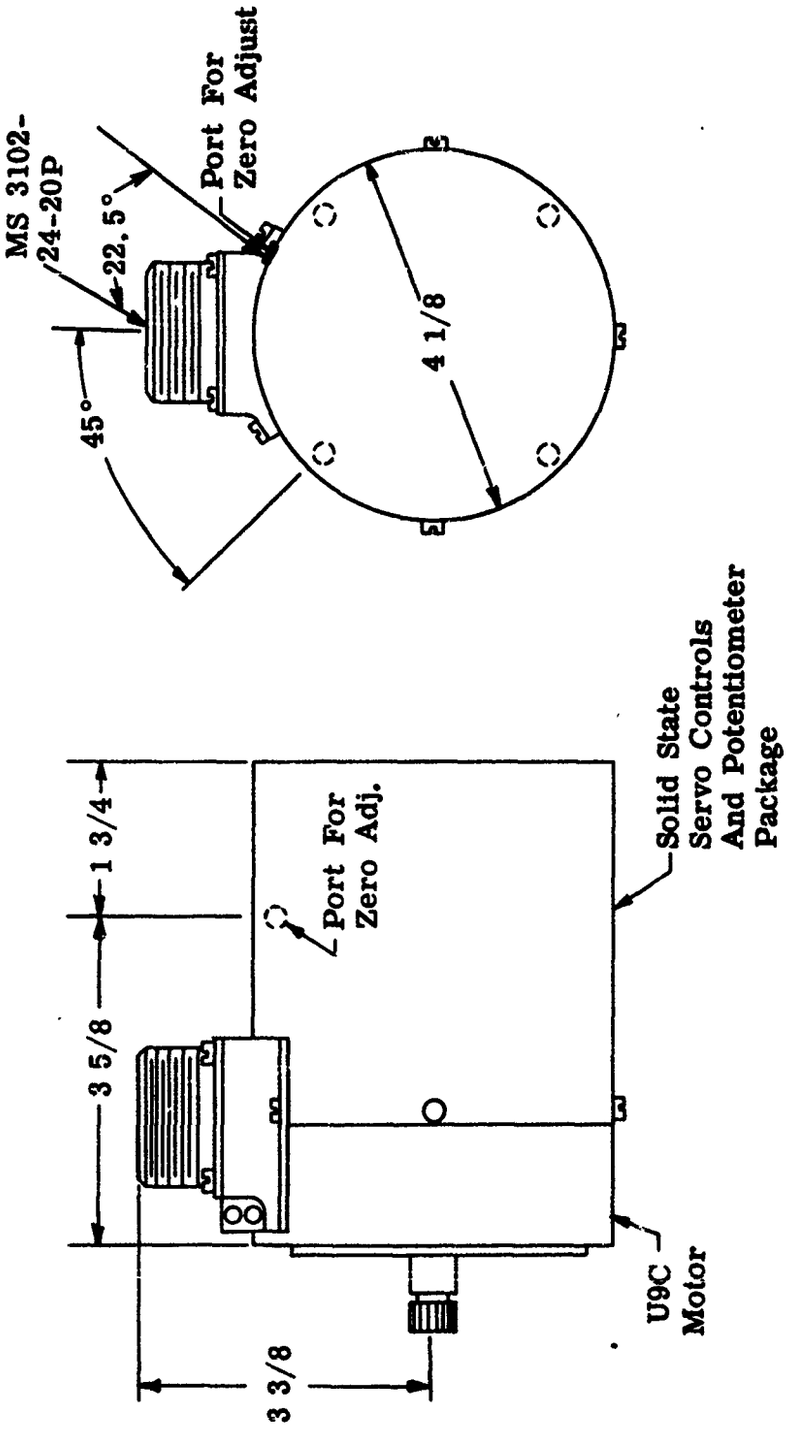


Figure 87. WSR-101 prototype servo and motor system. (U)

20-688

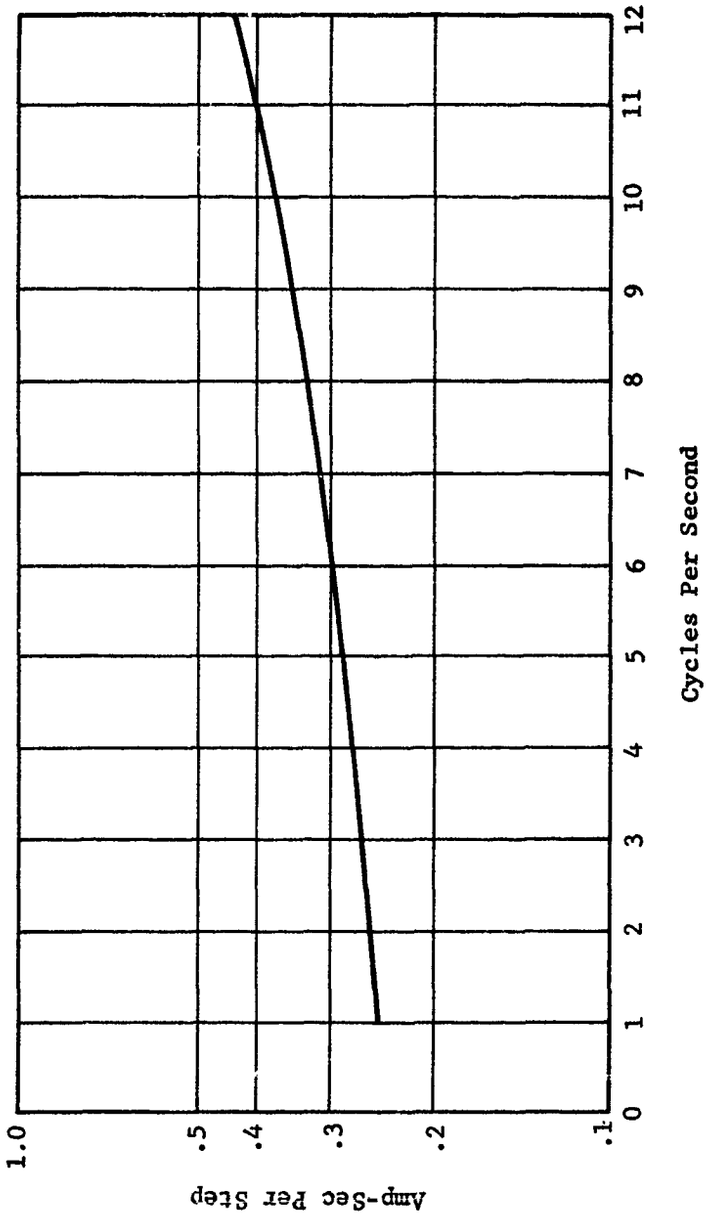
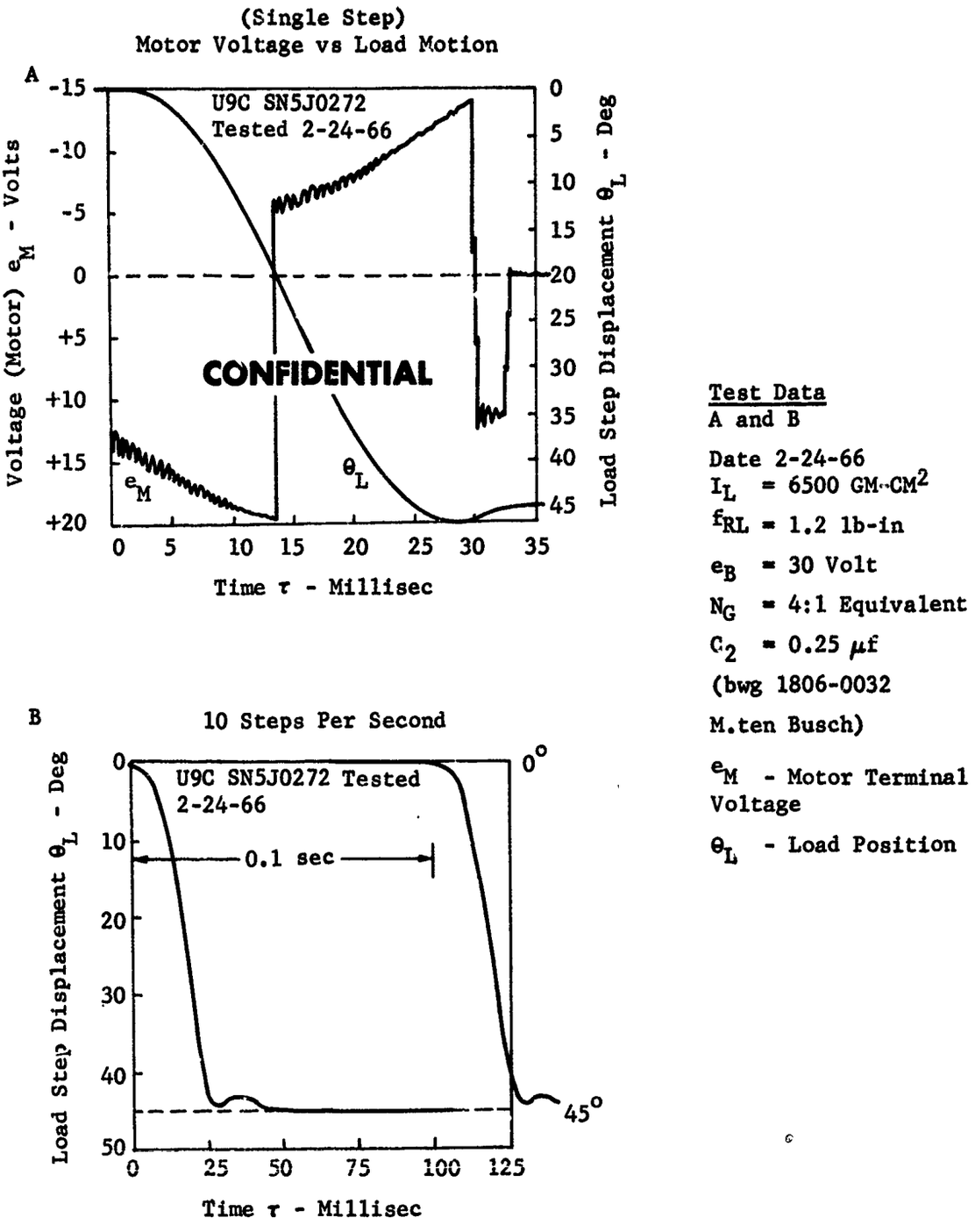


Figure 88. Prototype power requirements. (U)



Test Data
A and B

Date 2-24-66
I_L = 6500 GM-CM^2
f_{RL} = 1.2 lb-in
e_B = 30 Volt
N_G = 4:1 Equivalent
C_2 = 0.25 μf
(bwg 1806-0032
M.ten Busch)

e_M - Motor Terminal Voltage

θ_L - Load Position

Figure 89. WSR-101 prototype pulser (acceptance test data). (U)

20-826

PRECEDING PAGE BLANK-NOT FILMED

SECTION VII

FABRICATION

(U) Molds were procured for the expandable dome, the nozzle base, and the premolded inhibitor. After parts had been molded for dimensional inspection, pieces were made for initial firing tests and for development of assembly techniques.

(U) Following the selection of Dow Corning Silastic 55 as the dome material, 150 pieces were molded for the initial static firing tests. The two-cavity mold and a sample dome are shown in Figure 90. After completion of the initial pieces, production was initiated for the quantity required for the program. The molded parts were inspected visually prior to assembly.

(U) The single cavity mold for nozzle bases is shown in Figure 91. This mold is used in a Hull Corporation transfer molding press employing the usual techniques required for transfer molding. Dimensional inspection of the parts produced showed that they conformed to blueprint requirements. In addition, each part molded was visually inspected at a magnification of 13 diameters. Five different materials, Fiberite FM 4005, MX 1344-50, MX 2199A, MX 3264-2, and Allied Chemical Corporation Epial 1907 were used to make the first few pieces for firing tests as part of the materials evaluation phase. Following the selection of the quartz fiber filled phenolic compound MX 1344-50 as the nozzle base material, a total of 1650 pieces were molded. This operation produced an acceptance level of 93%, an improvement over the predicted 85%.

(U) Nine hundred pieces of the premolded propellant inhibitor were made in a single cavity mold using conventional compression molding techniques on the Gen Gard V-57 compound. The first group of parts was used for the development of assembly techniques and the remainder were used for final assemblies.

(U) A number of RTV silicone molds were prepared for inhibitor application to the propellant grains of asbestos filled epoxy. Upon development of the premolded inhibitor, fixtures were used for assembly of the inhibitor to provide the required dimensional control. Several acrylic plastic molds were cast for use in bonding the domes to the nozzle-propellant subassemblies. This temporary tooling was used for assembly of motors for the early static firing tests.

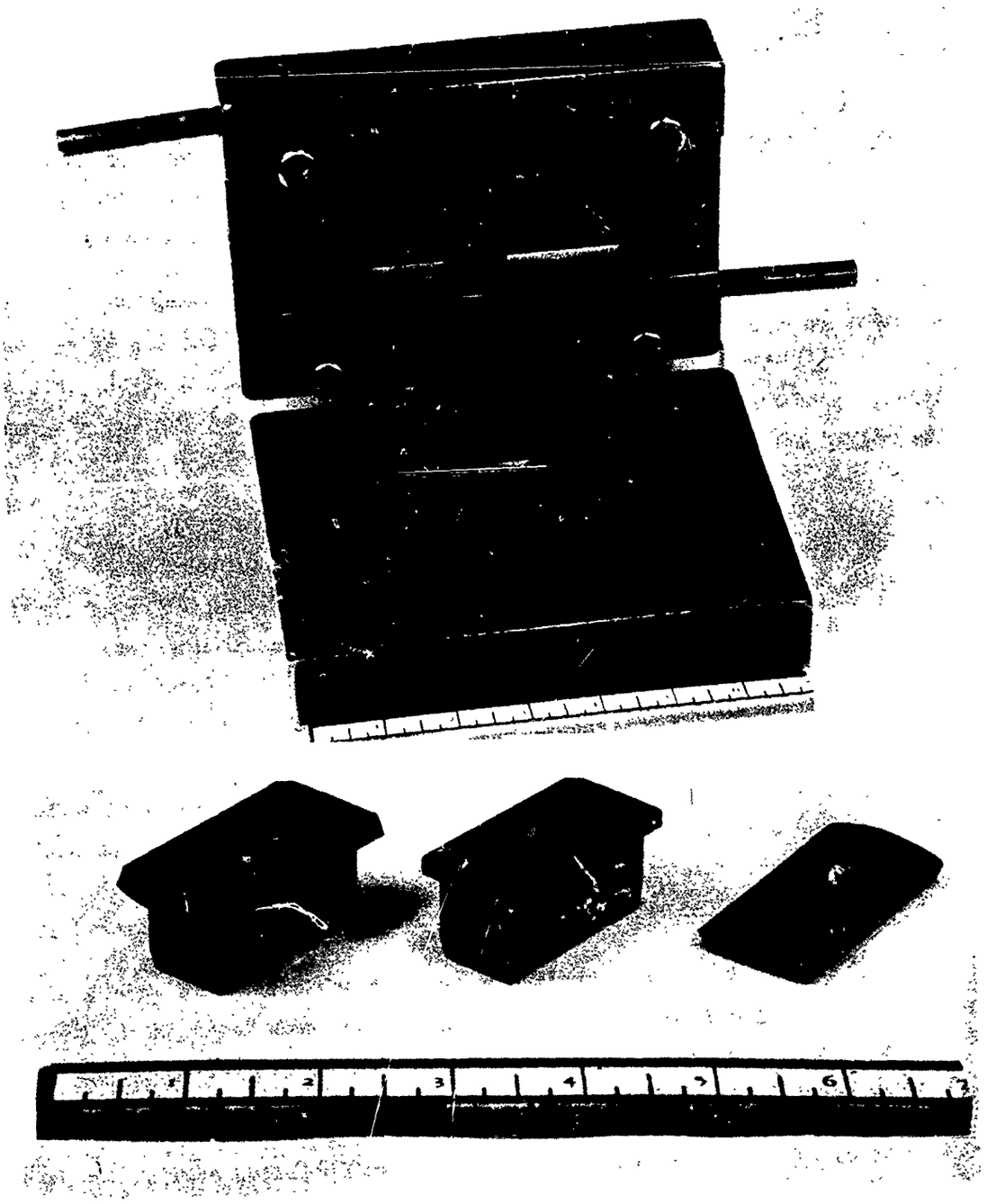


Figure 90. Two cavity "E" dome mold. (U)

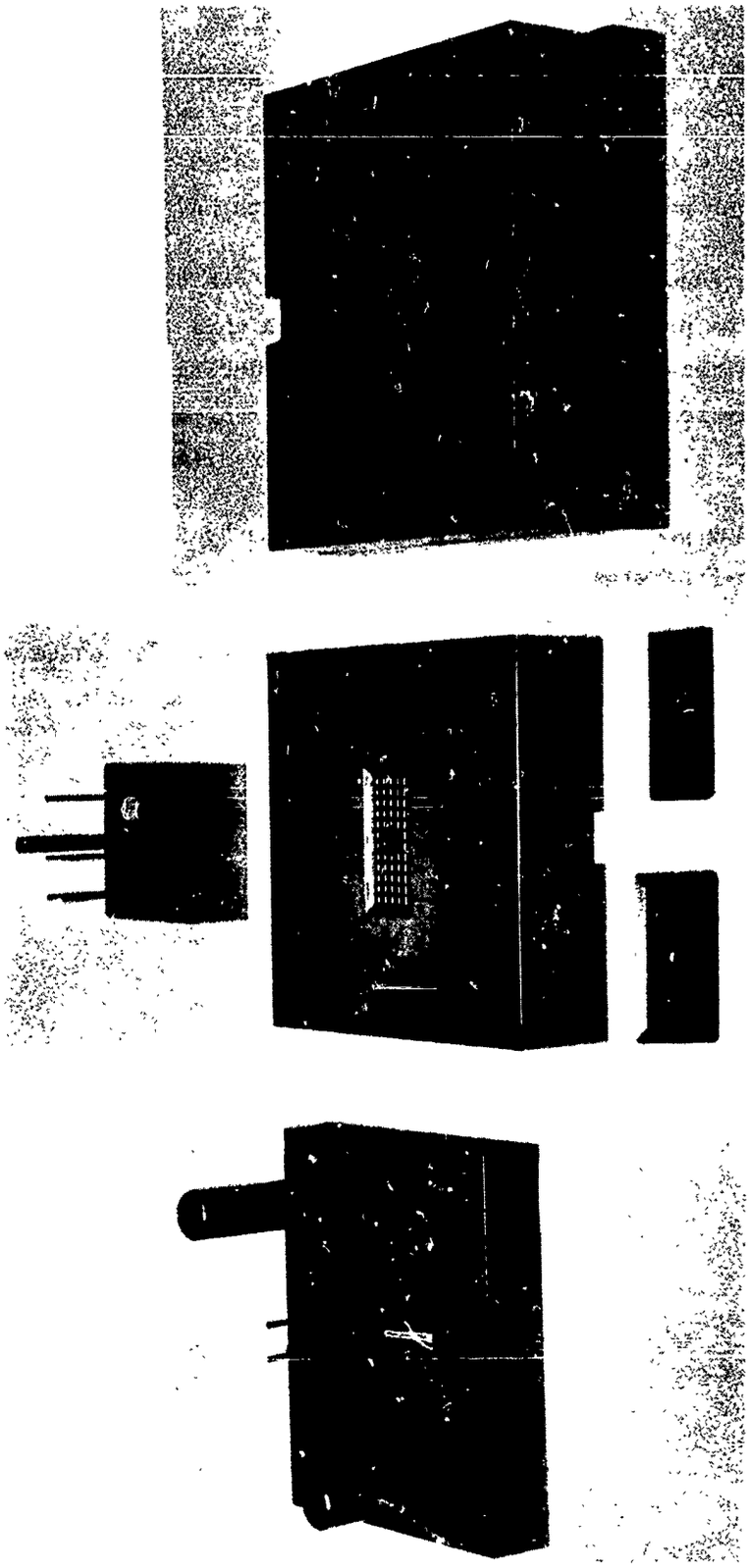


Figure 91. Single cavity nozzle base mold. (U)

14-681

(U) Assembly of the majority of motors and their application to tapes was made by a sub-contractor, High Temperature Instrument Co., Philadelphia, Pa. This organization produced its own tooling and fabricated the assemblies under the direction of WAD personnel and in accordance with WAD developed procedures.

(U) The assembly procedures utilized silicone adhesives to attach the premolded inhibitor to the propellant grain and to attach this subassembly to the nozzle base. Close dimensional control is maintained during curing of the adhesives by the assembly tooling. Similarly, closely dimensioned fixtures are used to attach the motors to the tape to maintain proper alignment.

(U) A transport tape punch was procured and was used by the vendor to provide suitably punched Teflon-Fiberglass tape for the program.

(U) A mold for the transport belt for the pulser inlet-outlet chute was designed and procured. Five belts were molded using a urethane resin.

SECTION VIII

TEST

A. Rocket Motor Tests

1. Development Tests

(U) All static testing of the rocket motor was performed using the test fixture shown in Figure 92. Individual motors were mounted on short lengths of tape and placed in the test fixture pocket which simulates the sprocket wheel cavity. The clearances and relationship of the ignition contacts are identical to the pulser assembly. The test fixture is mounted on a thrust stand, shown in Figure 93, which uses a Kistler piezoelectric force transducer to measure thrust. A schematic of the firing set-up and instrumentation circuitry is shown in Figure 94. The motor is fired by a current pulse which simultaneously triggers the oscilloscope sweep circuit. The signal generated by the force cell is amplified and displayed on a dual beam oscilloscope along with the ignition current. Force calibration and time calibration signals are also displayed on the scope. All of this data is recorded for each firing on a Polaroid photograph.

The initial WSR-101 rocket motor static firings were made to establish a baseline configuration and evaluate candidate nozzle base and E dome materials. The propellant (CWP-9), igniter (CWIC-4) and nozzle plug configurations were fixed while the following base and dome materials were evaluated.

BASE MATERIALS

FM 4005 Fiberglass reinforced phenolic
MX 1344-50M Quartz - fiber reinforced phenolic
MX 1299A Magnesium-oxide fiber reinforced phenolic
MX 3264-2 Silica-fiber reinforced flexible phenolic
Epial 1907 Fiberglass reinforced epoxy

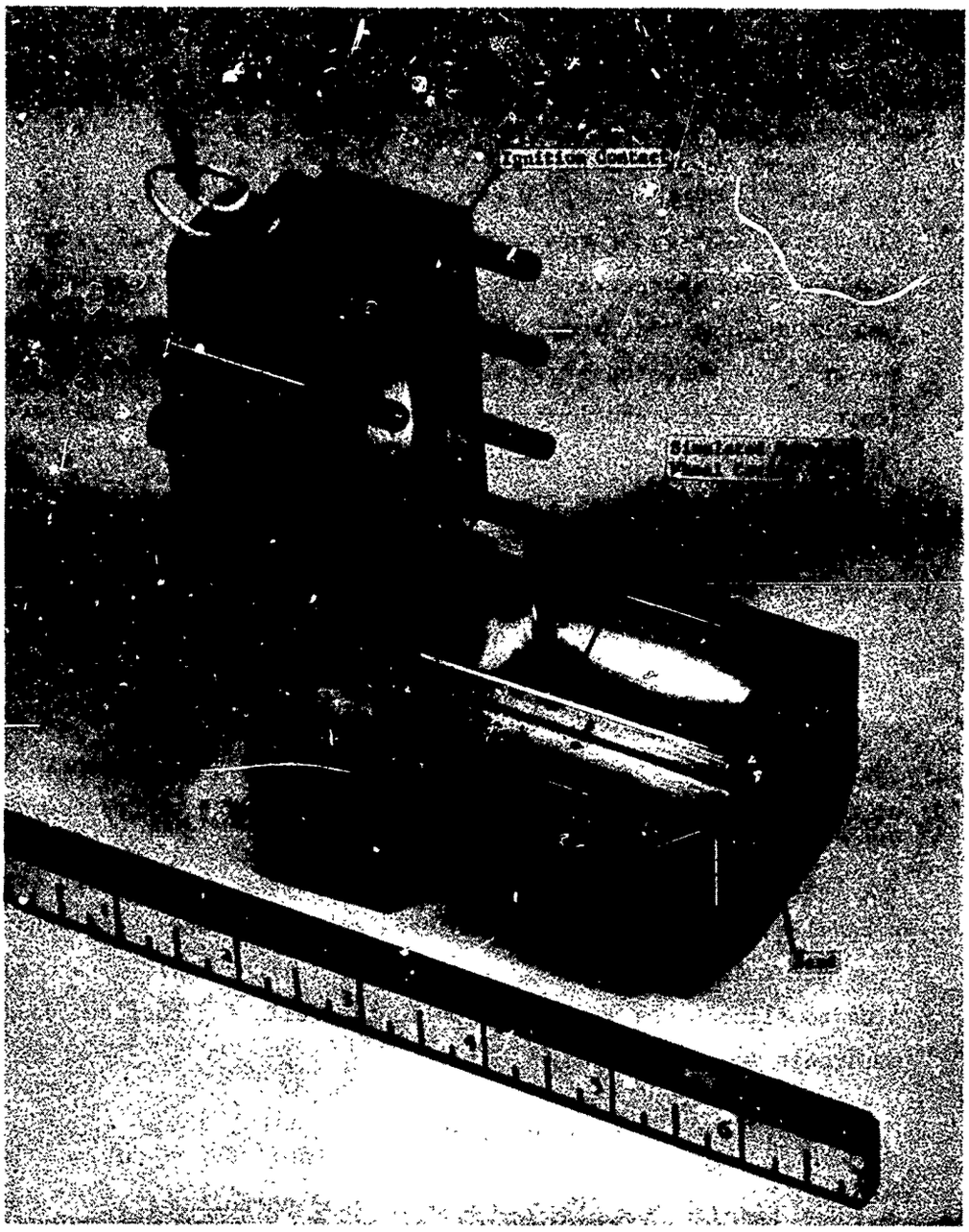


Figure 92. WSR-101 static firing fixture. (U)

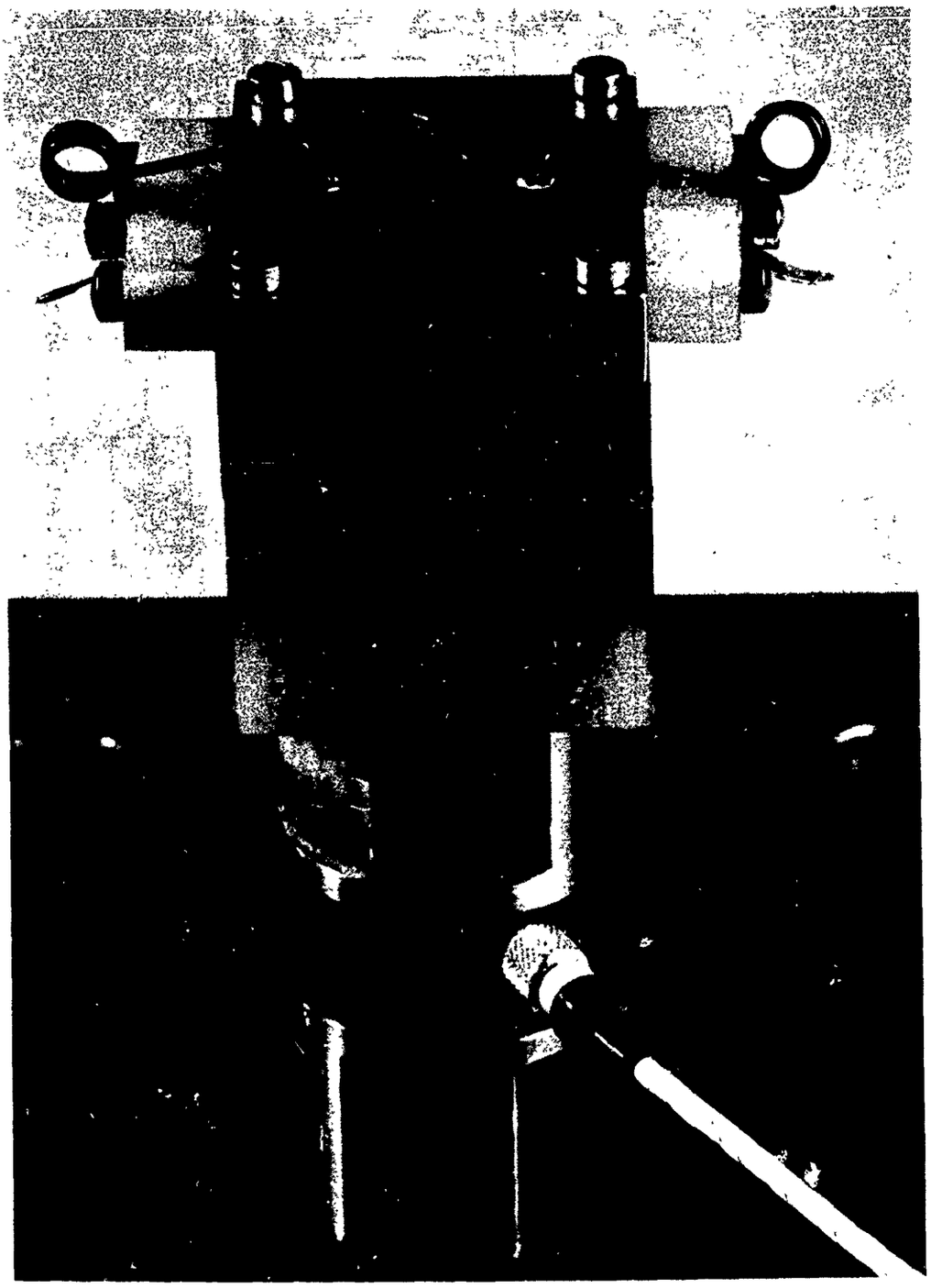


Figure 93. Static firing fixture on thrust cell. (U)

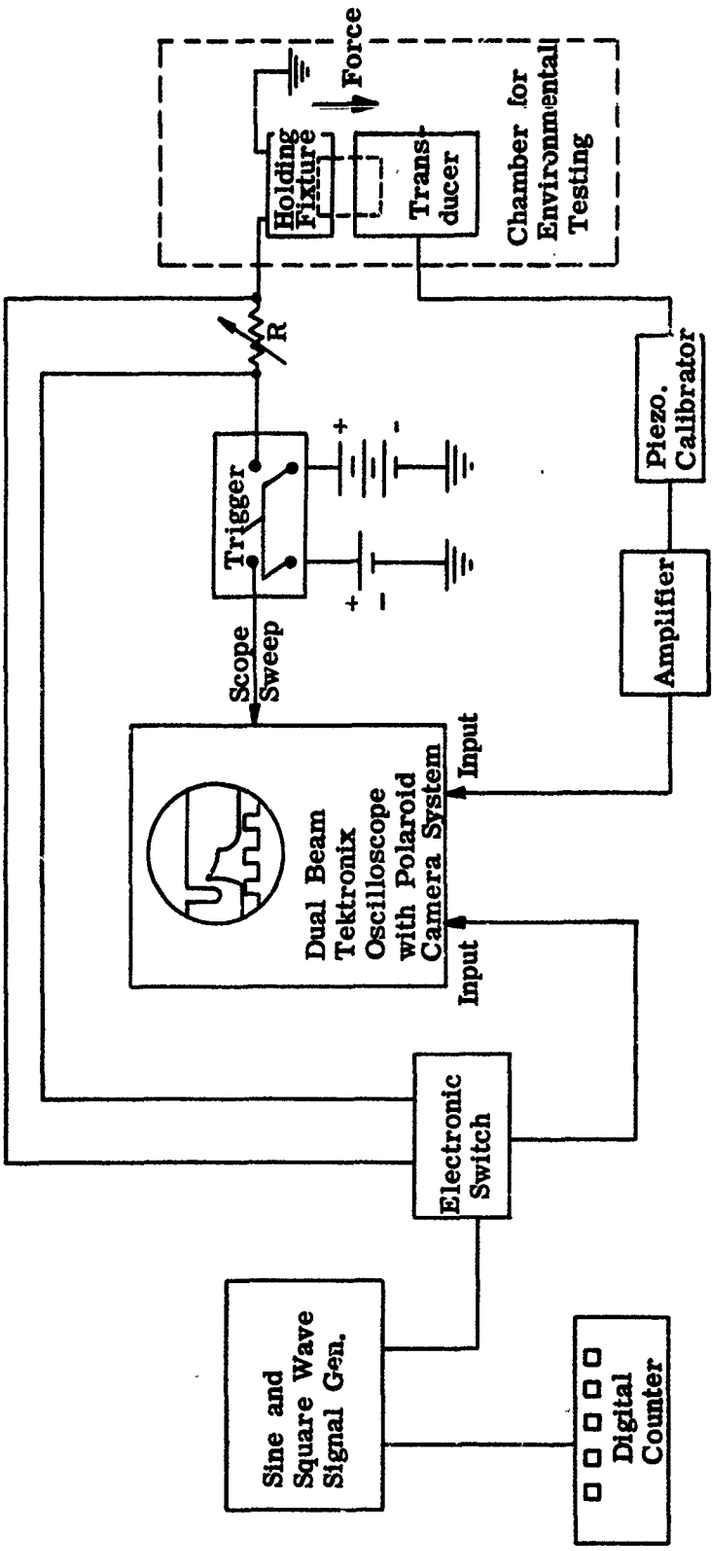


Figure 94. Schematic of static test set-up. (U)

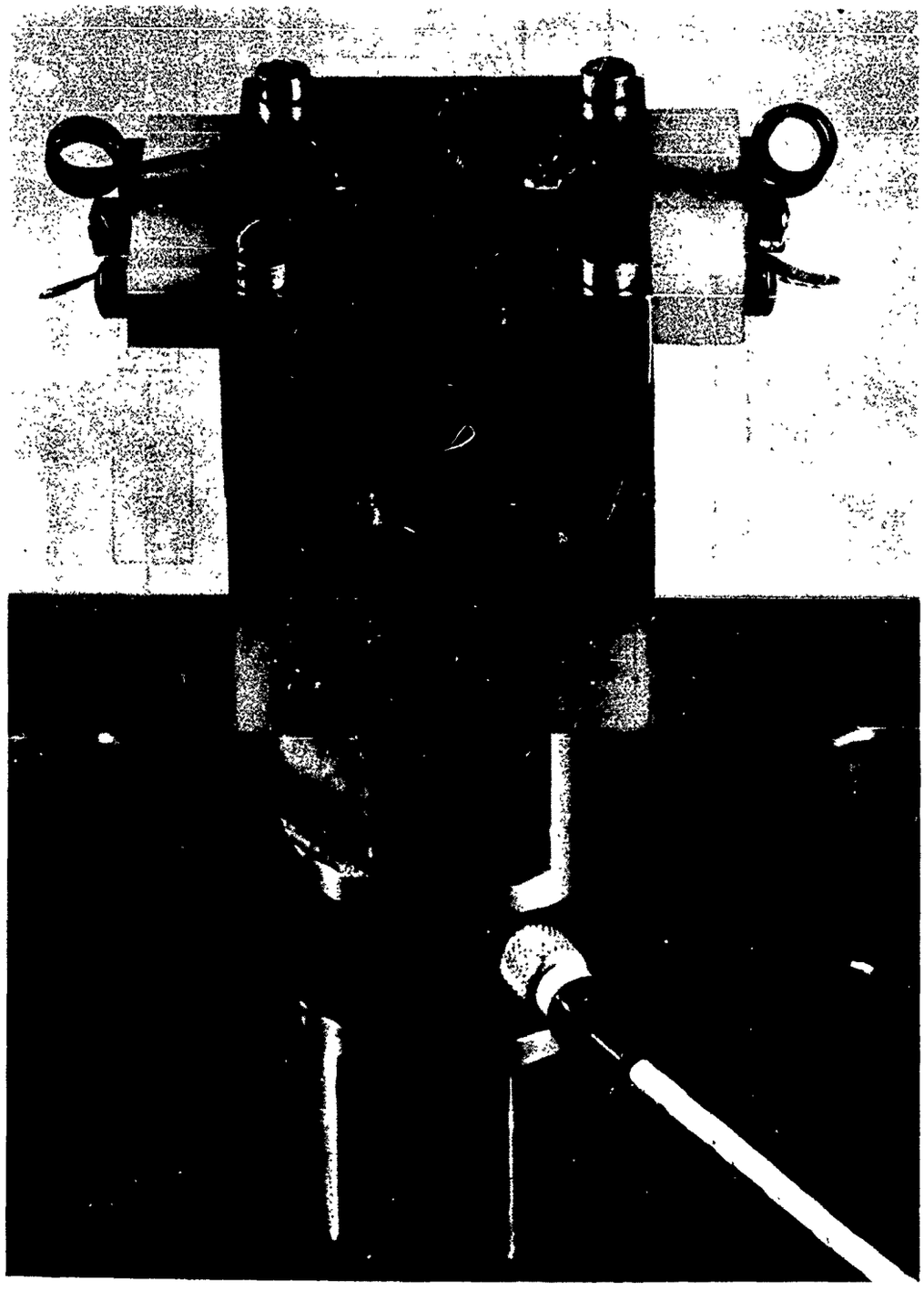


Figure 93. Static firing fixture on thrust cell. (U)

13-468

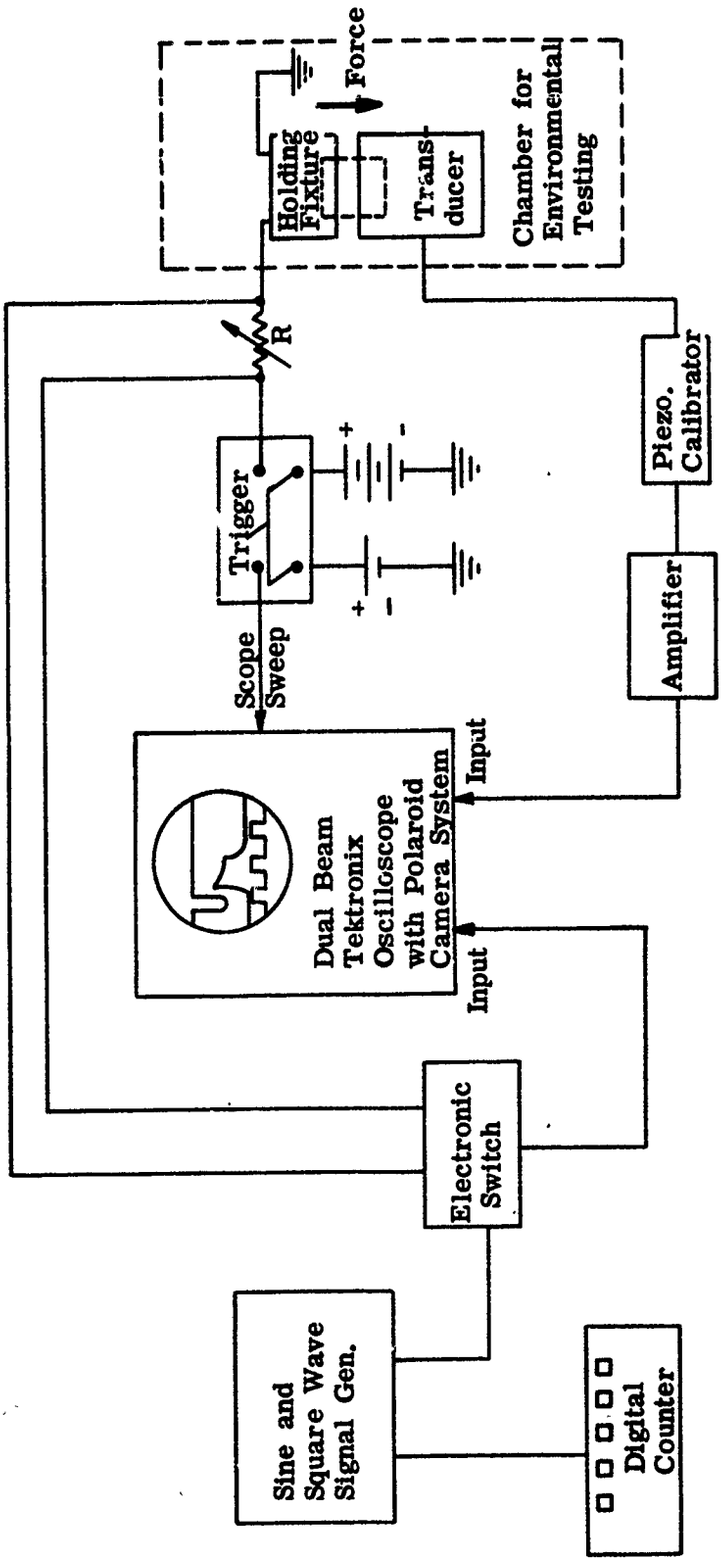


Figure 94. Schematic of static test set-up. (U)

DOME MATERIALS

(U) Silica-filled Buna-N Rubber (V-57)
Silicone Rubber (Silastic -55)

(U) These material evaluation tests were made using a closed fixture with no sprocket wheel-to-housing gap allowance. A total of seven firings were made and the results clearly indicated that the MX 1344-50M Quartz-fiber reinforced phenolic exhibited the best resistance to nozzle erosion and provided the highest strength. The flexible phenolic and the epoxy materials had the highest nozzle erosion. Both dome materials functioned satisfactory, however, the Silastic 55 silicone rubber was chosen because of the low temperature requirements.

(U) The next series of twelve static firings were conducted to establish an initial grain inhibitor configuration. Two epoxy materials were used, Epon 907 and an unfilled Epon 907 to which 50% asbestos powder was added. Both materials were molded around the periphery of the grain. The asbestos filled epoxy gave more consistent results and was used for the remaining development tests.

(U) To determine the margin of safety for the nozzle base, hydrostatic tests were conducted on four units to establish the rupture pressure. Table XIX lists the results of these tests and Figure 95 shows a typical failure of the base. The results show an average rupture pressure of 6900 psi and a 3.25 margin of safety.

(C) In establishing the final rocket motor design, the established nozzle base, E-dome, inhibitor, and nozzle plug configurations were used. Two propellants (CWP-9 and CWP-13) and three igniter compositions (CWIC-4, -6, -8) were evaluated. The results of these tests showed that the CWP-13 propellant and the CWIC-8 igniter produced an optimum configuration for minimum ignition delay, minimum action time and high performance. Figures 96 and 97 show the thrust-time curves achieved using CWP-9 and CWP-13 propellants

Table XIX. Nozzle base hydrotest.(U)

Test No.	Test Pressure psi	Rupture Pressure psi	Remarks
1	6,000 7,000 7,500	7,500	No. Cracks - Seal Leak
2	7,000	7,000	
3	6,500 6,750	6,750	
4	6,500	6,500	

(This page is unclassified)

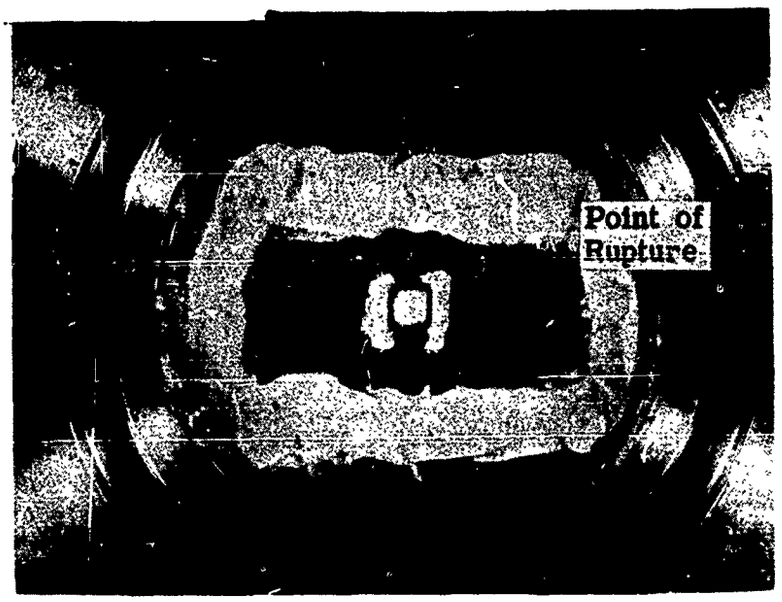
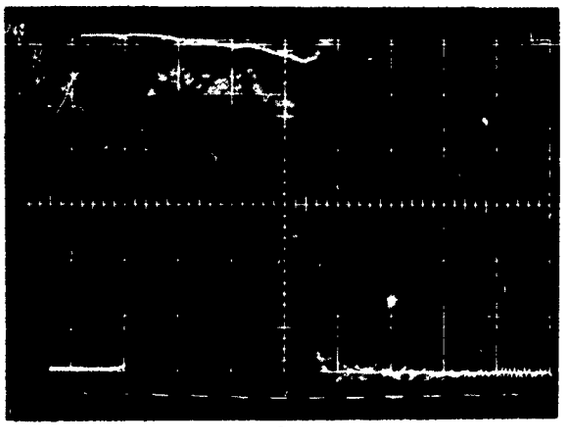
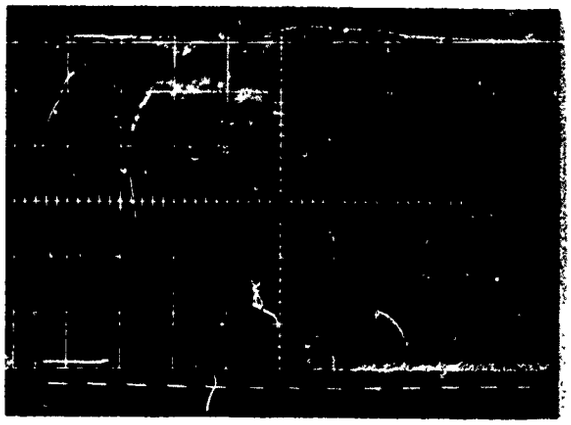


Figure 95. Hydrostatic test of nozzle base. (U)

(This page is unclassified)

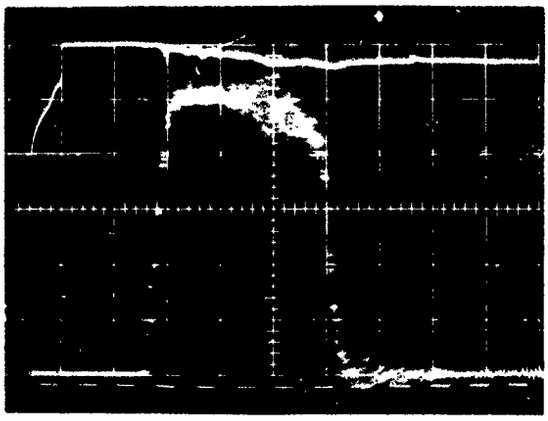


C^2-43



C^2-44

CONFIDENTIAL



C^2-47

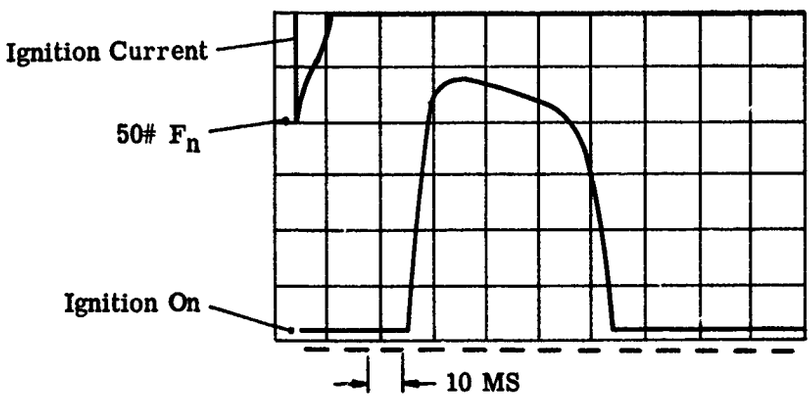
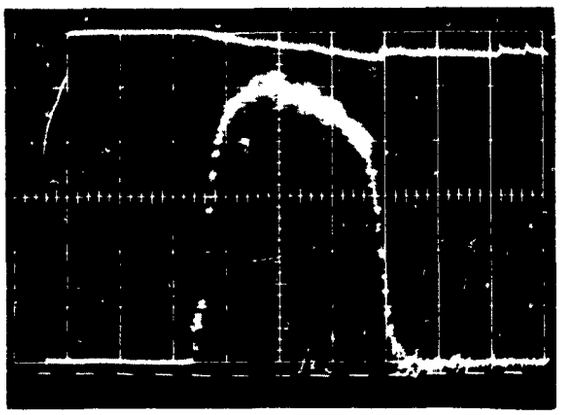
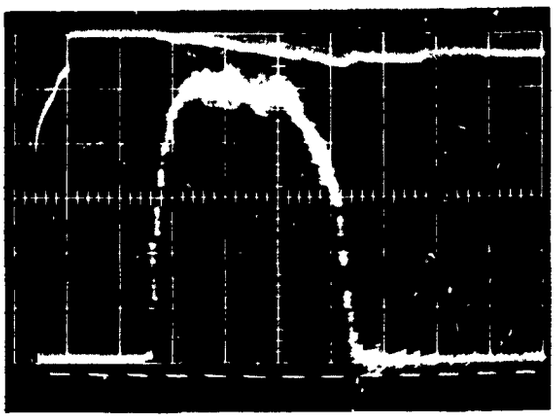


Figure 96. Thrust time traces, WSR-101, CWP-9. (U)

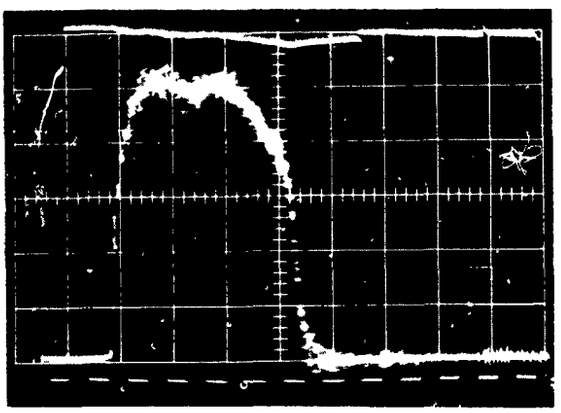


C^2-41

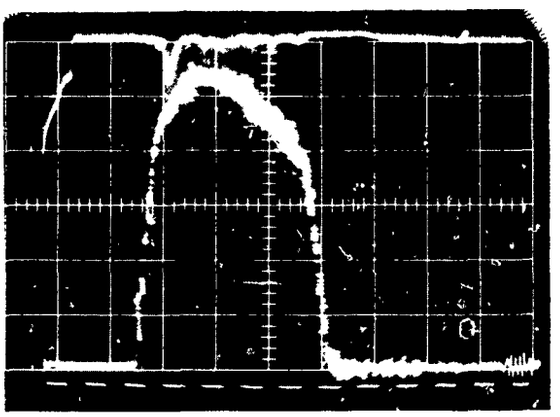


C^2-42

CONFIDENTIAL

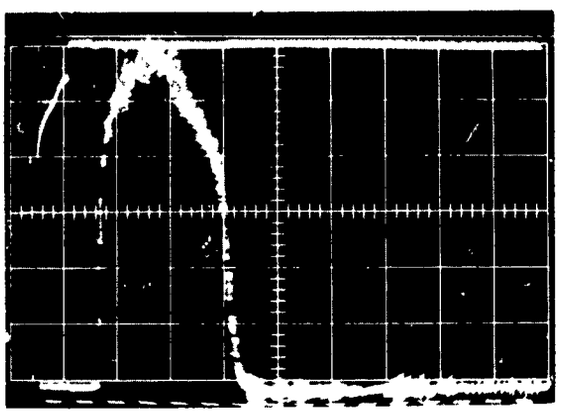


C^2-45

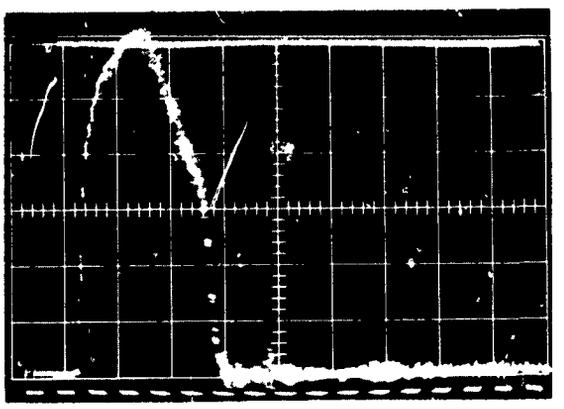


C^2-46

Figure 96. (cont.)

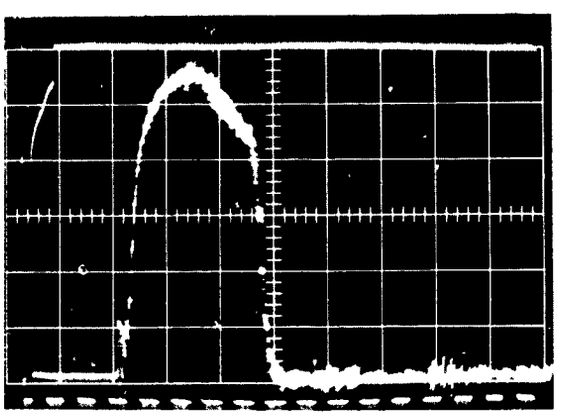


C-122

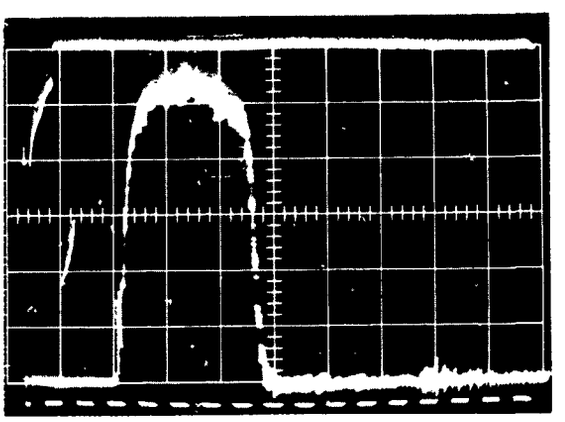


C-123

CONFIDENTIAL



C-126



C-127

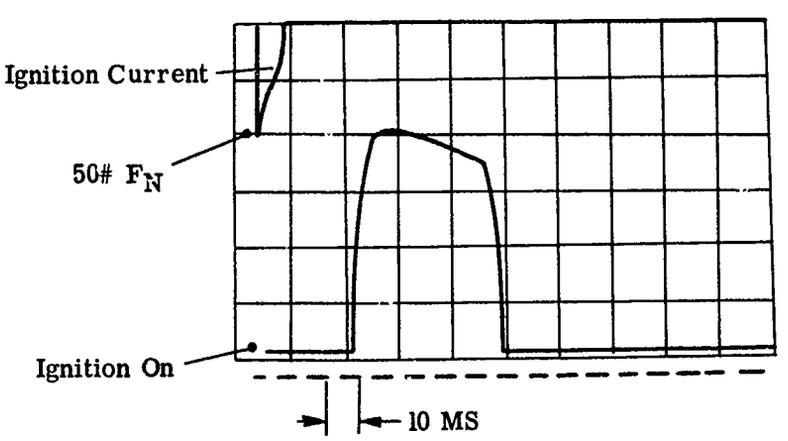
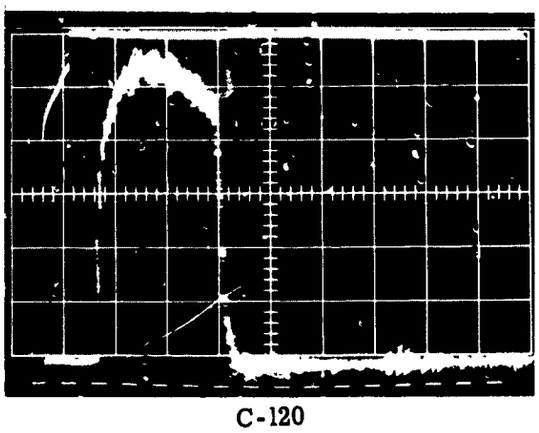
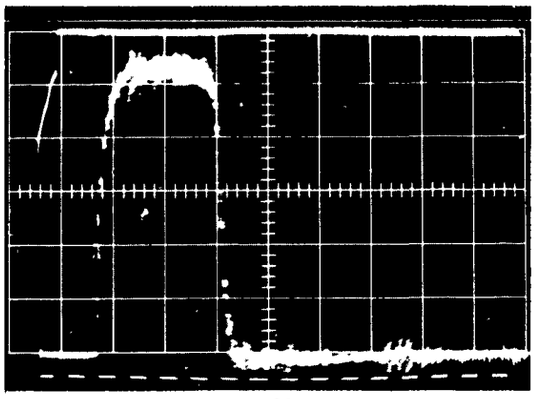


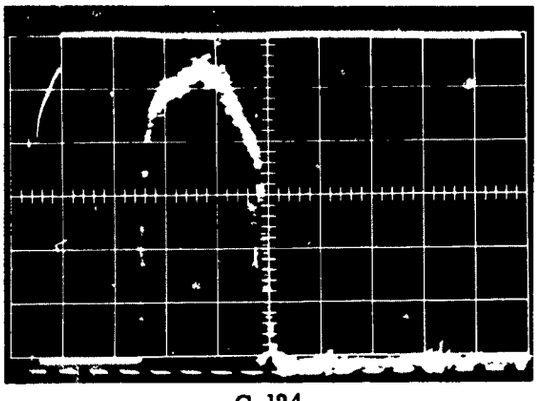
Figure 97. Thrust time traces, WSR-101, CWP-9. (U)



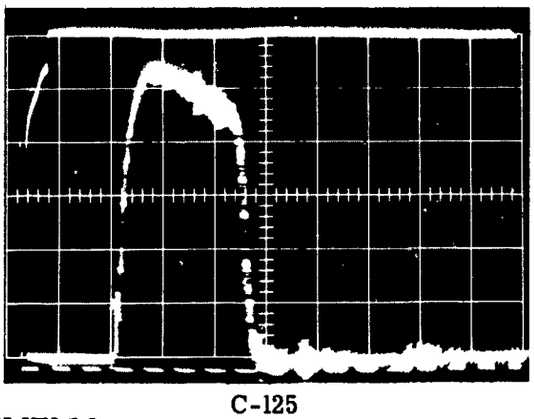
C-120



C-121

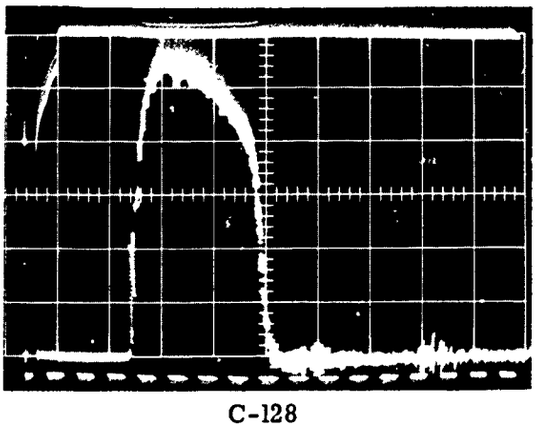


C-124



C-125

CONFIDENTIAL



C-128

Figure 97. (cont.)

(C) respectively. The performance obtained is presented in Table XX. The average specific impulse achieved with either propellant was 250 seconds, however, the overall action time for the CWP-13 propellant was shorter. The test results on ablation of the "E" dome and erosion of the exhaust nozzle throat are summarized in Table XXI.

(U) Once the rocket motor configuration was established, fabrication of approximately 1000 units was started to support the remaining static firing and repetitive firing tests. These units were to be assembled manually using fixtures to hold the components during handling and curing. A sampling of these motors were fired for comparison with previous performance to check on the quality and assembly techniques.

(U) The initial firings indicated that the change from laboratory assembly to semi-production assembly reduced quality and the number of successful firings decreased 30%. During the subsequent investigation to improve the quality of the motors a structural problem was uncovered concerning the gold ignition lead in the plastic nozzle base. As shown in Figure 98, the gold lead was not being properly positioned by the molding die. This resulted in either exposure of the lead or thinning down of the nozzle material. During firing, this weakened section would break out causing nozzle blockage and a resultant motor failure. Several new configurations were fabricated and tested to resolve this problem. These included placing the ignition lead through the nozzle and allowing them to blow out during ignition as well as modification to the die to prevent the gold leads from being skewed during the molding process. The problem was finally resolved by placing the ignition leads at the ends of the capsule. This completely removed the leads from the exhaust nozzle area. Firing tests with this configuration were completely successful.

(U) Continued investigations to improve the quality of the semi-production units showed the major problem to be with the asbestos filled epoxy inhibitor. The application of the inhibitor to the propellant grain and the integrity of the bond between the grain and epoxy during

Table XX. WSR-101 sea level static firings. (U)

E = 14:1

Motor Number	Propellant	Igniter	Total Impulse Lb-Sec	Specific Impulse Sec	Ignition Delay M.secs	Thrust Duration M.secs
41	CWP-9	CWIC-6	2.60	250	38	50
42	CWP-9	CWIC-6	2.80	251	29	50
43	CWP-9	CWIC-6	2.94	267	20	49
44	CWP-9	CWIC-6	2.82	259	18	49
45	CWP-9	CWIC-6	2.81	256	18	49
46	CWP-9	CWIC-6	2.67	249	23	48
47	CWP-9	CWIC-6	2.75	251	30	48
120	CWP-13	CWIC-8	2.78	257	17	42
121	CWP-13	CWIC-8	2.78	258	18	42
122	CWP-13	CWIC-8	2.83	256	20	45
123	CWP-13	CWIC-8	2.74	252	15	45
124	CWP-13	CWIC-8	2.59	255	34	43
125	CWP-13	CWIC-8	2.72	255	30	45
126	CWP-13	CWIC-8	2.76	258	29	47
127	CWP-13	CWIC-8	2.79	258	28	46
128	CWP-13	CWIC-8	2.76	256	32	45

Table XXI. Ablation of dome and exhaust nozzle throat erosion.(U)

	DOME		THROAT		
Motor Number	Before Firing	After Firing	Before Firing	After Firing	Propellant
120	.021 / .020	.016 / .015	.1495	.150 / .148	CWP-13
121	.021 / .020	.018 / .014	.1495	.160 / .150	CWP-13
81	.021 / .020	.018 / .016	.1370	.150 / .140	CWP-9
75	.021 / .020	.018 / .015	.1370	.140 / .135	CWP-9
77	.021 / .020	.018 / .014	.1370	.145 / .140	CWP-9
49	.021 / .020	.019 / .014	.1370	.140 / .135	CWP-9

CONFIDENTIAL

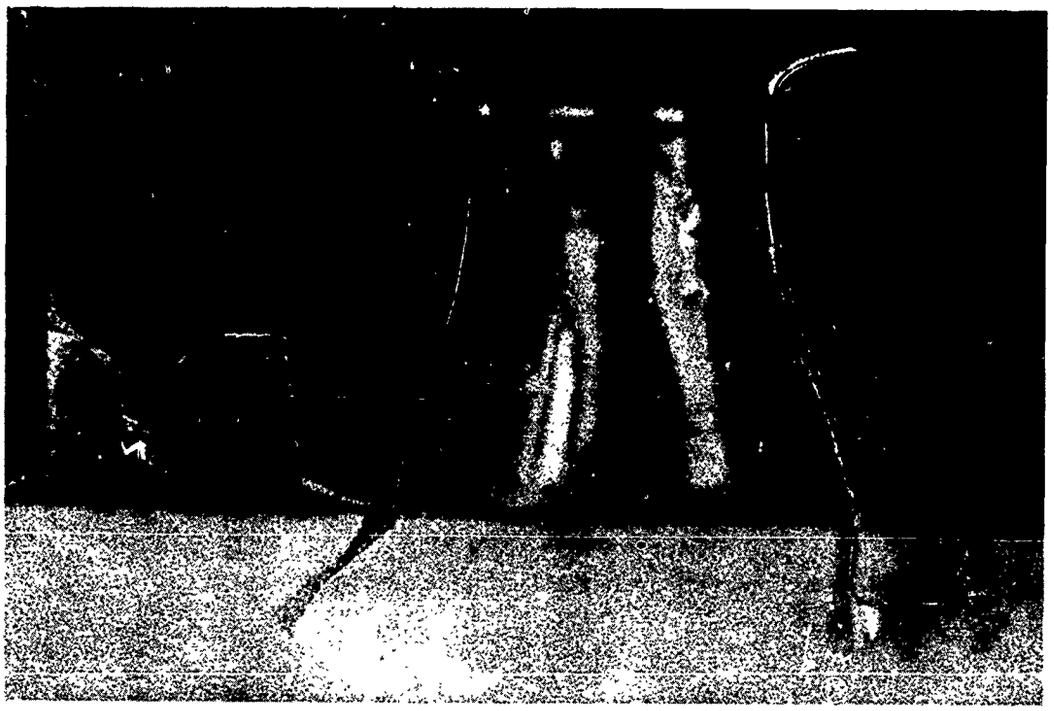


Figure 98. Nozzle base and gold lead configuration. (U)

(C) firing were marginal. Several schemes were investigated. The inhibitor tooling was modified to vent entrapped air in the inhibitor. Changes were made in techniques to ensure better wetting of the epoxy to the grain. Both of these approaches proved unsuccessful. A total of 77 static firings were made during this phase of the test program. A successful firing level of 58% was obtained which showed a negligible improvement over previous semi-production units. The failures were primarily due to the breakdown of the inhibitor bond between the grain and epoxy. This exposed more propellant area for burning and a resultant overpressurization and subsequent failure of the E-dome. Most of the changes which could be incorporated into the epoxy inhibitor configuration had been tried without success. Therefore, it was decided that a completely new inhibitor system was needed. The chosen configuration was a premolded rubber boot which fits tightly on all surfaces of the grain to be inhibited. This boot is adhered to the grain using DC-280 and 92-018 adhesives. Thirty-five units were fired at sea level static conditions as qualification units. A 100% successful firing level was achieved. Figure 99 shows eight typical thrust-time traces during these tests. These series of firings established the final rocket motor configuration and concluded the motor development phase of the program.

2. Performance and Repeatability Tests

(C) The final rocket motor configuration defined in the development series of tests was used to establish the performance level and repeatability of the system. One hundred motors were fired at static sea level conditions with an expansion ratio of 14:1. Table XXII summarizes the performance obtained and Figure 100 shows typical thrust-time traces for the 100 firings. A successful firing level of 99% was achieved for this series. Table XXIII summarizes the repeatability analysis of the firings.

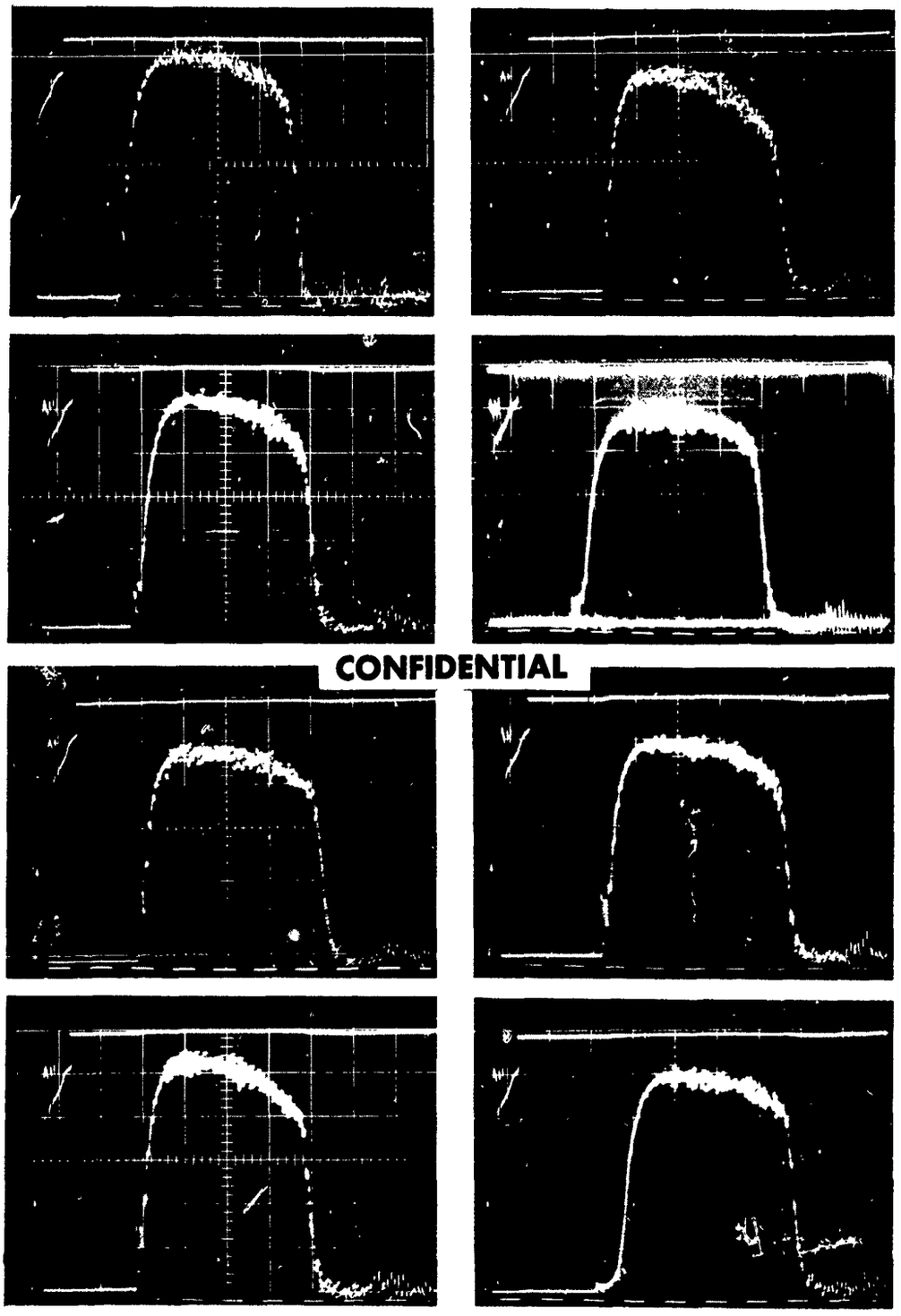


Figure 99. WSR-101 thrust time traces qualification motors. (U)

Table XXII. WSR-101 rocket motor static firing tests.(U)

MOTOR CONFIGURATION

PROPELLANT: CWP-13 IGNITER: CWIC-8
BASE: MX 134-50M DOME: SILASTIC 55
INHIBITOR: GEN GARD V-57

Capsule No.	Grain Wt. gms.	I_t Total Impulse lb-secs	Isp Specific Impulse Secs	Total Time M.secs	Ignition Delay M.secs	Thrust Duration M.secs	Remarks
1	4.8155	2.68	252	68	19	49	
2	4.8902	2.69	249	67	20	47	
3	4.9018	2.73	252	66	18	48	
4	4.8947	2.68	249	70	23	47	
5	4.8869	2.69	250	67	18	49	
6	4.8829	2.64	245	69	22	47	
7	4.9153	2.87	265	67	18	49	
8	4.8593	2.75	256	72	27	45	
9	4.8681	2.79	260	67	20	47	
10	4.8726	2.66	248	69	21	48	
11	4.8562	2.70	252	67	20	47	
12	4.8596	2.70	252	72	23	49	
13	4.7994	2.74	259	80	33	47	
14	4.8404	2.72	255	63	18	45	
15	4.8744	2.72	253	72	26	46	
16	4.8660	2.68	249	70	23	47	
17	4.8693	2.69	251	63	18	45	
18	4.7545	2.54	243	66	22	44	
19	4.8552	2.54	237	63	22	41	
20	4.8659	2.58	240	82	33	49	
21	4.8552	2.68	251	84	39	45	
22	4.8699	2.64	245	77	31	46	
23	4.8346	2.64	248	67	22	45	
24	4.8798	2.72	253	73	28	45	

Table XXII (Cont)

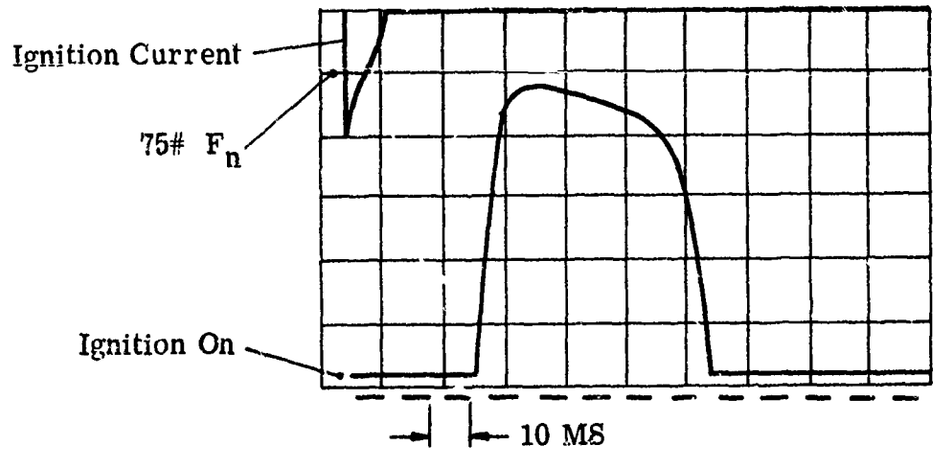
Capsule No.	Grain Wt. gms.	I_t Total Impulse lb-secs	I_{sp} Specific Impulse Secs	Total Time M.secs	Ignition Delay M.secs	Thrust Duration M.secs	Remarks
25	4.8908	2.75	235	72	23	49	
26	4.8599	2.63	245	72	26	46	
27	4.8667	2.69	251	62	20	42	
28	4.8193	2.61	245	72	27	45	
29	4.8539	2.68	250	66	18	48	
30	4.8753	2.64	246	64	18	46	
31	4.8757	2.61	242	72	25	47	
32	4.8616	2.57	240	72	23	49	
33	4.8865	2.62	243	70	22	48	
34	4.8799	2.69	249	70	25	55	
35	4.9012	2.72	251	67	18	49	
36	4.8542	2.64	246	74	27	47	
37	4.8817	2.6'	243	77	28	49	
38	4.8722	2.62	244	68	22	46	
39	4.8715	2.68	249	67	22	45	
40	4.8865	2.69	250	66	19	47	
41	4.8869	2.74	255	77	26	51	
42	4.8563	-	-	-	-	-	Good firing- Data recording malfunction
43	4.8509	2.59	242	67	21	46	
44	4.9147	2.64	243	67	19	48	
45	4.9510	2.73	249	73	26	47	
46	4.8753	2.63	245	70	22	48	
47	4.8674	2.62	244	95	46	49	
48	4.8211	2.61	245	65	18	47	
49	4.8581	2.62	244	72	23	49	
50	4.8978	2.64	244	67	19	48	
51	4.9148	2.70	250	72	23	49	
52	4.8665	2.59	242	67	20	47	
53	4.7924	2.54	241	70	23	47	

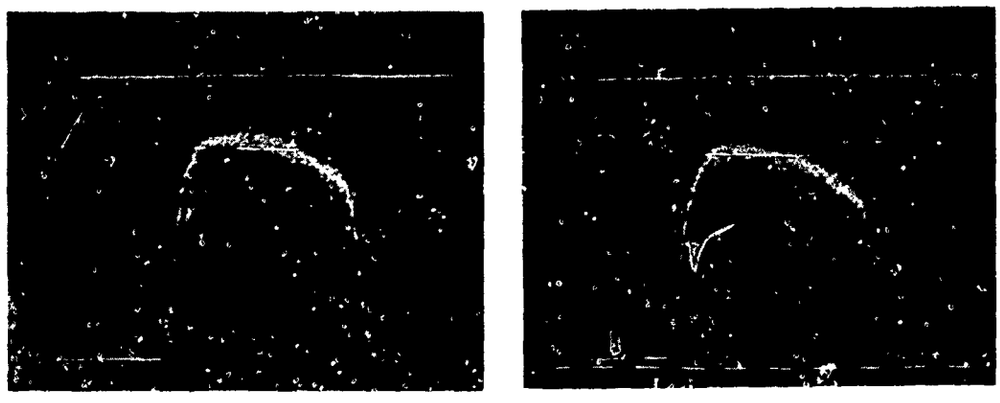
Table XXII (Cont)

Capsule No.	Grain Wt. gms.	I_t Total Impulse lb-secs	I_{sp} Specific Impulse Secs	Total Time M.secs	Ignition Delay M.secs	Thrust Duration M.secs	Remarks
54	4.8769	2.64	245	75	27	48	
55	4.8494	-	-	-	-	-	Capsule dome corner failure
56	4.8543	2.60	243	67	19	48	
57	4.8251	2.75	259	72	22	50	
58	4.8767	2.74	254	65	19	47	
59	4.8821	2.73	253	70	25	45	
60	4.8647	2.73	254	75	28	47	
61	4.9050	2.74	253	74	29	45	
62	4.8821	2.72	252	63	18	45	
63	4.8494	-	-	-	-	-	Good firing - Data recording malfunction
64	4.9339	2.64	242	62	18	44	
65	4.8899	2.67	247	72	23	49	
66	4.8894	2.65	246	72	25	47	
67	4.8428	2.64	247	62	17	45	
68	4.9115	2.73	251	64	20	44	
69	4.9007	2.68	248	65	19	47	
70	4.8328	2.61	245	65	18	47	
71	4.8578	2.64	247	66	20	46	
72	4.8865	2.65	246	63	15	48	
73	4.9577	2.74	250	67	20	47	
74	4.8008	2.67	250	64	18	46	
75	4.8945	2.77	256	63	18	45	
76	4.8741	2.79	260	66	18	48	
77	4.9594	2.77	253	65	18	47	
78	4.8693	2.71	252	68	20	48	
79	4.8776	2.61	243	72	28	44	
80	4.8617	2.62	244	65	18	47	
81	4.8535	2.56	239	64	19	45	

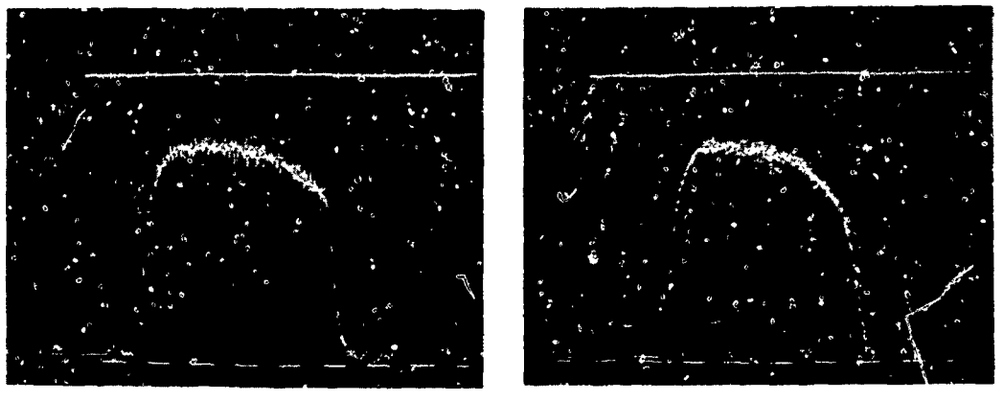
Table XXII (Cont)

Capsule No.	Grain Wt. gms.	I_t Total Impulse lb-secs	I_{sp} Specific Impulse Secs	Total Time M.secs	Ignition Delay M.secs	Thrust Duration M.secs	Remarks
82	4.8752	2.57	239	72	23	49	
83	4.8921	2.66	246	67	22	45	
84	4.8367	2.61	244	67	22	45	
85	4.8838	2.70	251	73	25	48	
86	4.8799	2.76	256	75	30	45	
87	4.8375	2.71	254	70	24	46	
88	4.8960	2.73	253	75	30	45	
89	4.8786	2.78	258	67	21	46	
90	4.8976	2.74	254	65	20	45	
91	4.8824	2.79	259	71	24	47	
92	4.8660	2.81	262	72	27	45	
93	4.8594	2.72	253	67	23	44	
94	4.8748	2.73	254	64	18	46	
95	4.8768	2.81	261	73	25	48	
96	4.8368	2.72	254	67	22	45	
97	4.8904	2.73	254	72	26	46	
98	4.9008	2.74	253	75	25	50	
99	4.8817	2.74	255	73	25	48	
100	4.8860	2.67	247	76	26	50	



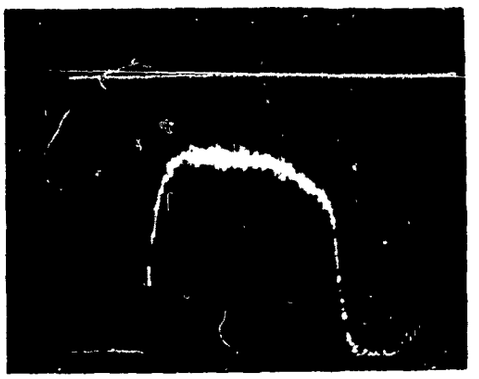


1077 1343



1371 1375

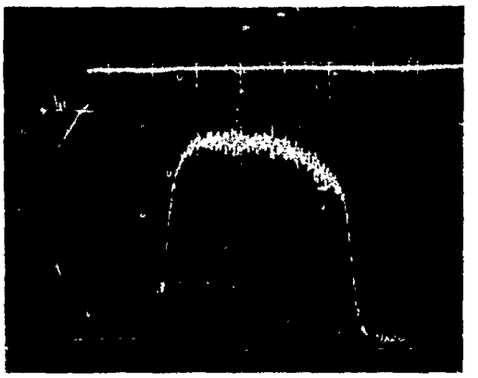
Figure 100. Thrust time traces, WSR-101, CWP-13. (U)



1406



1451



1473

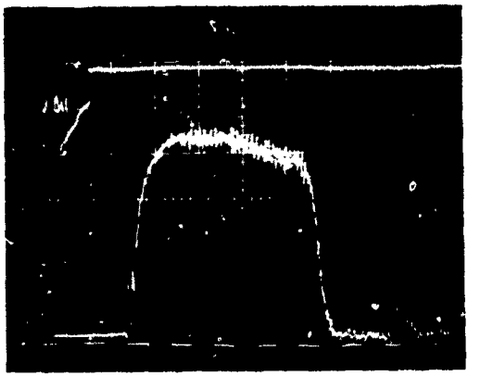


1864

CONFIDENTIAL



1933



1957

Figure 100. (cont.)

Table XXIII. WSR-101 rocket motor static sea level firing tests.

	Total Impulse LB-SEC	Specific Impulse SEC 14:1 S.L.	Thrust Duration M.secs	Ignition Delay M.secs
Mean	2.68	249.4	46.78	22.77
Range	2.54 to 2.87	237 to 265	41.0 to 55.0	15.0 to 46.0
Standard Deviation	0.0662	5.72	2.05	4.78
% Deviation	2.47%	2.30%	4.4%	20.9%

3. Aluminized Propellant Motor Tests

(C) The objective of this series of tests was to assess the performance characteristics of propellants containing aluminum. The particular composition (CWP-17A8) tested in the motors was selected as part of the propellant tailoring effort which is reported in Section V of this report. Two motor failures were experienced during the total of 25 firings. A summary of the performance obtained is presented in Table XXIV.

(C) Based on the theoretical sea level specific impulse for CWP-17A8 propellant of 265 seconds at a 14:1 expansion ratio, a specific impulse efficiency of 96% was obtained. This is 2% lower than obtained with the CWP-13 propellant, however, an increase of five seconds in delivered specific impulse was realized. The lower specific impulse efficiency for the CWP-17A8 can be attributed to incomplete combustion of the aluminum in the chamber because of the short dwell time.

4. Vacuum Tests

(C) To assess the capability of the rocket motor components to withstand the thermal and vacuum conditions of space the following schedule was established.

25 tests - Sea Level firings after vacuum storage at -30°F

25 tests - Sea Level firings after vacuum storage at +150°F

10 tests - Vacuum firings at -30°F

10 tests - Vacuum firings at 150°F

5 tests - Vacuum firings at Ambient

(C) The ignition of the propellant grain was recognized as a major obstacle in this series of tests. It was therefore decided to con-

Table XXIV. WSR-101 performance of aluminized propellant CWP-17A8.(U)

Motor Number	I_t Total Impulse) lb-secs	I_{sp} (Specific Impulse) Secs
282	2.96	260
284	2.92	259
287	2.98	263
289	2.66	246
293	2.74	246
294	2.61	245
295	2.69	245
298	2.72	244
299	2.62	237
300	2.74	254
301	2.88	261
296	2.95	267
297	Good Firing	Data recording malfunction
356	2.88	260
257	2.85	259
358	2.94	266
359	2.89	263
360	2.87	259
167	2.83	262
168	2.85	262
169	2.60	241
AL1	2.85	259
AL2	2.83	256

I_t Avg = 2.81 lb-secs

I_{sp} Avg = 255 secs

(C) duct a preliminary investigation of vacuum ignition prior to running the scheduled vacuum tests.

(U) Four igniter compositions were evaluated using full scale motor firings in vacuum. Table XXV shows the firing conditions and the ignition delays obtained. The CWIC-16 igniter composition, which produced the best results based on minimum delay time and ignition spike, was selected for the scheduled vacuum tests.

(C) Twenty-five units were installed in the vacuum chamber and exposed for three days at -30°F and an average of 10^{-6} torrs. The units were removed and fired at sea level ambient conditions. The results of the firings are presented in Table XXVI. The results show that no deterioration in performance or durability was experienced. The total impulse and specific impulse calculated from the data obtained were approximately 7% higher than previous data. This increase is attributed to a malfunction of the instrumentation during firing which could not be detected until the data was reduced. This was corrected for the remaining tests. Another 25 units were exposed for three days at +150°F and 10^{-6} torrs. vacuum. These units were also fired at sea level ambient conditions and the results are presented in Table XXVII. As before, no deterioration in performance was experienced. It is therefore concluded that exposure to temperature and vacuum have no effect on the rocket motor components.

(C) The final series of the thermal vacuum tests were conducted to evaluate thermal vacuum ignition delay. The tests were conducted at an average pressure of 0.20 millimeter of Mercury and temperatures of ambient, +150 and -30 degrees F. The results of these tests are shown in Tables XXVIII, XXIX, and XXX. The ignition delays are two to three times longer dependent upon the temperature than those obtained for the sea level ambient firings. Several theories and modification to the igniter overspray to reduce thermal vacuum ignition delay are presented for future consideration.

Table XXV. WSR-101 vacuum ignition firing test summary. (U)

Motor Number	Igniter Composition	Vacuum mm. Hg.	Exposure Time Hrs.	Temperature °F	Ignition Delay M.secs	Remarks
176W	CWIC-8	1.3	2	ambient	180	
179W	CWIC-8	2.5	3.5	ambient	38	
180W	CWIC-8	.13	1.8	ambient	120	
181W	CWIC-8	.12	1	ambient	-	No ignition
185	CWIC-16	.40	.5	ambient	28	
186	CWIC-16	.15	.5	ambient	50	
187	CWIC-16	.30	.7	ambient	30	
188	CWIC-16	.35	.7	ambient	22	
189	CWIC-17	.40	.7	ambient	25	
190	CWIC-17	.25	.75	ambient	32	
191	CWIC-19	.25	.75	ambient	70	
192	CWIC-19	.25	.75	ambient	45	
193	CWIC-16	S.L.	-	ambient	15	Datum firing
194	CWIC-16	S.L.	-	ambient	14	Datum firing
195	CWIC-16	.13	1.3	150	42	
196	CWIC-16	.15	1.5	150	50	
197	CWIC-16	.18	2.3	-30	75	
198	CWIC-16	.06	2.5	-30	110	

Table XXVI. WSR-101 rocket motor thermal vacuum tests. (U)

Firing No.	Total Impulse (I_t) lb-secs	Specific Impulse I_{sp} Secs	Action Time M.secs	Ignition Delay M.secs	Total Time M.secs	Remarks
1	Malfunction of recording equipment produced values of I_t and I_{sp} 10-7% in excess of norm.		45	18	63	
2			50	20	70	
3			48	22	70	
4			47	18	65	
5			47	18	65	
6			48	22	70	
7			47	20	67	
8			47	20	67	
9			46	18	64	
10			-	-	-	No trace* Good firing observed on C.R.T.
11			46	17	63	
12			48	18	66	
13			-	-	-	No trace*. Good firing observed on C.R.T.
14			-	-	-	No trace*. Good firing observed on C.R.T.
15			48	20	68	

*Defective Polaroid film.

Table XXVI (Cont)

Firing No.	Total Impulse (It) lb-secs	Specific Impulse I_{sp} Secs	Action Time M.secs	Ignition Delay M.secs	Total Time M.secs	Remarks
16			49	23	72	
17			48	22	70	
18			50	16	66	
19			47	18	65	
20			45	21	66	
21	Malfunction of recording equipment produced values of I_t and I_{sp} 10-7% in excess of norm.		-	-	-	No trace*. Good firing observed on C.R.T.
22			44	18	62	
23			54	22	72	
24			45	19	64	
25			46	20	66	

*Defective Polaroid film.

Table XXVII. WSR-101 rocket motor thermal vacuum tests. (U)

Firing No.	Total Impulse (I_t) lb-secs	Specific Impulse (I_{sp}) Secs	Action Time M.secs	Ignition Delay M.secs	Total Time M.secs	Remarks
1	2.64	246	48	15	63	
2	-	-	-	-	-	No trace*. Good firing observed on C.R.T.
3	-	-	-	12	-	Failed dome, 4 corners
4	-	-	-	-	-	No trace*. Good firing observed on C.R.T.
5	2.68	252	44	18	62	
6	2.69	251	48	15	63	
7	2.70	258	46	17	63	
8	2.72	254	48	22	70	Small slit in dome, end of run.
9	-	-	-	-	-	No trace*. Good firing observed on C.R.T.
10	2.64	244	45	15	60	
11	2.72	253	46	16	62	
12	2.73	255	47	15	62	
13	-	-	-	-	-	No trace*. Good firing observed on C.R.T.
14	2.65	247	44	16	60	
15	-	-	-	22	-	Dome end failure.

*Defective Polaroid film.

Table XXVII (Cont)

Firing No.	Total Impulse (I_t) lb-secs	Specific Impulse (I_{sp}) Secs	Action Time M.secs	Ignition Delay M.secs	Total Time M.secs	Remarks
16	2.71	253	44	18	62	
17	2.75	254	45	15	60	
18	2.63	245	35	17	52	
19	-	-	-	-	-	No trace*. Good firing observed on C.R.T.
20	-	-	-	18	-	Dome failure, 4 corners
21	-	-	-	24	-	Dome failure, 2 corners
22	2.68	248	46	22	68	
23	2.66	248	48	20	68	
24	2.66	247	50	18	68	
25	2.69	251	48	18	66	

* Defective Polaroid film.

CONFIDENTIAL

CONFIDENTIAL

Table XXVIII. WSR-101 rocket motor vacuum firing tests. (U)

Motor No.	Vacuum Torrs	Exposure Time-Hrs.	Temperature °F	Ignition Delay M.secs	Remarks
51	S.L.	-	AMB.	25	S.L. reference firing
52	.25	1.0	AMB.	35	
53	.12	1.0	AMB.	63	
54	.20	1.0	AMB.	45	
55	.15	1.0	AMB.	65	

Table XXIX. WSR-101 rocket motor vacuum firing tests. (U)

Motor No.	Vacuum Torrs	Exposure Time-Hrs.	Temperature °F	Ignition Delay M.secs	Remarks
56	.25	.8	+150°	25	
57	.25	.8	+150°	45	
58	.28	.3	+150°	75	
59	.20	.8	+150°	32	
60	.30	.7	+150°	50	
61	.28	.7	+150°	48	Small hole in dome.
62	.18	.7	+150°	60	
63	.25	.7	+150°	34	
64	.25	.7	+150°	35	
65	.12	.7	+150°	80	

Table XXX. WSR-101 rocket motor vacuum firing tests.(U)

Motor No.	Vacuum Torrs	Exposure Time-Hrs.	Temperature °F	Ignition Delay M.secs	Remarks
66	.09	3.0	-28	-	No ignition
67	.10	2.0	-21	48	
68	.12	5.0	-23	85	
69	.18	2.0	-22	-	Motor fired-data equip. malfunction
70	.18	1.6	-22	185	
71	.15	1.7	-23	75	
72	.10	3.0	-23	39	
73	.11	2.0	-27	-	No ignition
74	.18	2.0	-27	35	
75	.20	2.0	-24	-	No ignition

(U) The present igniter system is designed as a minimal gas producer to prevent spiking and overpressurization of the small motor. The combination of larger motors (i.e. WSR-101 or larger) and vacuum conditions indicate the possibility of reducing ignition delay by introducing gas producers into the composition. Metallic hydrides are very energetic and produce water as a combustion product which may serve as the pressurizing medium at combustion temperatures. A change of the resin binder to one that will produce greater quantities of gaseous products may also provide the necessary pressurization.

(U) A major factor in rapid ignition of the propellant grain is the rate of heat transfer from particle to particle within the pyrotechnic overspray. The igniter used is a porous structure and therefore does not provide optimum heat transfer in vacuum. A reduction in the porosity of the pyrotechnic can be achieved by method of application, however, an additive to the composition will be required to maintain the present burn rate.

(U) In summary, ignition delays of the WSR-101 system can be reduced by improving the rate of heat transfer in the composition and by additives which produce gas thereby increasing the rate of pressurization within the motor during initial ignition.

B. Repetitive Firing Tests

1. Pulser Deflection Tests

(U) Before conducting the repetitive tests, three single firings were made in the pulser assembly to determine the compatibility of the rocket motor and pulser. These motors failed at the corners of the dome section. It was suspected that the radial clearance between the sprocket wheel OD and the housing ID increased due to pressure exerted within the capsule combustion chamber during firing. Such excessive radial clearance would permit extrusion and failure of the capsule dome.

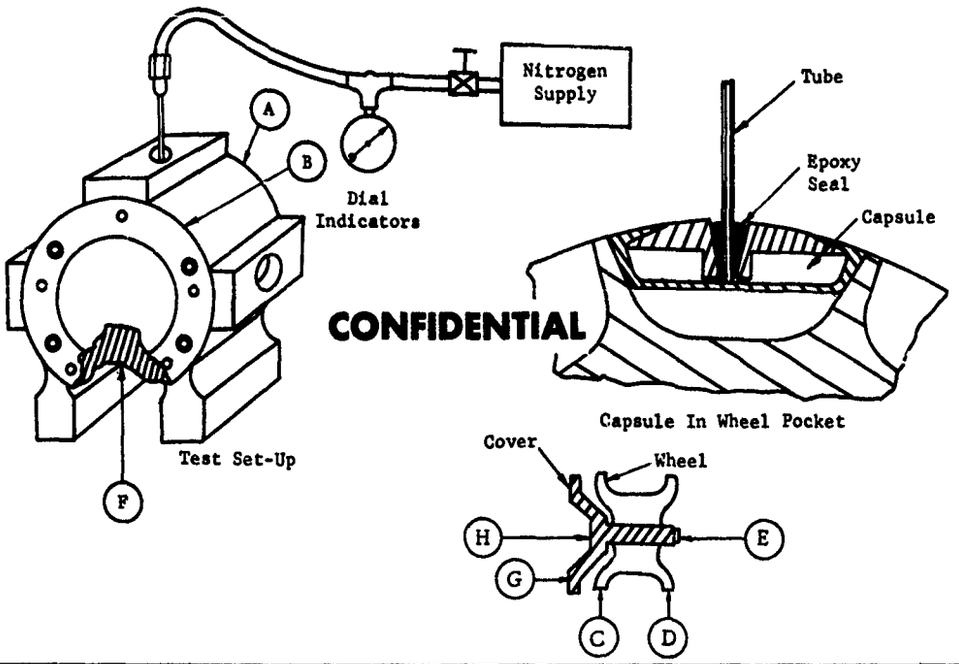
(This page is unclassified)

(C) A series of tests were made to measure deflections using dial indicators, at the housing, wheel, sprocket wheel shaft, and cover flange. A test capsule was installed in the pulser assembly and pressurized with nitrogen through a tube inserted and sealed at the nozzle. Bearing radial play (about .003 inch) was taken up before each test with a 50 psig preload. The results are shown in Figures 101, 102, and 103 and summarized as follows:

		Maximum Deflection - inches				
Capsule Position	Capsule Pressure psig	Wheel	Shaft	Housing	Cover Flange	Deflection Point
No. 2 port (12 o'clock position)	500	.006 ↓	.0037 ↓	.0006 ↑	.002	6 o'clock (outward)
	1000	.013 ↓	.007 ↓	.0015 ↑	--	
No. 2 port (12 o'clock position) (Pulser clamped fore and aft)	500	.0026 ↓	.0029 ↓	---	.0003 .0003	6 o'clock-out 12 o'clock-in
	1000	.0045 ↓	.0057 ↓	---	.0010 .0009	6 o'clock-out 12 o'clock-in
No. 1 port (3 o'clock position)	500	← .005	← .0048	→ .0002	.0015 .0000	9 o'clock-out 3 o'clock-in
	1000	← .0075	← .0075	→ .0006	.0031 .0000	9 o'clock-out 3 o'clock-in

(C) These tests showed that capsule pressure increases the pulser radial clearance. The stiffening of the cover flange using heavy plates with fore and aft clamping, (Figure 103) reduced the shaft deflection a small amount.

(C) The radial clearance at the outer rim of the pulser wheel (where extrusion during firing had occurred) is normally .006 inch. At 1000 psig capsule pressure, this .006 inch clearance increases to .0235 inches. This increase results from the following incremental increases: wheel deflection .013 inch, housing expansion .0015 inch, and bearing system clearance take-up .003 inch. At a 2000 psig capsule operating pressure (nominal operating point) the clearance could be expected to reach .040 inch. Successful tests of capsules in the firing fixtures had been conducted with a .007 - .008 inch simulated radial clearance.



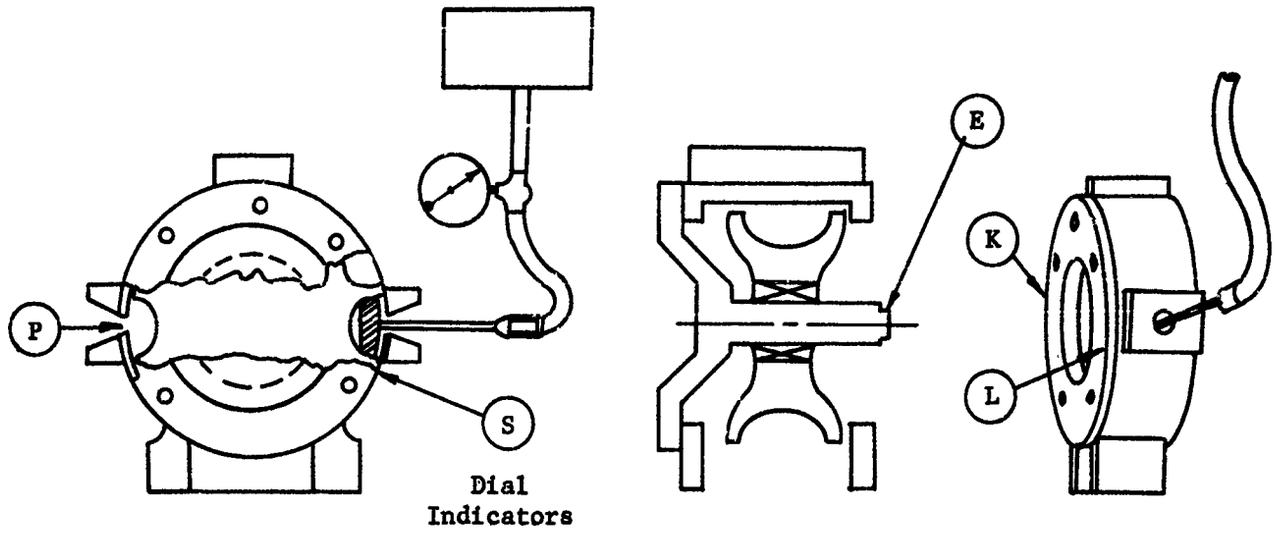
CONFIDENTIAL

Deflection - Inches						Deflection - Inches					
Capsule Pressure p.s.i.g.	A	B	C	D	F	Capsule Pressure p.s.i.g.	C	D	E	G	H
500	.0002	.0005	-	-	.004	100	.000	.0018	.0003		
1000	.0007	.0012	-	-	.009	200	.000	.0028	.0006		
1000	.0012	.001	-	-	.008	500	.0016	.0051	.0031		
All Readings Zeroed With 25 p.s.i.g. Preload						800	.0042	.006	.0067		
100	0	0	.0045	.0043		1000	.0057	.0068	.007		
200	0	0	.005	.005		500	.002	.0061	.0037		
300	0	0	.0055	.0065		200	.000	.0007	.0007		.000
350	.0015	0	.006	.0075		500	.002	.0027	.0033		.000
400	.0004	.0003	.0065	.0085							
600	.0006	.0015	.009	.0105		500	-	-	-	.002	
850	.0011	.0012	.0115	.0115		Bearing Clearance Take-up At 25 p.s.i.g.					
1000	.0015	.0015	.013	.0118		25	.004	.004			
						25	.0025	.002			
						20	.0035	.002			

Figure 101. WSR-101 pulser deflection test. (U)

66-433

CONFIDENTIAL



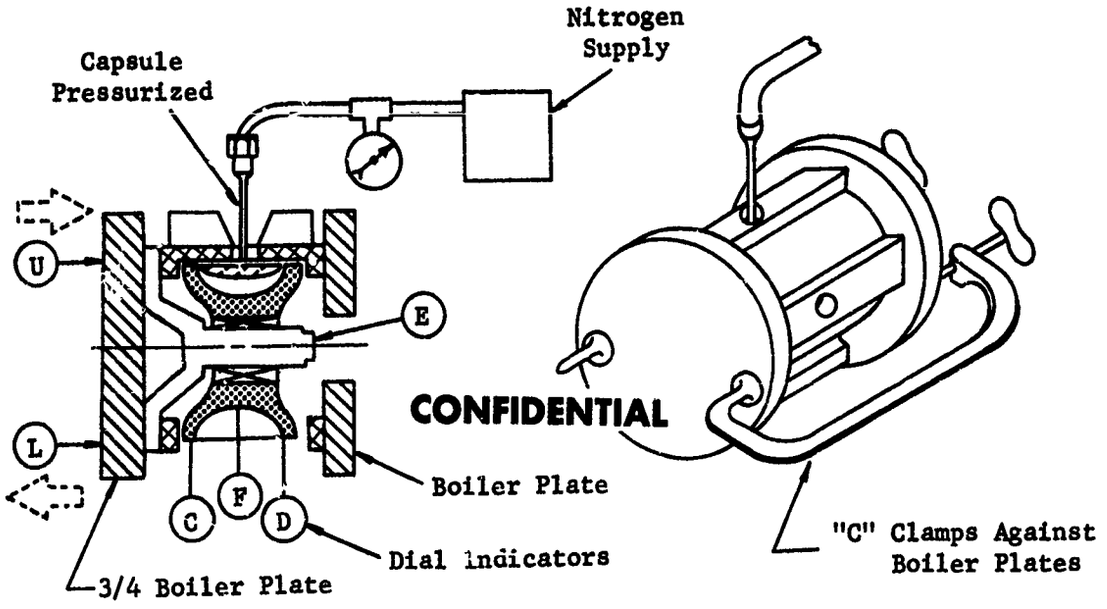
Deflection Out From Pulser ←

Capsule Pressure p.s.i.a.	Deflection - Inches				
	E	S	P	K	L
500	.0048	.0002	.0050	.0008	-
1000	-	.0006	.0075	.0025	-
500	.0055	.0002	.0025	.0014	.0000
1000	.0075	.0003	.0048	.0028	.0000
500	.0042	.0002	.0024	.0015	.0000
1000	.0070	-	.0050	.0031	.0000

All Dial Indicators Zeroed In At 50 p.s.i.g. Preload

Figure 102. WSR-101 pulser deflection tests (deflection simulating side port firing). (U)

67-1870



All Dial Indicators Zeroed at 50 p.s.i.g. Preload

Capsule Pressure	Deflection - Inches					
	C	D	E	F	U	L
500	-	.0025	.0029	.0023	.000	.000
1000	-	.0039	.0055	.0048	.0009	.0009
500	-	.0026	.0028	.0024	.00015	.0003
1000	-	.0038	.0057	.0048	.0006	.0010
500	-	.0026	.0028	.0022	.0002	.0003
1000	-	.0038	.0057	.0045	.0007	.0010
500	.0013	.0025	.0026	-	.0003	.0002
1000	.0045	.0040	.0057	-	.0008	.0009

Figure 103. WSR-101 pulser deflection test. (U)

66-434

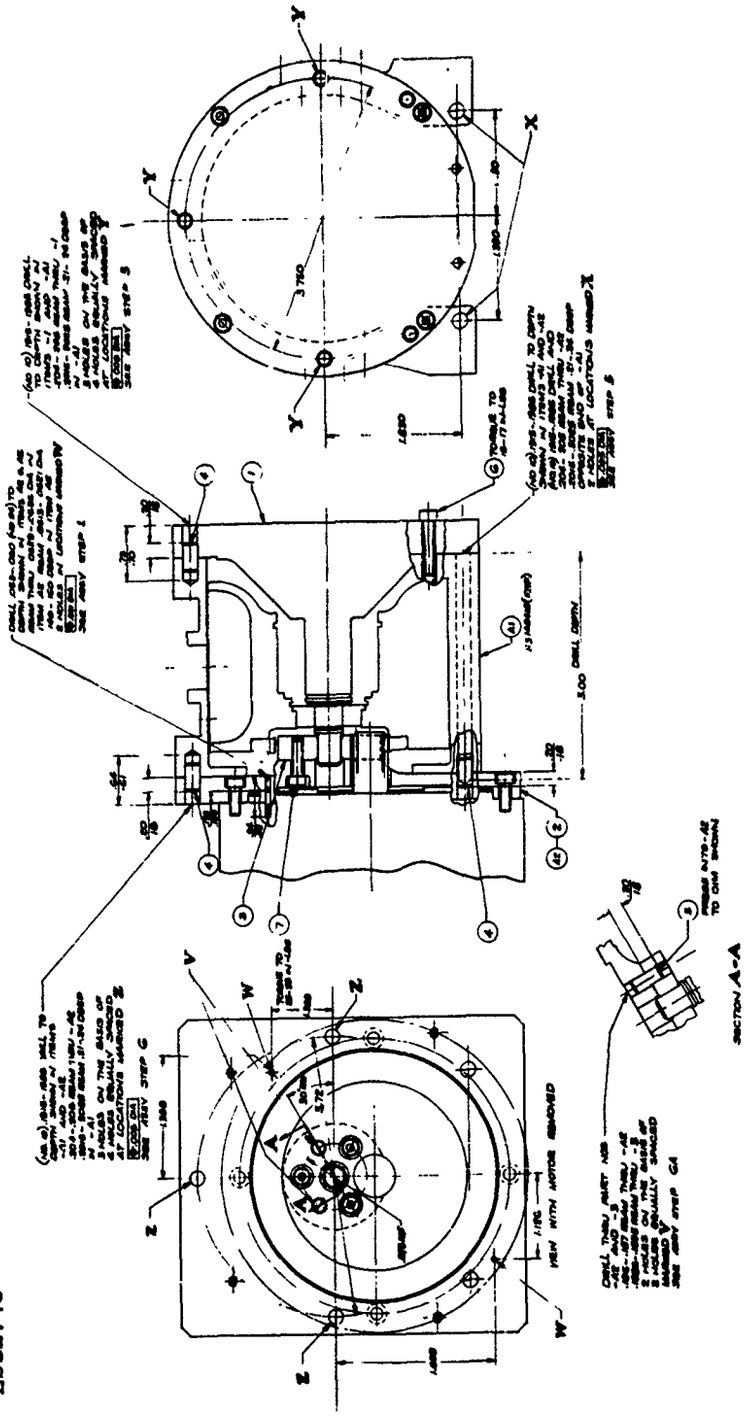
(U) A modification was made to the front cover and rear adapter plate which supported the free end of the shaft and strengthened both plates as illustrated in Figure 104. Deflection tests were conducted for this configuration and the results are shown in Figure 105. A before-and-after comparison (Figure 101 vs Figure 105) shows that the modification to the pulser virtually eliminated all of the shaft and front cover deflections. To fully evaluate these modifications the next task of the test program was to conduct single firings in the modified pulser assembly.

2. Single Firings

(U) A single rocket motor was first fired from port number two of the modified aluminum pulser assembly. The E dome section failed and the pulser housing showed an elongation of the dowel pin holes at the number two port as well as a permanent set in the housing. It was concluded that the load distribution in the housing changed as a result of modifying the pulser housing assembly and that the pulser configuration and materials had to be changed.

(C) Several stainless steel housings were designed, fabricated and tested in conjunction with modifications to the bearing system, sprocket wheel and E dome. The results of this series of single firings are illustrated in Figure 106. The first housing was a rig configuration used to establish the internal configuration of the housing. Two bearing configurations were used for these tests; the standard roller bearing from the previous design and a steel sleeve which replaced the bearings and provided no clearance in the sprocket wheel shaft system. The results showed that a .007 inch pocket at the firing port produced good results. However, several failures of E dome corners was experienced. A second housing was designed and fabricated of stainless steel. This housing was light weight and approached the prototype design. This housing was utilized to further develop the internal contour at the firing ports and establish an optimum bearing configuration. The results of this series of single pulser firings provided the following prototype configuration.

- A .005 inch recess step in the ID of the housing.
- An angled thrust roller bearing

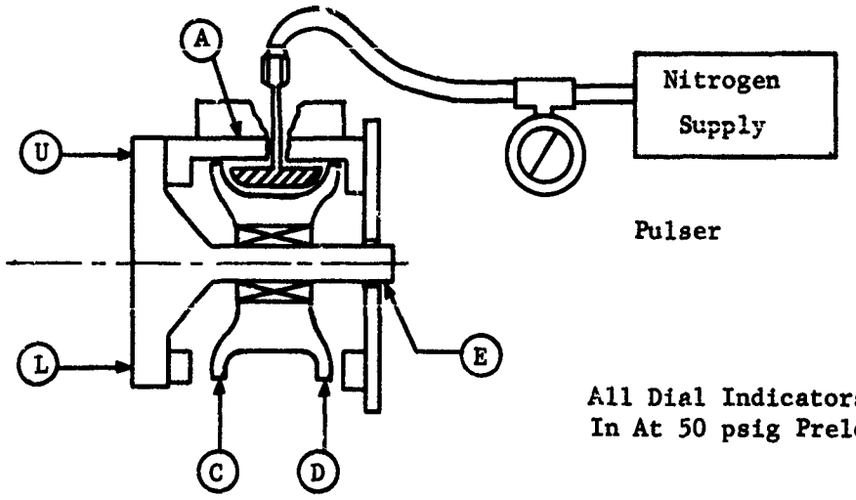


For Dimensions, Notes, Picture and Specs
Not Shown See LS32275
LS32748

Figure 104. WSR-101 sprocket wheel shaft modifications. (U)

66-431

(This page is unclassified)



Capsule Pressure psig	Deflection - inches					
	(E)	(C) ↓	(D) ↓	(U) →	(L) ←	(A) ↑
500	.0006 ↓	.0011	.0016	.000	.000	.0007
1000	.0015 ↑	.0034	.0034	.000	.0005	.0017
500	.0003 ↑	.001	.0008	.000	.000	.0004
1000	.001 ↑	.0023	.0023	.000	.0008	.0008
500	.00035 ↑	.0009	.001	.000	.000	.0002
1000	.0011 ↑	.0022	.0023	.000	.0003	.0006
500	.0004 ↑	.0009	.0011	.000	.000	.000
1000	.0011 ↑	.0022	.0023	.000	.0002	.0004
500	.0006 ↑	.0007	.0008	.000	.000	.0003
1000	.0013 ↑	.0021	.0022	.000	.000	.0007
500	.0004 ↑	.001	.0011	.000	.000	.000
1000	.0013 ↑	.0023	.0024	.0002	.0004	.0007
500	.0006 ↑	.001	.0011	.000	.000	.0002
1000	.0009 ↑	.0022	.0024	.0002	.0003	.0003
1500	.0018 ↑	.0039	.0038	.0005	.0006	.0009

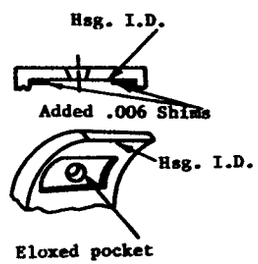
Figure 105. WSR-101 pulser deflection tests (revised pulser housing shaft supported at both ends). (U)

67-1864

CONFIDENTIAL

ROCKET MOTOR NO.	TAPE NO.	ST. STEEL HSG.	PULSER HOUSING CONFIGURATION HOUSING INSIDE DIAMETER	REMARKS	BEARING CONFIGURATION	SPROCKET WHEEL	FIRING PORT NO.	CAPSULE CONDITION
1703	-	Rig Hsg.	Same as Alum. Hsg.		Std. Roller	Standard	2	Good Firing
1701	-	"	"		"	"	"	Dome Failure - Front Corner
1702	-	Lt. Wt. Hsg.	"		"	"	"	"
1090	-	Rig Hsg.	"		Solid Bushing	"	"	"
1534	-	"			"	"	"	"
1705	-	"	"		"	"	"	Good Firing
985	-	Lt. Wt. Hsg.	Eloxed #2 Port Pocket (.007" deep)		"	"	"	"
1	1A (Std. Domes)	Rig Hsg.	"		"	"	"	"
2	"	"	"	"	"	"	"	"
3	"	"	"	"	"	"	"	"
4	"	"	"	"	"	"	"	"
5	"	"	"	"	Std. Roller	"	"	Dome Failure - Front Corner
6	"	"	"	"	"	"	"	"
7	"	Lt. Wt. Hsg.	"	"	Low Clearance Long Rollers	"	"	Good Firing

CONFIDENTIAL



CONFIDENTIAL

Figure 106. WSR-101 pulser housing assembly development. (U)

ROCKET MOTOR NO.	TAPE NO.	ST. STEEL HSG.	PULSER HOUSING CONFIGURATION HOUSING INSIDE DIAMETER	REMARKS	BEARING CONFIGURATION	SPROCKET WHEEL	FIRING PORT NO.	CAPSULE CONDITION
8	1A (Std. Domes)	Lt. Wt. Hsg.	Eloxed #2 Port Pocket (007" deep)	"	Low Clearance Long Rollers	Standard	2	Good Firing
9	"	"	"	"	"	"	"	"
10	"	"	"	"	"	"	"	Dome Failure - Defect in Wheel Pocket.
11	"	"	"	"	"	"	"	Capsule Leaked Near Nozzle
12	"	"	"	"	"	"	"	Good Firing
13	"	"	"	"	"	"	"	Dome Failure - Defect in Wheel Pocket.
14	"	"	"	Added .003" Tape into Eloxed Pocket	"	"	"	Good Firing
15	"	"	"	"	No Bearing Used	"	"	"
16	"	"	(Eloxed Pockets (.007" Deep at (Location #1, (#2, #3 Ports	"	High Clearance Long Rollers	"	"	Dome Failure - Front Corner
17	"	"	"	"	"	"	"	"
18	"	"	"	"	Low Clearance Long Rollers	"	"	Good Firing
19	"	"	"	"	"	"	"	Dome Failure - Rear Corner
20	"	"	"	"	"	"	3	Good Firing
21	"	"	"	"	"	"	"	Dome Failure - Front Corner
22	"	"	"	"	Solid Bushing	"	"	Good Firing

CONFIDENTIAL



Figure 106. (cont.)

CONFIDENTIAL

ROCKET MOTOR NO.	TAPE NO.	ST. STEEL HSG.	PULSER HOUSING CONFIGURATION HOUSING INSIDE DIAMETER	REMARKS	BEARING CONFIGURATION	SPROCKET WHEEL	FIRING PORT NO.	CAPSULE CONDITION
23	1A (Std. Domes)	Lt. Wt. Hsg.	(Eloxed Pockets (.007" Deep at (Location #1, (#2, #3 Ports	"	Solid Bushing	Standard	3	Good Firing
24	"	"	"	"	Low Clearance Long Rollers	"	2	Dome Failure - Front Corner
1	1 (Std Domes)	"	.	"	"	(Filled (Pocket (Corners With (Epon 907 (to Reduce (Clearance (With Capsule	"	Good Firing
2	"	"	"	"	"	"	3	"
3	"	"	"	"	"	"	"	"
4	"	"	"	"	"	"	"	"
5	"	"	"	"	"	"	2	Dome Failure - Front Corner
6	"	"	"	"	Std. Roller	(Filled (907) (Pocket (Corners (More (Uniformly (By Casting	"	Good Firing
7	"	"	"	"	"	"	3	"
8	"	"	"	"	"	"	"	"

CONFIDENTIAL

Figure 106. (cont.)

ROCKET MOTOR NO.	TAPE NO.	ST. STEEL HSG.	HOUSING INSIDE DIAMETER	REMARKS	BEARING CONFIGURATION	SPROCKET WHEEL	FIRING PORT NO.	CAPSULE CONDITION
			PULSER HOUSING CONFIGURATION					
7	5 Unit, New Dome Tape	Lt. Wt. Hsg.	.015" Step / Hsg. I.D.		Std. Roller	Standard	2	Excessive Step Caused Dome Failure
9	1 (Std. Domes)	"	Hsg I.D. Shim / .006" Step	Hsg. I.D. Recess	Low Clearance Long Roller	(Filled (907) (Pocket (Corners - (Cast	"	Good Firing
10	"	"	"	"	"	"	"	"
11	"	"	"	"	"	"	"	"
12	"	"	"	"	"	"	"	"
13	1 (Std. Domes)	"	"	"	"	"	"	"
3	"	"	"	"	"	Standard	"	"
4	"	"	"	"	"	"	"	"
5	"	"	"	"	"	"	"	"
1	3 (New Domes)	"	"	"	Angle Roller Bearings	"	"	"
2	"	"	"	"	"	"	"	"
3	"	"	"	"	"	"	"	"
4	"	"	"	"	"	"	"	"
5	"	"	"	"	"	"	"	Dome Break
6	"	"	"	"	"	"	"	Good Firing

CONFIDENTIAL

Figure 106. (cont.)

CONFIDENTIAL

ROCKET MOTOR NO.	TAPE NO.	LT. STEEL HSG.	PULSER HOUSING CONFIGURATION HOUSING INSIDE DIAMETER	REMARKS	BEARING CONFIGURATION	SPROCKET WHEEL	FIRING PORT NO.	CAPSULE CONDITION
7	3 (New Domes)	Lt. Wt. Hsg.	"	"	Angle Roller Bearings	Standard	2	Dome Failure - Suspect Grain Mishandling Damage
8	"	"	"	"	"	"	"	Good Firing
9	"	"	"	"	"	"	"	"
10	"	"	"	"	"	"	"	Capsule Blow - 3 Others Damaged Hsg. Pressurized Failing Cover Bolts
1	4 (New Domes)	Prototype Hsg.	.005" Step	" Plus Gas Vent Holes in Hsg. & Cover	"	" Plus Teflon Coat	"	Good Firing
2	"	"	" Teflon Coat On Hsg I.D.	"	"	" Plus Teflon Coat	"	"
3	"	"	"	"	"	" Removed Teflon Coat	"	"
4	"	"	"	"	"	"	"	"
5	"	"	"	"	"	"	"	Minor Dome Break
6	"	"	"	"	"	"	"	Good Firing
7	"	"	"	"	"	"	"	"
8	"	"	"	"	"	"	"	"
9	"	"	"	"	"	"	"	"
10	"	"	"	"	"	"	"	"
11	"	"	"	"	"	"	"	"

CONFIDENTIAL

Figure 106. (cont.)

(U) During this series of tests, a modification was incorporated to the E dome to eliminate corner failures during firing. This modification consisted of adding material to the corners to provide support during firing in the critical clearance area between the sprocket wheel and housing.

(U) A pulser housing assembly failure was experienced during the last single firing. The cause of failure was attributed to insufficient venting of the pulser housing assembly when a rocket motor failed. This was resolved in the final prototype pulser design by incorporating three 3/8 inch diameter holes in the front and rear face plates and six 1/8 inch and one 1/4 inch diameter holes in the pulser housing between firing ports. Several severe over-pressurizations occurred during subsequent repetitive firings, yet the pulser operation was unaffected and no pulser assembly damage was experienced. A prototype pulser housing assembly was fabricated to the design described in Section II of this report. Several single firings were successfully accomlished. With those indications the single firing series of tests were concluded.

3. Repetitive Firing Tests

(U) The most significant tests of the program were the repetitive firings. These tests established the overall operating capabilities of the propulsion system.

(C) To effectively conduct these tests, the control panel, shown schematically in Figure 107, was fabricated. This panel supplied the input signals to the system as well as the necessary monitoring of critical parameters and safety features to protect the propulsion system in the event of a malfunction. The control panel consists of three major units: a pulse generator capable of 3 to 20 cps with a maximum pulse width of 50 milliseconds to supply the input signal to step the pulser; an ignition unit which timed the ignition of the rocket motor with the end of the input pulse; and a main control panel which provided for manual or automatic stepping of the pulser as well as power to the various components.

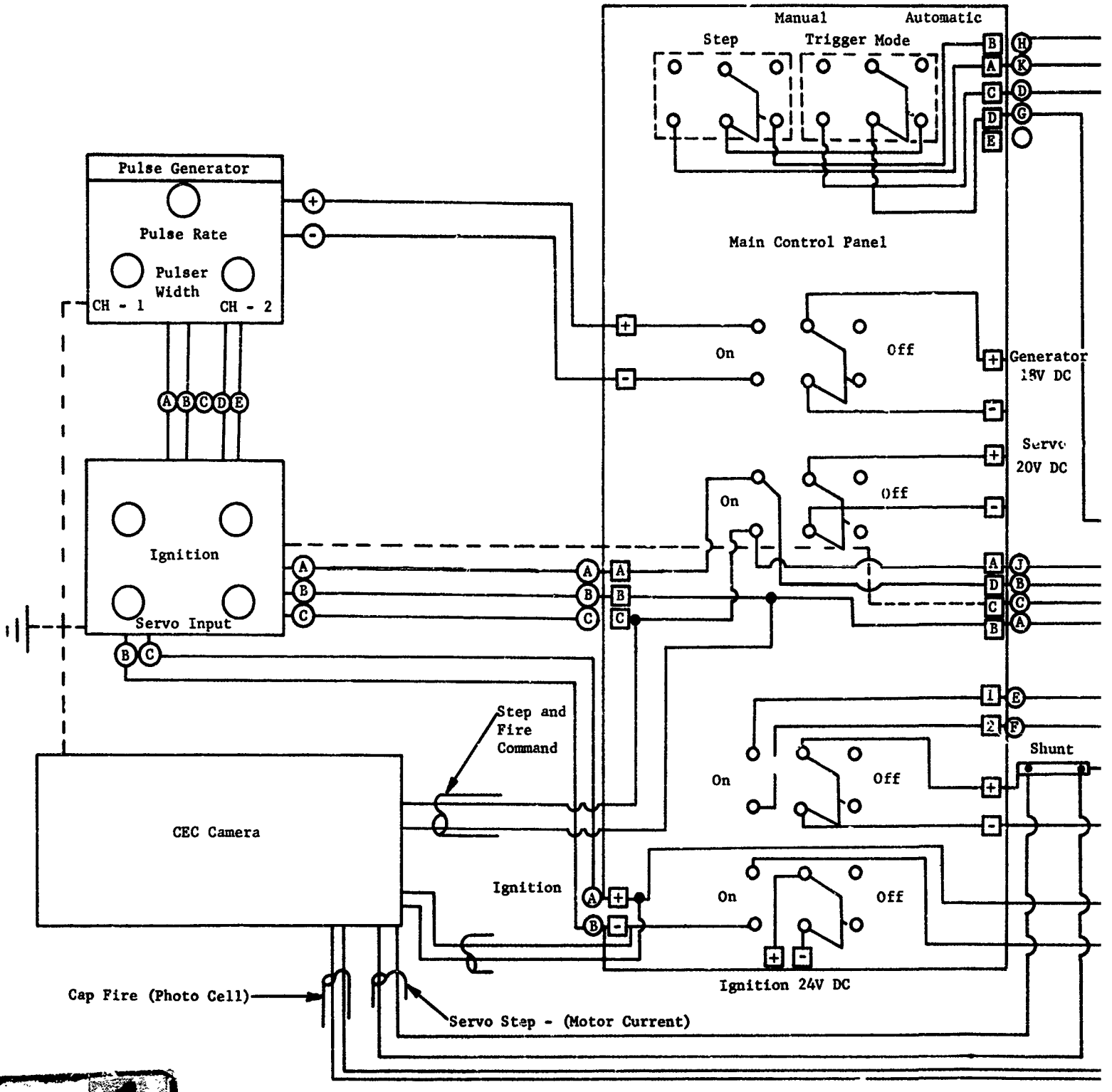
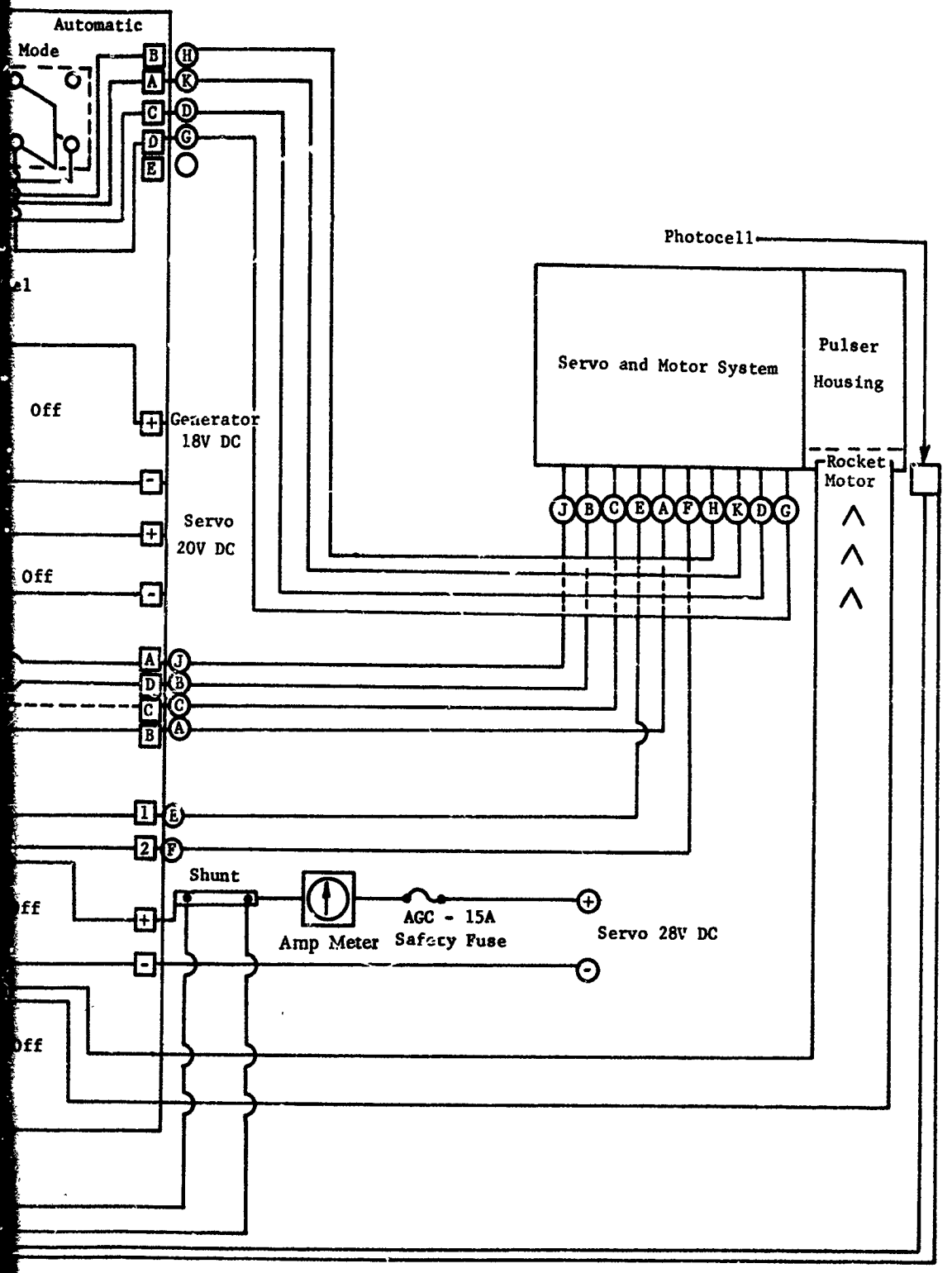


Figure 107. WSR-101 repetitive firing control panel.

66-426



ring control panel. (U)

(U) A direct read-out CEC was used to record the following data for each continuity check of the tapes and repetitive firings.

- Input Pulse
- Rocket Motor Igniter Continuity
- Ignition Voltage
- Motor Firing (Photo Cell at Nozzle Exit)
- Pulser Motor Current

(U) In addition, high speed (200 to 400 frames per second) and standard 16 mm movies were taken for each series of firings. Preliminary testing was conducted with tapes which incorporated "dummy" rocket motors. These motors contained only the pyrofuze element of the igniter to provided a continuity signal (rocket motor position) as the tape passed through the pulser. This series of tests were made to optimize the inlet and exit chute position for minimum friction load and positive entrance and expulsion of the rocket motor into and out of the sprocket wheel. In addition, the ignition brush load for minimum friction and positive contact with the ignition leads of the rocket motor were established.

(C) The repetitive firing tests were conducted using eight 25 shot tapes, four 50 shot tapes and one 100 shot tape. The pulser configuration established during the single firings in the pulser was used. Initially, the breadboard servo was used for stepping but was replaced (during firing of tapes 5 through 13) with the prototype servo and motor system. Firing rates of 3 to 8 cps were achieved during the tests. Prior to repetitive firing, each multi-shot tape was X-rayed for possible rocket motor defects. No defects were found. Each tape was also run through the pulser before firing to check on proper step timing, continuity of the rocket motor igniter, and operation of the brushes and instrumentation. A typical check-out trace is shown in Figure 108.

(C) Tables XXXI through XLIV summarize the results of the repetitive firings for each tape. These tables list the number of motors on the tape, firing rate and number of rocket motors fired. The results are categorized as follows:

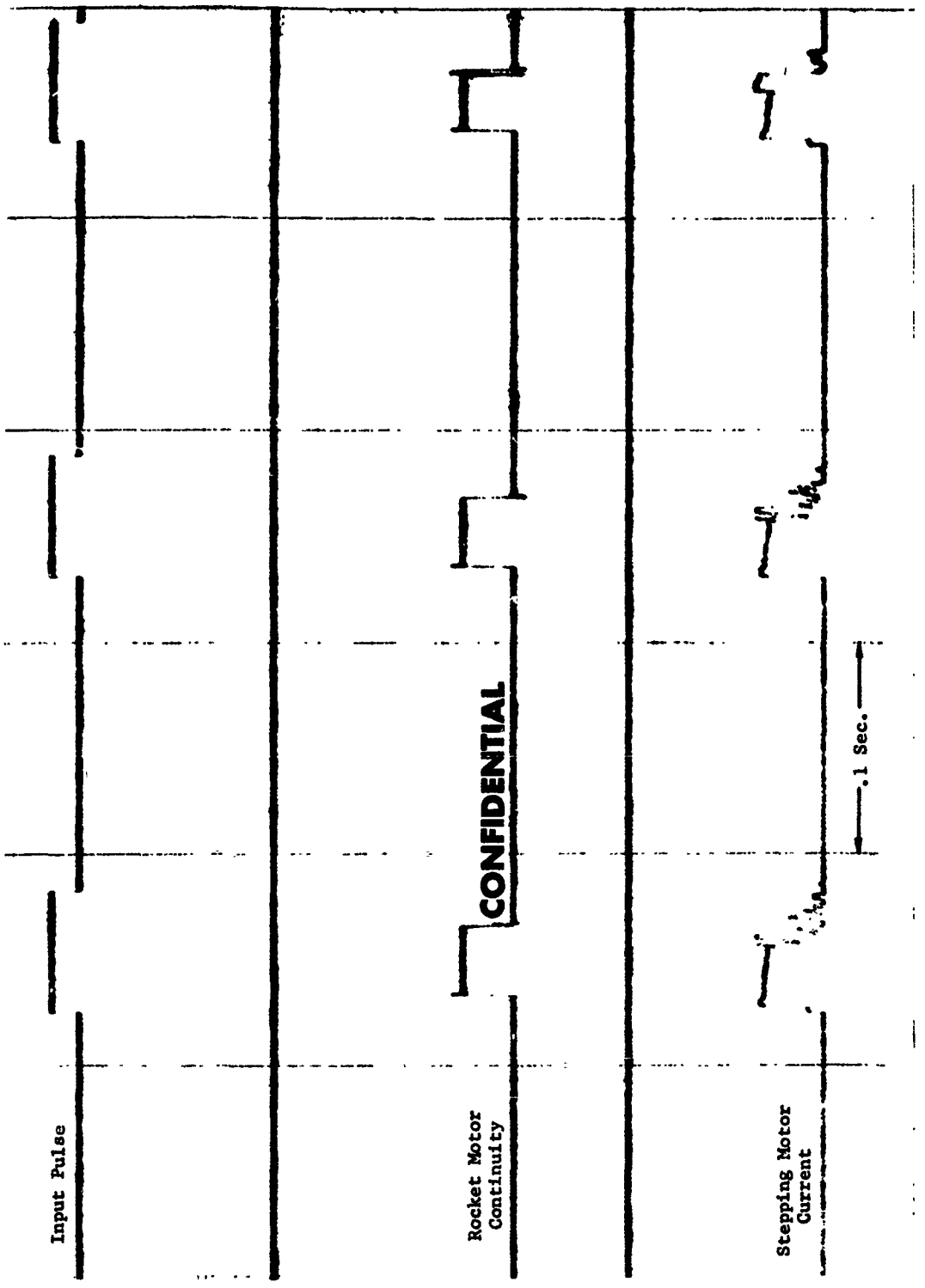


Figure 108. WSR-101 repetitive check-out trace. (U)

67-1862

Table XXXI. WSR-101 repetitive firing summary. (U)

TAPE NO. 1A

			Remarks
Number of Motors on Tape		24	Original domes with thin corners.
Firing Rate, c.p.s.		Manual	Tape fabricated prior to establishment of final rocket motor configuration.
Total Number of Motors Fired		24	
Results:	Good	14	
	Minor Dome Breaks	9	
	Dome Failures	1	
	Not Fired	0	

Table XXXII. WSR-101 repetitive firing summary. (U)

TAPE NO. 1

			Remarks
Number of Motors on Tape		25	Original domes with thin corners.
Firing Rate, c.p.s.		Manual	Last twelve not fired because of weak dome corners.
Total Number of Motors Fired		13	
Results:	Good	12	
	Minor Dome Breaks	1	
	Dome Failures	0	
	Not Fired	12	

Table XXXIII. WSR-101 repetitive firing summary. (U)

TAPE NO. 2

		Remarks
Number of Motors on Tape	25	Tape reworked. Weak corner domes removed and motors reassembled with V-57 domes. Tape designated as No. 12.

Table XXXIV. WSR-101 repetitive firing summary. (U)

TAPE NO. 3

			Remarks
Number of Motors on Tape		25	Strengthened S-55 domes used starting with this tape.
Firing Rate, c.p.s.		Manual	
Total Number of Motors Fired		13	Twelve not fired because of excessive handling of tape assembly during pulser check-outs.
Results:	Good	7	
	Minor Dome Breaks	1	
	Dome Failures	5	
	Not Fired	12	

Table XXXV. WSR-101 repetitive firing summary. (U)

TAPE NO. 4

			Remarks
Number of Motors on Tape		25	Fired eleven capsules with manual pulsing. Fired three capsules at 5 c.p.s. during one run. Fired eleven capsules at 3 c.p.s. during three runs. Two jams occurred due to partial capsule dome extrusion during firing. Motors missing firing signal caused by motor positioning on the tape during assembly.
Firing Rate, c.p.s.		3, 5 & Manual	
Total No. of motors fired		25	
Results:	Good	23	
	Minor Dome Breaks	2	
	Dome Failures	0	
	Not Fired	0	
Max. Motors Fired in One Run		3	
Total No. Motors Missing Firing Signal		4	

Table XXXVI. WSR-101 repetitive firing summary. (U)

TAPE NO. 5

			Remarks
Number of Motors on Tape		25	Fired 25 capsules during four runs. Run 1 stopped as result of a brush problem that was resolved. A jam, during run 2, was caused by partial extrusion of the motor dome during firing. Runs 3 and 4 were stopped at will.
Firing Rate, c.p.s.		4	
Total Number of Motors Fired		25	
Results:	Good	23	
	Minor Dome Breaks	2	
	Dome Failures	0	
	Not Fired	0	
Max. Motors Fired in One Run		9	
Total No. Motors Missing Firing Signal		5	

Table XXXVII. WSR-101 repetitive firing summary. (U)

TAPE NO. 6

			REMARKS
Number of Motors on Tape		25	Fired 22 motors at 4 c.p.s.
Firing Rate c.p.s.	Manual	,4	during 3 runs. Fired two motors
Total Number of Motors Fired		24	manually. One motor not fired
Results:	Good	22	due to dome defect. Two jams
	Minor Dome Breaks	1	occurred as result of partial
	Dome Failures	1	extrusion of the capsule dome
	Not Fired	1	during firing.
Max. Motors Fired in One Run		12	
Total No. Motors Missing Firing Signal		2	

Table XXXVIII. WSR-101 repetitive firing summary. (U)

TAPE NO. 7

			Remarks
Number of Motors on Tape		50	Fired 39 motors at 4 c.p.s.
Firing Rate, c.p.s.		4, 5	during two runs. Fired five
Total Number of Motors Fired		44	motors at 5 c.p.s. during one
Results:	Good	37	run. 6 motors not fired because
	Minor Dome Breaks	5	of poor tape transport with
	Dome Failures	2	expended capsules. Two jams
	Not Fired	6	occurred during runs as a result
Max. Motors Fired in One Run		27	of partial extrusion of dome
Total No. Motors Missing Firing Signal		8	motor during firing.

Table XXXIX. WSR-101 repetitive firing summary. (U)

TAPE NO. 8

			REMARKS
Number of Motors on Tape		50	Fired 27 motors at 5 c.p.s.
Firing Rate, c.p.s.		5, 6	during three runs. Fired 18 motors
Total Number of Motors Fired		45	at 6 c.p.s. during two runs,
Results:	Good	37	5 motors not fired because of
	Minor Dome Breaks	7	poor tape transport with expended
	Dome Failures	1	capsules. Three jams occurred
	Not Fired	5	as a result of dome extrusion
Max. Motors Fired in One Run		13	during firing.
Total No. Motors Missing Firing Signal		7	

Table XL. WSR-101 repetitive firing summary. (U)

TAPE NO. 9

			REMARKS
Number of Motors on Tape		50	Fired 45 motors at 6 c.p.s.
Firing Rate c.p.s.		6	during 6 runs. Five motors
Total Number of Motors Fired		45	remain unfired due to poor tape
Results:	Good	38	transport problem with expended
	Minor Dome Breaks	5	motors. Four jams occurred as
	Dome Failures	2	a result of dome extrusion during
	Not Fired	5	firing. One stoppage was caused
Max. Motors Fired in One Run		21	by a blown fuse and another by
Total No. Motors Missing Firing Signal		4	a hung-up contact brush.

Table XLI. WSR-101 repetitive firing summary. (U)

TAPE NO. 10

			Remarks
Number of Motors on Tape		100	Fired 43 motors at 6 c.p.s.
Firing Rate, c.p.s.		6, 7	during four runs. Fired 36
Total Number of Motors Fired		79	motors at 7 c.p.s. during four
Results:	Good	57	runs. Twenty-one unfired motors
	Minor Dome Breaks	15	because of extrusion problem.
	Dome Failures	7	Six jams occurred as a result of
	Not Fired	21	dome extrusion during firing.
Max. Motors Fired in One Run		29	
Total No. Motors Missing Firing Signal		6	

Table XLII. WSR-101 repetitive firing summary. (U)

TAPE NO. 11

			Remarks
Number of Motors on Tape		42	Fired 41 motors at 8 c.p.s.
Firing Rate, c.p.s.		8	during four runs. Fired one
Total Number of Motors Fired		42	motor manually. One jam
Results:	Good	37	occurred as a result of dome
	Minor Dome Breaks	5	extrusion. Another run was
	Dome Failures	0	stopped by a blown fuse.
	Not Fired	0	
Max. Motors Fired in One Run		27	

Table XLIII. WSR-101 repetitive firing summary. (U)

TAPE NO. 12

Number of Motors on Tape		25
Firing Rate, c.p.s.		5
Total Number of Motors Fired		22
Results:	Good	22
	Minor Dome Breaks	0
	Dome Failures	0
	Not Fired	3
Max. Motors Fired in One Run		20
Total No. Motors Missing Firing Signal		0

Remarks

Special tape with following feature: E-dome of V-57 material which is stiffer, to prevent extrusion during firing. Note: This tape was made with motors removed from tape No. 2 which had old domes removed. Two motors were fired manually as tape checkout firings. Twenty motors were fired at 5 c.p.s. during one run. Two capsules were igniter duds due to the considerable extra handling all capsules received during rework. One capsule left unfired.

Table XLIV. WSR-101 repetitive firing summary.(U)

TAPE NO. 13

Number of Motors on Tape		25
Firing Rate, c.p.s.		5
Total Number of Motors Fired		25
Results:	Good	24
	Minor Dome Breaks	1
	Dome Failures	0
	Not Fired	0
Max. Motors Fired in One Run		25
Total No. Motors Missing Firing Signal		0

Remarks

Special tape with following features:
E-dome of stiffer V-57 material to prevent extrusion during firing.
Higher burn rate propellant CWP-19 for shorter burn time.
Igniter (CWIC 16) for minimum ignition delays.
Fired 25 of 25 motors at 5 c.p.s. in one run. One capsule had a minor dome break. A temporary stopping delay was also encountered but was overcome at the next stepping command.

(U) Good Firings; Minor Dome Failures, defined as a very small puncture or slit in the dome which had no effect on the firing; Dome Failures defined as a major failure of the E dome; motors Not Fired because of thin dome configuration, extrusion problem or location of the unfired motors on the tape which provided a problem in repetitive firing; Maximum Motors Fired in One Run; and Motors Missed Firing Signal because of poorly positioned motors on the tape as a result of manual assembly.

(C) A section of a repetitive firing trace is shown in Figure 109. The input pulse signal for this run was five cps and the pulse width was 55 milliseconds. The ignition voltage trace indicates when the motor is in position, igniter continuity and ignition. The photo cell, which records the exhaust flame, shows the ignition of the propellant grain and end of burning. The stepping motor current is recorded to monitor the operation of the stepping-servo motor system.

(C) Although the operation or performance of each component has been demonstrated to the established requirements, the integration of these units into a system introduces new problems. The repetitive firing tests which combined the operation of the components into a system uncovered two problems, namely, missed ignition of the rocket motor during a firing run and E dome extrusion which jammed the pulser system. The ignition problem resulted from the manual assembly of the rocket motors and tapes. The use of inexpensive and expendable tooling fixtures made it difficult to properly position the rocket motors on the tape. The misalignment which resulted caused the contact brushes to miss the ignition leads on the rocket motor during repetitive firing. This misalignment also created additional friction within the pulser system and thereby increased the overall stepping load. This overloading condition caused the rocket motor to come into the firing position after the ignition signal was given. The condition was resolved by modification to the tooling which insured better positioning and spacing of the rocket motors on the tape. The E dome extrusion problem was resolved by using a higher durometer material for the dome. Tapes 12 and 13, as described in Tables XLIII and XLIV, utilized this material for the domes. There was no extrusion experienced with these tapes and the tests were completely successful.

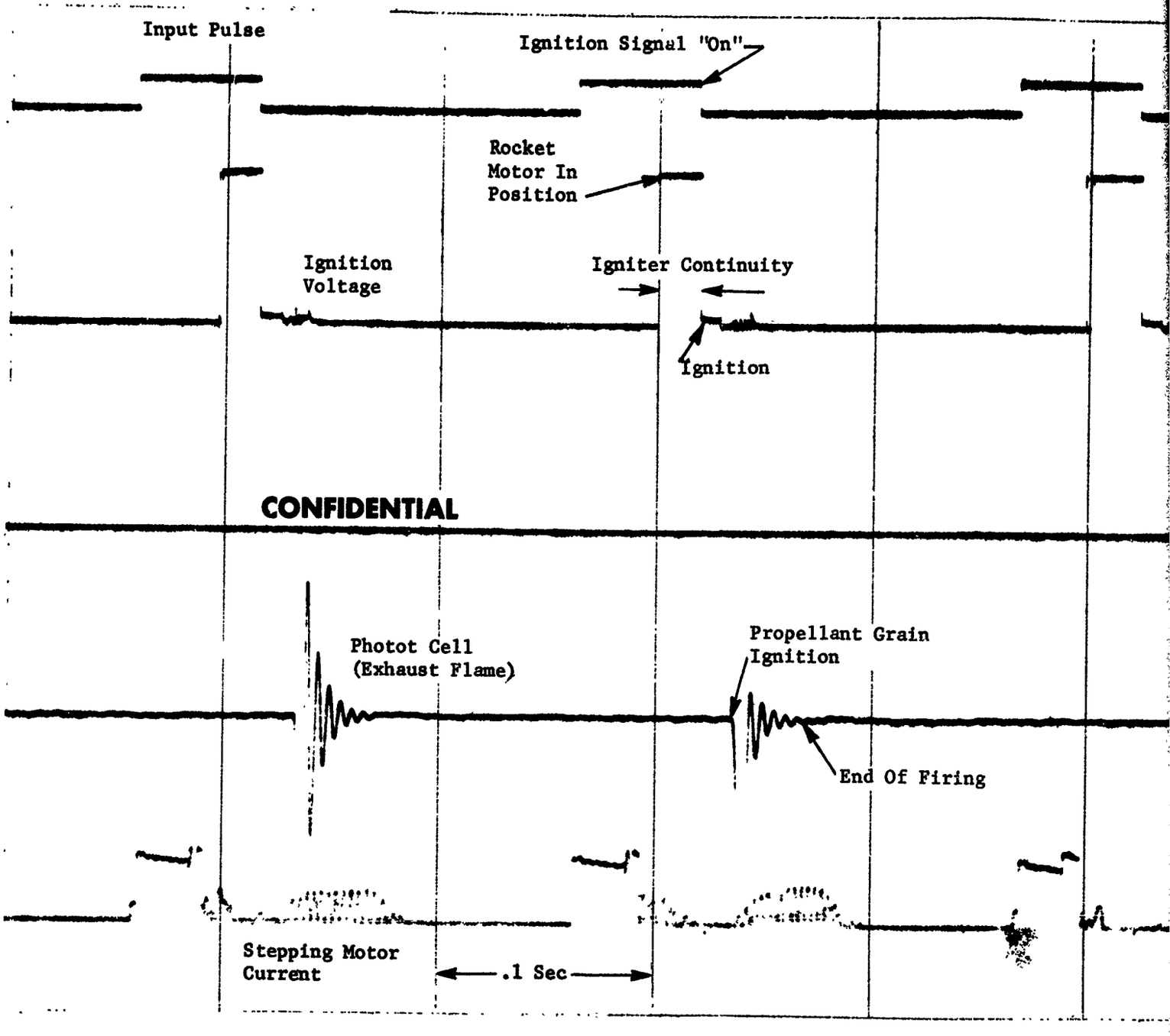
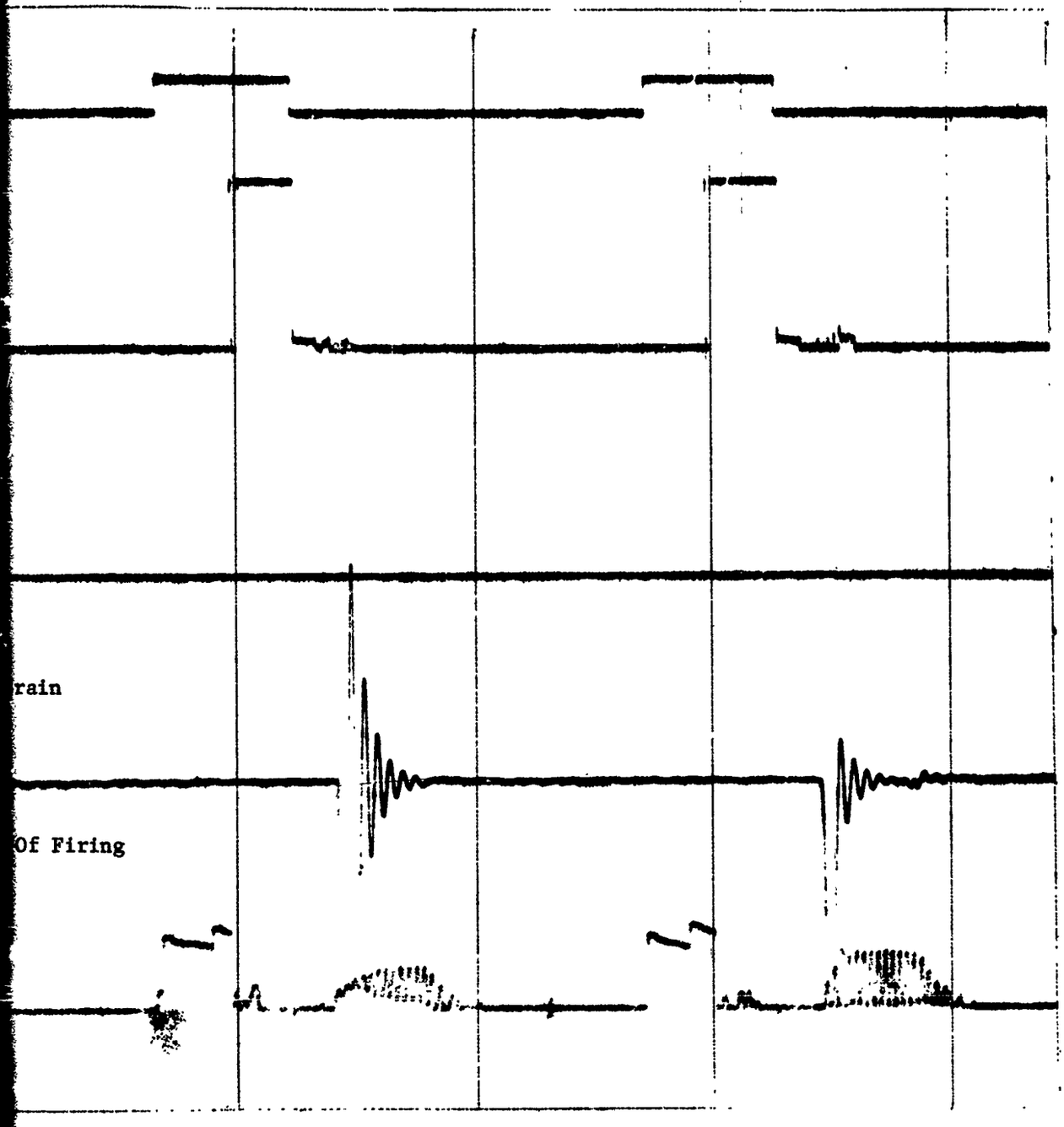


Figure 109. WSR-101 repetitive firing trace. (U

PRECEDING PAGE BLANK-NOT FILMED



epetitive firing trace. (U)

(U) It is therefore concluded that the problems encountered during repetitive firings have been resolved. For future tape assemblies more sophisticated assembly fixtures will be used to insure proper positioning of the rocket motors and higher durometer rubber will be used for the E dome to prevent extrusion.

SECTION IX
CONCLUSIONS

(U) 1. The solid propellant propulsion system designated WSR-101 incorporating the expandable (E dome) design concept, has demonstrated that it is capable of rapid, precise command-stop-restart functions and high performance.

(U) 2. A rectangular rocket motor with an L/D ratio of 2:1 with a simple, flat end-burning grain is optimum for minimum weight, volume, and sprocket wheel inertia.

(C) 3. Performance summary for WSR-101 rocket motor:
   a. Total impulse - 2.68 lb-sec
   b. Specific impulse - 249.4 lb-sec/lb
   c. Average thrust duration - 46.8 milliseconds
   d. Average ignition delay - 22.8 milliseconds

(C) 4. Weight summary for system:
   a. Pulser weight - 9.83 lb
   b. Rocket motor weight - .0246 lb

(C) 5. Firing test of the rocket motor accomplished successfully at -30° and +150°F.

(C) 6. Repetitive firing tests demonstrated a firing rate of 8 cps that the system is capable of firing at a rate of 10 cycles per second with additional modifications.

(C) 7. The CWP-13 propellant delivers an Isp of 250 seconds at an expansion ratio of 14:1 at sea level conditions.

(C) 8. The CWP-17A8 aluminized propellant delivers an Isp of 255 seconds at an expansion ratio of 14:1 at sea level conditions. The specific impulse efficiency is 96%.

(C) 9. The CWP series propellants are space storable and non-toxic.

(U) 10. Vacuum tests of each system component showed them to be operable under space conditions.

(C)11. System analyses for the encapsulated solid propellent pulse rocket motor showed it to be applicable for a post boost propulsion system.

(C)12. The observed reliability for the repetitive firings is .926.

CONFIDENTIAL
Security Classification

DOCUMENT CONTROL DATA - R&D
(Security classification of title, body of abstract and indexing annotation must be entered when the overall report is classified)

1. ORIGINATING ACTIVITY (Corporate author)
Curtiss-Wright Corporation
Wright Aeronautical Division
Wood-Ridge, New Jersey

2a. REPORT SECURITY CLASSIFICATION
CONFIDENTIAL

2b. GROUP
FOUR

3. REPORT TITLE
Preliminary Final Report For the Feasibility Demonstration of a Large Impulse Solid Rocket Attitude Control Motor (U)

4. DESCRIPTIVE NOTES (Type of report and inclusive dates)
Final Report January 1965 - August 1966

5. AUTHOR(S) (Last name, first name, initial)
Rolleri, Norman J.

6. REPORT DATE	7a. TOTAL NO. OF PAGES	7b. NO. OF REFS
August 1966	35	

8a. CONTRACT OR GRANT NO.	9a. ORIGINATOR'S REPORT NUMBER(S)
AF 04(611)-10531 b. PROJECT NO. 3059 c. AF Program Structure No. 750G d BPSN 623059	WAD: R-424-F 9b. OTHER REPORT NO(S) (Any other numbers that may be assigned this report) AFRPL-TR-66-135

10. AVAILABILITY/LIMITATION NOTICES

11. SUPPLEMENTARY NOTES	12. SPONSORING MILITARY ACTIVITY
	Air Force Rocket Propulsion Laboratory Edwards, California

13. ABSTRACT (Confidential)

Design, Analyses, and Reliability

(U) Rocket motor optimization studies show that a rectangular motor configuration with an L/D ratio of 2:1 using a simple flat end-burning grain was optimum to provide minimum weight, volume, and sprocket wheel inertia. The design of the rocket motor was based on a quartz-phenolic base, a pre-molded rubber grain inhibitor, a silicone expandable (E) dome, CWP-13 propellant, and a pyrofuze wire pyrotechnic overspray ignition system. The weight of the WSR-101 rocket motor is .0246 pounds.

(U) The final version of the pulser housing assembly was made of stainless steel. The titanium sprocket wheel included provisions to withstand rocket motor failures. The weight of the pulser housing assembly is 5.64 pounds.

(U) The inlet-exit chute assembly design incorporates a cleated belt to feed the rocket motors into the pulser and extract fired rocket motors from the sprocket wheel. The weight of this unit is 1.01 pounds.

(U) A static firing fixture was designed to house the rocket motors during sea level and vacuum firing tests and simulate the firing conditions in the pulser housing assembly.

DD FORM 1 JAN 64 1473

CONFIDENTIAL
Security Classification

(U) Heat transfer analyses showed that no problems would exist with the E dome, nozzle throat, sprocket wheel, or pulser housing. A problem would be encountered, however, with the exit cone for extended periods of firing. This did not present a problem for this program. For system applications which would require long periods of firing, suitable materials could be incorporated in the exhaust nozzle extension cone to meet the duty cycle.

(C) System analyses, using the requirements of a post boost propulsion system were conducted for the encapsulated solid propellant pulse rocket system. (Volume II)

(C) Specific impulse computations were perormed which showed that 8% aluminum was optimum for the WSR-101 motor. Motor tests produced an Isp of 255 seconds at sea level conditions and an expansion ratio of 14:1, and an Isp efficiency of 96%.

(C) Vacuum stability tests on the CWP series propellants showed excellent storability characteristics at 10^{-6} Torrs and 150°F.

Pulser Development

(U) The pulser system consists of those components which combined together produce the sprocket wheel stepping action to move capsules into firing position.

(U) A prototype solid state, high response relay type, feedback servo combined with a printed electrical motor was developed which met the program requirements for torque and step time.

Fabrication

(U) Standard transfer and compression molds were used to fabricate the rocket motor components. The assembly of the rocket motor components and tape assemblies was accomplished by manual methods using fixtures as required for curing and positioning.

Test

(U) Rocket motor development tests were conducted to establish the configuration of the motor.

(C) Performance repeatability tests on 100 motors showed the reproducibility of total impulse and specific impulse to be 2.47% and 2.3% respectively.

(C) Thermal vacuum firing tests of the rocket motors showed the components to be compatible in space and operable over a temperature range of -30 to +150°F. Ignition delays obtained in vacuum were two to three times longer than those experienced at sea level depending upon the exposure temperature.

(C) A failure mode analysis was made for each component of the WSR-101 system. The observed reliability for the repetitive firings is .926.

(C) A preliminary study of the maintainability requirements for an encapsulated solid propellant pulse rocket motor system shows that only routine checks need be performed to assure operational readiness. The system also has unique characteristics which permit effective checkout and maintenance procedures.

Materials Evaluation

(U) The selection and evaluation criteria for rocket motor materials were based on design requirements and consideration of methods of component fabrication. The materials selected for each rocket motor component are as follows:

Nozzle Base - Fiberite MX 1344-50
E - Dome - Silicone Rubber S-55 and Gen Gard V-57
Inhibitor - Gen Gard V-57
Nozzle Plug - Urethane Foam
Tape - Teflon - Fiberglass TB-5E
Adhesives - Aerospace Sealant 92-018 with Silicone Primer 4094

Igniter Development

(U) Several experimental igniter compositions were prepared and tested in the WSR-101 rocket motor. The aluminum based igniters performed well in the motors but require further improvement. Magnesium based igniters produced rapid rates of pressure rise which ruptured the elastic motor dome.

(U) A spray pyrotechnic igniter was selected as being the most feasible and reliable for the final motor configuration. The ignition system incorporates a Hi-R .004 inch diameter, Pyrofuze initiator and a pyrotechnic booster.

Propellant Development

(C) By means of processing changes, which can be precisely controlled, a reproducible burn rate of 1.9 inches per second was achieved.

(U) Repetitive firing tests were made which combined the operation of all components (rocket motor tape assembly, pulser housing assembly, stepping servo and motor system) of the system.

(U) Two problems were encountered during these tests, namely missed ignition of the rocket motor and E dome extrusion which jammed the pulser assembly. These problems were resolved by modification to the tooling to insure better positioning and spacing of the rocket motors on the tape and the use of higher durometer material for the dome.